DISCRIMINATING AMONG METALS

BY

JULIA ELIZABETH MARTIN

DISSERTATION

Submitted in partial fulfillment of the requirements
for the degree of Doctor of Philosophy in Microbiology
in the Graduate College of the
University of Illinois at Urbana-Champaign, 2013

Urbana, Illinois

Doctoral Committee:

Professor James A. Imlay, Chair
Associate Professor Cari Vanderpool
Professor James M. Slauch
Professor John E. Cronan

ABSTRACT

Role of the iron-dependent NrdAB homologue, NrdEF

The genome of *Escherichia coli* encodes two class I ribonucleotide reductases. The first, NrdAB, is a well-studied iron-dependent enzyme that is essential for aerobic growth. The second, NrdEF, is not functional under routine conditions, and its role is obscure. Recent studies demonstrated that NrdEF can be activated *in vitro* by manganese as well as iron. Since iron enzymes are potential targets for hydrogen peroxide (H_2O_2), and since the *nrdHIEF* operon is induced during H_2O_2 stress, we hypothesized that H_2O_2 might inactivate NrdAB and that NrdEF might be induced to compensate. This idea was tested using *E. coli* mutants that are chronically stressed by H_2O_2. Contrary to expectation, NrdAB remained active. Its resistance to H_2O_2 depended upon YfaE, which helps to activate NrdB. The induction of NrdEF during H_2O_2 stress was mediated by the inactivation of Fur, an iron-dependent repressor. This regulatory arrangement implied that NrdEF has a physiological role during periods of iron starvation. Indeed, NrdEF supported cell replication in iron-depleted cells. Iron bound to NrdF when it was expressed in iron-rich cells, but NrdEF was functional only in cells that were both iron-depleted and manganese-rich. Thus NrdEF supports DNA replication when iron is unavailable to activate the housekeeping NrdAB enzyme.

Role of *mntS* in manganese metabolism

Iron is involved in many cellular processes and is essential for almost all organisms. However, it is sometimes scarce in the contemporary aerobic world due to

oxidation. When *Escherichia coli* is deficient in iron or stressed by hydrogen peroxide, it uses manganese rather than iron to populate mononuclear enzymes. When iron becomes available, excess manganese is exported out of the cell through the efflux pump, MntP. It is unclear how these cells traffic intracellular manganese, since cells maintain manganese at concentrations below those of most other metals. Recent identification and characterization of the novel manganese homeostasis gene, *mntS*, sparked our interest in this problem. The *mntS* RNA encodes an extremely small protein of 42 amino acids that is repressed by the transcriptional regulator, MntR, in response to high intracellular manganese levels. Furthermore, hydrogen peroxide-stressed cells need manganese to sustain enzyme activity, and we confirmed that *mntS* allowed cells to cope with H_2O_2-stress. We hypothesized that MntS makes manganese more available to proteins when manganese is scarce. We showed that *mntS* assists the activation of two manganese-dependent enzymes: manganese-superoxide dismutase and manganese-ribonucleotide reductase. Titration experiments demonstrated that *mntS* is needed only when manganese is scarce. Conversely, MntS overexpression made cells more vulnerable to high concentrations of manganese, via activation of Fur, the ferric uptake regulator. These cells exhibited profound repression of the Fur regulon, which resulted in a significant reduction in intracellular free iron (<2 µM compared to ~90 µM under routine aerobiosis) and accumulation of 3-fold more manganese. This ultimately led to the failure of heme synthesis. Furthermore, a similar effect was observed in *mntP* mutants with respect to manganese toxicity. Taken together, this study reveals that the small protein MntS makes manganese more available to proteins possibly by inhibiting MntP function.

To my loving and supportive husband, Thomas Sullivan

ACKNOWLEDGEMENTS

I would like to thank all my colleagues, instructors, friends, and family members for their guidance, encouragement, and support during my graduate studies. I especially want to thank my advisor, Dr. James A. Imlay, for his exceptional guidance in helping me develop myself as a scientist. He is a very bright scientist and instructor that is very understanding. I admire him for his ability to balance time between his career and family. The work presented here would not have been possible without his advice and support.

I would like to thank my thesis committee, Dr. John E. Cronan, Dr. James M. Slauch, and Dr. Cari Vanderpool, for questioning my research and providing me with insightful research directions.

I would like to thank Dr. Mark Nilges for his help with the electron paramagnetic resonance spectroscopy studies, and members of the Vanderpool lab for their guidance on RNA preparations.

I would like to thank my current and past colleagues in the Imlay lab: Dr. Adil Anjem, Dr. Mianzhi Gu, Dr. Soojin Jang, Dr. Sergei Korshunov, Dr. Yuanyuan Liu, Dr. Zheng Lu, Dr. Lee Macomber, Dr. Stefano Mancini, Dr. Surabhi Mishra, Dr. Fangfang Xu, Kari Imlay, Maryam Khademian, and Jason Sobota. They are all smart, friendly, and kind people that have made working in the laboratory an enjoyable and exciting experience every day. I especially want to thank Dr. Lee Macomber for his creativity in helping develop the Imlay Lab Olympics. Many memories were created here that I will cherish forever.

I would like to thank several other mentors, Dr. Elena Maria Zavala and Dr. Larry Baresi, for their enthusiastic support and guidance that they have given me. They helped me find the confidence, determination, and perserverance to enter into graduate school and attain a higher educational degree.

I would like to thank my friends and family for their love, patience, and support. I especially want to thank my husband, Thomas Sullivan, who has stood by my side through my college education. His positive attitude has helped keep me sane during my graduate studies. Together we have two beautiful daughters, Gwendolyn and Elora. Their smiles have erased many long tough days in the lab.

Lastly, I want to thank God for reminding that I am never alone. I would like to end with my favorite bible verse from Mathew 7:7-8, "Ask and it will be given to you; seek and you will find; knock and the door will be opened to you. For everyone who asks receives; the one who seeks finds; and to the one who knocks, the door will be opened."

TABLE OF CONTENTS

CHAPTER 1: INTRODUCTION 1

1.1 Iron homeostasis 1
1.1.1 Role and properties of iron in biology 1
1.1.2 Strategies used to maintain intracellular iron homeostasis 4
1.1.2.1 Iron acquisition and import 5
1.1.2.2 Iron storage 6
1.1.2.3 Iron export 7
1.1.2.4 Regulation of iron homeostasis 8

1.2 Manganese homeostasis 11
1.2.1 Role and properties of manganese in biology 11
1.2.2 Manganese import 12
1.2.3 Regulating manganese import 12
1.2.4 Avoiding too much manganese 13

1.3 Other important transition metals 14
1.3.1 Copper 14
1.3.2 Nickel 17
1.3.3 Zinc 19

1.4 Intracellular metal trafficking 21
1.4.1 How is mismetallation avoided? 21
1.4.2 Metal insertion by delivery proteins 23
1.4.3 Trafficking of iron and manganese 25

1.5 Scope of this thesis 26
1.5.1 What is the physiological role of the alternative *Escherichia coli* aerobic ribonucleotide reductase, NrdEF? 26
1.5.2 What is the physiological role of the *Escherichia coli* small protein, MntS? 27

1.6 Figures 29

1.7 References 36

CHAPTER 2: WHAT IS THE PHYSIOLGICAL ROLE OF THE ALTERNATIVE *ESCHERICHIA COLI* AEROBIC RIBONUCLEOTIDE REDUCTASE, NRDEF? 48

2.1 Introduction 48

2.2 Materials and methods 50
2.2.1 Reagents 50
2.2.2 Growth conditions 51
2.2.3 Bacterial strain and plasmid construction 52
2.2.4 Cell viability 54
2.2.5 Enzyme assays 54
2.2.6 Disk diffusion assay 55
2.2.7 Total thymidine incorporation 56
2.2.8 Whole-cell EPR measurements of tyrosyl radical 57
2.2.9 RNA isolation 58
2.2.10 Quantitative real-time PCR 59
2.2.11 5′ RLM-RACE 59

2.3 Results 60
2.3.1 NrdEF is induced during H_2O_2 stress, but H_2O_2 does not inhibit NrdAB function 60
2.3.2 NrdEF is functional during H_2O_2 stress 63
2.3.3 Fur and IscR regulate *nrdHIEF* transcription 64
2.3.4 Expression of *nrdHIEF* is not sufficient for function 67
2.3.5 NrdEF requires manganese to function 68
2.3.6 NrdEF becomes active during protracted iron starvation 69
2.3.7 YfaE is required for continued NrdAB function during H_2O_2 stress 72

2.4 Discussion 72
2.4.1 Ribonucleotide reductase and iron starvation 74
2.4.2 Ribonucleotide reduction during oxidative stress 76

2.5 Tables 79

2.6 Figures 84

2.7 References 102

CHAPTER 3: WHAT IS THE PHYSIOLOGICAL ROLE OF THE *ESCHERICHIA COLI* SMALL PROTEIN, MNTS?.....109

3.1 Introduction.....109

3.2 Materials and methods.....112
3.2.1 Reagents.....112
3.2.2 Bacterial strain and plasmid construction.....113
3.2.3 Growth conditions.....115
3.2.4 Cell viability.....116
3.2.5 Enzyme assays.....116
3.2.6 Electron paramagnetic resonance (EPR) measurements of unincorporated intracellular iron.....119
3.2.7 Detection of manganese by EPR.....120
3.2.8 Inductively coupled plasma-mass spectrometry (ICP-MS) of intracellular iron and manganese.....120
3.2.9 Porphyrin quantification.....121

3.3 Results.....122
3.3.1 MntS facilitates manganese delivery to manganese-dependent enzymes when manganese is scarce.....122
3.3.2 In manganese-rich medium overproduced MntS disrupts metal pools.....125
3.3.3 Metal imbalance blocks growth by inhibiting the synthesis of heme.....126
3.3.4 MntS protein exerts manganese toxicity.....129
3.3.5 MntS overproduction mimics the effect of eliminating the MntP manganese exporter.....130

3.4 Discussion.....132
3.4.1 Manganese poisoning of iron-dependent processes by overexpression of MntS or deletion of *mntP*.....133
3.4.2 Regulating intracellular manganese concentrations.....135
3.4.3 Does MntS and RybA act within the same physiological pathway to increase manganese availability?.....136

3.5 Tables.....137

3.6 Figures.....142

3.7 References 166

CHAPTER 4: CONCLUSIONS 170

4.1 Summary of current work 170
4.1.1 NrdEF is a manganese-dependent ribonucleotide reductase that enables cell replication during periods of iron-starvation 170
4.1.2 MntS and MntP make manganese more available to enzymes 170

4.2 Future directions 171
4.2.1 What is the physiological relavance for the regulation of *nrdHIEF* by apo-IscR? 171
4.2.2 What parameters determine metal specificity of NrdB and NrdF *in vivo*? 172
4.2.3 Does NrdEF help pathogens tolerate the iron restriction that is imposed by the host? 173
4.2.4 Can enteric bacteria persist in the absence of iron? 174
4.2.5 How is manganese imported in the *mntH* mutants? 175
4.2.6 Is HemH poisoned by manganese? 176
4.2.7 Does MntS inhibit MntP function? 176
4.2.8 Do metal chaperones exist that help allocate iron and manganese to proteins? 177

4.3 References 178

APPENDIX A: EXPRESSION OF THE *E. COLI* TRX2 AND GRX1 ARE NOT INDUCED DURING HYDROGEN PEROXIDE STRESS TO COMPENSATE FOR INACTIVATION OF THE PRIMARY THIOREDOXIN, TRX1, SINCE IT REMAINS ACTIVE 179

A.1 Materials and methods 181
A.1.1 Bacterial strain construction 181
A.1.2 Growth conditions 182

A.2 Tables 183

A.3 Figures 184

A.4 References 186

APPENDIX B: *KATG* TRANSCRIPTION IS HIGHLY REPRESSED IN *ΔFUR* MUTANTS 188

B.1 Materials and methods 190
B.1.1 Bacterial strain construction 190
B.1.2 Growth conditions 191
B.1.3 Enzyme assays 192

B.2 Tables 194

B.3 Figures 195

B.4 References 198

APPENDIX C: *HEMA* TRANSCRIPTION IS DOWN-REGULATED DURING MANGANESE TOXICITY 200

C.1 Materials and methods 201
C.1.1 Bacterial strain construction 201
C.1.2 Growth conditions 202
C.1.3 β-galactosidase activity 203

C.2 Tables 204

C.3 Figures 205

C.4 References 209

APPENDIX D: DOES MNTS WORK AS A SMALL RNA IN ADDITION TO ITS FUNCTION AS A PROTEIN? 211

D.1 Introduction 211

D.2 Results 211
D.2.1 A small RNA helps activate MnSOD 211

D.2.2 Val10 residue is important for MntS/RybA function....213
D.2.3 MntS possibly functions as a small RNA to help activate NrdEF....214
D.2.4 MntS confers both protein and small RNA function during hydrogen peroxide stress....214

D.3 Conclusion....214

D.4 Materials and methods....215
D.4.1 Strain and plasmid constructions....215
D.4.2 Growth conditions....217
D.4.3 Cell viability....218
D.4.4 Superoxide dismutase activity....219
D.4.5 Purification of MntS protein....219
D.4.6 *In vitro* manganese uptake by apo-MnSOD in cell extracts....220

D.5 Tables....221

D.6 Figures....226

D.7 References....241

CHAPTER 1: INTRODUCTION

1.1 IRON HOMEOSTASIS

1.1.1 Role and properties of iron in biology

Iron is the fourth most abundant metal on Earth [4]. It is classified as a first row transition metal with an unfilled *d*-orbital (six electrons), which permits adoption of multiple oxidation states from Fe^{2+} to Fe^{6+}, with the two most common states being the reduced ferrous form Fe^{2+} and the oxidized ferric form Fe^{3+}. The ability to adopt different oxidation states makes iron extremely versatile and renders it capable of participating in both redox- and non-redox-based reactions inside cells. Iron can also bind to a wide variety of ligands (up to six at a time) depending on the intracellular microenvironment, but it is typically coordinated to negatively charged residues such as glutamate, aspartate, cysteine, and histidine. Taken together, these chemical properties make iron conducive for use in many major biological processes including respiration, TCA cycle, gene regulation, and DNA biosynthesis.

In redox-based reactions, iron is used as a prosthetic group that facilitates electron transfer in three different classes of enzymes: (i) iron-sulfur [Fe-S] cluster enzymes such as NADH dehydrogenase I (Ndh-1), (ii) heme-based enzymes such as catalase, and (iii) mononuclear enzymes such as iron-dependent superoxide dismutase (FeSOD). For example, Ndh-1 of *Escherichia coli* contains nine [Fe-S] clusters, each possessing a different reduction potential, which permits electron travel from one cluster to the next through the enzyme. Similar [Fe-S] clusters are found in succinate dehydrogenase, fumarate reductase, and sulfite reductase.

Iron performs an equally important redox role in the heme-based enzyme catalase, in which porphyrin-Fe^{3+} quickly converts to porphyrin-Fe^{4+} and back again in a two-step process during the disproportionation of hydrogen peroxide [39]. Iron is also known to cycle between the ferric Fe^{3+} and ferrous Fe^{2+} forms during the course of catalysis in the mononuclear enzymes FeSOD and ribonucleotide reductase NrdAB [22, 119]. It is imperative to note that these enzymes require iron as a cofactor to function and that no other redox-active metal can be used as a substitute, because those metals are not poised at the right potential to interact with substrate.

Iron can also participate in non-redox-based reactions by providing a local positive charge and coordinating substrate in [Fe-S] cluster-containing enzymes, such as dehydratases. These enzymes contain an [Fe-S] cluster, where one iron atom is solvent exposed and has the capacity to bind substrate. Upon binding substrate, the exposed iron atom shifts from a tetrahedral to octahedral (six-coordinate) geometry. This shift occurs with minimal activation energy, since no bonds are broken [54, 56]. Dehydratases are not the only enzymes that use iron in non-redox-based reactions. Isocitrate dehydrogenase, methionine aminopeptidase, and peptide deformylase have also been observed to use iron in a similar manner to dehydratases *in vitro* [12, 18, 86].

The chemical properties stated above have made iron essential for almost all organisms. Exceptions may include *Lactobacillus, Borrelia burgdorferi*, and *Treponema pallidum*, which seem to lack iron-dependent proteins and were found to contain minuscule amounts of intracellular iron [9, 101]. Although the later two bacteria may formally not require iron, they may rely on their hosts' iron-dependent processes for

energy, especially since they are obligate parasites. In hindsight, organisms that forgo iron may have a competitive advantage under specific growth conditions.

For present-day organisms that inhabit aerobic environments, iron dependence comes at a price: iron also exhibits toxic effects as a metal cofactor. In oxic conditions, iron is capable of interacting with oxygen and reduced oxygen species (H_2O_2 and superoxide) which results in the (1) production of harmful reactive oxygen species (ROS) that damage biomolecules and the (2) reduction of bioavailable iron. Note that both H_2O_2 and superoxide are strong univalent oxidants that cannot damage biomolecules by themselves, but rather their toxicity depends on their reaction with iron. For example, H_2O_2 can react with ferrous iron resulting in the formation of a hydroxyl radical in the Fenton reaction (Reaction 1.1). The hydroxyl radical produced is extremely toxic as it can damage any cellular biomolecule (Reaction 1.2)

$$H_2O_2 + Fe^{2+} \rightarrow OH^- + FeO^{2+} + H^+ \rightarrow Fe^{3+} + OH^- + HO^{\bullet} \quad \text{(Reaction 1.1)}$$

$$HO^{\bullet} + \text{DNA or Polypeptide} \rightarrow \text{Damage} \quad \text{(Reaction 1.2)}$$

Diminution of bioavailable iron also poses a serious problem for organisms. Cells deprived of iron grow poorly due to inefficient metallation of key enzymes, like ribonucleotide reductase, cytochrome oxidase, and those that detoxify ROS. Continual influx of iron and exposure to ROS will ultimately lead to cell death. Thus, it is critical for organisms to maintain optimal intracellular iron concentrations, as well as to retain iron in a controlled environment.

Technically speaking, bacteria lack specialized compartments for sequestration, storage, and distribution of metals. However, upon closer investigation one might consider the cytoplasm and periplasm as separate entities, with the cytoplasm exemplifying a stronger reducing environment than the periplasm. This type of compartmentalization ensures that metals are maintained in a safe environment. For example, iron would remain in its reduced state and uncomplexed or free within the cytoplasm. Similarly, other metals such as copper would be kept in their oxidized and less toxic form in the periplasm.

Lastly, there is no good way to study iron-limitation. Removal of iron from lab media using common metal chelators does not work well because they also bind other metals such as manganese. Moreover, I am not sure if *E. coli* can grow without iron in oxic environments because iron is necessary for isoprenoid and heme synthesis. Isoprenoids are needed to maintain the membrane, while heme is used in enzymes such as cytochrome oxidase. These enzymes appear to be essential for *E. coli*. To my knowledge, there is no way to get around these processes.

1.1.2 Strategies used to maintain intracellular iron homeostasis

Since iron is both essential and potentially, many organisms have evolved several strategies that keep intracellular iron levels within a non-detrimental range: high enough to keep iron-dependent metabolic processes from failing, yet low enough to prevent cell damage by ROS or mismetallation of enzymes. These strategies can be grouped into four basic categories: acquisition, transport, storage, and regulation. Organisms that use these approaches collectively to manage iron homeostasis have a better chance at survival.

1.1.2.1 Iron acquisition and import

Ferrous iron Fe^{2+} is the preferred form of iron used by bacteria, but on Earth iron is primarily found in its much less soluble ferric form Fe^{3+}due to oxidation by oxygen, thereby making iron less bioavailable. Bacteria employ two methods that help render ferric iron more soluble. (1) Some bacteria can actively reduce extracellular Fe^{3+} to its more soluble form before it is taken up, while (2) others secrete iron-chelator complexes termed siderophores that carry Fe^{3+} to be transported into the cell. The exact mechanism by which bacteria reduce extracellular Fe^{3+} is not known, but it can be said that Fe^{2+} import occurs both aerobically and anaerobically in bacteria via FeoB. Fe^{2+} can also be taken up by the putative EfeUOB transporter in *E. coli* strain Nissle 1917 under conditions of iron limitation and low pH [38]. Note that typical laboratory *E. coli* K-12 derivatives lack a functional iron permease EfeU (encoded by *ycdN*) protein. However, overexpression of EfeU in a *E. coli* K-12 derivative deficient in iron-uptake showed increased iron accumulation by measuring the uptake of radiolabeled ^{55}Fe [38]. The physiological role of the EfeUOB transporter has not been resolved despite its wide distribution among bacteria.

Unlike Fe^{2+}, Fe^{3+} can only be imported as a siderophore-complex through transport systems that possess receptors that specifically recognize corresponding siderophore-iron complexes [114]. For example, the two well known siderophores, ferri-enterobactin (a catecholate) and ferrichrome (a hydroxamate), are transported into the cell by the outer membrane receptors FepA and FhuA, respectively [6]. Fe^{3+} can also form a complex with citrate which is specifically imported by FecA. Commensal

microorganisms use similar high-affinity transport systems to scavenge various forms of iron, including heme, from their host for survival.

The transport of extracellular iron across the membrane into the cytoplasm requires energy. For the above-mentioned outer membrane receptors, this energy is supplied in the form of a proton motive force generated by the TonB-ExbB-ExbD complex (Fig. 1.1) [109]. Each outer membrane receptor is associated with an inner membrane ATP-dependent transporter that aids the transfer of the siderophore-iron complex into the cytoplasm (Fig. 1.1). It is unclear how siderophore-iron complexes are translocated through their respective transport systems, but once internalized it is hypothesized that the iron is either (i) liberated from the siderophore complex by reduction or (ii) released by hydrolysis. In *E. coli*, the release of iron from enterobactin requires the esterase protein Fes, which seems to employ both mechanisms to release iron from the siderophore [27].

1.1.2.2 Iron storage

Many bacteria deposit intracellular reserves of iron into iron-storage proteins, which can be drawn upon when iron is scarce. There are three types of iron-storage proteins: ferritin, heme-containing bacterioferritin, and Dps [5, 6]. These proteins are composed of multiple identical subunits that form a sphere with a hollow center in which iron atoms are sequestered. Dps has the capacity to store up to 500 iron atoms per protein molecule, whereas bacterioferritin and ferritin can hold at least 2000 iron atoms per protein molecule [6]. Ferritin, encoded by *ftnA*, is the primary iron-storage protein in *E. coli* and is regulated in response to intracellular iron [87]. The cellular role of

bacterioferritin, encoded by *bfr*, remains unknown, since *bfr* mutants do not show a defect in iron storage [1]. The third iron-storage protein, Dps, is induced during special growth conditions such as H_2O_2 stress, where it most likely functions to protect cells from damage by ROS through iron sequestration rather than storage for iron scarcity [134]. In summary, bacteria employing iron-storage proteins have established a way to accommodate their need for iron, as well as to protect themselves from cellular damage by maintaining iron in a safe controlled environment.

1.1.2.3 Iron export

In many organisms excess metal ions, including copper, zinc, nickel, and cobalt, are exported out of the cell and into the environment by efflux pumps. There are no known iron efflux systems in eukaryotes and only recently was the first putative iron efflux pump (FieF, encoded by *fieF*, formerly *yiiP*) identified for prokaryotes in *E. coli* [36]. FieF is a member of the cation diffusion facilitator (CDF) family of membrane-bound transporters. It is important to note that all CDF family members transport zinc in addition to other divalent metal ions across the membrane [91]. Zinc and iron induce *fieF* to similar levels [35]. Transport assays clearly show that FieF transports zinc in a proton-dependent manner, while the iron transport mechanism remains unclear [36, 125]. Indirect evidence suggests that FieF may be involved in the removal of iron from *E. coli* cells, since the presence of FieF leads to decreased accumulation of iron in cells [36]. If FieF were a true iron efflux pump, then one might predict it to be important during H_2O_2 stress. However, deletion of *fieF* in peroxidase/catalase-deficient cells showed no growth defect [71]. It is possible that ferric iron surplus induces *fieF* to eliminate zinc from the

cytoplasm, since recent published data shows that mononuclear enzymes are inactivated by zinc during superoxide stress where iron is mostly present in its oxidized form [41]. According to the Irving-William series, which predicts the tendency for metals to follow a universal order of preference for ligands ($Mn^{2+} < Fe^{2+} < Co^{2+} < Ni^{2+} < Cu^{2+} > Zn^{2+}$) [57], the metal affinity of a binding site may be higher for the incorrect metal. In the case above, zinc binds more tightly than iron to mononuclear enzymes. Other examples include copper displacing iron from [Fe-S] cluster-containing proteins *in vivo* due to its high ability to adhere to sulfhydryls.

1.1.2.4 Regulation of iron homeostasis

Many bacteria regulate iron metabolism in response to intracellular iron availability via Fur, the ferric uptake regulator protein. Fur exists as a homodimer that is activated by binding ferrous iron [23]. Under iron-replete conditions, activated Fur protein binds to the promoters of most iron-acquisition genes and represses transcription [28, 45]. In contrast, when iron levels decrease, Fur becomes inactive and the repression is relieved. It is important to point out that *E. coli* does not contain an iron-responsive regulator that acts in response to excessive intracellular iron concentrations. During iron surplus, *E. coli* possibly responds by simply increasing ferritin production to bind iron. Fur:Fe^{2+} displaces the histone-like protein, H-NS, from the *ftn* promoter, allowing induction when iron levels are high [87]. More research is needed to determine the reason for induction of *ftn*.

Note that there are several iron-utilizing genes (*sdhCDAB, acnA, fumABC, ftnA, bfr,* and *sodB*) in *E. coli* that are positively regulated by Fur; their expression is increased

under iron-replete conditions [6]. These genes, with the exception of *ftnA*, do not contain Fur-binding boxes and are regulated indirectly through Fur via the small regulatory RNA RyhB [77]. The RyhB sRNA acts as an iron-sparing mechanism by pairing to target mRNAs and promoting degradation of RNA encoding dispensable iron-containing proteins (Fig. 1.2). Hence, RyhB eliminates Fe-using enzymes that are abundant but not essential. RyhB activity is dependent on the RNA chaperone Hfq [33]. Hfq helps mediate the interaction between RyhB and RNase E and prevents degradation of RyhB by RNase E [3, 81, 83].

In addition to reducing non-essential iron-dependent process by down-regulation, bacteria can also replace iron-dependent proteins with iron-free isozymes during iron restriction. For example, the *sodB* gene that encodes the FeSOD enzyme is induced by Fur:Fe^{2+} under iron-replete conditions in *E. coli*, whereas the *sodA* gene that encodes the manganese-superoxide dismutase (MnSOD) protein is repressed by Fur:Fe^{2+} [89]. A similar regulatory relationship exists between the fumarase isozymes, in which the iron-sulfur cluster-containing fumarases (FumA and FumB) are induced by Fur:Fe^{2+} whereas the iron-free fumarase (FumC) is repressed [6, 97].

Fur also indirectly regulates the [Fe-S] cluster assembly systems: Isc (genes *iscRSUA-hscBA-fdx*) and Suf (genes *sufABCDSE*) [78, 95, 98]. As described before, RyhB is expressed when iron is limited. In the case of the Isc system, RyhB binds to an untranslated region between *iscR* and *iscS* and promotes degradation of the *iscSUA* mRNA [25]. This ultimately results in a lower [Fe-S] cluster pool, which is sensed by IscR. Apo-IscR, containing no [Fe-S] cluster, binds to the promoter of the *suf* operon and induces its transcription [69, 131]. In contrast to the Isc system, Fur:Fe^{2+} directly

represses expression of the Suf system. Hence, during iron depletion, the Isc system is repressed, while the Suf system is induced. For reasons that are not yet clear, the Suf system is more efficient than the Isc system when iron pools are low.

Iron deficiency is also compensated in *E. coli* by importing manganese via Fur:Fe^{2+}-dependent repression of the sole dedicated manganese transporter, *mntH* [66, 100]. Thus, *mntH* is induced when iron is scarce. Imported manganese apparently replaces iron in mononuclear metalloenzymes and in the activation of other non-iron requiring proteins, such as MnSOD, that are up-regulated when iron is scarce. Note that MnSOD is a redox enzyme that requires manganese as a cofactor to function; no other redox-active metal can substitute.

Iron-responsive regulation is much different in alpha-proteobacteria compared to *E. coli*, a gamma-proteobacterium; and its distant firmicute relatives like *Bacillus*. Two types of iron regulators are present in alpha-proteobacteria: RirA and Irr. Unlike Fur, these iron-responsive regulators do not directly interact with Fe^{2+}, but rather form complexes with an [Fe-S] cluster or heme. During iron-rich conditions, RirA likely binds an [Fe-S] cluster co-factor that causes it to actively repress expression of downstream genes [63]. In contrast, Irr represses downstream genes in iron-depleted conditions and is inactivated by degradation in iron-replete conditions. Degradation of Irr is mediated by its interaction with heme [76]. The ability to sense iron-complexes, rather than iron itself, may provide more metal selectivity, thereby reducing interference by other metal cations.

1.2 MANGANESE HOMEOSTASIS

1.2.1 Role and properties of manganese in biology

Like iron, manganese can participate in redox reactions. However, it does not contribute to the harmful effects associated with oxidative stress *in vivo*, but rather helps protect cells against H_2O_2 by replacing iron in non-redox mononuclear metalloenzymes in *E. coli*, such as peptide deformylase, threonine dehydrogenase, and ribulose-5-phosphate epimerase [7, 112]. Manganese can serve the role of iron in these enzymes because it preferentially binds the same ligands as iron. Manganese also helps *E. coli* cells tolerate periods of iron limitation. Note that *E. coli* is an iron-dependent organism and does not normally use manganese. Only when iron is scarce or H_2O_2 is present does manganese become critical for *E. coli* growth.

In other bacteria, manganese is necessary for several metabolic pathways, including oxygenic photosynthesis in cyanobacteria and glycolysis in several Gram-positive endospore-forming bacteria [19, 132]. A number of enzymes also require manganese for activity, including MnSOD and the mangani-catalase of *Salmonella* [30, 126]. Manganese does not only aid in enzyme catalysis. Signal transduction proteins, such as the eukaryotic serine/threonine protein phosphatases (PrpA and PrpB), also rely on manganese [11]. These proteins have also been identified in *E. coli* [80].

In essence, manganese is used for a wide variety of functions, most likely because it shares similar properties to iron, including charge states, ionic radius, and ligand affinity. This is not surprising, since manganese is located direct adjacent to iron on the periodic table. Manganese does not share the same reduction potential as iron. Thus, it may interfere with iron-requiring processes when metal homeostasis is not

accurately maintained. In fact, too much manganese can poison *E. coli* but not *fur* mutants [46]. The mechanism of manganese toxicity is a topic of this thesis.

1.2.2 Manganese import

A wealth of information exists regarding the importance of manganese in bacteria during oxidative stress, iron-limitation, and infection. At least three types of manganese import systems have been identified in bacteria: (1) the natural resistance-associated macrophage protein (Nramp) MntH, (2) the ATP-binding cassette (ABC-transporter) SitABC (*alias* MntABC), and (3) the unique P-type ATPase MntA [42, 49, 55, 93]. Citrate and other tricarboxylic acids can stimulate Mn^{2+} import by the latter transporter [49]. This raises the possibility that Mn^{2+}-chelated complexes may also be imported similarly to iron-siderophores. Note that *E. coli* only contains a single specific manganese transporter, MntH, which is required for growth during protracted H_2O_2 stress and is induced when iron is limited via derepression of the Fur protein [8, 67].

1.2.3 Regulating manganese import

In many bacteria, manganese homeostasis depends upon the regulation of transport by the manganese-dependent transcriptional regulator MntR, which belongs to the DtxR family of metal-dependent corepressors. Divalent metals directly bind to members of this family and allosterically activate DNA binding, which turns off the expression of metal uptake systems [34]. For example, under manganese-sufficient conditions, activated MntR:Mn^{2+} protein binds to the promoters of both *mntH* and *sitABC* and represses transcription (Fig. 1.3) [28, 43, 45]. In contrast, when manganese levels

decrease, MntR becomes inactive and repression is relieved. The well-studied prototypical *Bacillus subtilis* MntR binds two metal ions in a binuclear cluster per subunit, in which site-A functions as a selective filter that recognizes a metal based on its coordination with residues and determines whether site-C will be filled with manganese [34]. Thus, manganese bound to site-C will lead to the activation of MntR. As a reminder, *mntH* is repressed by both Fur:Fe^{2+} and MntR:Mn^{2+} in *E. coli*, which suggests that iron and manganese homeostasis are interconnected.

An alternate manganese-uptake regulator, Mur, exists within the Fur-family of corepressors. In comparison to MntR, Mur binds only one manganese ion per subunit compared to two for MntR [13]. Mur also actively represses *sitABC* in *Rhizobium leguminosarum* during manganese-replete conditions [26]. What's more interesting is that Mur has difficulty distinguishing between Mn^{2+} and Fe^{2+}: apparently either metal can activate it *in vitro* and possibly *in vivo* under iron-replete conditions [13]. This is also true for Fur. Mur:Fe^{2+} can bind to Fur boxes and repress transcription of Fur-regulated genes, such as *bfd* encoding bacterioferritin, when expressed in *E. coli* during iron-rich growth [13]. The ability of Mur to respond to multiple metals *in vitro* elicits the need for bacteria to maintain metal homeostasis *in vivo*.

1.2.4 Avoiding too much manganese

High intracellular manganese concentrations may interfere with iron-requiring processes, resulting from similar characteristics between manganese and iron. In many cases, excess metals are redirected out of the cytoplasm by induction of efflux pumps. Recent identification of manganese efflux systems in *E. coli* (MntP), *Streptococcus*

pneumonia (MntE), and *Neisseria spp.* (MntX) suggest that bacteria remove excess manganese when levels become toxic [106, 120, 124]. The putative efflux pump MntP from *E. coli* was discovered by whole genome expression analysis of wild type and *mntR* mutants. Water *et al*. (2011) showed that *mntP* (formerly, *yebN*) mutants are sensitive to manganese but not to other divalent metals (Zn, Mg, Fe, Ni, and Cu). This sensitivity most likely originates from accumulation of intracellular manganese. Expression of *mntP* is also induced rapidly by manganese via MntR, which suggests that MntR is involved in metal resistance in addition to controlling manganese homeostasis. Hence, MntR can shut off manganese import and turn on export when manganese levels become toxic (Fig. 1.2).

N. meningitidis mntX and *S. pneumoniae mntE* mutants also accumulate high levels of intracellular manganese and are less virulent compared to wild type strains [106, 120]. Although *S. pneumoniae* MntE appears to be involved in manganese export, it is a member of the CDF family which has been characterized to export primarily zinc [91]. Further studies are needed to validate the functional role of these putative manganese transporters.

1.3 OTHER IMPORTANT TRANSITION METALS

1.3.1 Copper

In contrast to iron, the introduction of oxygen in the atmosphere increased the bioavailability of copper, by oxidizing the insoluble cuprous form Cu^{1+} to the more soluble cupric form Cu^{2+} [4]. Differences also exist within the coordination chemistry of Cu^{1+} and Cu^{2+}; Cu^{1+} tends to bind to sulfur-containing ligands such as cysteine, whereas

Cu^{2+} typically binds to nitrogen-containing ligands such as histidine. These chemical properties make copper conducive for electron transfer. Thus, copper is commonly used as a metal cofactor in redox-based reactions within bacterial proteins, such as the membrane-bound cytochrome *bo* oxidase (*cyo*), the membrane-bound phenylethylamine oxidase (*tynA* or *maoA*), and the periplasmic copper/zinc superoxide dismutase (*sodC*). Copper centers are also found in plastocyanin of photosynthetic cyanobacteria [79] and cupredoxin azurin of *Pseudomonas aeruginosa* [2]. In summary, bacteria have taken advantage of the ability of copper to quickly convert from one oxidation state to another.

Many strictly anaerobic and facultative bacteria, including *E. coli*, do not require copper for growth. This is most logically due to the fact that copper is often unavailable in the anoxic habitats in which these microorganisms reside. Although copper is not essential for many bacteria, it is still used in minute amounts. In eukaryotes, Cu^{1+} enters the cytoplasm through Ctr transporters and is handed off immediately to copper chaperones (CCS and Atx1-like proteins), which deliver Cu^{1+} to target enzymes. Ctr transport proteins have not been identified in bacteria. However, copper may possibly enter through other non-specific routes.

Excess intracellular copper is toxic. In eukaryotes, reports show that copper stress stimulates oxidative DNA damage and can deplete glutathione levels, which normally aid in maintaining a reducing cytoplasmic environment [10, 84, 108, 113]. In *E. coli*, excess intracellular copper can displace iron from catalytic exposed [Fe-S] clusters of dehydratases [74]. The released iron atoms can potentially poison the cell by participating in Fenton chemistry, thereby causing further cellular damage. As a

consequence, organisms cannot afford for intracellular copper levels to go beyond what is needed for routine aerobic metabolism.

It is important to note that all known Cu-requiring enzymes in *E. coli* are periplasmic or membrane-bound, which strongly suggests that this organism does not need to import copper into the cytoplasm at all, but does so only inadvertently. Entry of copper into the cytoplasm is sensed by the cytoplasmic protein CueR. When bound to copper, CueR induces the transcription of genes *copA* and *cueO*, which are involved in copper detoxification [96]. CopA is a P-type ATPase cytoplasmic membrane-bound protein that pumps Cu^{1+} from the cytoplasm to the periplasm (Fig. 1.4) [104]. CueO is a multicopper oxidase that oxidizes periplasmic Cu^{1+} to Cu^{2+} (Fig. 1.4) [37, 110]. The oxidation of copper by CueO is thought to slow down re-entry of copper into the cytoplasm.

Excess copper may also accumulate in the periplasm, where it is detected by CusRS, a two-component regulatory system. CusS is a cytoplasmic membrane-bound copper sensor protein, and CusR is a regulatory protein that induces *cusCFBA* when it is phosphorylated by CusS [85, 130]. The CusCFBA system involves four proteins for export of Cu^{1+} from the periplasm: CusA is an inner-membrane H^+ antiporter; CusC is an outer-membrane protein; CusB is a membrane fusion protein that possibly brings CusA and CusC closer together; and CusF is a periplasmic copper-binding protein that delivers Cu^{1+} to CusB (Fig. 1.4) [16].

In summary, bacteria reduce copper toxicity using three mechanisms: (1) compartmentalization of copper-requiring proteins, (2) induction of copper efflux systems, and (3) oxidation of Cu^{1+} to the potentially less toxic Cu^{2+} form. Note that

compartmentalization combined with localized protein folding potentially increases a cell's ability to correctly populate metal-dependent enzymes. Such examples of compartmentalization have been observed in cyanobacteria.

1.3.2 Nickel

Like iron, nickel is mostly inaccessible on Earth as it is typically bound to sulfur atoms and is found in the sediment as a precipitant. Nickel can adopt multiple oxidation states from Ni^0 to Ni^{4+}, with the most common oxidation state being Ni^{2+}. A number of microbial enzymes require nickel as a metal cofactor, including [NiFe] hydrogenase, urease, Ni-superoxide dismutase, carbon monoxide dehydrogenase, acetyl-CoA synthase, acireductone dioxygenase, methyl-CoM reductase, and glyoxylase I [70]. Nickel is coordinated by histidine and/or cysteine residues within these enzymes. Note that aspartate and glutamate can also contribute to the coordination chemistry of nickel.

Nickel is considered an essential micronutrient for anaerobiosis in many bacteria and has been shown to be important for the fitness of pathogenic bacteria, including *E. coli*, *S. enterica*, and *Helicobacter pylori*. *E. coli* imports nickel into the cytoplasm using the ATP-dependent (ABC) importer NikABCDE (Fig. 1.5). In this system, NikA is a soluble periplasmic binding protein that binds nickel and delivers it to the NikBC inner transmembrane pore. NikD and NikE are proteins that bind to and hydrolyze ATP for the translocation of nickel across the inner membrane [88]. Nik homologs have been found in several pathogens, including *Vibrio parahemolyticus, Helicobacter hepaticus, Yersinia,* and *Staphylococcus aureus*. Many bacteria also contain a secondary high-affinity nickel permease from the NiCoT family of transporters. The most prominent

member of this family is HoxN from *Cupriavidus necator*. NiCoT family transporters are able to transfer both nickel and cobalt but may prefer one metal over the other.

Nickel uptake by NikABCDE in *E. coli* is regulated by the nickel-dependent repressor, NikR. This tetrameric protein contains four metal binding sites: two high-affinity Ni^{2+} binding sites that allosterically activate promoter DNA binding and two low-affinity Ni^{2+} binding sites that further enhance DNA binding affinity [20]. Thus, nickel binding to NikR triggers repression of *nikABCDE* transcription (Fig.1.2). This does not completely eliminate nickel entry into the cytoplasm, as nonspecific nickel import can occur through the magnesium importer, CorA, as well as other adventitious transporters (Fig. 1.5) [90].

As with other transition metals, excess nickel is potentially toxic to all organisms, including humans. The mechanism of nickel toxicity in humans involves the oxidation of lipids and proteins [73]. In contrast, less is known about the mechanism of nickel toxicity in microorganisms, despite the immense amount of research that shows its harmful effects. Only recently has the presence of excess nickel in bacteria been shown to inhibit the function of several iron-dependent deoxygenases and zinc metallopeptidases [73]. It is hypothesized that nickel inhibits these enzymes by displacing the essential metal cofactor from the active site or by binding to an allosteric site. Nickel has also been shown to interfere with the function of several non-metal enzymes that contain catalytic cysteine residues [72, 73]. In summary, nickel homeostasis is a general biological concern for all organisms.

When nickel levels rise above that needed, some bacteria will induce the membrane-bound efflux system RcnA, which pumps nickel and cobalt out of the

cytoplasm (Fig. 1.5) [61, 68, 105]. Transcription of *rcnA* is repressed by the RcnR regulator. Increasing concentrations of nickel or cobalt release repression by RcnR [58, 60]. The transcription of *rcnR* is repressed by itself in addition to Fur:Fe^{2+} [68]. What's more puzzling is that iron supplementation induces *rcnR* transcription even the absence of *fur*, which suggests that RcnR may respond to intracellular iron concentration [68].

Unlike other transition metals, the surplus of nickel is sensed by two independent regulators, NikR and RcnR. NikR:Ni^{2+} represses import whereas RcnR:Ni^{2+} allows export of nickel. NikR ($K_d \leq 1$ pM) and RcnR ($K_{app} < 26$ nM) have relatively similar nickel-binding affinities [59]. Thus, these regulators likely compete for nickel at low concentrations. This might explain why there is very little evidence of nickel deficiency or toxicity in bacteria.

1.3.3 Zinc

Zinc is an essential trace element for all organisms. It is required for activity of many enzymes, including the metallopeptidase FtsH and the alcohol dehydrogenase GS-FDH [44, 117]. Zinc is also present in structurally important sites, like zinc-fingers. Some zinc finger proteins are significant for metabolic regulation.

Unlike other transition metals, zinc is only a moderately reactive metal and does not participate in redox reactions. The lack of redox activity makes zinc favorable for use in redox reactions that require a stable metal cofactor, such as PerR and [Cu/Zn]-SOD. Zinc functions as a Lewis acid to accept a pair of electrons in these reactions [127]. Contrary to popular belief, zinc does not preferentially coordinate with oxygen, nitrogen, or sulfur atoms. In proteins, zinc is typically coordinated by several different amino acid

residues, including aspartate, glutamate, histidine, and cysteine. Furthermore, all ligand geometries formed by zinc are equally stable, since zinc has a completely filled *d*-orbital [53]. Thus, these chemical properties make zinc conducive for (1) participating in chemical catalysis and for (2) maintaining protein structure and stability.

Bacteria import zinc into the cytoplasm using the high-affinity ATP-dependent (ABC) transport system ZnuABC (Fig. 1.6). In this system ZnuA is a soluble periplasmic binding protein that binds zinc and delivers it to the membrane permease ZnuB. The ZnuC protein binds to and hydrolyzes ATP for the translocation of zinc across the inner membrane [47]. During zinc scarcity, a second low-affinity transporter ZupT may also be critical for zinc import (Fig. 1.5). Experiments indicate that a proton motive force may be needed for ZupT-mediated metal uptake [115]. It was also shown that other metal cations may be accidently imported by ZupT.

Zinc uptake by ZnuABC in *E. coli* is regulated by the zinc-dependent Fur family repressor, Zur (ZnuR). In the presence of excess zinc, Zur:Zn^{2+} binds DNA and prevents transcription of *znuABC*. In contrast, derepression of *znuABC* is observed when cells are starved for zinc [99]. The apparent affinity of Zur for Zn^{2+} is about 1×10^{-4} pM, which suggests strict control of zinc import and gives rise to the possibility that free intracellular zinc is toxic [94].

In fact, the high affinity of zinc for sulfhydryl groups can promote toxicity by blocking essential cellular processes. One study showed that low doses of zinc led to the inactivation of fumarase A, a member of the dehydratase family, by displacing iron from the exposed iron-sulfur cluster [129]. Zinc also seems to bind and inactivate mononuclear *E. coli* enzymes during oxidative stress (Mianzhi Gu, unpublished data).

Thus, it is most favorable for organisms to maintain zinc concentrations within narrow limits that will keep zinc-requiring proteins active, yet won't inhibit proteins that require active-site thiols for activity.

Storage proteins may possibly play a role in the management of excess zinc, since researchers have found that zinc is stored in metallothionein SmtA of cyanobacteria. Storage of zinc is thought to be advantageous in niches in which zinc concentrations change abruptly and frequently [15]. Note that storage is not a major mechanism used by bacteria to maintain zinc homeostasis.

Export systems (ZntA and Czc-like transporters) are more commonly used to remove surplus zinc. The ZntA protein is a P-type ATPase whose synthesis is activated by ZntR during periods of zinc abundance (1.7) [14, 17, 123]. *E. coli* also encode two other putative zinc efflux pumps, ZitB and FieF (formerly YiiP). Both exporters are members of the CDF family of transporters and have been shown to transport other metal cations. Furthermore, their regulation is not well characterized. Thus, only speculation can be made about their physiological role.

1.4 INTRACELLULAR METAL TRAFFICKING

1.4.1 How is mismetallation avoided?

Intracellular metal concentration or metal availability is greatly influenced by the niche in which microorganisms dwell. In aerobic habitats, metal availability is dictated by the presence of oxygen and the distribution of organic complexes. By contrast, pH may be the primary determinant of metal availability in anoxic environments. This is especially true for iron. Its availability on Earth has declined tremendously over the past

4 billion years with the emergence of photosynthesis which gave rise to oxygen. In aerobic (oxic) environments, iron is sparingly soluble and extremely scarce, where as in anaerobic (anoxic) conditions iron is more soluble and available. Note that small environmental changes can alter the composition of bioavailable metals, which may be deleterious to microorganisms. Thus, microorganisms are constantly under pressure to maintain metal homeostasis in order to survive.

Metal homeostasis in microorganisms is dictated by the balance of metal transporters which are regulated by metal-responsive regulatory proteins as described above in previous sections. Each bacterial species possesses a different complement of transporters and regulators that handle the various metals required for metabolism. Bacteria also use regulatory proteins to control the number of proteins available for some metals. For example, MnSOD is up-regulated by derepression of Fur protein when iron is scarce, while FeSOD is down-regulated. Minimizing certain metal-dependent proteins lessens the metal demand and allows essential metal-dependent enzymes to remain active, thereby permitting proliferation of the organism.

Even with these systems in place, many of these proteins will still fail to select the correct metal. In fact, many enzymes can bind the wrong metal with high avidity as predicted from the Irving-William series ($Mn^{2+} < Fe^{2+} < Co^{2+} < Ni^{2+} < Cu^{2+} > Zn^{2+}$). For example, the mononuclear enzyme ribulose-5-phosphate epimerase binds zinc more tightly than it does iron, which prevents catalytic turnover [112]. Even metal-responsive regulatory, import, and export proteins have difficulty discerning metal ions, and they are the first line of defense against intracellular metal toxicity. Thus, how do bacteria

overcome these challenges of imperfect metal selection and maximize metal specificity once metal ions are imported?

In summary, bacteria can establish metal specificity and correctly populate metal-dependent proteins using several mechanisms: (1) regulating metal pools by excluding or permitting metal entry into the cell; (2) regulating the expression of metal-dependent proteins; and (3) compartmentalization of metals and metal-requiring proteins. In some cases, bacteria have been observed to use metal delivery and accessory proteins to facilitate correct metal insertion into metal-requiring proteins.

1.4.2 Metal insertion by delivery proteins

Once imported, metals must be delivered to their cognate proteins, but how cells accomplish this remains unclear. There is only minimal understanding of how copper and nickel are trafficked *in vivo,* and we are definitely clueless when it comes to iron and manganese. Only a few metal chaperones have been identified, including the well-studied Atx1-like eukaryotic copper chaperone CCS and the nickel chaperone HypA. These chaperones are required for *in vivo* metal delivery to relevant copper- or nickel-dependent proteins.

To date, researchers have only identified one Atx1-like bacterial copper chaperone, designated CopZ in *B. subtilis*, *Enterococcus hirae*, and *Lactococcus lactis* [75, 103]. The cytosolic CopZ protein shuttles cytoplasmic Cu^{1+} to CopA for export into the periplasm [111]. *In vitro*, CopZ can also interact with the CopY copper repressor, which regulates the *cop* operon [21]. Identification of copper chaperones suggests the

possibility that all organisms possess the capacity to prevent inappropriate copper interactions with other cellular proteins by transporting it in designated vehicles.

HypA-type nickel chaperones are present in every organism that encodes a [NiFe]-hydrogenase. *E. coli* contains four hydrogenases, each of which are synthesized in response to different physiological conditions and are thought to require nickel for function. The maturation of *E. coli* hydrogenases requires several nickel chaperones: HypA, HypF, HypB, and SlyD. It is postulated that these chaperones work collectively to deliver nickel to the hydrogenase after delivery of iron by other accessory proteins. HypA or its homologue HypF is thought to form a heterodimer with HypB and together generate a nickel scaffold. SlyD has been shown to interact with HypB and transfers Ni^{2+} to it [65, 133]. Although SlyD can interact with several metal cations [128], its expression is only influenced by intracellular Ni^{2+}, since Ni^{2+} binding increases its stability [50, 64]. HypA and HypB have also been shown to deliver nickel to the enzyme urease in *H. pylori* [92].

A putative zinc chaperone YodA has also recently been identified in *E. coli*. YodA is predicted to be regulated by Zur [48]. *yodA* is also induced by cadmium, SoxS, and Fur [102]. Furthermore, it is unclear whether YodA is a true zinc chaperone, since several different metal binding forms are observed for the crystal structure of YodA, i.e. it can bind other metals [24]. If YodA is a zinc chaperone, then metal promiscuity could elicit a potential problem for the cell, as mismetallation of target proteins could be bacteriostatic.

In summary, metal chaperones have been identified in bacteria that bind to and direct copper, nickel, and possibly zinc to metal-dependent enzymes. It is not surprising

to find metal chaperones for these three metals, as they have high ligand-binding affinities and without a chaperone these metals would stick to adventitious ligands.

1.4.3 Trafficking of iron and manganese

It is well-known that *E. coli* stores excess iron in Dps, bacteroferritin and ferritin for protection against ROS or as a source to be drawn upon during periods of iron scarcity, but how iron is delivered and retrieved from these storage proteins is still unknown. In general, very little is known about how iron is trafficked once imported into cells.

Over the past several years, researchers have speculated that proteins such as YggX, YaaA, and CyaY (frataxin homolog) could be iron carriers that are involved in iron trafficking [40, 71, 116, 121]. More recent hypotheses have included the involvement of small proteins of less than 50 amino acids as modulators of metal delivery to larger proteins for activation. There are roughly 60 small proteins that have been identified to date in both Gram-positive and Gram-negative bacteria [51]. One group has shown that the *B. subtilis* small protein FbpC (29 aa) assists the function of the small regulatory RNA FsrA in the iron-sparing response [31]. The physiological roles of these proteins still remains questionable and more definitive experiments are needed.

To date, only one manganese chaperone (MntS) has been proposed to assist *E. coli* and is encoded within the *rybA* gene. MntS encodes a novel small protein of 42 amino acids [124]. Its expression is regulated by MntR in response to high manganese, which suggests that it may be involved in manganese homeostasis. Furthermore, *E. coli*

cells overexpressing MntS are sensitive to manganese but not to other divalent metal cations [124].

1.5 SCOPE OF THIS THESIS

1.5.1 What is the physiological role of the alternative *Escherichia coli* aerobic ribonucleotide reductase, NrdEF?

Ribonucleotide reductases (RNRs) catalyze the *de novo* synthesis of deoxyribonucleotides, the precursors for DNA synthesis and repair in all organisms. *E. coli* encodes two iron-dependent RNRs: NrdDG and NrdAB. NrdDG is essential for anaerobic growth and it is not active aerobically. In contrast, NrdAB is essential for the routine aerobic growth of *Escherichia coli*. By sequence homology to NrdAB, a second aerobic RNR was identified: NrdEF. The role of NrdEF is not apparent. It is not functional under standard aerobic growth conditions, since a Δ*nrdAB* mutant cannot replicate its DNA. However, H_2O_2 was shown to strongly induce *nrdEF* [82]. Since H_2O_2 inactivates some mononuclear enzymes by oxidizing iron, I hypothesized that (i) NrdAB function is inhibited by H_2O_2 and that (ii) *nrdEF* is induced to compensate.

H_2O_2 might plausibly inhibit NrdAB by reacting directly with the di-iron center in the R2 subunit through Fenton chemistry, thereby damaging the polypeptide or preventing the formation of the essential tyrosyl radical (Fig. 1.7). H_2O_2 might also inhibit NrdAB indirectly through Fenton chemistry by limiting the pool of iron, thereby preventing metallation of NrdAB. In fact, several studies indicated that superoxide and H_2O_2 can inhibit NrdAB function *in vitro* by more than 55 % [29, 32, 107]. Hristova and coworkers (2008) also observed lower NrdAB activity in crude extracts compared to purified enzyme and proposed that the decreased activity resulted from oxidation of the

NrdAB tyrosyl radical by unknown small molecules/proteins present in the crude extract. Furthermore, recent *in vitro* studies have shown that the 2Fe-2S cluster ferredoxin protein in *E. coli*, YfaE, can help convert the non-radical diferrous form of NrdB back to its active form containing the tyrosyl radical stress [52]. The exact mechanism of reactivation remains unknown. Taken together, these data indicate that the *E. coli* NrdAB may be inherently unstable in the presence of ROS. If this were true, then it would be advantageous for cells to possess a second aerobic RNR that is resistant to ROS and can offset the failure of NrdAB.

Although the leading literature states that the *E. coli* NrdEF is active with iron, I wondered whether NrdEF might use another metal cofactor for activation. Researchers have shown that manganese increases the expression of the *Corynebacterium ammoniagenese* NrdEF and that the *Chlamydia trachomatis* NrdEF uses a mixed manganese/iron metal cofactor for activation, making it resistant to millimolar H_2O_2 [62, 118, 122]. Since the *E. coli* NrdEF and the manganese transporter, MntH, are both induced during H_2O_2 stress [8, 82], I speculated that NrdEF might be resistant to H_2O_2 stress because it uses manganese, as opposed to iron, as a metal cofactor for activation.

1.5.2 What is the physiological role of the *Escherichia coli* small protein, MntS?

Iron is involved in many cellular processes and is essential for almost all organisms. However, it is sometimes scarce in the contemporary aerobic world due to oxidation. When *E. coli* is deficient in iron or stressed by hydrogen peroxide, it uses manganese rather than iron to populate mononuclear enzymes. When iron becomes available, excess manganese is exported out of the cell through the efflux pump, MntP. It

is unclear how these cells traffic intracellular manganese to these enzymes, since cells maintain manganese at concentrations below those of most other metals. The recent identification and characterization of the novel manganese homeostasis gene, *mntS*, sparked our interest in how cells get manganese to metalloproteins when it is needed.

The *mntS* RNA encodes an extremely small protein of 42 amino acids, the expression of which is repressed by the transcriptional regulator, MntR, in response to high intracellular manganese levels [124]. Furthermore, the MntS protein contains several residues that have been shown in other proteins to bind manganese. Taken together with its small size, these features suggest that MntS might act as chaperone that makes manganese more available to proteins. This study attempts to identify the role of *mntS* in *E. coli* and to further our understanding of how bacteria might use small proteins to facilitate intracellular metal delivery.

1.6 FIGURES

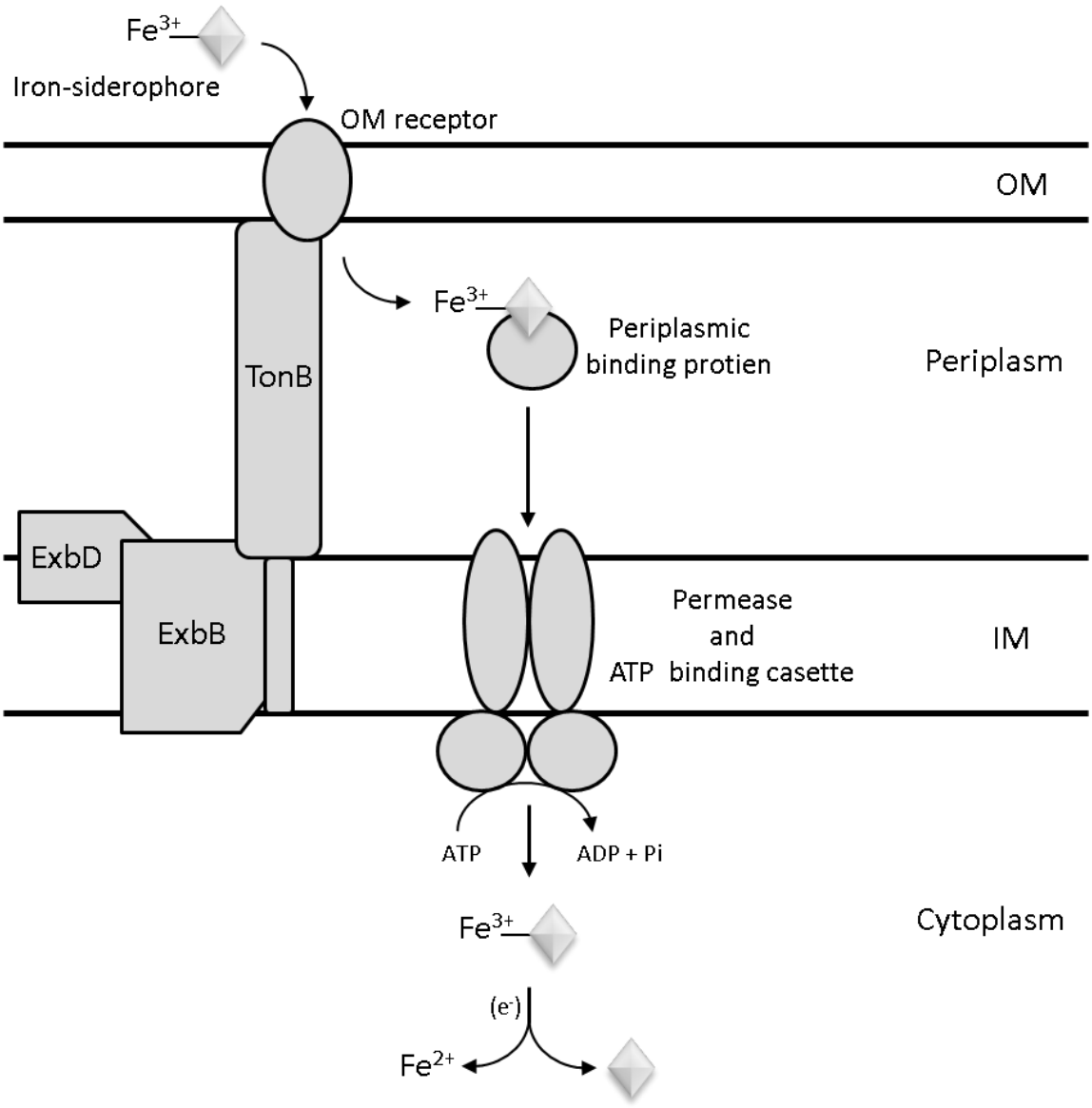

Figure 1.1. Schematic representation of siderophore-mediated iron uptake in *E. coli*.

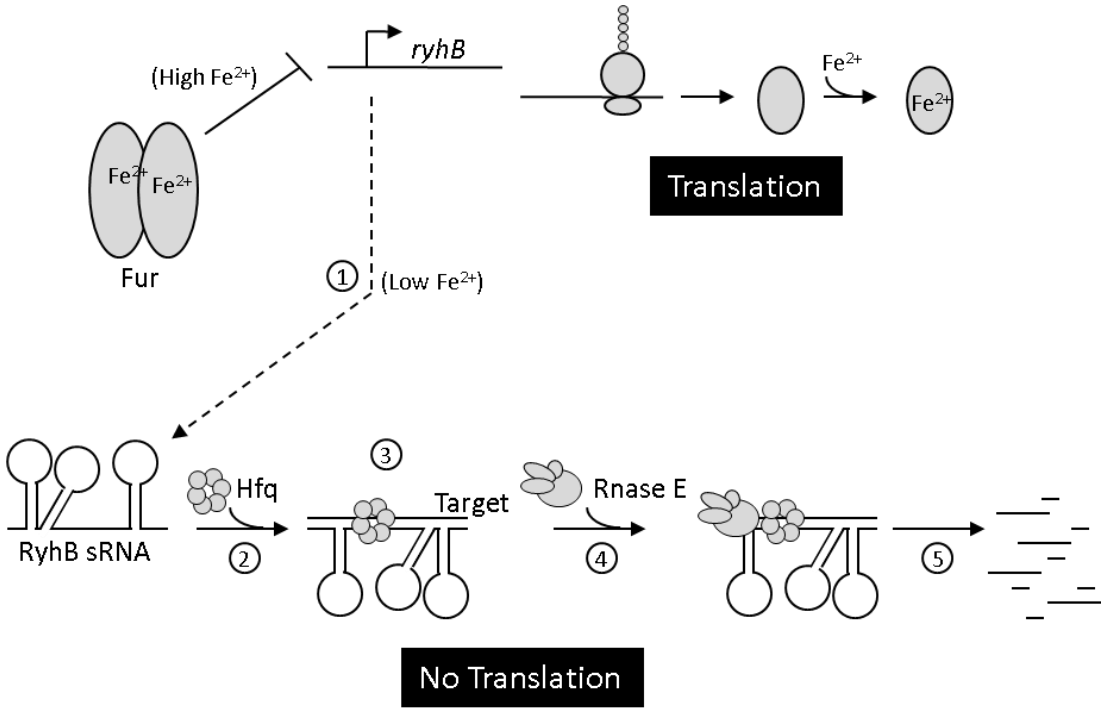

Figure 1.2. Mechanism of RyhB during iron starvation; (1) Fur inactivation leads to RyhB expression, (2) RyhB is stabilized by the RNA chaperone Hfq, (3) sRNA RyhB pairs with mRNA target and blocks translation, (4) RNase E degradasome is recruited, and (5) sRNA-mRNA target complex is degraded.

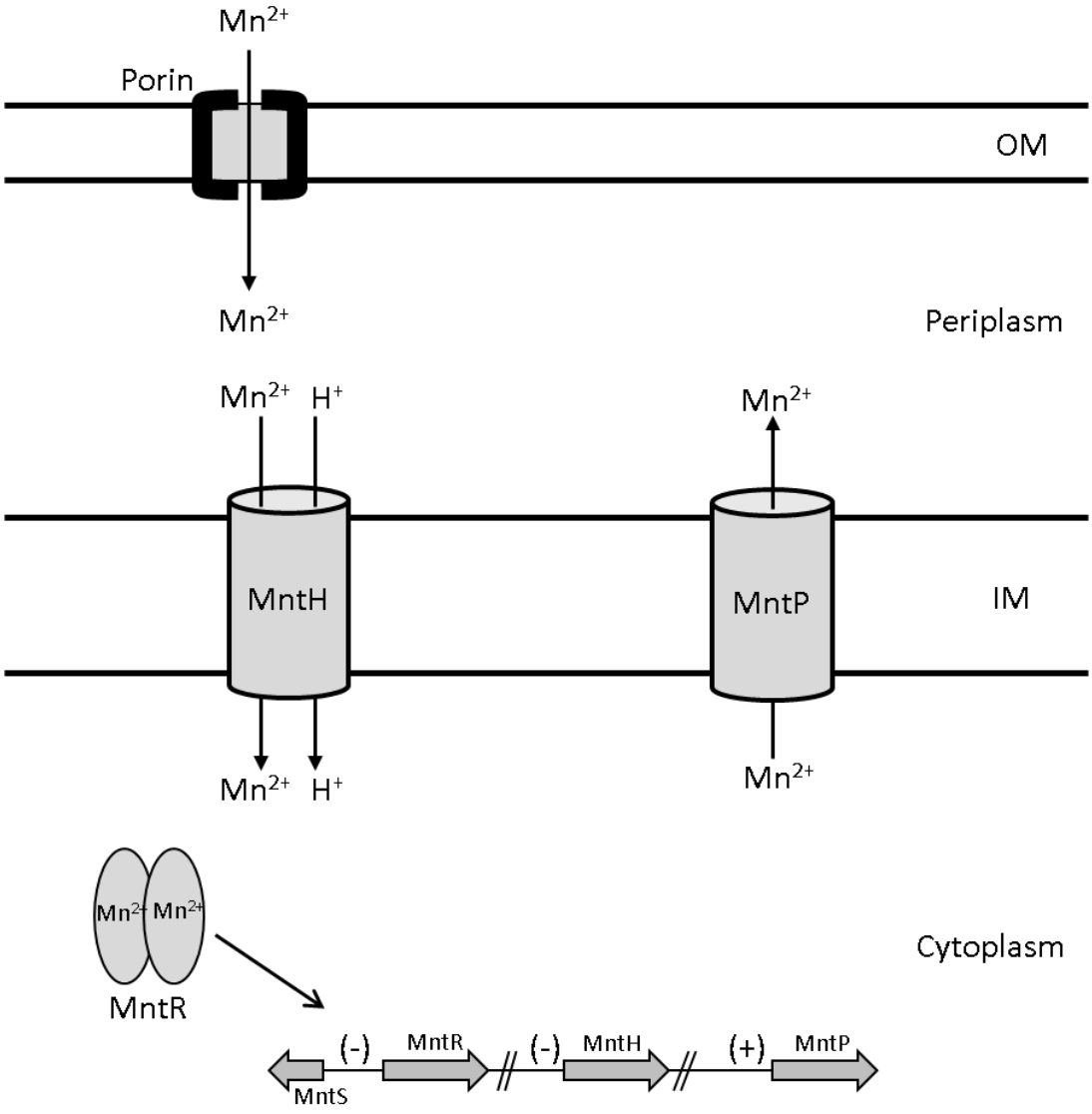

Figure 1.3. Manganese resistance proteins in *E. coli* and their proposed functions.

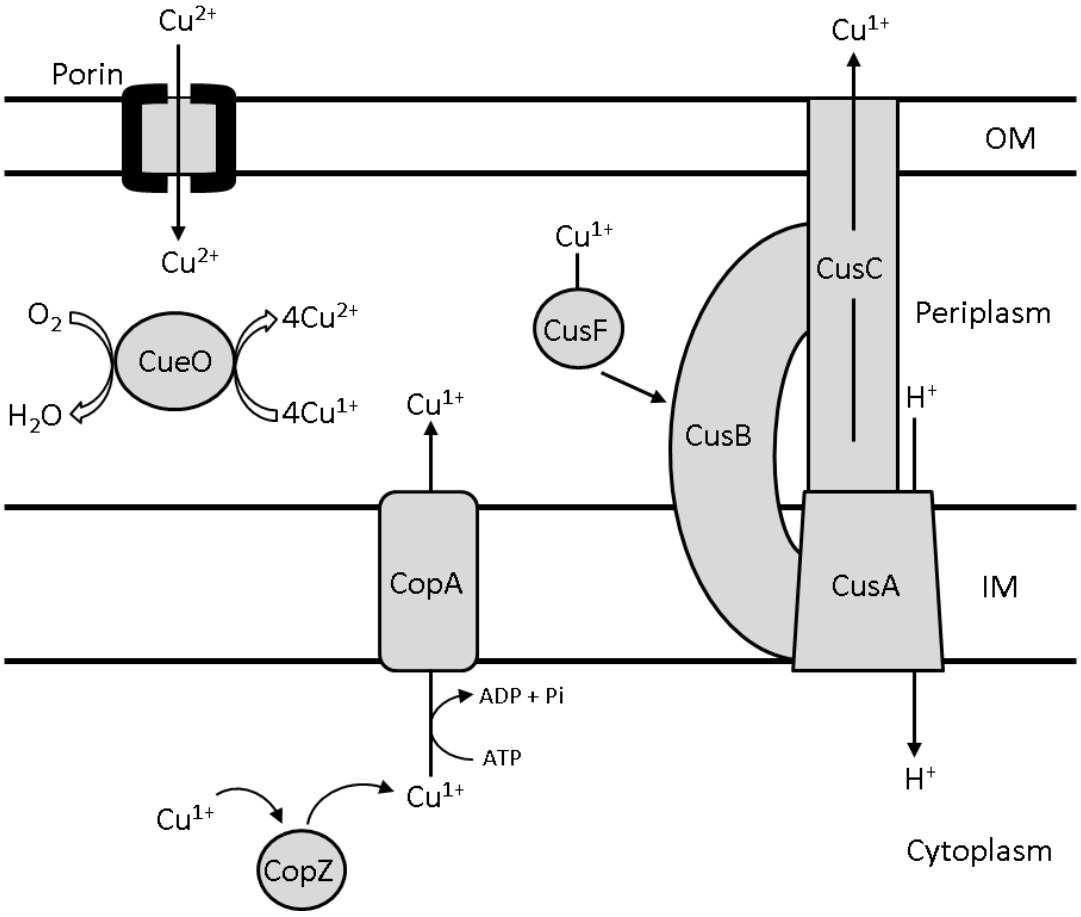

Figure 1.4. Copper resistance proteins in bacteria and their proposed functions.

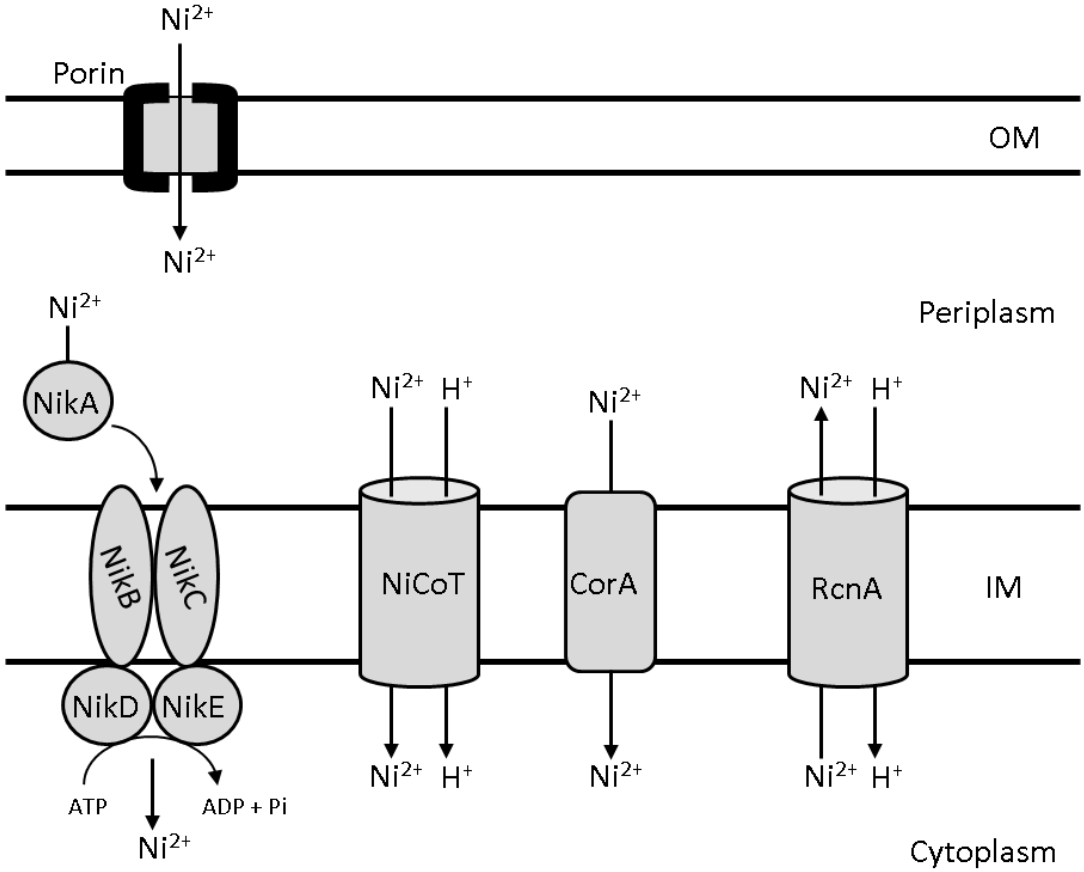

Figure 1.5. Nickel uptake and efflux proteins in bacteria and their proposed functions.

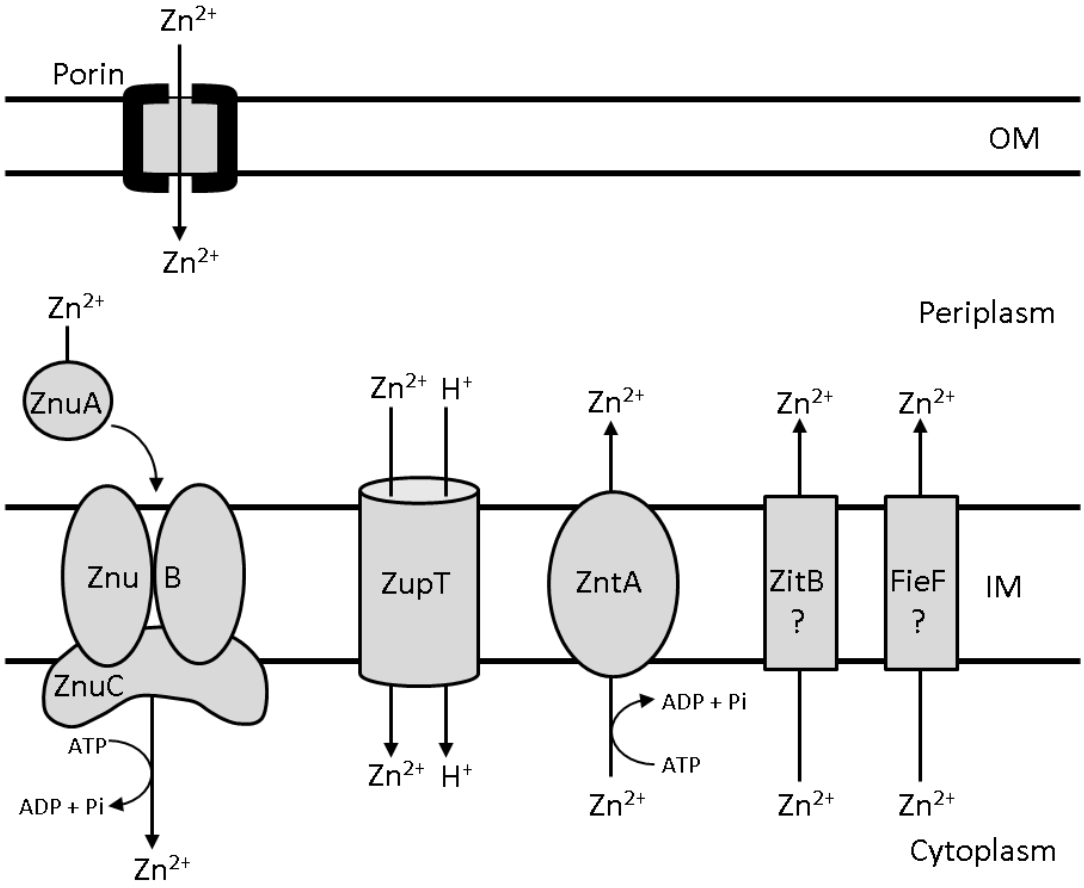

Figure 1.6. Zinc uptake and efflux proteins in *E. coli* and their proposed functions.

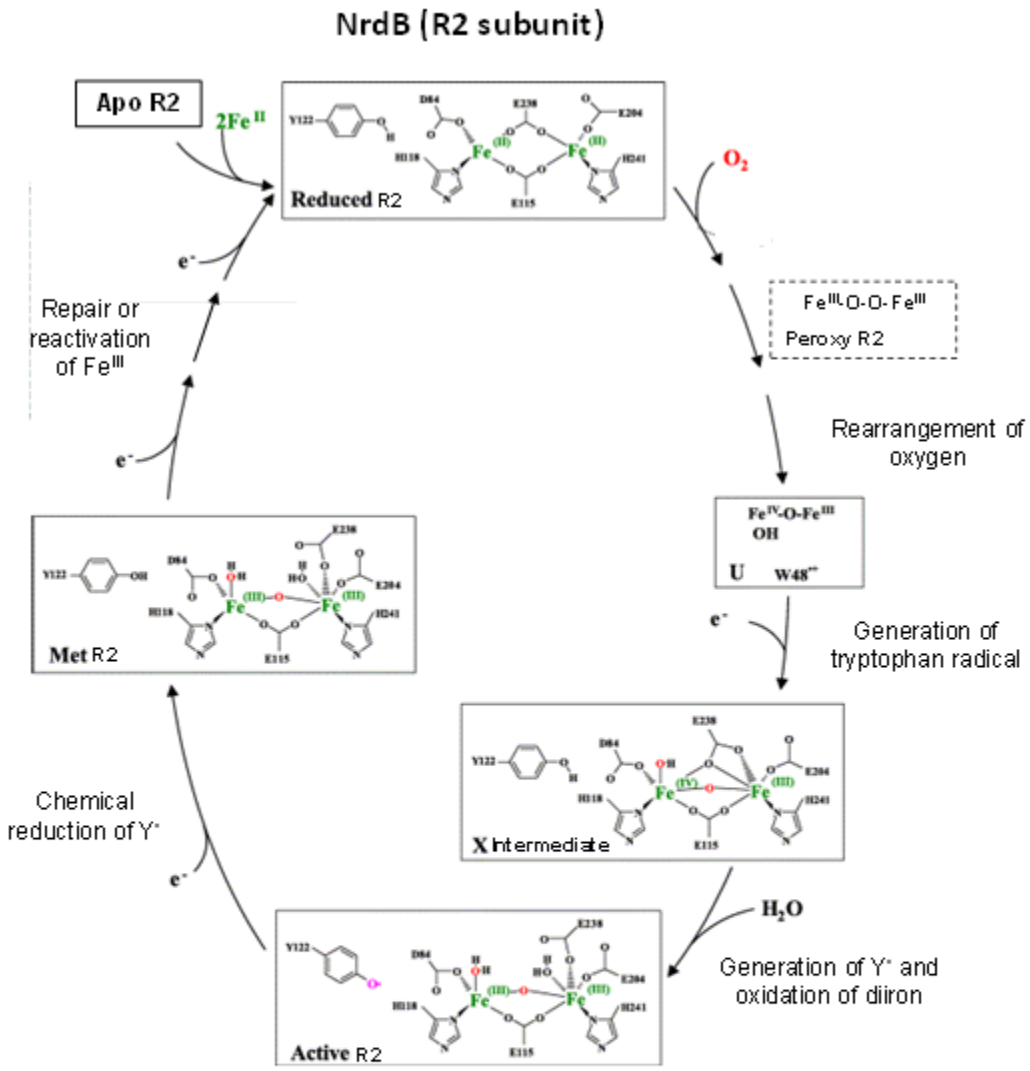

Figure 1.7. Possible iron-oxygen activation states of the *E. coli* NrdAB, R2 subunit. Iron (Fe) is loaded into apo R2 by an unknown mechanism generating reduced R2. Oxygen binds to the reduced iron center and through a series of intermediates generates active R2 containing the tyrosine radical. MetR2 may be alternately formed from reduced R2 during H_2O_2 stress. MetR2 also acts as an intermediate during repair or reactivation of R2.

1.7 REFERENCES

1. **Abdul-Tehrani, H., A. J. Hudson, Y. S. Chang, A. R. Timms, C. Hawkins, J. M. Williams, P. M. Harrison, J. R. Guest, and S. C. Andrews.** 1999. Ferritin mutants of *Escherichia coli* are iron deficient and growth impaired, and fur mutants are iron deficient. J. Bacteriol. **181:**1415-1428.

2. **Adman, E. T.** 1991. Copper protein structures. Adv. Protein Chem. **42:**145-197.

3. **Afonyushkin, T., B. Vecerek, I. Moll, U. Blasi, and V. R. Kaberdin.** 2005. Both RNase E and RNase III control the stability of *sodB* mRNA upon translational inhibition by the small regulatory RNA RyhB. Nucleic Acids Res. **33:**1678-1689.

4. **Anbar, A. D.** 2008. Oceans. Elements and evolution. Science. **322:**1481-1483.

5. **Andrews, S. C.** 1998. Iron storage in bacteria. Adv. Microb. Physiol. **40:**281-351.

6. **Andrews, S. C., A. K. Robinson, and F. Rodriguez-Quinones.** 2003. Bacterial iron homeostasis. FEMS Microbiol. Rev. **27:**215-237.

7. **Anjem, A., and J. A. Imlay.** 2012. Mononuclear iron enzymes are primary targets of hydrogen peroxide stress. J. Biol. Chem. **287:**15544-15556.

8. **Anjem, A., S. Varghese, and J. A. Imlay.** 2009. Manganese import is a key element of the OxyR response to hydrogen peroxide in *Escherichia coli*. Mol. Microbiol. **72:**844-858.

9. **Archibald, F.** 1983. *Lactobacillus plantarum*, an organism not requiring iron. FEMS Microbiology Letters. **19:**29-32.

10. **Arciello, M., G. Rotilio, and L. Rossi.** 2005. Copper-dependent toxicity in SH-SY5Y neuroblastoma cells involves mitochondrial damage. Biochem. Biophys. Res. Commun. **327:**454-459.

11. **Barford, D.** 1996. Molecular mechanisms of the protein serine/threonine phosphatases. Trends Biochem. Sci. **21:**407-412.

12. **Becker, A., I. Schlichting, W. Kabsch, D. Groche, S. Schultz, and A. F. Wagner.** 1998. Iron center, substrate recognition and mechanism of peptide deformylase. Nat. Struct. Biol. **5:**1053-1058.

13. **Bellini, P., and A. M. Hemmings.** 2006. In vitro characterization of a bacterial manganese uptake regulator of the Fur superfamily. Biochemistry. **45:**2686-2698.

14. **Binet, M. R., and R. K. Poole.** 2000. Cd(II), Pb(II) and Zn(II) ions regulate expression of the metal-transporting P-type ATPase ZntA in *Escherichia coli*. FEBS Lett. **473:**67-70.

15. **Blindauer, C. A., M. D. Harrison, A. K. Robinson, J. A. Parkinson, P. W. Bowness, P. J. Sadler, and N. J. Robinson.** 2002. Multiple bacteria encode metallothioneins and SmtA-like zinc fingers. Mol. Microbiol. **45:**1421-1432.

16. **Boal, A. K., and A. C. Rosenzweig.** 2009. Structural biology of copper trafficking. Chem. Rev. **109:**4760-4779.

17. **Brocklehurst, K. R., J. L. Hobman, B. Lawley, L. Blank, S. J. Marshall, N. L. Brown, and A. P. Morby.** 1999. ZntR is a Zn(II)-responsive MerR-like transcriptional regulator of *zntA* in *Escherichia coli*. Mol. Microbiol. **31:**893-902.

18. **Chai, S. C., W. L. Wang, and Q. Z. Ye.** 2008. Fe(II) is the native cofactor for *Escherichia coli* methionine aminopeptidase. J. Biol. Chem. **283:**26879-26885.

19. **Chander, M., B. Setlow, and P. Setlow.** 1998. The enzymatic activity of phosphoglycerate mutase from gram-positive endospore-forming bacteria requires Mn2+ and is pH sensitive. Can. J. Microbiol. **44:**759-767.

20. **Chivers, P. T., and R. T. Sauer.** 2002. NikR repressor: high-affinity nickel binding to the C-terminal domain regulates binding to operator DNA. Chem. Biol. **9:**1141-1148.

21. **Cobine, P., W. A. Wickramasinghe, M. D. Harrison, T. Weber, M. Solioz, and C. T. Dameron.** 1999. The *Enterococcus hirae* copper chaperone CopZ delivers copper(I) to the CopY repressor. FEBS Lett. **445:**27-30.

22. **Coves, J., B. Delon, I. Climent, B. M. Sjoberg, and M. Fontecave.** 1995. Enzymic and chemical reduction of the iron center of the *Escherichia coli* ribonucleotide reductase protein R2. The role of the C-terminus. Eur. J. Biochem. **233:**357-363.

23. **Coy, M., and J. B. Neilands.** 1991. Structural dynamics and functional domains of the fur protein. Biochemistry. **30:**8201-8210.

24. **David, G., K. Blondeau, M. Schiltz, S. Penel, and A. Lewit-Bentley.** 2003. YodA from *Escherichia coli* is a metal-binding, lipocalin-like protein. J. Biol. Chem. **278:**43728-43735.

25. **Desnoyers, G., A. Morissette, K. Prevost, and E. Masse.** 2009. Small RNA-induced differential degradation of the polycistronic mRNA *iscRSUA*. EMBO J. **28:**1551-1561.

26. **Diaz-Mireles, E., M. Wexler, G. Sawers, D. Bellini, J. D. Todd, and A. W. Johnston.** 2004. The Fur-like protein Mur of *Rhizobium leguminosarum* is a Mn(2+)-responsive transcriptional regulator. Microbiology. **150:**1447-1456.

27. **Earhart, C.** 1996. Uptake and metabolism of iron and molybdenum. In: *E. coli* and *Salmonella*. Cellular and molecular biology, p. 1075-1090. *In* F. C. Neidhardt (ed.), , 2nd ed., . ASM press, Washington, DC.

28. **Escolar, L., J. Perez-Martin, and V. de Lorenzo.** 1999. Opening the iron box: transcriptional metalloregulation by the Fur protein. J. Bacteriol. **181:**6223-6229.

29. **Fontecave, M., A. Graslund, and P. Reichard.** 1987. The function of superoxide dismutase during the enzymatic formation of the free radical of ribonucleotide reductase. J. Biol. Chem. **262:**12332-12336.

30. **Fridovich, I.** 1995. Superoxide radical and superoxide dismutase. Annual Review of Biochemistry. **64:**97-112.

31. **Gaballa, A., H. Antelmann, C. Aguilar, S. K. Khakh, K. B. Song, G. T. Smaldone, and J. D. Helmann.** 2008. The *Bacillus subtilis* iron-sparing response is mediated by a Fur-regulated small RNA and three small, basic proteins. Proc. Natl. Acad. Sci. U. S. A. **105:**11927-11932.

32. **Gaudu, P., V. Niviere, Y. Petillot, B. Kauppi, and M. Fontecave.** 1996. The irreversible inactivation of ribonucleotide reductase from *Escherichia coli* by superoxide radicals. FEBS Lett. **387:**137-140.

33. **Geissmann, T. A., and D. Touati.** 2004. Hfq, a new chaperoning role: binding to messenger RNA determines access for small RNA regulator. EMBO J. **23:**396-405.

34. **Giedroc, D. P., and A. I. Arunkumar.** 2007. Metal sensor proteins: nature's metalloregulated allosteric switches. Dalton Trans. **(29):**3107-3120.

35. **Grass, G., B. Fan, B. P. Rosen, S. Franke, D. H. Nies, and C. Rensing.** 2001. ZitB (YbgR), a member of the cation diffusion facilitator family, is an additional zinc transporter in *Escherichia coli*. J. Bacteriol. **183:**4664-4667.

36. **Grass, G., M. Otto, B. Fricke, C. J. Haney, C. Rensing, D. H. Nies, and D. Munkelt.** 2005. FieF (YiiP) from *Escherichia coli* mediates decreased cellular accumulation of iron and relieves iron stress. Arch. Microbiol. **183:**9-18.

37. **Grass, G., and C. Rensing.** 2001. CueO is a multi-copper oxidase that confers copper tolerance in *Escherichia coli*. Biochem. Biophys. Res. Commun. **286:**902-908.

38. **Grosse, C., J. Scherer, D. Koch, M. Otto, N. Taudte, and G. Grass.** 2006. A new ferrous iron-uptake transporter, EfeU (YcdN), from *Escherichia coli*. Mol. Microbiol. **62:**120-131.

39. **Groves, J. T., R. C. Haushalter, M. Nakamura, T. E. Nemo, and B. J. Evans.** 1981. High-valent iron-porphyrin complexes related to peroxidases and chytochrome P-450. J. Amer. Chem. Soc. **103:**2884-2886.

40. **Gu, M., and J. A. Imlay.** 2011. The SoxRS response of *Escherichia coli* is directly activated by redox-cycling drugs rather than by superoxide. Mol. Microbiol. **79:**1136-1150.

41. **Gu, M., and J. A. Imlay.** 2013. Superoxide poisons mononuclear iron enzymes by causing mismetallation. Mol. Microbiol.

42. **Guedon, E., and J. D. Helmann.** 2003. Origins of metal ion selectivity in the DtxR/MntR family of metalloregulators. Mol. Microbiol. **48:**495-506.

43. **Guedon, E., C. M. Moore, Q. Que, T. Wang, R. W. Ye, and J. D. Helmann.** 2003. The global transcriptional response of *Bacillus subtilis* to manganese involves the MntR, Fur, TnrA and sigmaB regulons. Mol. Microbiol. **49:**1477-1491.

44. **Gutheil, W. G., B. Holmquist, and B. L. Vallee.** 1992. Purification, characterization, and partial sequence of the glutathione-dependent formaldehyde dehydrogenase from *Escherichia coli*: a class III alcohol dehydrogenase. Biochemistry. **31:**475-481.

45. **Hantke, K., and V. Braun.** 1998. Control of bacterial iron transport by regulatory proteins, p. 11-44. *In* S. Silver and W. Walden (eds.), Metal ions in gene regulation. Chapman and Hall, New York.

46. **Hantke, K.** 1987. Selection procedure for deregulated iron transport mutants (fur) in *Escherichia coli* K-12: Fur not only affects iron metabolism. Mol. Gen. Genet. **210:**135-139.

47. **Hantke, K.** 2001. Bacterial zinc transporters and regulators. Biometals. **14:**239-249.

48. **Hantke, K.** 2005. Bacterial zinc uptake and regulators. Curr. Opin. Microbiol. **8:**196-202.

49. **Hao, Z., S. Chen, and D. B. Wilson.** 1999. Cloning, expression, and characterization of cadmium and manganese uptake genes from *Lactobacillus plantarum*. Appl. Environ. Microbiol. **65:**4746-4752.

50. **Haupt, C., U. Weininger, M. Kovermann, and J. Balbach.** 2011. Local and coupled thermodynamic stability of the two-domain and bifunctional enzyme SlyD from *Escherichia coli*. Biochemistry. **50:**7321-7329.

51. **Hobbs, E. C., F. Fontaine, X. Yin, and G. Storz.** 2011. An expanding universe of small proteins. Curr. Opin. Microbiol. **14:**167-173.

52. **Hristova, D., C. H. Wu, W. Jiang, C. Krebs, and J. Stubbe.** 2008. Importance of the maintenance pathway in the regulation of the activity of *Escherichia coli* ribonucleotide reductase. Biochemistry. **47:**3989-3999.

53. **Huheey, J. E., E. A. Keiter, and R. L. Keiter.** 1993. Inorganic Chemistry: principles of structure and reactivity. Harper Collins College Publishers, New York.

54. **Huynen, M. A., B. Snel, P. Bork, and T. J. Gibson.** 2001. The phylogenetic distribution of frataxin indicates a role in iron-sulfur cluster protein assembly. Hum. Mol. Genet. **10:**2463-2468.

55. **Ikeda, J. S., A. Janakiraman, D. G. Kehres, M. E. Maguire, and J. M. Slauch.** 2005. Transcriptional regulation of sitABCD of *Salmonella enterica* serovar Typhimurium by MntR and Fur. J. Bacteriol. **187:**912-922.

56. **Imlay, J. A.** 2006. Iron-sulphur clusters and the problem with oxygen. Mol. Microbiol. **59:**1073-1082.

57. **Irving, H., and R. J. P. Williams.** 1953. 637. The stability of transition-metal complexes. Journal of the American Chemical Society (Resumed). 3192-3210.

58. **Iwig, J. S., and P. T. Chivers.** 2009. DNA recognition and wrapping by *Escherichia coli* RcnR. J. Mol. Biol. **393:**514-526.

59. **Iwig, J. S., and P. T. Chivers.** 2010. Coordinating intracellular nickel-metal-site structure-function relationships and the NikR and RcnR repressors. Nat. Prod. Rep. **27:**658-667.

60. **Iwig, J. S., S. Leitch, R. W. Herbst, M. J. Maroney, and P. T. Chivers.** 2008. Ni(II) and Co(II) sensing by *Escherichia coli* RcnR. J. Am. Chem. Soc. **130:**7592-7606.

61. **Iwig, J. S., J. L. Rowe, and P. T. Chivers.** 2006. Nickel homeostasis in *Escherichia coli* - the *rcnR-rcnA* efflux pathway and its linkage to NikR function. Mol. Microbiol. **62:**252-262.

62. **Jiang, W., J. Xie, H. Norgaard, J. M. Bollinger Jr, and C. Krebs.** 2008. Rapid and quantitative activation of chlamydia trachomatis ribonucleotide reductase by hydrogen peroxide. Biochemistry. **47:**4477-4483.

63. **Johnston, A. W., J. D. Todd, A. R. Curson, S. Lei, N. Nikolaidou-Katsaridou, M. S. Gelfand, and D. A. Rodionov.** 2007. Living without Fur: the subtlety and complexity of iron-responsive gene regulation in the symbiotic bacterium *Rhizobium* and other alpha-proteobacteria. Biometals. **20:**501-511.

64. **Kaluarachchi, H., J. F. Siebel, S. Kaluarachchi-Duffy, S. Krecisz, D. E. Sutherland, M. J. Stillman, and D. B. Zamble.** 2011. Metal selectivity of the *Escherichia coli* nickel metallochaperone, SlyD. Biochemistry. **50:**10666-10677.

65. **Kaluarachchi, H., J. W. Zhang, and D. B. Zamble.** 2011. *Escherichia coli* SlyD, more than a Ni(II) reservoir. Biochemistry. **50:**10761-10763.

66. **Kehres, D. G., A. Janakiraman, J. M. Slauch, and M. E. Maguire.** 2002. Regulation of *Salmonella enterica* serovar Typhimurium *mntH* transcription by H_2O_2, Fe(2+), and Mn(2+). J. Bacteriol. **184:**3151-3158.

67. **Kehres, D. G., M. L. Zaharik, B. B. Finlay, and M. E. Maguire.** 2000. The NRAMP proteins of *Salmonella typhimurium* and *Escherichia coli* are selective manganese transporters involved in the response to reactive oxygen. Mol. Microbiol. **36:**1085-1100.

68. **Koch, D., D. H. Nies, and G. Grass.** 2007. The RcnRA (YohLM) system of *Escherichia coli*: a connection between nickel, cobalt and iron homeostasis. Biometals. **20:**759-771.

69. **Lee, K. C., W. S. Yeo, and J. H. Roe.** 2008. Oxidant-responsive induction of the suf operon, encoding a Fe-S assembly system, through Fur and IscR in *Escherichia coli*. J. Bacteriol. **190:**8244-8247.

70. **Li, Y., and D. B. Zamble.** 2009. Nickel homeostasis and nickel regulation: an overview. Chem. Rev. **109:**4617-4643.

71. **Liu, Y., S. C. Bauer, and J. A. Imlay.** 2011. The YaaA protein of the *Escherichia coli* OxyR regulon lessens hydrogen peroxide toxicity by diminishing the amount of intracellular unincorporated iron. J. Bacteriol. **193:**2186-2196.

72. **Macomber, L., S. P. Elsey, and R. P. Hausinger.** 2011. Fructose-1,6-bisphosphate aldolase (class II) is the primary site of nickel toxicity in *Escherichia coli*. Mol. Microbiol. **82:**1291-1300.

73. **Macomber, L., and R. P. Hausinger.** 2011. Mechanisms of nickel toxicity in microorganisms. Metallomics. **3:**1153-1162.

74. **Macomber, L., and J. A. Imlay.** 2009. The iron-sulfur clusters of dehydratases are primary intracellular targets of copper toxicity. Proc. Natl. Acad. Sci. U. S. A. **106:**8344-8349.

75. **Magnani, D., O. Barre, S. D. Gerber, and M. Solioz.** 2008. Characterization of the CopR regulon of *Lactococcus lactis* IL1403. J. Bacteriol. **190:**536-545.

76. **Martinez, M., R. A. Ugalde, and M. Almiron.** 2005. Dimeric *Brucella abortus* Irr protein controls its own expression and binds haem. Microbiology. **151:**3427-3433.

77. **Masse, E., and S. Gottesman.** 2002. A small RNA regulates the expression of genes involved in iron metabolism in *Escherichia coli*. Proc. Natl. Acad. Sci. U. S. A. **99:**4620-4625.

78. **Masse, E., C. K. Vanderpool, and S. Gottesman.** 2005. Effect of RyhB small RNA on global iron use in *Escherichia coli*. J. Bacteriol. **187:**6962-6971.

79. **Merchant, S. S., M. D. Allen, J. Kropat, J. L. Moseley, J. C. Long, S. Tottey, and A. M. Terauchi.** 2006. Between a rock and a hard place: trace element nutrition in *Chlamydomonas*. Biochim. Biophys. Acta. **1763:**578-594.

80. **Missiakas, D., and S. Raina.** 1997. Signal transduction pathways in response to protein misfolding in the extracytoplasmic compartments of *E. coli*: role of two new phosphoprotein phosphatases PrpA and PrpB. EMBO J. **16:**1670-1685.

81. **Moll, I., T. Afonyushkin, O. Vytvytska, V. R. Kaberdin, and U. Blasi.** 2003. Coincident Hfq binding and RNase E cleavage sites on mRNA and small regulatory RNAs. RNA. **9:**1308-1314.

82. **Monje-Casas, F., J. Jurado, M. Prieto-Alamo, A. Holmgren, and C. Pueyo.** 2001. Expression analysis of the *nrdHIE*F operon from *Escherichia coli*. Conditions that trigger the transcript level *in vivo*. J. Biol. Chem. **276:**18031-18037.

83. **Morita, T., K. Maki, and H. Aiba.** 2005. RNase E-based ribonucleoprotein complexes: mechanical basis of mRNA destabilization mediated by bacterial noncoding RNAs. Genes Dev. **19:**2176-2186.

84. **Moriwaki, H., M. R. Osborne, and D. H. Phillips.** 2008. Effects of mixing metal ions on oxidative DNA damage mediated by a Fenton-type reduction. Toxicol. in. Vitro. **22:**36-44.

85. **Munson, G. P., D. L. Lam, F. W. Outten, and T. V. O'Halloran.** 2000. Identification of a copper-responsive two-component system on the chromosome of *Escherichia coli* K-12. J. Bacteriol. **182:**5864-5871.

86. **Murakami, K., R. Tsubouchi, M. Fukayama, T. Ogawa, and M. Yoshino.** 2006. Oxidative inactivation of reduced NADP-generating enzymes in *E. coli*: iron-dependent inactivation with affinity cleavage of NADP-isocitrate dehydrogenase. Arch. Microbiol. **186:**385-392.

87. **Nandal, A., C. C. Huggins, M. R. Woodhall, J. McHugh, F. Rodriguez-Quinones, M. A. Quail, J. R. Guest, and S. C. Andrews.** 2010. Induction of the ferritin gene (*ftnA*) of *Escherichia coli* by Fe(2+)-Fur is mediated by reversal of H-NS silencing and is RyhB independent. Mol. Microbiol. **75:**637-657.

88. **Navarro, C., L. F. Wu, and M. A. Mandrand-Berthelot.** 1993. The nik operon of *Escherichia coli* encodes a periplasmic binding-protein-dependent transport system for nickel. Mol. Microbiol. **9:**1181-1191.

89. **Niederhoffer, E. C., C. M. Naranjo, K. L. Bradley, and J. A. Fee.** 1990. Control of *Escherichia coli* superoxide dismutase (*sodA* and *sodB*) genes by the ferric uptake regulation (fur) locus. J. Bacteriol. **172:**1930-1938.

90. **Niegowski, D., and S. Eshaghi.** 2007. The CorA family: structure and function revisited. Cell Mol. Life Sci. **64:**2564-2574.

91. **Nies, D. H.** 2003. Efflux-mediated heavy metal resistance in prokaryotes. FEMS Microbiol. Rev. **27:**313-339.

92. **Olson, J. W., N. S. Mehta, and R. J. Maier.** 2001. Requirement of nickel metabolism proteins HypA and HypB for full activity of both hydrogenase and urease in *Helicobacter pylori.* Mol. Microbiol. **39:**176-182.

93. **Osman, D., and J. S. Cavet.** 2011. Metal sensing in *Salmonella*: implications for pathogenesis. Adv. Microb. Physiol. **58:**175-232.

94. **Outten, C. E., and T. V. O'Halloran.** 2001. Femtomolar sensitivity of metalloregulatory proteins controlling zinc homeostasis. Science. **292:**2488-2492.

95. **Outten, F. W., O. Djaman, and G. Storz.** 2004. A *suf* operon requirement for Fe-S cluster assembly during iron starvation in *Escherichia coli*. Mol. Microbiol. **52:**861-872.

96. **Outten, F. W., C. E. Outten, J. Hale, and T. V. O'Halloran.** 2000. Transcriptional activation of an *Escherichia coli* copper efflux regulon by the chromosomal MerR homologue, cueR. J. Biol. Chem. **275:**31024-31029.

97. **Park, S. J., and R. P. Gunsalus.** 1995. Oxygen, iron, carbon, and superoxide control of the fumarase *fumA* and *fumC* genes of *Escherichia coli*: role of the *arcA*, *fnr*, and *sox*R gene products. J. Bacteriol. **177:**6255-6262.

98. **Patzer, S. I., and K. Hantke.** 1999. SufS is a NifS-like protein, and SufD is necessary for stability of the [2Fe-2S] FhuF protein in *Escherichia coli*. J. Bacteriol. **181:**3307-3309.

99. **Patzer, S. I., and K. Hantke.** 2000. The zinc-responsive regulator Zur and its control of the *znu* gene cluster encoding the ZnuABC zinc uptake system in *Escherichia coli*. J. Biol. Chem. **275:**24321-24332.

100. **Patzer, S. I., and K. Hantke.** 2001. Dual repression by Fe(2+)-Fur and Mn(2+)-MntR of the *mntH* gene, encoding an NRAMP-like Mn(2+) transporter in *Escherichia coli*. J. Bacteriol. **183:**4806-4813.

101. **Posey, J. E., and F. C. Gherardini.** 2000. Lack of a role for iron in the Lyme disease pathogen. Science. **288:**1651-1653.

102. **Puskarova, A., P. Ferianc, J. Kormanec, D. Homerova, A. Farewell, and T. Nystrom.** 2002. Regulation of *yodA* encoding a novel cadmium-induced protein in *Escherichia coli*. Microbiology. **148:**3801-3811.

103. **Radford, D. S., M. A. Kihlken, G. P. Borrelly, C. R. Harwood, N. E. Le Brun, and J. S. Cavet.** 2003. CopZ from *Bacillus subtilis* interacts in vivo with a copper exporting CPx-type ATPase CopA. FEMS Microbiol. Lett. **220:**105-112.

104. **Rensing, C., B. Fan, R. Sharma, B. Mitra, and B. P. Rosen.** 2000. CopA: An *Escherichia coli* Cu(I)-translocating P-type ATPase. Proc. Natl. Acad. Sci. U. S. A. **97:**652-656.

105. **Rodrigue, A., G. Effantin, and M. A. Mandrand-Berthelot.** 2005. Identification of *rcnA* (*yohM*), a nickel and cobalt resistance gene in *Escherichia coli*. J. Bacteriol. **187:**2912-2916.

106. **Rosch, J. W., G. Gao, G. Ridout, Y. D. Wang, and E. I. Tuomanen.** 2009. Role of the manganese efflux system *mntE* for signalling and pathogenesis in *Streptococcus pneumoniae*. Mol. Microbiol. **72:**12-25.

107. **Sahlin, M., B. M. Sjoberg, G. Backes, T. Loehr, and J. Sanders-Loehr.** 1990. Activation of the iron-containing B2 protein of ribonucleotide reductase by hydrogen peroxide. Biochem. Biophys. Res. Commun. **167:**813-818.

108. **Saleha Banu, B., M. Ishaq, K. Danadevi, P. Padmavathi, and Y. R. Ahuja.** 2004. DNA damage in leukocytes of mice treated with copper sulfate. Food Chem. Toxicol. **42:**1931-1936.

109. **Schalk, I. J., G. L. Mislin, and K. Brillet.** 2012. Structure, function and binding selectivity and stereoselectivity of siderophore-iron outer membrane transporters. Curr. Top. Membr. **69:**37-66.

110. **Singh, S. K., G. Grass, C. Rensing, and W. R. Montfort.** 2004. Cuprous oxidase activity of CueO from *Escherichia coli*. J. Bacteriol. **186:**7815-7817.

111. **Singleton, C., S. Hearnshaw, L. Zhou, N. E. Le Brun, and A. M. Hemmings.** 2009. Mechanistic insights into Cu(I) cluster transfer between the chaperone CopZ and its cognate Cu(I)-transporting P-type ATPase, CopA. Biochem. J. **424:**347-356.

112. **Sobota, J. M., and J. A. Imlay.** 2011. Iron enzyme ribulose-5-phosphate 3-epimerase in *Escherichia coli* is rapidly damaged by hydrogen peroxide but can be protected by manganese. Proc. Natl. Acad. Sci. U. S. A. **108:**5402-5407.

113. **Speisky, H., M. Gomez, F. Burgos-Bravo, C. Lopez-Alarcon, C. Jullian, C. Olea-Azar, and M. E. Aliaga.** 2009. Generation of superoxide radicals by copper-glutathione complexes: redox-consequences associated with their interaction with reduced glutathione. Bioorg. Med. Chem. **17:**1803-1810.

114. **Stintzi, A., C. Barnes, J. Xu, and K. N. Raymond.** 2000. Microbial iron transport via a siderophore shuttle: a membrane ion transport paradigm. Proc. Natl. Acad. Sci. U. S. A. **97:**10691-10696.

115. **Taudte, N., and G. Grass.** 2010. Point mutations change specificity and kinetics of metal uptake by ZupT from *Escherichia coli*. Biometals. **23:**643-656.

116. **Thorgersen, M. P., and D. M. Downs.** 2009. Oxidative stress and disruption of labile iron generate specific auxotrophic requirements in *Salmonella enterica.* Microbiology. **155:**295-304.

117. **Tomoyasu, T., J. Gamer, B. Bukau, M. Kanemori, H. Mori, A. J. Rutman, A. B. Oppenheim, T. Yura, K. Yamanaka, and H. Niki.** 1995. *Escherichia coli* FtsH is a membrane-bound, ATP-dependent protease which degrades the heat-shock transcription factor sigma 32. EMBO J. **14:**2551-2560.

118. **Torrents, E., I. Roca, and I. Gibert.** 2003. *Corynebacterium ammoniagenes* class Ib ribonucleotide reductase: transcriptional regulation of an atypical genomic organization in the nrd cluster. Microbiology. **149:**1011-1020.

119. **Vance, C. K., and A. F. Miller.** 2001. Novel insights into the basis for *Escherichia coli* superoxide dismutase's metal ion specificity from Mn-substituted FeSOD and its very high E(m). Biochemistry. **40:**13079-13087.

120. **Veyrier, F. J., I. G. Boneca, M. F. Cellier, and M. K. Taha.** 2011. A novel metal transporter mediating manganese export (MntX) regulates the Mn to Fe intracellular ratio and *Neisseria meningitidis* virulence. PLoS Pathog. **7:**e1002261.

121. **Vivas, E., E. Skovran, and D. M. Downs.** 2006. *Salmonella enterica* strains lacking the frataxin homolog CyaY show defects in Fe-S cluster metabolism in vivo. J. Bacteriol. **188:**1175-1179.

122. **Voevodskaya, N., F. Lendzian, A. Ehrenberg, and A. Graslund.** 2007. High catalytic activity achieved with a mixed manganese-iron site in protein R2 of *Chlamydia* ribonucleotide reductase. FEBS Lett. **581:**3351-3355.

123. **Wang, D., O. Hosteen, and C. A. Fierke.** 2012. ZntR-mediated transcription of *zntA* responds to nanomolar intracellular free zinc. J. Inorg. Biochem. **111:**173-181.

124. **Waters, L. S., M. Sandoval, and G. Storz.** 2011. The *Escherichia coli* MntR miniregulon includes genes encoding a small protein and an efflux pump required for manganese homeostasis. J. Bacteriol. **193:**5887-5897.

125. **Wei, Y., and D. Fu.** 2005. Selective metal binding to a membrane-embedded aspartate in the *Escherichia coli* metal transporter YiiP (FieF). J. Biol. Chem. **280:**33716-33724.

126. **Whittaker, J. W.** 2012. Non-heme manganese catalase--the 'other' catalase. Archives of Biochemistry and Biophysics. **525:**111-120.

127. **Williams, R. J. P.** 1987. The biochemistry of zinc. Polyhedron. **6:**61-69.

128. **Wulfing, C., J. Lombardero, and A. Pluckthun.** 1994. An *Escherichia coli* protein consisting of a domain homologous to FK506-binding proteins (FKBP) and a new metal binding motif. J. Biol. Chem. **269:**2895-2901.

129. **Xu, F. F., and J. A. Imlay.** 2012. Silver(I), mercury(II), cadmium(II), and zinc(II) target exposed enzymic iron-sulfur clusters when they toxify *Escherichia coli*. Appl. Environ. Microbiol. **78:**3614-3621.

130. **Yamamoto, K., K. Hirao, T. Oshima, H. Aiba, R. Utsumi, and A. Ishihama.** 2005. Functional characterization in vitro of all two-component signal transduction systems from *Escherichia coli*. J. Biol. Chem. **280:**1448-1456.

131. **Yeo, W. S., J. H. Lee, K. C. Lee, and J. H. Roe.** 2006. IscR acts as an activator in response to oxidative stress for the *suf* operon encoding Fe-S assembly proteins. Mol. Microbiol. **61:**206-218.

132. **Yocum, C. F., and V. L. Pecoraro.** 1999. Recent advances in the understanding of the biological chemistry of manganese. Curr. Opin. Chem. Biol. **3:**182-187.

133. **Zhang, J. W., G. Butland, J. F. Greenblatt, A. Emili, and D. B. Zamble.** 2005. A role for SlyD in the *Escherichia coli* hydrogenase biosynthetic pathway. J. Biol. Chem. **280:**4360-4366.

134. **Zhao, G., P. Ceci, A. Ilari, L. Giangiacomo, T. M. Laue, E. Chiancone, and N. D. Chasteen.** 2002. Iron and hydrogen peroxide detoxification properties of DNA-binding protein from starved cells. A ferritin-like DNA-binding protein of *Escherichia coli*. J. Biol. Chem. **277:**27689-27696.

CHAPTER 2: WHAT IS THE PHYSIOLGICAL ROLE OF THE ALTERNATIVE *ESCHERICHIA COLI* AEROBIC RIBONUCLEOTIDE REDUCTASE, NRDEF?

2.1 INTRODUCTION

Ribonucleotide reductases provide the building blocks for DNA replication in all organisms. The reaction is chemically difficult, and it is achieved by free-radical chemistry that originates with an amino-acid radical in the protein active site. Life evolved in a world that for two billion years was anaerobic and iron-replete, and the prevailing ribonucleotide reductase isozyme was likely a class III enzyme of the glycyl-radical enzyme family. As in all members of this enzyme family, however, the glycyl radical of this ribonucleotide reductase is rapidly quenched by direct adduction with molecular oxygen; thus, the eventual oxygenation of the atmosphere forced the evolution of alternative enzymes. While anaerobes retain class III ribonucleotide reductases, organisms that dwell in oxic environments typically have been found to use either a B12-dependent (class II) enzyme or, more commonly, a di-ferric (class Ia) enzyme.

E. coli, which in its life cycle moves between the anaerobic gut and oxic surface waters, relies upon a class III enzyme (NrdD) for anoxic replication and a class Ia enzyme (NrdAB) for aerobic replication. Genetic experiments show that mutants lacking the former enzyme cannot grow in the absence of oxygen, while those lacking the latter enzyme cannot grow in its presence [22, 36]. The diferric NrdAB isozyme acquires iron in its ferrous state, and the NrdB subunit is then activated to its resting di-ferric/tyrosyl-radical form by molecular oxygen and an electron donor. In the resting enzyme the tyrosyl radical is buried in the protein interior, an arrangement that shields it from outside solutes and minimizes inadvertent inactivation. When substrate binds, the radical is

transiently conducted to a cysteinyl residue within the NrdA active site, where the chemistry occurs. Thioredoxin is the coreactant that delivers the electrons that are channeled to the catalytic residues, ultimately reducing the ribonucleotide. NrdAB is oxygen-resistant and apparently sufficient to enable *E. coli* replication in aerobic habitats.

Thus, it was puzzling when the genomic sequence of *E. coli* revealed the presence of a NrdAB homologue. It is denoted NrdEF, and these subunits are encoded within a four-gene operon (*nrdHIEF*). NrdH is a thiol-based redoxin, which evidently replaces thioredoxin as the electron donor for ribonucleotide reduction [38]. NrdI is a flavodoxin. *In vitro* studies confirmed that NrdEF can exhibit ribonucleotide reductase activity [10]. Members of this sequence group have been identified in a variety of bacterial genomes and are now denoted as class Ib enzymes. Although they comprise the sole ribonucleotide reductases is many microbes, the reason that they are used in preference to class Ia enzymes has been uncertain [11].

The *E. coli* NrdEF is evidently not functional under standard aerobic growth conditions, since *nrdAB* mutants fail to grow [36]. This raises the question: What is its role? The *nrdHIEF* operon is somewhat induced in *nrdR* mutants, which lack the dATP-activated feedback repressor that controls *nrdAB* and *nrdDG* expression; thus a role in DNA replication, under some circumstance, seemed certain [62].

A hypothesis emerged from several disparate observations. First, early *in vitro* experiments suggested that oxygen species such as hydrogen peroxide and superoxide might be able to disrupt either NrdAB activation or function [21, 23]. Second, active NrdEF homologues that were purified from *Corynebacterium* species contained predominantly manganese rather than iron [1, 17]. Cotruvo and Stubbe showed that

NrdEF from *E. coli* could be activated *in vitro* by manganese (as well as iron) [11]. And finally, Monje-Casas *et al.* discovered that the *E. coli nrdHIEF* operon was highly expressed during hydrogen peroxide stress [48]. These observations would tentatively fit a notion that during oxidative stress *E. coli* prefers to employ a manganese-activated ribonucleotide reductase.

A reason that it might do so is suggested by studies with other iron-cofactored enzymes. Hydrogen peroxide rapidly oxidizes ferrous iron atoms in the Fenton reaction, and when cells are exposed to even micromolar H_2O_2, this reaction results in the inactivation of key iron-dependent enzymes and in iron-catalyzed DNA damage [35, 53]. Strikingly, when *E. coli* senses elevated levels of H_2O_2, it strongly induces the synthesis of its manganese importer, MntH [39]. The imported manganese has been proposed to replace iron in non-redox enzymes that require a mononuclear metal; since manganese does not react easily with H_2O_2, this substitution would ensure enzyme activity in the face of H_2O_2 stress [2]. Thus it seemed plausible that a similar situation might pertain to ribonucleotide reduction: H_2O_2 might interfere with the activation or activity of iron-dependent NrdAB, and the induction of putative manganese-dependent NrdEF might compensate. This study was undertaken to test that hypothesis.

2.2 MATERIALS AND METHODS

2.2.1 Reagents

All antibiotics, manganese (II) chloride tetrahydrate, ferrous ammonium sulfate, colbalt(II) chloride hexahydrate, 8-hydroxyquinoline-5-sulphonic acid, desferroxamine, 30% H_2O_2, *E. coli* manganese-containing superoxide dismutase, amino acids, casein acid

hydrolysate, *o*-nitrophenyl-β-D-galactopyranoside (ONPG), xanthine, bovine xanthine oxidase, and thymidine were purchased from Sigma. Guanidine hydrochloride, nitroblue tetrazolium, 3-(*N*-morpholino) propane-sulfonic acid (MOPS), and RNase inhibitor were from Fisher Scientific. Riboflavin and tricine were from Aldrich Chemical Co. Thymidine (methyl-^{3}H) was from MP biomedicals, Inc. DEPC water, hexamer random primer, and superscript II reverse transcriptase were from Invitrogen. Na-acetate, 20% SDS solution, EDTA, saturated phenol, acid phenol-chloroform, nuclease free water, and TE buffer were from Ambion.

2.2.2 Growth conditions

Anaerobic cultures were grown in an anaerobic chamber (Coy Laboratory Products Inc.) under an atmosphere of 85% nitrogen, 10% hydrogen, and 5% carbon dioxide. Aerobic cultures were grown with vigorous shaking. All cultures were grown at 37°C unless specified elsewhere. To ensure that cells were growing exponentially before they were exposed to oxygen, anaerobic overnight cultures of oxygen-sensitive strains were diluted to OD_{600} = 0.005 into fresh anaerobic medium. After approximately five generations of anaerobic growth, cells were diluted into fresh aerobic medium.

LB medium contained (per liter) 10 g of tryptone, 10 g of NaCl, and 5 g of yeast extract. Standard glucose/amino acids medium contained minimal A salts [47], 1 mM $MgSO_4$, 5 mg/liter thiamine, 0.2 % glucose, 0.2% casamino acids, and 0.5 mM tryptophan. Glucose/aromatic medium contained 0.5 mM aromatic amino acids and 0.5 mM histidine in place of casamino acids and tryptophan. For low-iron experiments, defined medium contained MOPS salts (lacking $FeSO_4$ and micronutrients) [49], 1.32

mM K_2HPO_4, 5 mg/liter thiamine, 0.2 % glucose, 0.2% casamino acids, and 0.5 mM tryptophan. The MOPS medium was adjusted to pH 7.2 and filter-sterilized before use. Antibiotics were used at concentrations of 100 μg/ml ampicillin, 20 μg/ml chloramphenicol, 30 μg/ml kanamycin sulfate, and 12.5 μg/ml tetracycline HCl.

2.2.3 Bacterial strain and plasmid construction

The bacterial strains and plasmids used in this study are described in Table 2.1. All oxygen-sensitive strains were constructed under anaerobic conditions to ensure that suppressor mutations were not selected during outgrowth. The λ red recombinase method was used to create null mutations [13]. Mutations were introduced into new strains by P1 transduction [47]. The resulting mutations were confirmed by PCR analysis or blue/white selection with Xgal. When necessary, the antibiotic cassette was removed by transformation with the temperature-sensitive plasmid pCP20, which encodes FLP recombinase [13].

Single-copy *lacZ* transcriptional fusions to the *nrdHIEF* promoter region were integrated into the λ attachment site, while the wild-type genes remained at their native positions [28]. The promoter region was amplified using the forward primer 5′-CACTGTCTGCAGCAGCTGCGGTAGGTAGGTA-3′ and the reverse primers 5′-GTGCATAGGAATTCGCATGATTCGTATTTCCG-3′ or 5′-AGCATCGAATTC AGCGCGTGGTAATCCATCGT-3′ that were designed with PstI and EcoR1 restriction sites. The plasmid pAH125 was modified by replacing the kanamycin-resistance cassette with a chloramphenicol-cassette flanked by FLP sites, to permit antibiotic selection under anaerobic conditions. The promoter region was inserted into pSJ501, and the resulting

plasmid was confirmed by restriction analysis and sequencing. After chromosomal integration and P1-transduction into recipient strains, the chloramphenicol-cassette was removed via pCP20.

Targeted single-copy transcriptional and translational *lac* fusions to the genes of the *nrdHIEF* operon were made using λ red and FLP-mediated site-specific recombination [16]. Chromosomal mutations were created using the λ red recombinase method and pKD13, which contains a FRT flanked kanamycin-resistant cassette for in-frame deletions. After confirmation and P1 transduction into a Lac^- strain, the kanamycin cassette was removed via pCP20 at 30°C. The resultant kanamycin-sensitive strain contained a single FRT site in the desired chromosomal location and retained pCP20. Construction of *lac* fusions were made by transformation and integration of pKG137 (transcriptional *lac* fusion) or pCE40 (in-frame translational *lac* fusion) into the chromosome at the FRT site. Transformants were recovered in LB broth and selected on LB kanamycin agar plates at 37°C. Growth at 37°C blocks the replication of the temperature-sensitive plasmid pCP20. Isolates that contained stable integration of the fusion plasmid were kanamycin-resistant, ampicillin-sensitive, and Lac^+ on Xgal. Colony PCR was used to confirm that single plasmid integrants were in the correct orientation and chromosomal location. P1 transduction was used to move the *lac* fusions into recipient strains.

For the construction of tetracycline inducible genes, I used the λ red recombinase method to replace the *nrdHIEF* and *mntH* promoter regions with *tetRA* [46]. The coding sequence of *tetRA* was amplified with the following primers 5′-GCTAT

GTTGTGTATGGAAGCTGAAAGTTATGTAAATGTGCTAGGTGGGTACGTTC-3′ and 5′-GCTGCTACTCTCAACGCGATAGTTCGTCATCTTCTCCTTGGTGACG AAATAA-3′ or 5′-CACTGTTAAGCATGCGCAAATCGTAGTGCAAAAATGAT ATAGGTGGGTACGTTG-3′ and 5'-TACGGCGCGATGATACGCGTCGGGTTGTC TTCTCTGTTGATTTGGTGACGAAATAA-3′ which are flanked by sequences from the *mntH* or *nrdHIEF* promoter regions, respectively. Products were electrophoresed on a 1% agarose gel. Resulting bands were excised, purified, and transformed into strains harboring the temperature-sensitive plasmid pKD46. Transformants were selected on LB containing tetracycline, the resulting mutations were confirmed by PCR analysis, and P1 transduction was used to move P_{tet} fusions into recipient strains.

2.2.4 Cell viability

Anaerobic overnight cultures were diluted to OD_{600} = 0.005 into fresh anaerobic medium. After approximately five generations of anaerobic growth, cells were diluted to OD_{600} = 0.0025 into fresh aerobic medium and grown aerobically at 37°C with vigorous shaking. At intervals, aliquots of cells were removed and serially diluted into aerobic medium. The diluted samples were mixed with anaerobic top agar and poured onto anaerobic medium agar plates. Colonies formed were counted after 24 (LB medium) or 48 h (defined medium) of anaerobic incubation at 37°C.

2.2.5 Enzyme assays

Aerobic cultures were grown to an OD_{600} of 0.25 in fresh medium, after which cells were centrifuged, washed, resuspended to 1/30 the original culture volume, and

lysed by French press in cold 50 mM Tris-HCl buffer, pH 8. β-galactosidase activities in cell extracts were determined by ONPG hydrolysis [47].

For SOD activity measurements, aliquots of aerobic cultures grown in MOPS glucose medium supplemented with casamino acids/tryptophan were taken at intervals over time, after which cells were centrifuged, washed, resuspended to 1/100 the original culture volume, and lysed by French press in cold 50 mM potassium phosphate buffer (pH 7.8). SOD activity was measured in cell extracts using the xanthine oxidase/cytochrome *c* method [44]. To track the activity of the MnSOD, I used a *sodB* mutant. The fraction of MnSOD that was active in the cell extracts was determined after extracts were subjected to partial denaturation and renaturation in the presence of manganese to ensure full activation of MnSOD protein [2, 40]. Briefly, MnSOD was denatured at pH 3.8 in the presence of 5 mM Tris-HCl/2.5 M guanidinium chloride/20 mM 8-hydroxyquinoline-5-sulphonic acid/0.1 mM EDTA for approximately 12 hr in the dark and then renatured at pH 7.8 in the presence of 5 mM HEPES/0.1 mM $MnCl_2$ for 2 periods of approximately 12 hr each. Excess metal was removed by dialysis at pH 7.8 in 5 mM Tris-HCl/0.1 mM EDTA for 2 periods of 4 hr each. The entire reconstitution process was performed at 4°C. Purchased *E. coli* manganese-containing SOD was used as a control for the reconstitution procedure. For both enzymes assays, total protein content was determined using the Coomassie blue dye-binding assay (Thermo Scientific).

2.2.6 Disk diffusion assay

Anaerobic overnight cultures were diluted to OD_{600} = 0.005 into fresh anaerobic minimal A glucose medium supplemented with aromatic amino acids/histidine. After

approximately five generations of anaerobic growth, cells were harvested by centrifugation. The cells were suspended in 1/10 the original volume with minimal A glucose medium supplemented with aromatic amino acids/histidine. Concentrated cells were spread plated aerobically onto minimal A glucose agar plates supplemented with aromatic amino acids/histidine. Sterile paper disks impregnated with 5 µmoles of H_2O_2 or 5 nmoles of metal solution were placed on each plate. The plates were incubated for 48 h aerobically at 37°C.

2.2.7 Total thymidine incorporation

Thymine auxotrophs (*thyA* null mutants) were constructed, in order to incorporate thymidine linearly for extended periods of time. P1 transduction was used to move the *thyA*-null mutation into recipient strains. Transductants were selected on minimal A glucose medium supplemented with casamino acids/tryptophan, 50 µg/ml thymidine, and chloramphenicol. The resultant *thyA* mutants were unable to grow on defined medium unless supplemented with thymidine.

Anaerobic overnight cultures were diluted to OD_{600} = 0.005 into fresh anaerobic minimal A glucose medium supplemented with aromatic amino acids/histidine and 50 µg/ml thymidine. After approximately five generations of anaerobic growth, cells were harvested by centrifugation and suspended in 1/10 the original volume with warm medium. Concentrated cells were diluted to OD_{600} = 0.025 into aerobic minimal A glucose medium supplemented with aromatic amino acids/histidine and 32 µM thymidine/^{3}H-thymidine (1 µCi/ml) with vigorous shaking. At intervals, aliquots of cells were mixed with cold 5% trichloroacetic acid (TCA) to stop the labeling reaction and

stored on ice until all intervals were collected. Lysed cells were filtered through a G6 glass fiber filter using a manifold. Filters were washed with cold 5% TCA followed by cold 100% ethanol, then spotted with 0.1 M KOH to quench intrinsic fluorescence during counting. Filters were air dried and the radioactivity was counted using a Coulter multipurpose scintillation counter (Beckman, LS6500).

2.2.8 Whole-cell EPR measurements of tyrosyl radical

In vivo EPR samples were prepared with strains that overproduce NrdB or NrdF [30]. To overexpress the structural genes, 5 mM (for LB) or 20 mM arabinose (for defined medium) was added to aerobic cultures when cells reached OD_{600} = 0.25. After another 2 hours of incubation, the cells were harvested by centrifugation and washed two times in cold buffer A [100 mM Tris-HCl, 150 mM NaCl, and 5% glycerol (pH 7.6)]. The cell pellet was resuspended in 1/250 of the original volume in buffer A. A cell suspension (250 µl) was incubated with H_2O_2 for 5 min at 37°C. As a control, a cell suspension was incubated with 160 mM hydroxyurea for 1 h at 37°C [30]. The cell suspension was then transferred into an EPR tube and frozen in dry ice/ethanol. EPR spectra of the NrdB tyrosyl radical were obtained at the following settings: 9.08 GHz frequency; 110 K temperature; 0.2 mW power, 4 G modulation amplitude, 0.032 s time constant, and 10 scans at 30 s per scan. Spectra of the NrdF signal were obtained at 0.5 mW power. Due to interactions of the metal centers with the tyrosyl radicals, the spectra of manganese- and iron-loaded enzymes differ substantially in field position and sharpness [11].

2.2.9 RNA isolation

Anaerobic overnight cultures were diluted to OD_{600} = 0.005 into LB medium. After approximately five generations of anaerobic growth, cells were moved to aerobic conditions and vigorously shaken until cells reached OD_{600} = 0.45. Total RNA was isolated from cells by hot phenol extraction. Briefly, an aliquot of cells was mixed with pre-warmed fresh 8x lysis solution (0.32 M Na-acetate pH 5.5, 0.4% SDS, 16 mM EDTA pH 8 in DEPC water) containing saturated phenol and incubated at 65°C for 15 min with vigorous shaking. After microcentrifugation at room temperature for 10 min, the aqueous-layer was transferred to a clean tube with phenol-chloroform. Repeated phenol-chloroform extractions were performed until the interface was clean. The aqueous-layer was then transferred to ethanol and incubated at -80°C overnight. Samples were microcentrifuged at max speed for 10 min at 4°C. The supernatant was discarded and the precipitated RNA was rinsed with cold 75% ethanol by gentle palpitation. The RNA pellet was air dried, suspended in 10mM Tris-HCl/1mM EDTA (RNase free) buffer, pH 7, and stored at -80°C.

Contaminating DNA was removed from isolated RNA by rigorous DNase treatment using the Turbo DNA-*free*™ kit (Ambion, #AM1907) according to the manufacturer's directions. The product was amplified by PCR using 2 µl aliquot and subjected to gel-electrophoresis. The absence of product confirmed that the RNA samples were DNA-free. Clean RNA was then converted to cDNA by reverse-transcription. Briefly, RNA (1 µg) was mixed with 20 nmol dNTPs in 12 µl ddH_2O and incubated at 65°C for 5 min, then quenched on ice. DTT (9mM), 5x first strand buffer, 40 units RNase inhibitor, and 3 ng of hexamer random primer were added to the RNA

solution and incubated at room temperature for 2 min. Two hundred units of Superscript II reverse transcriptase were added and the reaction was incubated for 10 min at room temperature, and then moved to 42°C for 50 min. The reaction was inactivated at 70°C for 15 min and stored at -20°C.

2.2.10 Quantitative real-time PCR

PCR amplification was carried out using the primer pairs listed in Table 2.2. *gapA* served as the housekeeping gene. PCR amplification was performed in a mixture (25 µl final volume) containing 2x iQ^{TM} Sybr green supermix (Qiagen, #170-8882), 800 nM each primer, and 1-10 ng cDNA. Cycling conditions were as follows: 95°C/3 min; 40 cycles of 94°C/1 min, 55°C/45 s, 70°C/45 s. The cDNA was amplified using primers listed in Table 2.2. PCR outcomes were normalized to the *gapA* gene and relative transcription levels were calculated by comparison of the ratio of treated to non-treated cells.

2.2.11 5′ RLM-RACE

5′ RNA ligase mediated-rapid amplification of cDNA ends (RLM-RACE) was carried out using the First Choice RLM-RACE kit (Ambion, #AM1700) according to the manufacturer's directions. RNA was extracted from cells and treated with DNase as described earlier. However, the reaction was terminated by bringing the reaction volume up to 200 µl with DEPC water and the addition of an equal amount of acid phenol-chloroform. The samples were microcentrifuged at maximum speed for 5 min at room temperature. The aqueous-layer was transferred to a clean tube and the RNA was

precipitated in 100% ethanol containing 80 mM Na-acetate at -80°C for 10 min. Precipitated RNA was pelleted by microcentrifugation, air dried, and then resuspended in 15 µl nuclease free water approximately. Approximately 1.2 µg of DNA-free RNA was reserved for the 'Minus-Tobacco Acid Pyrophosphatase (TAP)' control reaction which was used to assess whether the products produced by 5′ RLM-RACE are true. The remaining DNA-free RNA (3 µg) was treated with TAP to remove the phosphate from full length mRNA. The 5′ RACE adapter was ligated to monophosphate mRNA, and then reverse transcribed to make cDNA. Two subsequent nested PCRs were performed using the 5′ RACE adapter primers and a gene-specific reverse primer 5′-TGTGGCGCT GGATGCAGACGGTTAAT-3′, 5′-AATCACTACCGGCAACTGACGAAAGC-3′, 5′-TCTACCTGAATCCGTTCCCGCTCATT-3′, and 5′-GTGTTTTCGGAGCTGCTGGA GAAGTA-3′. Cycling conditions were as follows: 94°C/3 min; 35 cycles of 94°C/30 s, 65°C/30 s, 72°C/60 s; 72°C/7 min. Products were run on a 2% nusieve agarose gel. Resulting bands were excised, gel purified using Qiaquick gel extraction kit (Qiagen, #28704), and sequenced.

2.3 RESULTS

2.3.1 NrdEF is induced during H_2O_2 stress, but H_2O_2 does not inhibit NrdAB function

Previous workers demonstrated that the transcription of the *nrdHIEF* operon is elevated when a bolus of 100 µM H_2O_2 is added to exponentially growing cultures of *E. coli* [48]. That dose substantially exceeds the amount of H_2O_2 that *E. coli* is likely to experience in natural environments [31]. To impose constant, low doses of H_2O_2 upon

cells, we have used *katE katG ahpCF* (Hpx$^-$) strains that lack catalase and peroxidase activities. These strains cannot degrade the H_2O_2 that is generated as a by-product of metabolism, and during aerobic growth their internal concentration of H_2O_2 rises to 0.5-1 μM [58]. This dose is likely to represent a physiological degree of stress, since it exceeds the dose that triggers the OxyR response (0.2 μM) by only a moderate amount [3, 58]. Measurements of transcript levels confirmed that all four genes of the *nrdHIEF* operon were induced in Hpx$^-$ mutants (Fig. 2.1). A $P_{nrdHIEF}$ – lacZ fusion was constructed and integrated at the phage attachment site. When the Hpx$^-$ mutant was grown in defined medium, the β-galactosidase activity was consistently elevated by two-fold over the level in unstressed wild-type cells. This effect is lower than previously reported [48], but differences arise from the effects of the culture medium (see below).

Hydrogen peroxide inactivates some mononuclear iron enzymes by oxidizing their exposed iron cofactor, triggering iron dissociation and/or covalent modification of the protein by the hydroxyl radical that is formed [2, 60]. Thus I hypothesized (i) that NrdAB function might be inactivated by H_2O_2 and (ii) that NrdEF might be induced to compensate.

Ribonucleotide reductase activity is essential for cell viability, but the roles of the aerobic isozymes can be genetically tested by the construction of null mutants in an anaerobic chamber. Under those conditions replication depends upon NrdD, an oxygen-sensitive glycyl-radical enzyme, whereas NrdAB is non-functional, since it requires oxygen for activation. When wild-type *E. coli* cultures are diluted into aerobic medium, NrdD immediately loses activity, while NrdAB is activated.

Once exposed to oxygen, a Δ*nrdAB nrdEF*$^+$ mutant filamented and lost viability, while a *nrdAB*$^+$ Δ*nrdEF* mutant grew as well as a wild-type strain (Fig. 2.2A). Thus, in unstressed *E. coli*, NrdAB is necessary and sufficient for aerobic DNA replication, whereas NrdEF has no apparent function. To determine if NrdAB remains functional during H_2O_2 stress, an *E. coli* Hpx$^-$ Δ*nrdEF* strain was constructed, and cell viability was monitored subsequent to aeration. This mutant grew as well as the wild-type strain. Thus, contrary to our expectation, NrdAB appeared to retain function during H_2O_2 stress (Fig. 2.2B).

Measurements of total [^{3}H]-thymidine incorporation [14] confirmed that chromosomal replication continued to progress in the Hpx$^-$ Δ*nrdEF* strain (Figure 2.3). I was unable to reliably test the activity of ribonucleotide reductase by direct assay, since these methods are problematic in crude extracts, and purification steps can perturb the enzyme activity status. Therefore to directly test the stability of the NrdB iron center, I overexpressed *nrdB* and used whole-cell EPR to visualize its diferric/tyrosyl radical signal [30]. A characteristic signal was visible, and it was quenched when cells were treated by hydroxyurea, an established scavenger of the tyrosyl radical [15] (Fig. 2.4). However, the NrdB signal was not abolished when the Hpx$^-$ strain was exposed to up to 1 mM H_2O_2 (Fig. 2.4).

Finally, I tested whether the NrdR repressor is deactivated during H_2O_2 stress. When cellular ribonucleotide reductase activity is sufficient, NrdR binds dATP and/or dADP and, as a complex, represses expression of ribonucleotide reductases [27, 62]. In a wild-type cell, deletion of *nrdR* caused a 3-fold increase in P_{nrdH}-*lacZ* expression (Fig. 2.5). A similar effect resulted from a Δ*nrdAB* deletion, and minimal further induction

was observed when *nrdR* was additionally deleted, implying that in this strain the repressive effect of NrdR depends upon the function of NrdAB (Fig. 2.5). I then observed that the addition of the Δ*nrdR* allele to Hpx$^-$ mutants caused a similar degree of P_{nrdH}-*lacZ* induction (Fig. 2.5). This finding shows that NrdR still actively represses *nrdHIEF* transcription during H_2O_2 stress and affirms that NrdAB is not inactivated by H_2O_2.

Some *in vitro* experiments had suggested that NrdAB might be directly poisoned by superoxide, an oxidant whose reactivity with metal centers resembles that of H_2O_2 [19, 23]. However, I observed no replication defect when Δ*sodA* Δ*sodB* Δ*nrdEF* mutants were cultured in aerobic medium. Further, overproduced NrdB exhibited a normal tyrosyl radical in a SOD$^-$ strain (Fig. 2.6). The superoxide stress in these cells is sufficient to inactivate a variety of iron-sulfur enzymes and the metabolic pathways to which they belong [31]; I conclude, therefore, that NrdAB is not a significant target of superoxide stress *in vivo*.

2.3.2 NrdEF is functional during H_2O_2 stress

Mutants that lacked both NrdAB and NrdEF lost viability more quickly than did mutants that lacked only NrdAB (Fig. 2.2A), which indicated that under these circumstances NrdEF must provide some ribonucleotide reductase function, albeit not enough to enable normal aerobic growth. In fact, previous work indicated that the engineered overexpression of *nrdEF* could substantially compensate for *nrdAB* deficiency [25, 37, 38]. Since *nrdEF* is induced during H_2O_2 stress, it seemed plausible that NrdEF activity might rise to a level that would allow DNA replication. Indeed, the

Hpx$^-$ Δ*nrdAB* strain was able to successfully replicate under aerobic conditions (Fig. 2.2B), in contrast to the congenic Hpx$^+$ Δ*nrdAB* strain (Fig. 2.2A). Thus during oxidative stress the native *nrdEF* operon can generate enough ribonucleotide reductase activity to permit cell replication.

2.3.3 Fur and IscR regulate *nrdHIEF* transcription

I sought to identify the regulatory mechanism that triggers expression of *nrdHIEF* during oxidative H_2O_2 stress. Many of the proteins involved in protection against H_2O_2 stress are positively regulated by the OxyR transcription factor, which is fully activated by the H_2O_2 that accumulates in Hpx$^-$ mutants [67]. However, a constitutive *oxyR2* mutant allele had no effect on the level of P_{nrdH}-*lacZ* expression in an otherwise wild-type strain, indicating that this operon is not part of the OxyR regulon (data not shown). Others had made a similar conclusion from complementary experiments [48, 56].

Fur and IscR are the other global regulators that are perturbed by H_2O_2 stress [43, 63, 66]. In iron-replete cells Fur binds ferrous iron, and the Fur:Fe^{2+} complex binds to the promoter regions of iron-import genes, inhibiting their expression. It also represses the transcription of the small RNA RyhB, which otherwise targets for degradation mRNAs that encode iron-requiring enzymes; this system ensures that non-essential iron enzymes are only synthesized when iron is available to activate them [63]. Earlier work showed that the micromolar level of H_2O_2 inside Hpx$^-$ mutants can deactivate Fur, presumably due to the oxidation of its iron cofactor [63]. I believed this to be a plausible mechanism of *nrdHIEF* induction in Hpx$^-$ mutants, since several groups have reported that the transcription of *nrdHIEF* is elevated in cells devoid of *fur* [45, 64]. To assess the

effect of Fur on the transcription of *nrdHIEF*, quantitative measurements of mRNA levels were made using RT-PCR. In a wild-type background I detected elevated *nrdHIEF* mRNA levels in both Δ*fur* mutants and Δ*nrdR* single mutants (Fig. 2.7, left), thus confirming that under these growth conditions each regulator inhibits *nrdHIEF* transcription [62]. The combination of Δ*fur* and Δ*nrdR* alleles resulted in a synergistic effect on transcription, indicating that Fur and NrdR repress *nrdHIEF* independently of one another.

In the H_2O_2-stressed Hpx$^-$ background, NrdR still exerted a repressive effect on transcription, but Fur did not (Fig. 2.7, right). These data indicated that the induction of *nrdHIEF* by H_2O_2 occurs primarily because H_2O_2 inactivates the Fur repressor.

These results suggested that NrdEF is likely to respond to a diminution of cellular iron levels. I wished to test this idea without the involvement of H_2O_2 stress or *fur* mutations, which each exert physiological effects that would not be triggered by iron restriction. When wild-type cells were grown in the presence of the iron-chelator desferroxamine (DFO), a 17-fold increase in *nrdHIEF* levels occurred (Fig. 2.8A). Interestingly, DFO addition had a modest but consistent effect even upon a Δ*fur* mutant, potentially suggesting that iron starvation diminished NrdAB activity and thereby partially inactivated NrdR. A similar inducing effect was achieved by the deletion of *tonB*, thereby eliminating the energy source that drives the import of iron chelates (Fig. 2.8B). These approaches confirm that iron starvation triggers *nrdHIEF* induction.

Jordan and coworkers mapped the initiation of basal *nrdHIEF* transcription to a start site 67 bp upstream of the first translated gene [36]. I established by 5′ RNA ligase

mediated-rapid amplification of cDNA ends (RLM-RACE) that the same start site is used when transcription is elevated in a Δ*fur* Δ*nrdR* strain.

Genetic approaches have been used to locate Fur binding sites in *E. coli*, and a positive result was reported for clones carrying DNA upstream of the *nrdHIEF* operon [61, 64]. *In vitro* studies indicated that Fur protein can bind to this region of the *Salmonella* gene [52]. A region of similarity to a Fur binding box (GTAATTTCGACCACTATT) was reported 61 bp upstream of the transcriptional start site, near the transcriptional start of the divergently transcribed *ygaC* gene. However, Fur continued to regulate *nrdHIEF* transcription when this sequence was removed (Fig. 2.9A). Regulation also persisted in mutants lacking *ryhB* and *hfq*, which appears to rule out post-transcriptional regulation by a small RNA (Fig. 2.9B); further, the regulatory effect of Fur disappeared when the promoter was replaced by the *tetRA* expression system (Fig. 2.9C). I deduce that Fur regulates *nrdHIEF* transcription through an alternate binding site, either directly or through an intermediary; I did not further map this site.

Hydrogen peroxide also affects the function of IscR, a transcriptional regulator that can coordinate a [2Fe-2S] cluster [43, 66]. In its holoprotein form, IscR[2Fe-2S] represses a broad set of genes that includes those that encode the housekeeping iron-sulfur-cluster assembly system (*iscSUA-fdx-hscAB*) [24, 57]. In its apoprotein form, IscR is a positive activator of expression of other genes, including the alternative iron-sulfur-cluster assembly system that is encoded by the *sufABCDSE* operon. The level of H_2O_2 that accumulates in Hpx$^-$ mutants is sufficient to disrupt Isc-mediated cluster assembly, leading to the conversion of substantial IscR to its apoprotein form [34], with consequent

effects on the operons it regulates. I tested whether *nrdHIEF* might lie within its regulon. In fact, I observed a two-fold decrease in *nrdHIEF* transcription when *iscR* was deleted from wild-type cells (Fig. 2.8C), while overexpression of *iscR* did not affect *nrdHIEF* regulation (data not shown). These data suggested that IscR might activate *nrdHIEF* transcription. To test this idea further, the native *iscR* gene was replaced with *iscR*-(C92A/C98A/C104A) mutant allele, which is incapable of binding an iron-sulfur cluster and thereby forms apo-iscR protein [50]. A four-fold increase in *nrdHIEF* transcription resulted (Fig. 2.8C). The presence of the native *iscR* gene did not affect this increase, since up-regulation of *nrdHIEF* was still observed in a meroploid strain containing both alleles (data not shown). It appears that apo-IscR activates transcription of *nrdHIEF*. The effect of apo-IscR persisted in strains with deletions in *fur* and/or *nrdR* (Fig. 2.10). Thus these three regulatory proteins act independently of one another: NrdR:dATP and Fur:Fe^{2+} repress *nrdHIEF* transcription, while apo-IscR activates it.

2.3.4 Expression of *nrdHIEF* is not sufficient for function

The induction of *nrdHIEF* in the Δ*fur* mutants was substantially higher than that which occurred in the Hpx^- background, and so I anticipated that the Δ*fur* mutants might similarly produce enough NrdEF to compensate for a Δ*nrdAB* mutation. However, unlike the Hpx^- Δ*nrdAB* strain, the Δ*nrdAB* Δ*fur* mutant did not grow in aerobic medium (Fig. 2.11). Nor did a Δ*nrdAB* Δ*fur iscR*-(C92A/C98A/C104A) mutant, despite the simultaneous deactivation of NrdR, absence of Fur, and presence of apo-IscR (Fig. 2.11). Indeed, expression of *nrdHIEF* from the *tet* promoter also failed to enable growth (data not shown); thus transcription of *nrdHIEF* is not sufficient for NrdEF to become

functional. Since NrdEF becomes functional during H_2O_2 stress (Fig. 2.2B), I considered that another element of the cellular response to H_2O_2 might be essential to activate the enzyme.

2.3.5 NrdEF requires manganese to function

Superoxide dismutase, like ribonucleotide reductase, is a non-heme/non-metal-cluster enzyme that requires a redox-active metal. When cells are replete with iron, the iron-containing superoxide dismutase is synthesized. When iron is scant, a manganese-dependent isozyme is induced as a replacement [9]. The fact that NrdEF is induced in iron-poor cells suggested that it might similarly be manganese-dependent. In fact, when iron levels are low, the manganese transporter gene, *mntH*, is upregulated through derepression of the Fur regulon [39, 54], potentially facilitating this adjustment. The induction of *mntH* is especially pronounced during H_2O_2 stress, since OxyR directly activates its transcription [2, 39]. Furthermore, *in vitro* studies have suggested that *Corynebacterium glutamicum* and *Corynebacterium ammoniagenes* use manganese for ribonucleotide reductase function [1, 17]. If *E. coli* NrdEF Ire manganese-dependent, then the failure of this enzyme to function when the *nrdHIEF* operon was artificially expressed would be understandable, since manganese is not imported into *E. coli* under normal growth conditions [2].

A disk diffusion assay was employed to test whether NrdEF required manganese to function (Fig. 2.12). Unlike wild-type cells, Δ*nrdAB* mutants were unable to grow on this base aerobic medium. However, the Δ*nrdAB* mutants showed growth near a manganese-impregnated disk. Similarly, they grew in a halo close to a H_2O_2-containing

disk. This growth was abolished by the addition of either *nrdEF* or *mntH* null mutations (Fig. 2.12). Neither iron nor cobalt could substitute for manganese (Fig. 2.12, bottom). These data suggest that manganese is requisite for NrdEF to function.

Manganese did not influence *nrdHIEF* expression (Fig. 2.13a). These data support the idea that NrdEF uses manganese as a metal cofactor. The plate phenotype could also be replicated in liquid medium: Δ*nrdAB* mutants were able to grow in aerobic defined medium if it was supplemented with 1 μM manganese, but Δ*nrdAB* Δ*mntH* mutants could not (Fig. 2.13b).

2.3.6 NrdEF becomes active during protracted iron starvation

It is difficult to create protracted iron deficiency in lab cultures by simply minimizing iron in the medium, both because trace iron contaminates medium components and because the dense cultures that are used in lab studies will quickly drive low-iron levels to near zero. In the complete absence of iron, *E. coli* cannot grow, and so DNA replication cannot be monitored. In order to simulate persistent iron-poor environments that might be found in nature, I constructed *E. coli* strains that lack the primary iron uptake systems *(*Δ*tonB* Δ*feoABC* Δ*zupT*) [26]. The number of viable cells was tracked over time. Under these conditions, the low iron levels of unsupplemented medium enabled slow growth of the Δ*tonB* Δ*feoABC* Δ*zupT* strain, presumably because iron inefficiently slips into cells through low-affinity systems that are dedicated to other polyvalent cations. Iron-limited cells devoid of *nrdAB* showed a brief lag before they were able to grow (Fig. 2.14a). This outgrowth depended upon the function of NrdEF,

since iron-limited mutants lacking both aerobic ribonucleotide reductases were non-viable (Fig. 2.14a).

Similar growth patterns were also observed with defined medium supplemented with manganese (data not shown). To test whether the initial growth lag was due to delays in the induction of *mntH* or *nrdHIEF*, I followed the expression of P_{mntH} – lacZ and P_{nrdE} – lacZ over time. The iron-limited Δ*nrdAB* mutants showed that *nrdHIEF* was induced soon after aeration, presumably because NrdR was immediately derepressed; in contrast, *mntH* failed to be induced for several hours, which might be the time needed for depletion of cellular iron stores (Fig. 2.14b). The lag in *mntH* induction coincided with the lag in the outgrowth of the iron-limited Δ*nrdAB* mutants.

The native promoters of *mntH* and *nrdHIEF* were replaced with a tetracycline-inducible promoter in order to allow metal-independent control of *nrdHIEF* and *mntH* expression. Surprisingly, the over-expression of these genes still did not enable NrdEF to function in iron-replete cells, but it did allow it to function in the iron-limited mutants—after a residual delay (Fig. 2.15). These data indicated that low iron concentrations are needed not simply for *nrdHIEF* and *mntH* induction, but also for NrdEF polypeptide to become functional.

To verify our inference regarding intracellular metal availability, I monitored the activity of the cellular manganese superoxide dismutase, an enzyme that can bind either iron or manganese but is only active with the latter. By assaying the enzyme in cell extracts, partially denaturing and renaturing the protein in the presence of manganese, and assaying again, one can determine the fraction of enzyme that was initially active. In iron-replete cells, this enzyme is expressed, but metal-replacement experiments showed

that less than 5% of the enzyme was active, due to lack of manganese in the active site [2]. In contrast, 80% of this enzyme was active during outgrowth of the iron-limited Δ*nrdAB* mutants.

Recent *in vitro* studies have shown that NrdEF can form an active enzyme using either iron or manganese; however, in the studies that have been reported, the manganese-cofactored enzyme was about five-fold more active [11]. The two forms are distinguishable by the characteristic EPR spectra of the tyrosyl radical, which interacts with the metal cofactor. Whole-cell EPR of a NrdF-overproducing strain indicated that NrdF was loaded with manganese during the outgrowth of the iron-limited Δ*nrdAB* mutants (Fig. 2.16a).

In contrast, when cells were grown in iron-rich conditions, a signal denoting iron-loaded NrdF was observed (Fig. 2.16b). The Δ*nrdAB* mutants do not grow under these conditions, suggesting that iron-loaded NrdEF is not sufficiently functional to enable normal replication *in vivo*.

The EPR data cannot be used to compare the relative amounts of NrdF activation under these two conditions, since interference from cellular metal pools compromises spin quantification. However, they do show that the identity of the metal that binds NrdF depends upon the relative availability of iron and manganese. More broadly, these data collectively show that metallation by manganese is necessary for NrdEF to be functional *in vivo*, while iron is inadequate.

2.3.7 YfaE is required for continued NrdAB function during H_2O_2 stress

The competition between iron and manganese for the active site of NrdF suggested that the same might occur in NrdB. This would be problematic, since *in vitro* studies have shown that iron is required for NrdAB activity and manganese most likely cannot be used [4, 6, 29]. Recent evidence suggests that NrdB activation can be a catalyzed process that involves YfaE, a ferredoxin that is encoded immediately downstream of *nrdB* [30, 65]. I wondered whether the YfaE-mediated process excludes manganese.

The deletion of *yfaE* did not compromise the function of NrdAB in iron-replete cells (Fig. 2.17a). However, in Hpx^- mutants *yfaE* was essential (Fig. 2.17b). In LB medium, which has substantial manganese, the Hpx^- Δ*yfaE* defect could be substantially suppressed by deletion of *mntH* (Fig. 2.18a). The defect was less pronounced in defined medium, but it re-emerged when manganese was added (Fig. 2.18b). Thus an apparent effect of YfaE is to discriminate between iron and manganese during NrdB activation.

The *yfaE* phenotype was not apparent during iron limitation, as the Δ*tonB* Δ*feoABC* Δ*zupT* Δ*nrdEF* mutants continued to replicate their DNA even when *yfaE* was deleted (data not shown). It is plausible that H_2O_2 stress is a greater challenge for YfaE-independent metallation either because it oxidizes ferrous iron during the loading process or because it more strongly induces the manganese importer.

2.4 DISCUSSION

DNA synthesis in *E. coli* has long been known to rely upon NrdD, an oxygen-sensitive ribonucleotide reductase, in anaerobic habitats, and NrdAB, an oxygen-

dependent isozyme, in aerobic habitats. The goal of this work was to assess the physiological role of a NrdAB homologue, NrdEF. Its function was not apparent, as it is not active under standard laboratory growth conditions. Prior work had hinted that NrdAB might be vulnerable to oxidative stress and that NrdEF might be induced to compensate, but this was not so. Instead, NrdEF is a manganese-dependent enzyme that becomes functional only when iron is scarce; by doing so, it allows DNA synthesis to proceed when NrdAB, an iron-dependent enzyme, cannot be activated.

As this work approached completion, I learned from JoAnne Stubbe that a member of her lab, Joseph Cotruvo, Jr., had isolated biochemically active NrdEF from severely iron-limited *E. coli* mutant strain (personal communication). This strain, like those used in our study, contained mutations that eliminate the major iron-import systems (*feo ent fec zupT mntH*); in addition, they were cultured with dipyridyl, a cell-permeable iron chelator that further diminishes the availability of intracellular iron. Substantial manganese (100 μM) was added to the medium, and its import through non-specific metal channels presumably compensated for the lack of MntH. Combined EPR and western-blot analyses of cell extracts indicated that about 20% of the NrdEF recovered from these cells contained a tyrosyl radical, and metal-content measurements indicated that the NrdF subunit contained two manganese atoms. Although these culture conditions differ slightly from those used in our own experiments, it seems clear that their biochemical data affirm the conclusions of our physiological, genetic, and EPR results.

The physical features that determine the metal specificities of NrdB and NrdF are unclear; data from other workers established that each of these enzymes can bind either

iron or manganese *in vitro* [4, 11]. Binding constants have not been determined, but the results of this investigation indicate that they can be metallated with either metal *in vivo*, too. Surprisingly, while both iron and manganese can facilitate tyrosine activation in NrdF, biochemical measurements show that the iron-loaded radical enzyme is significantly less active than the manganese-loaded enzyme [11]. The data of Figure 2.16b and 2.2a support that conclusion: although the NrdF tyrosyl radical is generated in iron-loaded cells, the enzyme activity is evidently insufficient to drive replication. One possibility is that the electronic effect of the metal upon the radical—which is evidenced by the metal-dependency of the radical EPR spectrum—might control its reduction potential and thereby influence how adept the radical is at abstracting and then returning the cysteinyl electron during the course of the catalytic cycle. In addition, crystal structures of NrdF indicate that despite their similarities, the ligand sphere around iron does not exactly match that around manganese, a structural difference that might similarly degrade electron conduction [5]. Broadly speaking, both physiological and structural parameters will determine which metals load and activate metalloenzymes *in vivo*; this question is gaining currency.

2.4.1 Ribonucleotide reductase and iron starvation

E. coli is routinely iron-dependent; in laboratory media in which all biological metals are available, this microbe accumulates high concentrations of total iron (*ca.* 1 mM) but scant manganese (15 μM) [2]. This preference may originate in the conditions of its usual habitat, the large intestine, which is anaerobic and relatively iron-replete. However, once *E. coli* is excreted into surface waters, iron sources are less reliable. To

maintain metabolic activity, adaptations are made when environmental iron is scarce. Iron that has been stored in ferritins is released; siderophores are excreted; and, if the situation is especially dire, the synthesis of dispensable iron-requiring enzymes is suppressed. It is now becoming apparent that another adjustment is made: manganese is imported in order to preserve enzyme activities that might otherwise falter. Some non-redox enzymes rely upon iron as a mononuclear cofactor, and manganese can activate these very well [7, 32, 33, 60]; presumably, the induction of MntH, the manganese transporter, rescues these enzymes. However, such a strategy cannot easily work for enzymes that use iron as a redox cofactor, since the inherent reduction potentials of these metals differ. A co-ordination environment that poises iron at the optimal potential for a given reaction is unlikely to succeed with manganese. A long-standing example is bacterial superoxide dismutase: enteric bacteria use an iron-SOD as the housekeeping enzyme, but when iron levels are low, its transcripts are degraded, and a distinct isozyme is induced that is functional only with manganese.

The present study reveals that a similar arrangement pertains to ribonucleotide reductase: the manganese-dependent isozyme is induced when iron is scarce. This adaptation is especially striking because it had seemed that the essentiality of ribonucleotide reduction would impose upon bacteria an absolute requirement for iron. One wonders, now, whether enteric bacteria might adapt to dwindling iron levels so efficiently that growth could be established without it. To date *Borrelia burgdorferi* is the sole organism known to grow under rigorously iron-deplete conditions [55]; although it harvests its deoxynucleosides from its host, related *Borrelia* species employ a ribonucleotide reductase that is a homologue of the *E. coli* NrdEF enzyme. Lactic acid

bacteria, which also eschew major iron-dependent pathways, including the TCA cycle and respiratory chains, also rely on NrdEF homologues.

Iron sequestration is a key host strategy used by mammals to suppress invasion by bacteria, and so would-be pathogens rely upon iron-acquisition and -sparing strategies. NrdEF is found in many of them. An initial interpretation was that its role might be in tolerating the oxidative stress that is created by macrophages; however, the results of the current study suggest that it may help pathogens to tolerate the iron restriction that is imposed by the host.

2.4.2 Ribonucleotide reduction during oxidative stress

It has long been suspected that oxidants might interfere with conventional ribonucleotide reductases. This idea arose when superoxide dismutase (SOD) was determined to be necessary for the aerobic activation of *E. coli* NrdAB in an *in vitro* system that utilized flavin reductase as an electron source [19]. Further investigation determined that the SOD requirement could be circumvented if the loading of ferrous iron occurred anaerobically [20]. Flavin reductase (Fre) itself generates superoxide [21], and since superoxide efficiently oxidizes ferrous iron, one explanation for the early data might be that the superoxide introduced in the system by Fre interfered with metal loading, by converting ferrous to ferric iron. A later study showed that superoxide might degrade the tyrosine radical of pre-activated NrdAB *in vitro* [23]. However, the rate of this reaction was slow, with a half-time of *ca.* 10 min; in contrast, superoxide inactivates iron-sulfur dehydratases within seconds [18]. Similarly, although H_2O_2 exposure was observed to gradually quench the tyrosine radical [21], the conditions (5 mM x 30 min)

far exceeded the physiological micromolar doses. Thus our observation that NrdAB retains function in Hpx^- and SOD^- mutants indicates that this enzyme is not a physiologically important target of these oxygen species.

This finding is chemically reasonable. Hydrogen peroxide does not react with organic radicals; and, although superoxide may be chemically capable of doing so, the tyrosine radical is not solvent-exposed. Ferric iron itself is poorly reactive with H_2O_2, and I have found no evidence that H_2O_2 stress oxidizes the thioredoxin/glutaredoxin pool, the electron source for NrdAB. Thus the most obvious opportunity for H_2O_2 to disrupt NrdAB function might be through interference with the iron-loading stage of NrdB activation. This process is catalyzed, and YfaE is a participant [30]. Our data indicate that in wild-type cells iron is delivered to NrdB in a way that precludes problems from H_2O_2. In contrast, the persistent activity of NrdAB in *yfaE* mutants presumably arises from the passive, uncatalyzed binding of ferrous iron to nascent apo-NrdB. The data show that H_2O_2 interferes. In part this is due to the MntH-driven import of manganese, which apparently competes with iron to bind NrdB. The situation is likely aggravated by the action of Dps, an ferritin that sequesters cellular iron as a device to minimize Fenton chemistry [2, 53]. Further, the uncatalyzed (YfaE-independent) NrdB-activation process may be slow enough that H_2O_2 might interfere directly by oxidizing the newly bound ferrous iron, thereby aborting the activation cycle. I observed that YfaE was not essential for NrdAB activation in iron-starved cells absent H_2O_2 stress (data not shown); it is the combination of H_2O_2 stress and high manganese that imposes an absolute requirement that YfaE catalyze NrdB activation.

In contrast to NrdB, the wild-type NrdF activation process appears not to effectively exclude its non-cognate metal, iron. Since iron-loaded NrdEF is poorly active, the repression of *nrdHIEF* by Fur:Fe^{2+} makes sense. However, what is the physiological logic for *nrdHIEF* induction by apo-IscR? Plausibly this stems from the role of YfaE, a [2Fe-2S] enzyme, in activating NrdAB. When iron-sulfur synthesis is impeded—the situation that is sensed by IscR—YfaE may become unavailable to activate NrdAB, and so a shift to NrdEF could be salutary. Alternatively, apo-IscR may serve as an adjunct indicator of iron deficiency [51]. This may be useful in manganese-rich cells, since abundant manganese can restore the repressor activity of Fur protein.

2.5 TABLES

Table 2.1. Bacterial stains and plasmids used in this study.

Strain	Genotype	Reference
MG1655	F^- wild type	*E. coli* CGSC
LC106	Δ*ahpF::kan* Δ(*katG::*Tn*10*)1 Δ(*katE12::*Tn*10*)	[59]
BW25113	*lacI rrnB* Δ*lacZ hsdK* Δ*araBAD* Δ*rhaBAD*	[13]
JC10241	*thr-300* λ^- *slr300::*Tn*10 relA rpsE2300 spot1 ilv-318 thi-1* Hfr^+	[12]
CAG12178 *gyrA*$^+$	F^- λ^- *zfa-723::*Tn*10 rph-1*	*E. coli* CGSC
JEM80	As BW25113 Δ*nrdAB1::cat*	This study
JEM84	As MG1655 Δ*nrdAB1::cat*	P1(JEM80) X MG1655
JEM86	As LC106 Δ*nrdAB1::cat*	P1(JEM80) X LC106
JEM78	As BW25113 Δ*nrdEF1::cat*	This study
JEM89	As MG1655 Δ*nrdEF1::cat*	P1(JEM89) X MG1655
JEM90	As LC106 Δ*nrdEF1::cat*	P1(JEM89) X LC106
JEM110	As MG1655 Δ*nrdEF1::cat~srl300::*Tn*10*	This study
JEM118	As MG1655 Δ*nrdAB1* Δ*nrdEF1::cat~srl300::*Tn*10*	P1(JEM110) X JEM93
JEM119	As LC106 Δ*nrdAB1* Δ*nrdEF1::cat~srl300::*Tn*10*	P1(JEM110) X JEM94
AA19	As BW25113 Δ*mntH2::cat*	[2]
AA30	As LC106 Δ*mntH2::cat*	[2]
JEM128	As MG1655 Δ*nrdAB1* Δ*mntH2::cat*	P1(AA19) X JEM93
SJ130	As MG1655 Δ*lacZ1*	[34]
SJ108	As LC106 Δ*lacZ1*	[34]
JEM228	As SJ130 *attλ::*[pSJ501::*nrdH´-lacZ*$^+$]	This study
JEM233	As MG1655 Δ*lacZ1* Δ*nrdAB1 attλ::*[pSJ501::*nrdH´-lacZ*$^+$]	P1(JEM228) X JEM178
JEM235	As MG1655 Δ*lacZ1* Δ*nrdAB1* Δ*mntH2 attλ::*[pSJ501::*nrdH´-lacZ*$^+$]	P1(JEM228) X JEM180
JEM245	As SJ108 *attλ::*[pSJ501::*nrdH´-lacZ*$^+$]	P1(JEM228) X SJ108
JEM273	As MG1655 Δ*nrdEF1*	This study
EM1256	As MG1655 Δ*fur::kan*	C. Rensing
JEM275	As EM1256 Δ*lacZ1 attλ::*[pSJ501::*nrdH´-lacZ*$^+$]	P1(JEM228) X JEM272
JEM253	As BW25113 Δ*nrdR1::cat*	This study
JEM284	As MG1655 Δ*lacZ1* Δ*nrdR1 attλ::*[pSJ501::*nrdH´-lacZ*$^+$]	This study
JEM286	As JEM284 Δ*fur::kan*	P1(EM1256) X JEM284
JEM407	As SJ108 Δ*nrdR1*	P1(JEM253) X SJ108

Table 2.1. (continued)

JEM304	As SJ108 Δ*nrdR1 attλ::*[pSJ501::*nrdH´-lacZ*$^+$]	This study
JEM312	As MG1655 Δ*lacZ1* Δ*nrdAB1* Δ*nrdR1 attλ::*[pSJ501::*nrdH´-lacZ*$^+$]	This study
KK210	As AB1157 *fur::*Tn*5~zbf-507::*Tn*10*	Lab strain
JEM302	As EM1256 *zbf-507::*Tn*10*	P1(KK210) X EM1256
JEM311	As JEM304 Δ*fur::kan~zbf-507::*Tn*10*	P1(JEM302) X JEM304
JEM307	As MG1655 Δ*lacZ1* Δ*nrdAB1 attλ::*[pSJ501::*nrdH´-lacZ*$^+$] Δ*fur::kan~zbf-507::*Tn*10*	P1(JEM302) X JEM259
JEM309	As LC106 Δ*lacZ1 attλ::*[pSJ501::*nrdH´-lacZ*$^+$] Δ*fur::kan~zbf-507::*Tn*10*	P1(JEM302) X JEM261
JEM255	As BW25113 Δ*yfaE1::cat*	This study
JEM290	As MG1655 Δ*yfaE1::cat*	P1(JEM255) X MG1655
JEM296	As JEM273 Δ*yfaE1::cat*	P1(JEM255) X JEM273
JEM325	As LC106 Δ*yfaE1::cat*	P1(JEM255) X LC106
JEM326	As BW25113 Δ*nrdHIEF1::cat*	This study
JEM475	As LC106 Δ*nrdHIEF1* Δ*yfaE1::cat*	P1(JEM255) X JEM464
JEM504	As LC106 Δ*nrdHIEF1* Δ*yfaE1* Δ*mntH2::cat*	P1(AA19) X JEM492
AW25113	As BW25113 Δ*tonB1::cat*	Lab strain
W3110	F$^-$ λ$^-$ IN(*rrnD-rrnE*)1 *rph-1* Wild type	C. Rensing
GR538	As W3110 Δ*zupT::cat* Δ*feoABC* Δ*entC* Δ*fecABCDE::kan*	[26]
GR540	As W3110 Δ*feoABC::cat* Δ*entC* Δ*fecABCDE::kan*	C. Rensing
JEM609	As SJ130 Δ*tonB1* Δ*feoABC* Δ*zupT::cat*	This study
JEM715	As MG1655 Δ*nrdAB1::cat~zbf-723::*Tn*10*	This study
JEM720	As JEM609 Δ*nrdAB1::cat~zbf-723::*Tn*10*	P1(JEM715) X JEM609
JEM722	As SJ130 Δ*nrdHIEF1* Δ*nrdAB1::cat~zbf-723::*Tn*10*	P1(JEM715) X JEM610
JEM865	As JEM609 Δ*nrdAB1::cat*	P1(JEM80) X JEM609
JEM646	As SJ130 Δ(*nrdHIEF::kan*)*6*::φ(*nrdH´-lac*$^+$)*6*	This study
JEM648	As SJ130 Δ(*nrdHIEF6::kan*)*6*::φ(*nrdH´-´lacZ lacY*$^+$)*6*	This study
JEM806	As SJ130 Δ*nrdR1* Δ(*nrdHIEF6::kan*)*6*::φ(*nrdH´-´lacZ lacY*$^+$)*6*	This study
JW0669-2	*F-* Δ*(araD-araB)567* Δ*lacZ4787*(::rrnB-3) *rph-1* Δ*(rhaD-rhaB)568 hsdR514* Δ*fur-731::kan*	*E. coli* CGSC
JEM918	As SJ130 Δ*fur-731* Δ(*nrdHIEF6::kan*)*6*::φ(*nrdH´-´lacZ lacY*$^+$)*6*	This study
JEM814	As SJ130 *iscR*-(C92A/C98A/C104A) Δ(*zfh-3600::kan*)*1* Δ*fur::kan* Δ*nrdAB1::cat~zbf-723::*Tn*10*	This study
JEM824	As JEM806 Δ*fur::kan~zbf-507::*Tn*10*	This study
JEM657	As JEM648 Δ*fur::kan~zbf-507::*Tn*10*	P1(JEM302) X JEM648

Table 2.1. (continued)

JEM707	As JEM648 Δ*tonB1::cat*	P1(AW514) X JEM648
JEM709	As JEM657 Δ*tonB1::cat*	P1(AW25113) X JEM657
SMV41	*mntH9::kan~zff-1::*Tn*10*	Lab strain
JEM1144	As JEM609 *mntH9::kan~zff-1::*Tn*10*	P1(SMV41) X JEM609
JEM1137	As JEM609 Δ*nrdAB1 mntH9::kan~zff-1::*Tn*10*	P1(SMV41) X JEM609
SJ285	As SJ130 Δ*iscR1::cat*	Lab strain
JEM762	As SJ130 Δ*iscR1* Δ(*nrdHIEF::kan*)*6*::φ(*nrdH´-lac*$^{+}$)*6*	P1(JEM646) X JEM755
PK7887	*iscR*-(C92A/C98A/C104A)~*zfh-3600::kan*	[50]
JEM776	As SJ130 *iscR*-(C92A/C98A/C104A) Δ(*zfh-3600::kan*)*1* Δ(*nrdHIEF::kan*)*6*::φ(*nrdH´-lac*$^{+}$)*6*	P1(JEM646) X JEM766
JEM436	As SJ130 *attλ::*[pSJ501::*nrdE´-lacZ*$^{+}$] Cam^{R}	This study
JEM738	As MG1655 Δ*lacZ1* Δ*nrdAB1 attλ::*[pSJ501::*nrdE´-lacZ*$^{+}$]	P1(JEM436) X JEM178
JEM756	As MG1655 Δ*lacZ1* Δ*nrdAB1 attλ::*[pSJ501::*mntH´-lacZ*$^{+}$]	This study
JEM757	AS JEM609 Δ*nrdAB1::cat~zbf-723::*Tn*10 attλ::*[pSJ501::*mntH´-lacZ*$^{+}$]	This study
CAG18562	F^{-} *λ*$^{-}$ *zga-3114::*Tn*10*(*kan*) *rph-1*	*E. coli* CGSC
JEM955	As SJ130 ΔP*nrdH::tetRA-67*~Δ(*nrdHIEF::*kan)6::Φ(*nrdH'-'lacZ lacY*$^{+}$)6	This study
JEM979	As SJ130 Δ*fur-731* ΔP*nrdH::tetRA-67*~Δ(*nrdHIEF::kan*)6::Φ(*nrdH'-'lacZ lacY*$^{+}$)6	This study
JEM973	As SJ130 ΔP*mntH::tetRA*-7 ΔP*nrdH::tetRA*-67*~zga-3144::*Tn*10(kan)*	This study
JEM975	As JEM609 ΔP*mntH::tetRA*-7 ΔP*nrdH::tetRA*-67*~zga-3144::*Tn*10(kan)*	This study
JEM1040	As JEM973 Δ*nrdAB1::cat*	P1(JEM81) X JEM973
JEM1042	As JEM975 Δ*nrdAB1::cat*	P1(JEM81) X JEM975
KK183	As AB1157 (*sodA::*Mud PR13)25 (*sodB-kan*)1-Δ2~*zdg-299::*Tn*10*	Lab strain
JEM1133	As JEM865 (*sodB-kan*)1-Δ2~*zdg-299::*Tn*10*	P1(KK183) X JEM865
AAM1	F- *thr-1 leuB6 proA2 his-4 thi-1 argE2 lacY1 galK2 rpsL supE44 ara-14 xyl-15 mtl-1 tsx-33* Δ*thyA71::cat*	[42]
JEM198	As LC106 Δ*nrdEF1::cat* Δ*thyA71::cat*	This study
JEM206	As LC106 Δ*nrdAB1* Δ*nrdEF1::cat~srl300::*Tn*10* Δ*thyA71::cat*	This study
JEM1018	As SJ130 attλ::[pSJ501::*nrdE'-lacZ*$^{+}$]7	This study
JEM1024	As JEM1018 Δ*fur-731::kan*	This study
JEM1034	As SJ130 *attλ::*[pSJ501::*nrdE´-lacZ*$^{+}$] Cam^{s}	This study
JEM1054	As JEM1034 Δ*fur-731::kan*	This study
JEM659	As BW25113 Δ*hfq1::cat*	This study
JEM1154	As JEM1034 Δ*hfq1:: cat*	This study
JEM1156	As JEM1054 Δ*hfq1::cat*	This study

Table 2.1. (continued)

JEM1058	As JEM257 with pACYC184	This study
JEM1060	As JEM1034 with pACYC184	This study
JEM914	As MG1655 with pBAD-N-S-*nrdB*	This study
JEM915	As LC106 with pBAD-N-S-*nrdB*	This study
JEM1185	(*sodB-kan*)1-Δ2 Δ*sodA1* Δ*lacZ1* with pBAD-N-S-*nrdB*	This study
JEM1033	As MG1655 with pBAD-N-S-2-*nrdF*	This study
JEM1121	As MG1655 with pBAD-N-S-2-*nrdF*	This study

Plasmids	**Relevant characteristics**	**Reference**
pSJ501	pAH125 derivative with *cat* flanked by *flp* sites	[34]
pAH57	CRIM helper plasmid	[28]
pJEM51	pSJ501::*nrdH´-lacZ*$^+$	This study
pJEM54	pSJ501::*nrdE´-lacZ*$^+$	This study
pJEM66	pSJ501::(*nrdE´-lacZ*$^+$)7	This study
pAA03	pSJ501::*mntH´-lacZ*$^+$	[2]
pKD3	*bla* FRT *cat* FRT PS1 PS2 oriR6K	[13]
pKD46	*bla* P_{BAD} *gam bet exo* pSC101 oriTS	[13]
pKD13	*bla* FRT *ahp* FRT PS1 PS4 oriR6K	[13]
pCE40	*ahp* FRT ´*lacZY*$^+$ t_{his} oriR6K	[16]
pKG137	*ahp* FRT *lacZY*$^+$ t_{his} oriR6K	J. M. Slauch
pCP20	*bla cat cI857* λP_R *flp* pSC101 oriTS	[8]
pPK7312	pACYC184 containing EcoRI 1303-bp *FRT-kan-FRT* StuI-EcoRV 985-bp *iscR*	[50]
pPK7867	pACYC184 containing EcoRI 1303-bp *FRT-kan-FRT* StuI-EcoRV 985-bp *iscR*-(C92A/C98A/C104A)	[50]
pACYC184	Tet^r Cm^r	[41]
pGS058	pACYC184 containing *oxyR2* [A233V]	[41]
pBAD-N-S-*nrdB*	pBAD containing N-terminal StrepII-*nrdB*	[30]
pBAD-N-S-2-*nrdF*	pBAD containing N-terminal StrepII-*nrdF*	J. Stubbe

Table 2.2. qRT-PCR primers used in this study [48].

Primer	Sequence	Fragment Size (bp)
nrdH	5′-GTTGCGTGCTCAGGGCTTTCGTCAGT-3′	105
*nrdH**	5′-TGTGGCGCTGGATGCAGACGGTTAAT-3′	
nrdI	5′-GCCAGCTCGTCTACTTCTCCAGCAGC-3′	112
*nrdI**	5′-TCTACCTGAATCCGTTCCCGCTCATT-3′	
nrdE	5′-CGTCCGAACAGTGTGACCTTCAGTAGCC-3′	130
*nrdE**	5′-GTGCGTGGGTAAACAGCGTAATGACAAA-3′	
nrdF	5′-GGCTACGAACCGTTATTTCCCGCAGAA-3′	136
*nrdF**	5′-CAACCGCTTTCCCCATCACATAAGAGG-3′	
gapA	5′-CGTTCTGGGCTACACCGAAGATGACG-3′	143
*gapA**	5′-AACCGGTTTCGTTGTCGTACCAGGA-3′	

2.6 FIGURES

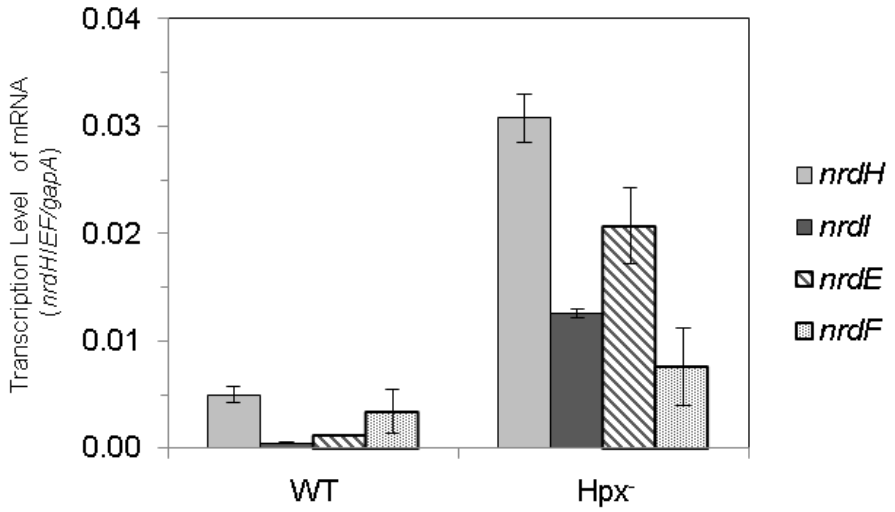

Figure 2.1. The *nrdHIEF* operon is induced during H_2O_2 stress. RNA was isolated from cells grown in aerobic LB medium. Data are representative of two independent experiments each measured in triplicate. Strains used were SJ130 (wild type) and SJ108 (Hpx^-).

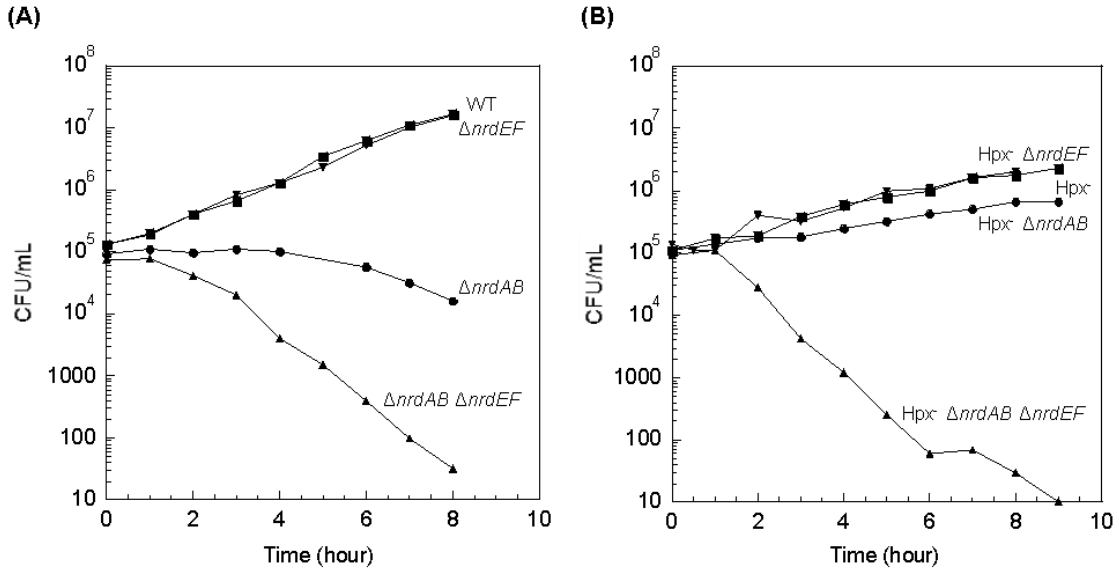

Figure 2.2. NrdAB and NrdEF are both functional during protracted H_2O_2 stress. Cells were pre-cultured in anaerobic glucose/aromatic medium and then diluted at time zero into the same aerobic medium. Viability was tracked by anaerobic plating.

A. Cell viability during routine growth. MG1655 (wild type), JEM84 (Δ*nrdAB*), JEM89 (Δ*nrdEF*), and JEM118 (Δ*nrdAB* Δ*nrdEF*).

B. Cell viability during protracted H_2O_2 stress (*ca.* 0.5 μM). LC106 (Hpx$^-$), JEM86 (Hpx$^-$ Δ*nrdAB*), and JEM90 (Hpx$^-$ Δ*nrdEF*), and JEM119 (Hpx$^-$ Δ*nrdAB* Δ*nrdEF*).

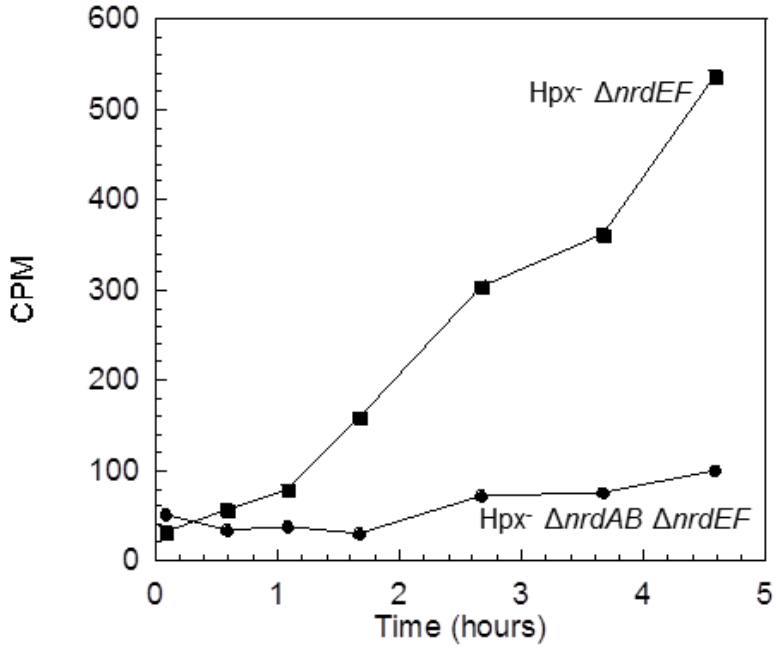

Figure 2.3. The NrdAB ribonucleotide reductase enables chromosome replication during H_2O_2 stress. Hpx$^-$ Δ*thyA* mutants were pre-cultured in anaerobic glucose/amino acids medium with thymidine and then diluted at time zero into aerobic medium containing ^{3}H-thymidine. Total thymidine incorporated into DNA was tracked by radioactivity measurements. Strains used were JEM198 (Hpx$^-$ Δ*nrdEF*) and JEM206 (Hpx$^-$ Δ*nrdAB* Δ*nrdEF*).

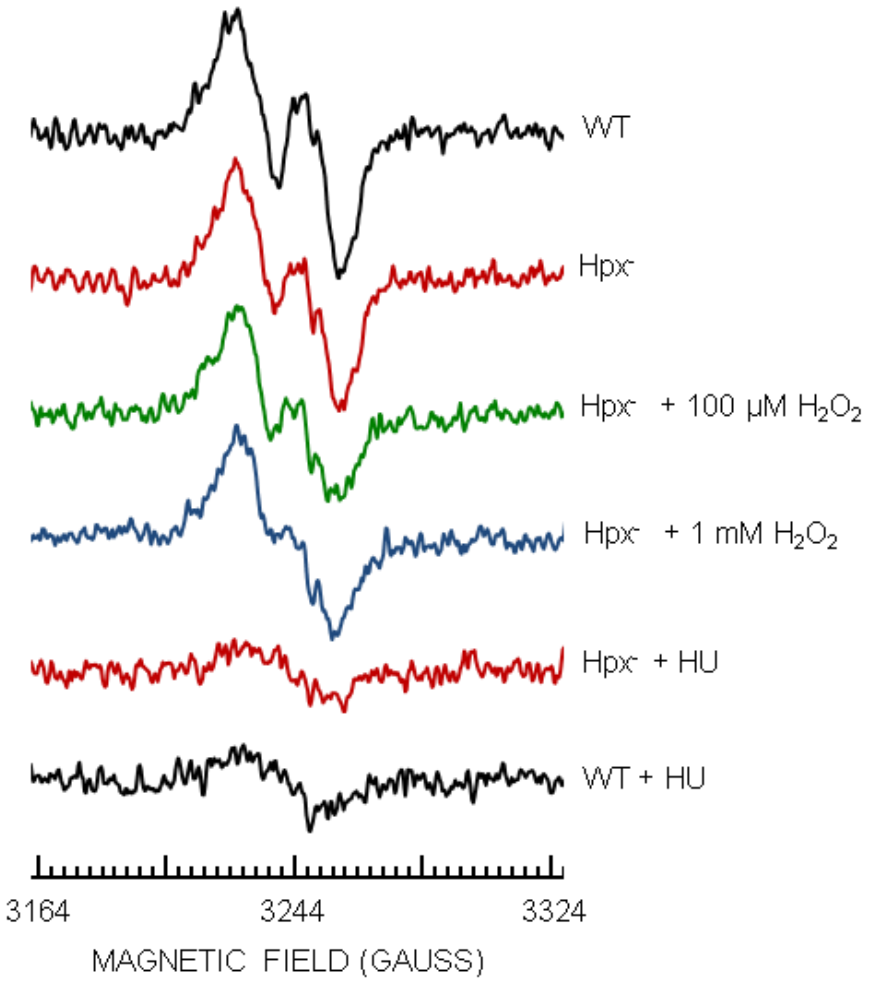

Figure 2.4. H_2O_2 does not eliminate the tyrosyl radical of NrdB. The expression of *nrdB* was induced in aerobic LB medium for 2 h in wild-type (JEM914) or Hpx$^-$ (JEM915) strains harboring pBAD-N-S-*nrdB*. Cells were washed and concentrated, and where indicated H_2O_2 was added for 5 min at 37°C. The intact cells were then transferred to EPR tubes and analyzed. HU: hydroxyurea was added to quench the NrdB tyrosyl radical.

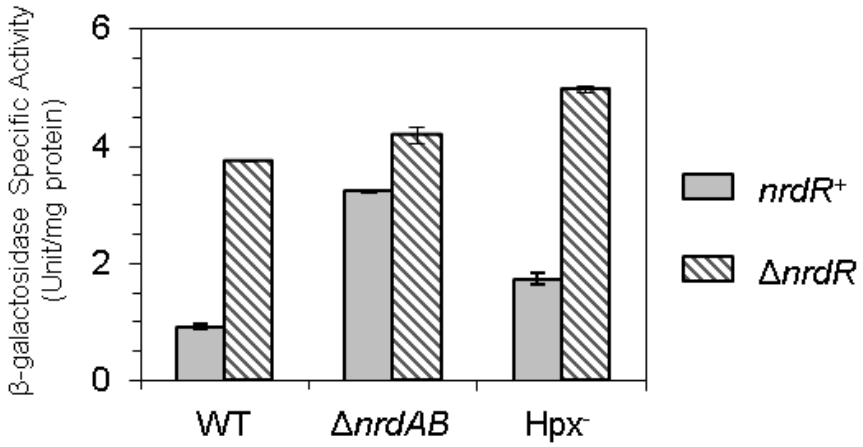

Figure 2.5. During H_2O_2 stress NrdAB retains sufficient function to activate NrdR. Cells bearing a P_{nrdH}-*lacZ* transcriptional fusion were grown in anaerobic glucose/amino acids medium and then aerated for 60 min before harvesting. Data represent the mean of three independent cultures. The strains used were JEM228 (wild type), JEM284 (Δ*nrdR*), JEM307 (Δ*nrdAB*), JEM312 (Δ*nrdAB* Δ*nrdR*), JEM245 (Hpx^-), and JEM304 (Hpx^- Δ*nrdR*).

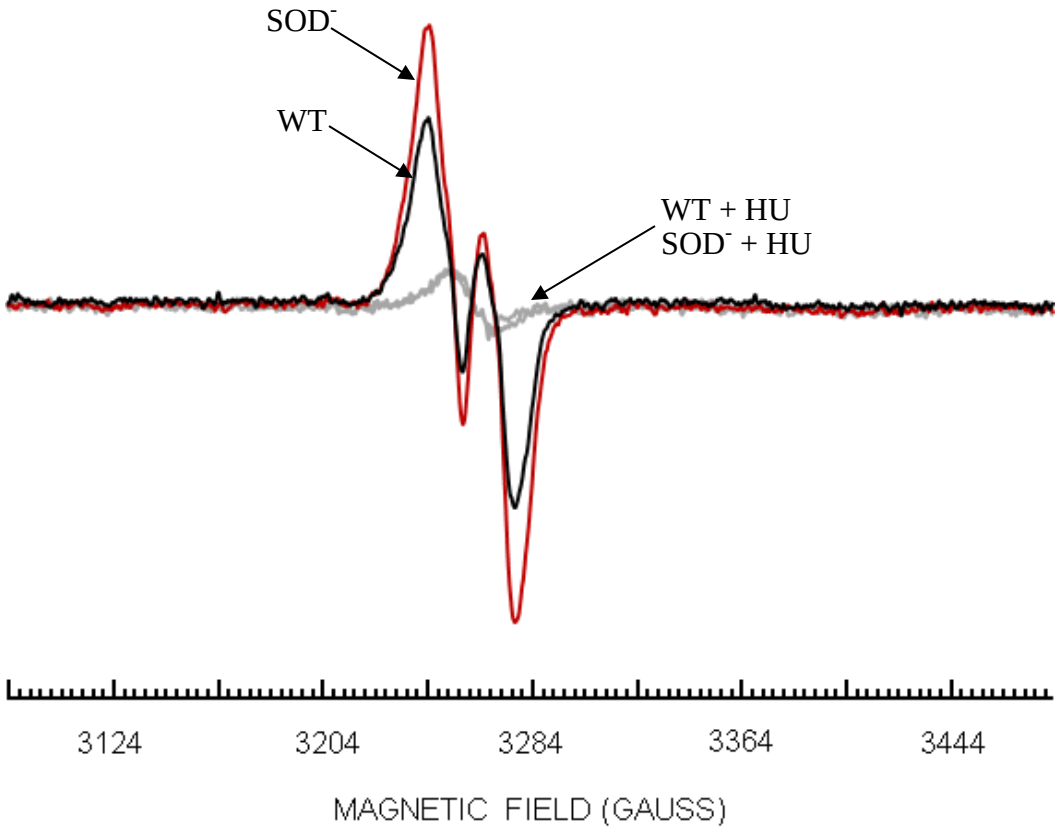

Figure 2.6. Superoxide does not eliminate the tyrosyl radical of NrdB *in vivo*. The expression of *nrdB* was induced in aerobic LB medium for two hours in wild-type (JEM914) or SOD$^-$ (JEM1185) strains harboring pBAD-N-S-*nrdB*. Cells were washed, concentrated, and transferred to EPR tubes and then analyzed. Gray (JEM914) and green (JEM1185): Hydroxyurea (160 mM) was added for 1 h after *nrdB* expression prior to EPR analysis.

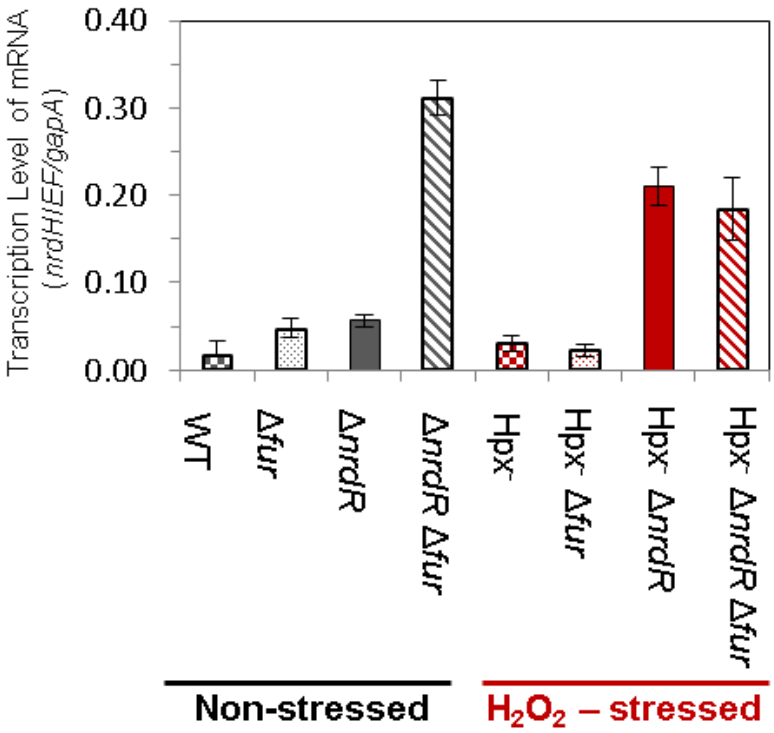

Figure 2.7. During H_2O_2 stress the expression of *nrdHIEF* is due to derepression of the Fur regulon. RNA was isolated from cells grown in aerobic LB medium. Data are representative of two independent experiments each measured in triplicate. Strains were SJ130 (wild type), JEM275 (Δ*fur*), JEM406 (Δ*nrdR*), JEM286 (Δ*nrdR* Δ*fur*), SJ108 (Hpx$^-$), JEM309 (Hpx$^-$ Δ*fur*), JEM407 (Hpx$^-$ Δ*nrdR*), and JEM311 (Hpx$^-$ Δ*nrdR* Δ*fur*).

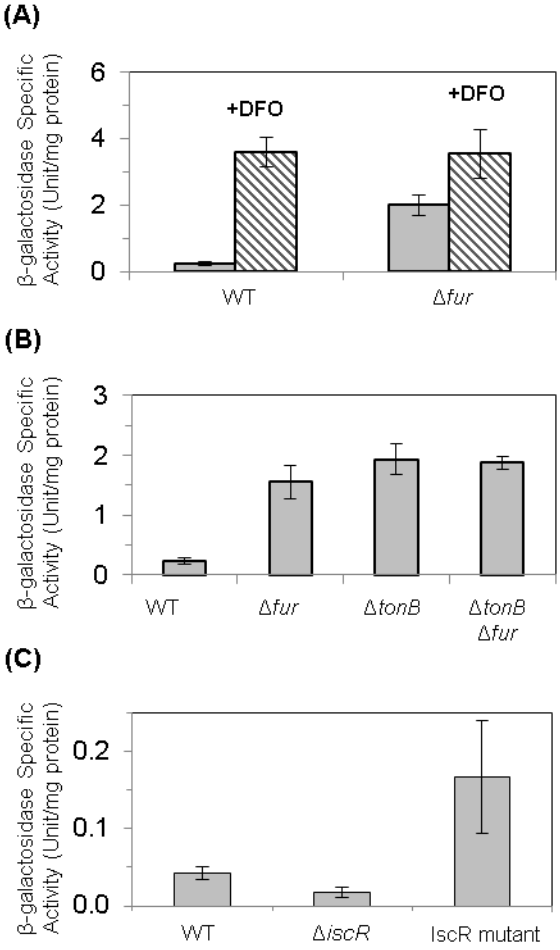

Figure 2.8. Fur and IscR both regulate the expression of *nrdHIEF*. Cells bearing the *nrdH'-'lacZ* translational fusion were grown in aerobic media. Data represent the mean of three independent cultures.

A. JEM648 (wild type) and JEM657 (Δ*fur*) were grown in glucose/amino acids medium with or without 100 µM of the iron chelator DFO.

B. JEM648 (wild type), JEM657 (Δ*fur*), JEM707 (Δ*tonB*), and JEM709 (Δ*tonB* Δ*fur*) were grown in LB medium.

C. Expression of a *nrdH'-lac*$^{+}$ transcriptional fusion in LB medium from JEM646 (wild type), JEM762 (Δ*iscR*), and JEM776 (*iscR*-C92A/C98A/C104A).

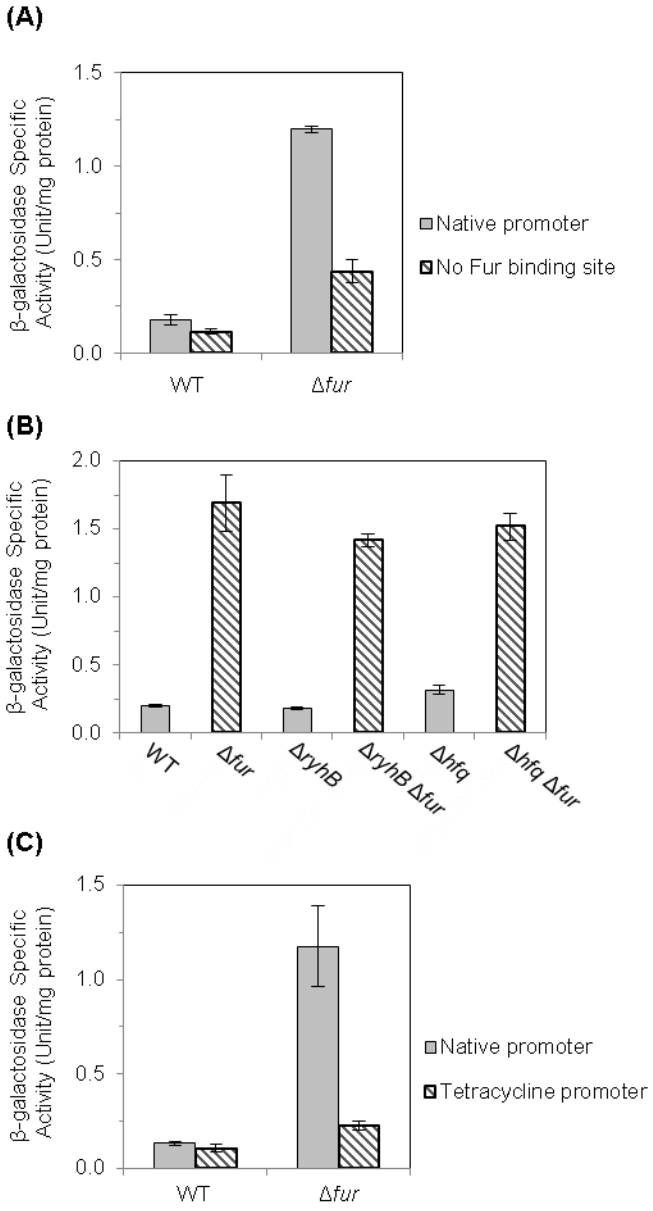

Figure 2.9. Fur regulates *nrdHIEF*. Cells bearing P_{nrdE}-*lacZ* transcription fusions were grown in aerobic LB medium. Data represent the mean of three independent cultures.
A. Expression with native promoter from JEM436 (wild type) and JEM1054 (Δ*fur*) or without Fur binding site from JEM1018 (wild type) and JEM1024 (Δ*fur*).
B. Expression from JEM1034 (wild type), JEM1054 (Δ*fur*), JEM1158 (Δ*ryhB*), JEM1160 (Δ*ryhB* Δ*fur*), JEM1154 (Δ*hfq*), and JEM1156 (Δ*hfq* Δ*fur*).
C. Expression of *nrdH'-'lacZ* with native promoter from JEM648 (wild type) and JEM918 (Δ*fur*) or with a tetracycline promoter from JEM955 (wildtype) and JEM979 (Δ*fur*).

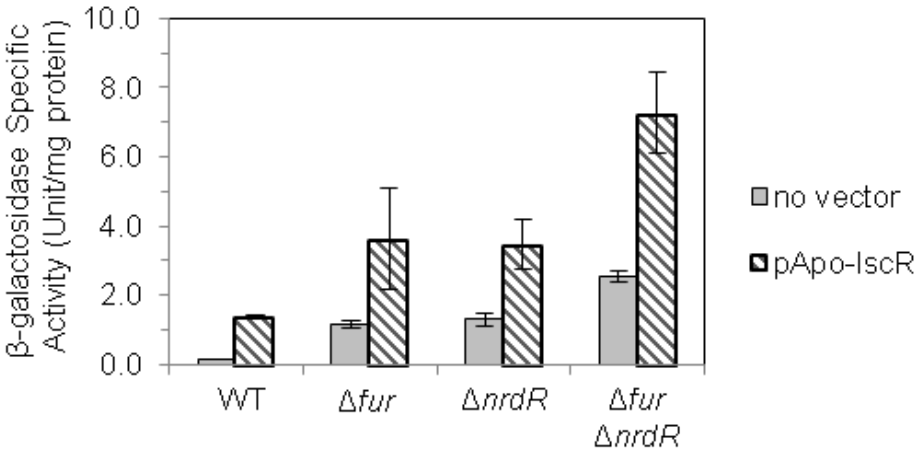

Figure 2.10. NrdR, Fur, and apo-IscR independently regulate *nrdHIEF* expression. Cell bearing a *nrdH'-'lacZ* translational fusion were grown in aerobic LB medium. Data represent the mean of three independent cultures. Strains used were JEM648 (wild type), JEM657 (Δ*fur*), JEM806 (Δ*nrdR*), and JEM824 (Δ*fur* Δ*nrdR*) with or without pPK7867 (*iscR*-(C92A/C98A/C104A).

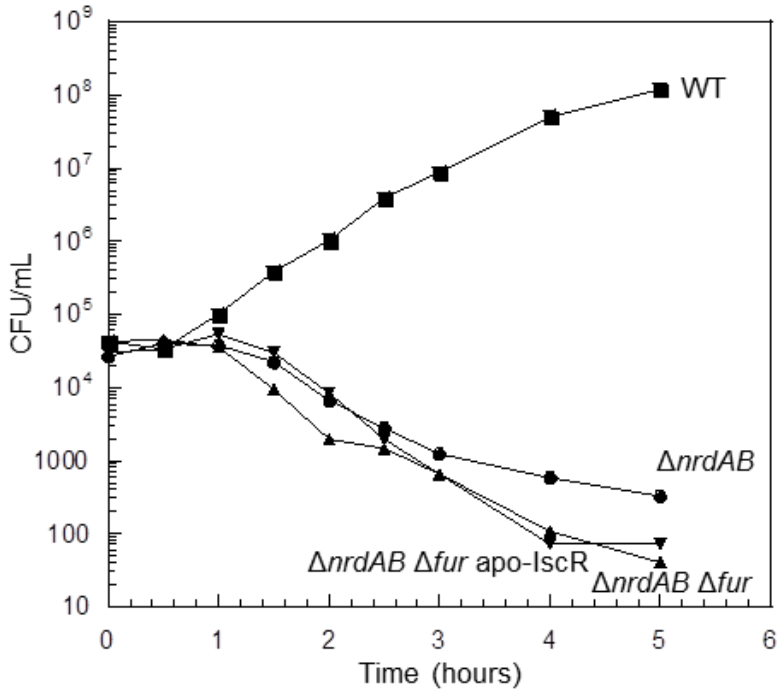

Figure 2.11. Transcription of *nrdHIEF* is not sufficient for NrdEF to become functional. Cells grown in anaerobic LB medium were diluted at time zero into aerobic medium and viability was tracked by anaerobic plating. Strains used were MG1655 (wild type), JEM84 (Δ*nrdAB*), JEM307 (Δ*nrdAB* Δ*fur*), and JEM814 (Δ*nrdAB* Δ*fur iscR*-(C92A/C98A/C104A)).

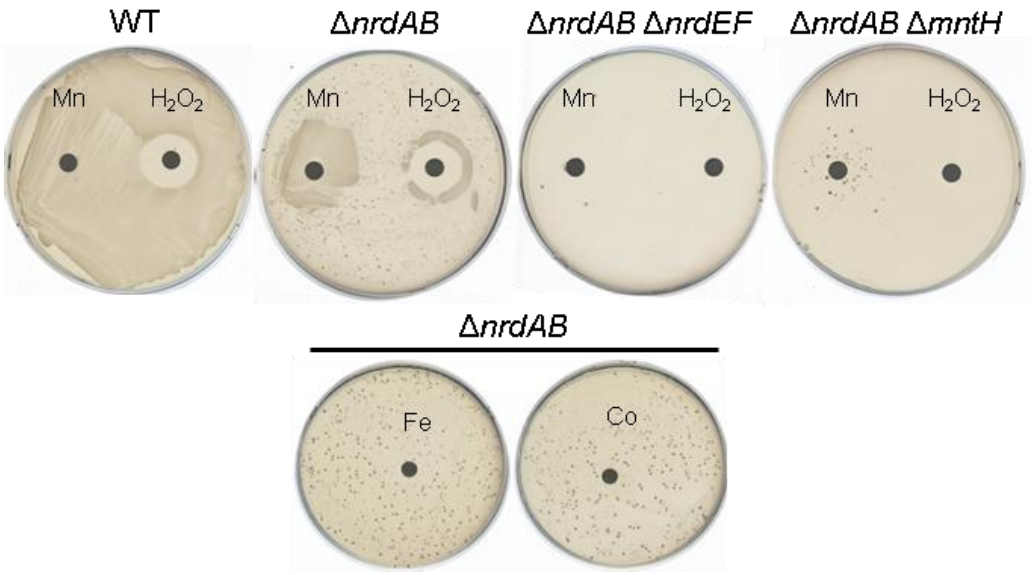

Figure 2.12. NrdEF function requires manganese import. Anaerobically grown cells were spread onto aerobic glucose/aromatic plates. Sterile disks impregnated with 5 µmol of H_2O_2 or 5 nmol of metal solution [$MnCl_2$, $Fe(NH_4)_2SO_4$ or $CoCl_2$] were placed on each plate. Results are shown after 48 h of aerobic incubation at 37°C. Strains were MG1655 (wild type), JEM84 (Δ*nrdAB*), JEM118 (Δ*nrdAB* Δ*nrdEF*), JEM128 (Δ*nrdAB* Δ*mntH*). Note: the scattered suppressor colonies were not stable and may represent the amplification of the *nrdHIEF* locus.

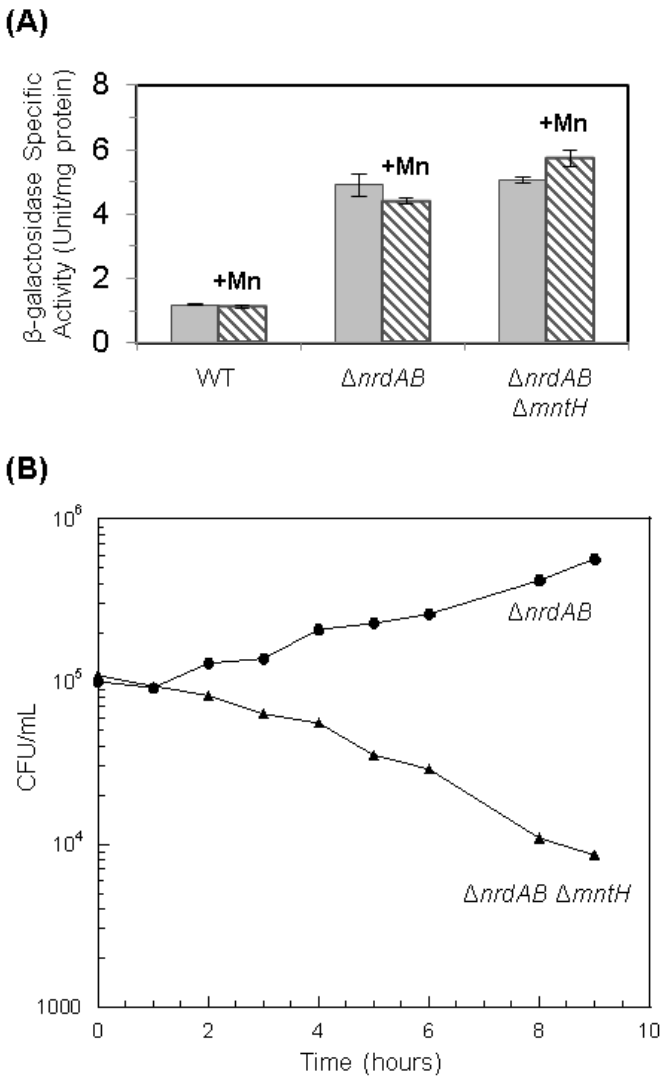

Figure 2.13. Manganese is required for NrdEF function but not expression.
A. Cells bearing a P_{nrdH}-*lacZ* transcriptional fusion were grown in anaerobic glucose/amino acids medium with or without 50 μM manganese and then aerated for 60 min before harvesting. Data represent the mean of three independent cultures. The strains were JEM228 (wild type), JEM233 (Δ*nrdAB*), and JEM235 (Δ*nrdAB* Δ*mntH*).
B. Cells were grown in anaerobic glucose/aromatic medium and diluted at time zero into aerobic medium with 1 μM $MnCl_2$. Viability was determined by plating on anaerobic medium. Strains used were JEM84 (Δ*nrdAB*) and JEM128 (Δ*nrdAB* Δ*mntH*).

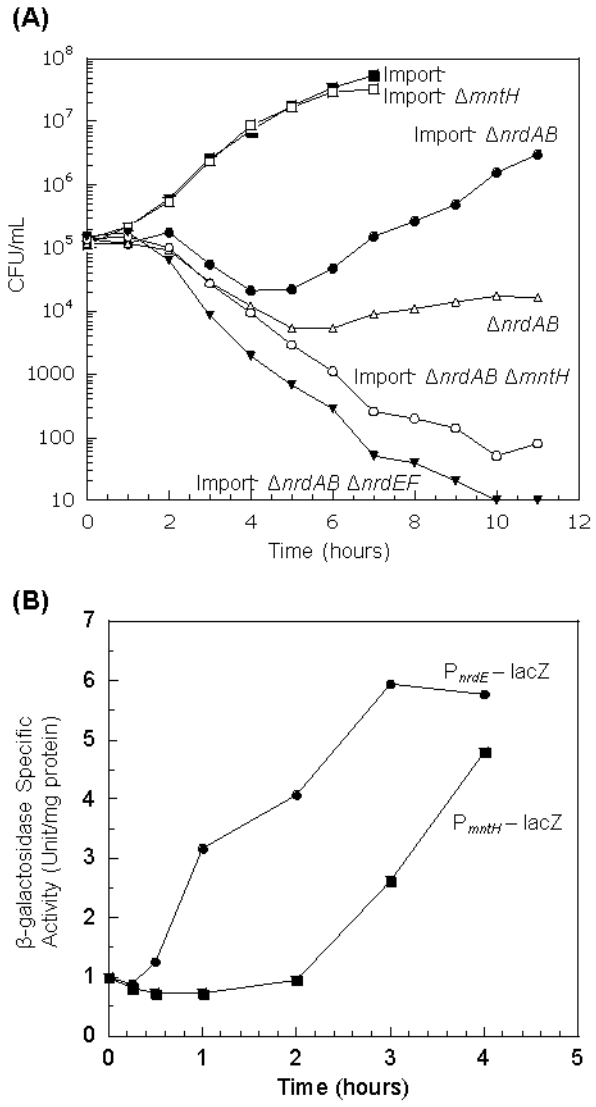

Figure 2.14. NrdEF is functional when iron is limited and manganese is available. **A.** Cells in anaerobic MOPS glucose/amino acids medium were diluted into aerobic medium at time zero, and viability was monitored. 'Import-minus' strains contain Δ*tonB* Δ*feoABC* Δ*zupT* null alleles and therefore have reduced iron import. Strains used were JEM609 (Import$^-$), JEM1144 (Import$^-$ Δ*mntH*), JEM720 (Import$^-$ Δ*nrdAB*), JEM1137 (Import$^-$ Δ*nrdAB* Δ*mntH*), JEM722 (Import$^-$ Δ*nrdAB* Δ*nrdHIEF*), and JEM756 (Δ*nrdAB*). **B.** Delayed expression of *mntH* during iron limitation coincides with delayed NrdEF function. Iron-limited Δ*nrdAB* strains bearing P_{nrdE} – *lacZ* (JEM738) or P_{mntH} – *lacZ* (JEM757) transcription fusions aerated at time zero. Data are normalized to the anaerobic expression level and are representative of at least two independent experiments.

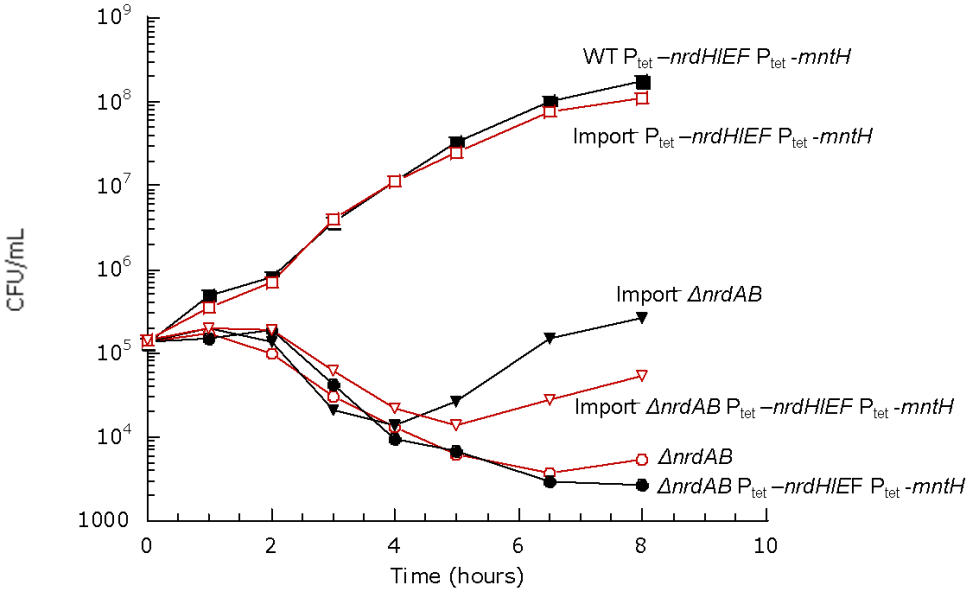

Figure 2.15. Iron limitation is necessary to activate NrdEF. Cells in anaerobic MOPS glucose/amino acids medium were diluted into aerobic medium at time zero, and the number of viable cells was monitored. "Import-minus" strains contain Δ*tonB* Δ*feoABC* Δ*zupT* null alleles and therefore have reduced iron import. Where *mntH* and *nrdHIEF* synthesis are directed by the tet promoter, 10 μM $MnCl_2$ and 2 μg/ml tetracycline were included in the medium. Strains using native promoters were JEM756 (Δ*nrdAB*) and JEM757 (Import$^-$ Δ*nrdAB*). Strains using P_{tet} – *nrdHIEF* and P_{tet} – *mntH* were JEM973 (wild type), JEM1040 (Δ*nrdAB*), JEM975 (Import$^-$), and JEM1042 (Import$^-$ Δ*nrdAB*).

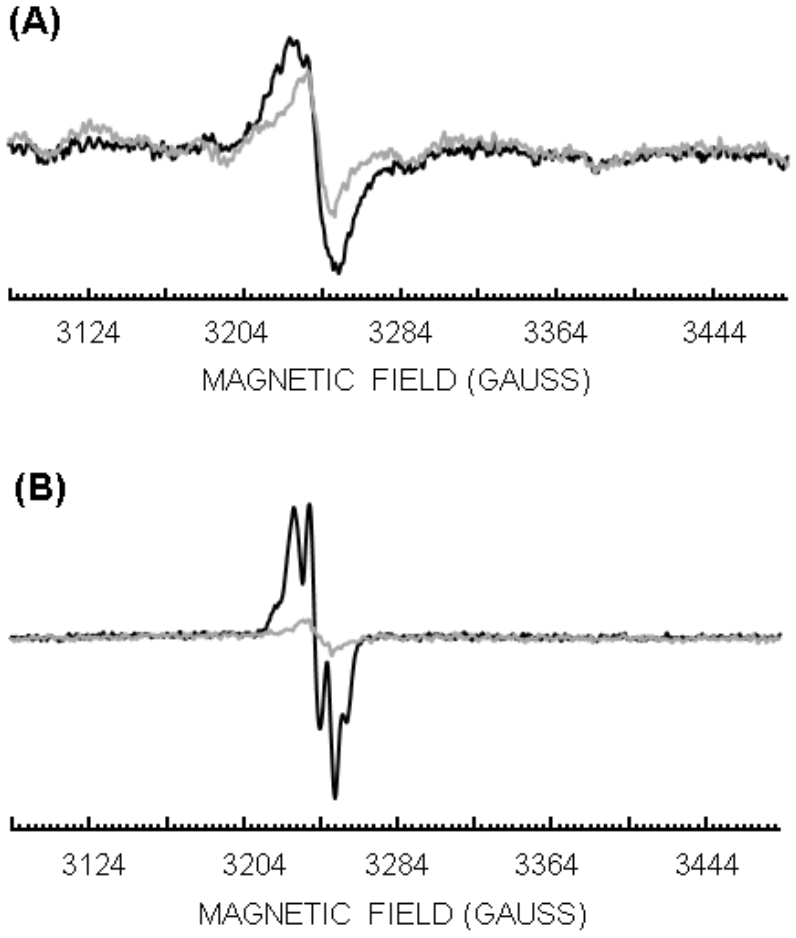

Figure 2.16. EPR spectra of NrdF expressed in iron-deficient and iron-replete cells.
A. Iron-deficient (Δ*tonB* Δ*feoABC* Δ*zupT*) cells with (JEM1121, black) or without (JEM865, gray) plasmid pBAD-N-S-2-*nrdF*. Cells were cultured in aerobic MOPS glucose/amino acids medium, and arabinose was added for 2 h before harvesting and whole-cell EPR analysis.
B. Iron-replete wild-type cells harboring pBAD-N-S-*nrdF* (JEM1033) were cultured in aerobic LB medium, and arabinose was added for 2 h before harvesting and whole-cell EPR analysis (black). Gray: 160 mM hydroxyurea was added for 1 h after *nrdF* expression prior to EPR analysis.

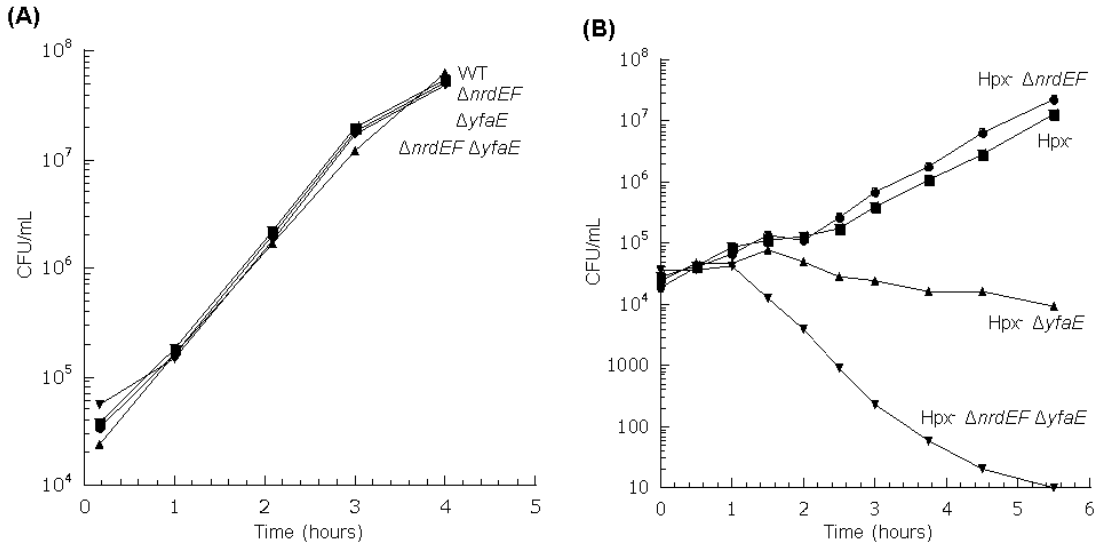

Figure 2.17. NrdAB exhibits activity during H_2O_2 stress only if YfaE is active. Cells in anaerobic LB medium were diluted into aerobic medium at time zero, and the number of viable cells was monitored.

A. Viable cells during routine (unstressed) aerobic growth. Strains were MG1655 (wild type), JEM273 (Δ*nrdEF*), JEM290 (Δ*yfaE*), and JEM296 (Δ*nrdEF* Δ*yfaE*).

B. Viable cells during protracted H_2O_2 stress. Strains were LC106 (Hpx^-), JEM646 (Hpx^- Δ*nrdEF*), JEM325 (Hpx^- Δ*yfaE*), and JEM475 (Hpx^- Δ*nrdEF* Δ*yfaE*).

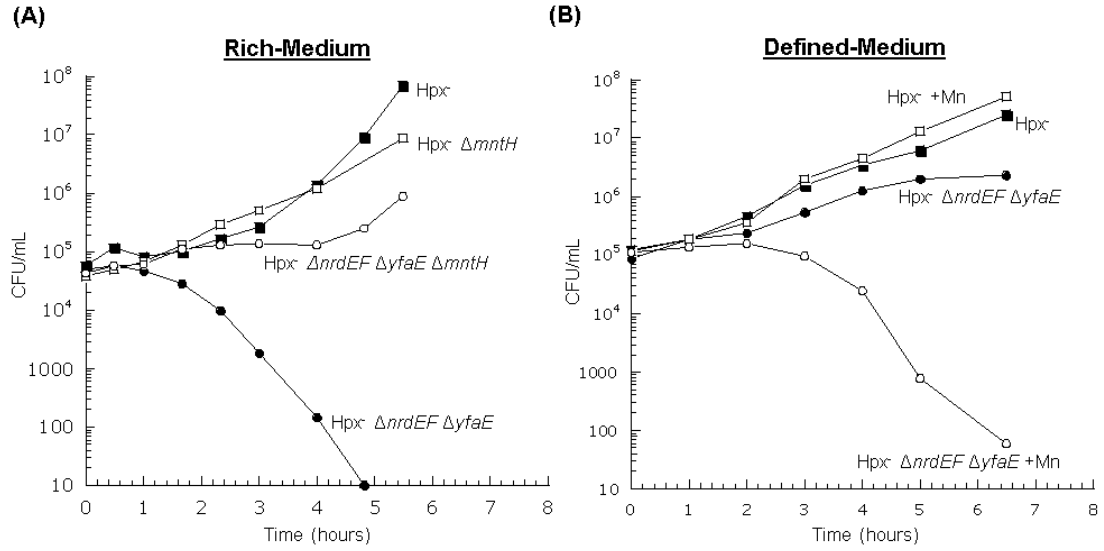

Figure 2.18. In H_2O_2-stressed cells, imported manganese can poison NrdAB if YfaE is absent.

A. Cells in anaerobic LB medium were diluted into aerobic medium at time zero. Strains were LC106 (Hpx$^-$), AA30 (Hpx$^-$ Δ*mntH*), JEM475 (Hpx$^-$ Δ*nrdEF* Δ*yfaE*), and JEM504 (Hpx$^-$ Δ*nrdEF* Δ*yfaE* Δ*mntH*).

B. Cells in anaerobic glucose/amino acids medium were diluted into aerobic medium. Where indicated, 50 μM $MnCl_2$ was included. Strains were LC106 (Hpx$^-$) and JEM475 (Hpx$^-$ Δ*nrdEF* Δ*yfaE*).

2.7 REFERENCES

1. **Abbouni, B., W. Oehlmann, P. Stolle, A. J. Pierik, and G. Auling.** 2009. Electron paramagnetic resonance (EPR) spectroscopy of the stable-free radical in the native metallo-cofactor of the manganese-ribonucleotide reductase (Mn-RNR) of *Corynebacterium glutamicum*. Free Radic. Res. **43:**943-950.

2. **Anjem, A., S. Varghese, and J. A. Imlay.** 2009. Manganese import is a key element of the OxyR response to hydrogen peroxide in *Escherichia coli*. Mol. Microbiol. **72:**844-858.

3. **Aslund, F., M. Zheng, J. Beckwith, and G. Storz.** 1999. Regulation of the OxyR transcription factor by hydrogen peroxide and the cellular thiol---disulfide status. Proc. Natl. Acad. Sci. U. S. A. **96:**6161-6165.

4. **Atta, M., P. Nordlund, A. Aberg, H. Eklund, and M. Fontecave.** 1992. Substitution of manganese for iron in ribonucleotide reductase from *Escherichia coli*. Spectroscopic and crystallographic characterization. J. Biol. Chem. **267:**20682-20688.

5. **Boal, A. K., J. A. Cotruvo Jr, J. Stubbe, and A. C. Rosenzweig.** 2010. Structural basis for activation of class Ib ribonucleotide reductase. Science. **329:**1526-1530.

6. **Brown, N. C., R. Eliasson, P. Reichard, and L. Thelander.** 1968. Nonheme iron as a cofactor in ribonucleotide reductase from *E. coli*. Biochem. Biophys. Res. Commun. **30:**522-527.

7. **Chai, S. C., W. L. Wang, and Q. Z. Ye.** 2008. FE(II) is the native cofactor for *Escherichia coli* methionine aminopeptidase. J. Biol. Chem. **283:**26879-26885.

8. **Cherepanov, P. P., and W. Wackernagel.** 1995. Gene disruption in *Escherichia coli*: TcR and KmR cassettes with the option of Flp-catalyzed excision of the antibiotic-resistance determinant. Gene. **158:**9-14.

9. **Compan, I., and D. Touati.** 1993. Interaction of six global transcription regulators in expression of manganese superoxide dismutase in *Escherichia coli* K-12. J. Bacteriol. **175:**1687-1696.

10. **Cotruvo, J. A., Jr, and J. Stubbe.** 2008. NrdI, a flavodoxin involved in maintenance of the diferric-tyrosyl radical cofactor in *Escherichia coli* class Ib ribonucleotide reductase. Proc. Natl. Acad. Sci. U. S. A. **105:**14383-14388.

11. **Cotruvo, J. A., Jr, and J. Stubbe.** 2010. An active dimanganese(III)-tyrosyl radical cofactor in *Escherichia coli* class Ib ribonucleotide reductase. Biochemistry. **49:**1297-1309.

12. **Csonka, L. N., and A. J. Clark.** 1980. Construction of an Hfr strain useful for transferring recA mutations between *Escherichia coli* strains. J. Bacteriol. **143:**529-530.

13. **Datsenko, K. A., and B. L. Wanner.** 2000. One-step inactivation of chromosomal genes in *Escherichia coli* K-12 using PCR products. Proc.Natl. Acad. Sci. U. S. A. **97:**6640-6645.

14. **Drlica, K., E. C. Engle, and S. H. Manes.** 1980. DNA gyrase on the bacterial chromosome: possibility of two levels of action. Proc. Natl. Acad. Sci. U. S. A. **77:**6879-6883.

15. **Ehrenberg, A., and P. Reichard.** 1972. Electron spin resonance of the iron-containing protein B2 from ribonucleotide reductase. J. Biol. Chem. **247:**3485-3488.

16. **Ellermeier, C. D., A. Janakiraman, and J. M. Slauch.** 2002. Construction of targeted single copy lac fusions using lambda Red and FLP-mediated site-specific recombination in bacteria. Gene. **290:**153-161.

17. **Fieschi, F., E. Torrents, L. Toulokhonova, A. Jordan, U. Hellman, J. Barbe, I. Gibert, M. Karlsson, and B. M. Sjoberg.** 1998. The manganese-containing ribonucleotide reductase of *Corynebacterium ammoniagenes* is a class Ib enzyme. J. Biol. Chem. **273:**4329-4337.

18. **Flint, D. H., J. F. Tuminello, and M. H. Emptage.** 1993. The inactivation of Fe-S cluster containing hydro-lyases by superoxide. J. Biol. Chem. **268:**22369-22376.

19. **Fontecave, M., R. Eliasson, and P. Reichard.** 1987. NAD(P)H:flavin oxidoreductase of *Escherichia coli*. A ferric iron reductase participating in the generation of the free radical of ribonucleotide reductase. J. Biol. Chem. **262:**12325-12331.

20. **Fontecave, M., R. Eliasson, and P. Reichard.** 1989. Enzymatic regulation of the radical content of the small subunit of *Escherichia coli* ribonucleotide reductase involving reduction of its redox centers. J. Biol. Chem. **264:**9164-9170.

21. **Fontecave, M., A. Graslund, and P. Reichard.** 1987. The function of superoxide dismutase during the enzymatic formation of the free radical of ribonucleotide reductase. J. Biol. Chem. **262:**12332-12336.

22. **Garriga, X., R. Eliasson, E. Torrents, A. Jordan, J. Barbe, I. Gibert, and P. Reichard.** 1996. *nrdD* and *nrdG* genes are essential for strict anaerobic growth of *Escherichia coli*. Biochem. Biophys. Res. Commun. **229:**189-192.

23. **Gaudu, P., V. Niviere, Y. Petillot, B. Kauppi, and M. Fontecave.** 1996. The irreversible inactivation of ribonucleotide reductase from *Escherichia coli* by superoxide radicals. FEBS Lett. **387:**137-140.

24. **Giel, J. L., D. Rodionov, M. Liu, F. R. Blattner, and P. J. Kiley.** 2006. IscR-dependent gene expression links iron-sulphur cluster assembly to the control of O2-regulated genes in *Escherichia coli*. Mol. Microbiol. **60:**1058-1075.

25. **Gon, S., M. J. Faulkner, and J. Beckwith.** 2006. In vivo requirement for glutaredoxins and thioredoxins in the reduction of the ribonucleotide reductases of *Escherichia coli*. Antioxid. Redox Signal. **8:**735-742.

26. **Grass, G., S. Franke, N. Taudte, D. H. Nies, L. M. Kucharski, M. E. Maguire, and C. Rensing.** 2005. The metal permease ZupT from *Escherichia coli* is a transporter with a broad substrate spectrum. J. Bacteriol. **187:**1604-1611.

27. **Grinberg, I., T. Shteinberg, A. Q. Hassan, Y. Aharonowitz, I. Borovok, and G. Cohen.** 2009. Functional analysis of the *Streptomyces coelicolor* NrdR ATP-cone domain: role in nucleotide binding, oligomerization, and DNA interactions. J. Bacteriol. **191:**1169-1179.

28. **Haldimann, A., and B. L. Wanner.** 2001. Conditional-replication, integration, excision, and retrieval plasmid-host systems for gene structure-function studies of bacteria. J. Bacteriol. **183:**6384-6393.

29. **Hogbom, M., M. E. Andersson, and P. Nordlund.** 2001. Crystal structures of oxidized dinuclear manganese centres in Mn-substituted class I ribonucleotide reductase from *Escherichia coli*: carboxylate shifts with implications for O2 activation and radical generation. J. Biol. Inorg. Chem. **6:**315-323.

30. **Hristova, D., C. H. Wu, W. Jiang, C. Krebs, and J. Stubbe.** 2008. Importance of the maintenance pathway in the regulation of the activity of *Escherichia coli* ribonucleotide reductase. Biochemistry. **47:**3989-3999.

31. **Imlay, J. A.** 2008. Cellular defenses against superoxide and hydrogen peroxide. Annu. Rev. Biochem. **77:**755-776.

32. **Ireton, G. C., G. McDermott, M. E. Black, and B. L. Stoddard.** 2002. The structure of *Escherichia coli* cytosine deaminase. J. Mol. Biol. **315:**687-697.

33. **Jain, R., B. Hao, R. P. Liu, and M. K. Chan.** 2005. Structures of *E. coli* peptide deformylase bound to formate: insight into the preference for Fe2+ over Zn2+ as the active site metal. J. Am. Chem. Soc. **127:**4558-4559.

34. **Jang, S., and J. A. Imlay.** 2010. Hydrogen peroxide inactivates the *Escherichia coli* Isc iron-sulphur assembly system, and OxyR induces the Suf system to compensate. Mol. Microbiol. **78:**1448-1467.

35. **Jang, S., and J. A. Imlay.** 2007. Micromolar intracellular hydrogen peroxide disrupts metabolism by damaging iron-sulfur enzymes. J. Biol. Chem. **282:**929-937.

36. **Jordan, A., E. Aragall, I. Gibert, and J. Barbe.** 1996. Promoter identification and expression analysis of *Salmonella typhimurium* and *Escherichia col*i nrdEF operons encoding one of two class I ribonucleotide reductases present in both bacteria. Mol. Microbiol. **19:**777-790.

37. **Jordan, A., E. Pontis, M. Atta, M. Krook, I. Gibert, J. Barbe, and P. Reichard.** 1994. A second class I ribonucleotide reductase in *Enterobacteriaceae*: characterization of the *Salmonella typhimurium* enzyme. Proc. Natl. Acad. Sci. U. S. A. **91:**12892-12896.

38. **Jordan, A., F. Aslund, E. Pontis, P. Reichard, and A. Holmgren.** 1997. Characterization of *Escherichia coli* NrdH. A glutaredoxin-like protein with a thioredoxin-like activity profile. J. Biol. Chem. **272:**18044-18050.

39. **Kehres, D. G., A. Janakiraman, J. M. Slauch, and M. E. Maguire.** 2002. Regulation of *Salmonella enterica* serovar Typhimurium *mntH* transcription by H_2O_2, Fe(2+), and Mn(2+). J. Bacteriol. **184:**3151-3158.

40. **Kirby, T., J. Blum, I. Kahane, and I. Fridovich.** 1980. Distinguishing between Mn-containing and Fe-containing superoxide dismutases in crude extracts of cells. Arch. Biochem. Biophys. **201:**551-555.

41. **Kullik, I., M. B. Toledano, L. A. Tartaglia, and G. Storz.** 1995. Mutational analysis of the redox-sensitive transcriptional regulator OxyR: regions important for oxidation and transcriptional activation. J. Bacteriol. **177:**1275-1284.

42. **Kuong, K. J., and A. Kuzminov.** 2009. Cyanide, peroxide and nitric oxide formation in solutions of hydroxyurea causes cellular toxicity and may contribute to its therapeutic potency. J. Mol. Biol. **390:**845-862.

43. **Lee, K. C., W. S. Yeo, and J. H. Roe.** 2008. Oxidant-responsive induction of the *suf* operon, encoding a Fe-S assembly system, through Fur and IscR in *Escherichia coli*. J. Bacteriol. **190:**8244-8247.

44. **McCord, J. M., and I. Fridovich.** 1969. Superoxide dismutase. An enzymic function for erythrocuprein (hemocuprein). J. Biol. Chem. **244:**6049-6055.

45. **McHugh, J. P., F. Rodriguez-Quinones, H. Abdul-Tehrani, D. A. Svistunenko, R. K. Poole, C. E. Cooper, and S. C. Andrews.** 2003. Global iron-dependent gene regulation in *Escherichia coli*. A new mechanism for iron homeostasis. J. Biol. Chem. **278:**29478-29486.

46. **Merighi, M., C. D. Ellermeier, J. M. Slauch, and J. S. Gunn.** 2005. Resolvase-in vivo expression technology analysis of the *Salmonella enterica* serovar Typhimurium PhoP and PmrA regulons in BALB/c mice. J. Bacteriol. **187:**7407-7416.

47. **Miller, J. H. (ed.),** 1972. Experiments in Molecular Genetics. Cold Springs Harbor Laboratory, Cold Springs Harbor, NY.

48. **Monje-Casas, F., J. Jurado, M. Prieto-Alamo, A. Holmgren, and C. Pueyo.** 2001. Expression analysis of the *nrdHIE*F operon from *Escherichia coli*. Conditions that trigger the transcript level *in vivo*. J. Biol. Chem. **276:**18031-18037.

49. **Neidhardt, F. C., P. L. Bloch, and D. F. Smith.** 1974. Culture medium for enterobacteria. J. Bacteriol. **119:**736-747.

50. **Nesbit, A. D., J. L. Giel, J. C. Rose, and P. J. Kiley.** 2009. Sequence-specific binding to a subset of IscR-regulated promoters does not require IscR Fe-S cluster ligation. J. Mol. Biol. **387:**28-41.

51. **Outten, F. W., O. Djaman, and G. Storz.** 2004. A *suf* operon requirement for Fe-S cluster assembly during iron starvation in Escherichia coli. Mol. Microbiol. **52:**861-872.

52. **Panosa, A., I. Roca, and I. Gibert.** 2010. Ribonucleotide reductases of *Salmonella typhimurium*: transcriptional regulation and differential role in pathogenesis. PLoS One. **5:**e11328.

53. **Park, S., X. You, and J. A. Imlay.** 2005. Substantial DNA damage from submicromolar intracellular hydrogen peroxide detected in Hpx^- mutants of *Escherichia coli*. Proc. Natl. Acad. Sci. U. S. A. **102:**9317-9322.

54. **Patzer, S. I., and K. Hantke.** 2001. Dual repression by Fe(2+)-Fur and Mn(2+)-MntR of the *mntH* gene, encoding an NRAMP-like Mn(2+) transporter in *Escherichia coli*. J. Bacteriol. **183:**4806-4813.

55. **Posey, J. E., and F. C. Gherardini.** 2000. Lack of a role for iron in the Lyme disease pathogen. Science. **288:**1651-1653.

56. **Pueyo, C., J. Jurado, M. J. Prieto-Alamo, F. Monje-Casas, and J. Lopez-Barea.** 2002. Multiplex reverse transcription-polymerase chain reaction for determining transcriptional regulation of thioredoxin and glutaredoxin pathways. Methods Enzymol. **347:**441-451.

57. **Schwartz, C. J., J. L. Giel, T. Patschkowski, C. Luther, F. J. Ruzicka, H. Beinert, and P. J. Kiley.** 2001. IscR, an Fe-S cluster-containing transcription factor, represses expression of *Escherichia coli* genes encoding Fe-S cluster assembly proteins. Proc. Natl. Acad. Sci. U. S. A. **98:**14895-14900.

58. **Seaver, L. C., and J. A. Imlay.** 2001. Hydrogen peroxide fluxes and compartmentalization inside growing *Escherichia coli*. J. Bacteriol. **183:**7182-7189.

59. **Seaver, L. C., and J. A. Imlay.** 2004. Are respiratory enzymes the primary sources of intracellular hydrogen peroxide? J. Biol. Chem. **279:**48742-48750.

60. **Sobota, J. M., and J. A. Imlay.** 2011. Iron enzyme ribulose-5-phosphate 3-epimerase in *Escherichia coli* is rapidly damaged by hydrogen peroxide but can be protected by manganese. Proc. Natl. Acad. Sci. U. S. A. **108:**5402-5407.

61. **Stojiljkovic, I., A. J. Baumler, and K. Hantke.** 1994. Fur regulon in gram-negative bacteria. Identification and characterization of new iron-regulated *Escherichia coli* genes by a fur titration assay. J. Mol. Biol. **236:**531-545.

62. **Torrents, E., I. Grinberg, B. Gorovitz-Harris, H. Lundstrom, I. Borovok, Y. Aharonowitz, B. M. Sjoberg, and G. Cohen.** 2007. NrdR controls differential expression of the *Escherichia coli* ribonucleotide reductase genes. J. Bacteriol. **189:**5012-5021.

63. **Varghese, S., A. Wu, S. Park, K. R. C. Imlay, and J. A. Imlay.** 2007. Submicromolar hydrogen peroxide disrupts the ability of Fur protein to control free-iron levels in *Escherichia coli*. Mol. Microbiol. **64:**822-830.

64. **Vassinova, N., and D. Kozyrev.** 2000. A method for direct cloning of Fur-regulated genes: identification of seven new Fur-regulated loci in *Escherichia coli*. Microbiology. **146:**3171-3182.

65. **Wu, C. H., W. Jiang, C. Krebs, and J. Stubbe.** 2007. YfaE, a ferredoxin involved in diferric-tyrosyl radical maintenance in *Escherichia coli* ribonucleotide reductase. Biochemistry. **46:**11577-11588.

66. **Yeo, W. S., J. H. Lee, K. C. Lee, and J. H. Roe.** 2006. IscR acts as an activator in response to oxidative stress for the suf operon encoding Fe-S assembly proteins. Mol. Microbiol. **61:**206-218.

67. **Zheng, M., X. Wang, L. J. Templeton, D. R. Smulski, R. A. LaRossa, and G. Storz.** 2001. DNA microarray-mediated transcriptional profiling of the *Escherichia coli* response to hydrogen peroxide. J. Bacteriol. **183:**4562-4570.

CHAPTER 3: WHAT IS THE PHYSIOLOGICAL ROLE OF THE *ESCHERICHIA COLI* SMALL PROTEIN, MNTS?

3.1 INTRODUCTION

The biology and metabolism of ancestral organisms were configured around the catalytic capabilities of iron. Iron-cofactored enzymes became the drivers of many fundamental cellular processes, including central metabolism, respiration, nucleic acid processing, nitrogen and sulfur assimilation, and the biosyntheses of amino acids, nucleotides, and organic cofactors. However, this dependency ultimately became problematic: after the advent of photosystem II, molecular oxygen gradually accumulated and caused the oxidation and precipitation of most environmental iron. As a result, iron is episodically unavailable in many contemporary habitats.

Because bacteria inherited the ancestral metabolic schemes, they were forced to evolve strategies to cope with iron scarcity. Many bacteria synthesize siderophores to solubilize and import ferric iron [39]; during times of high iron availability they store any excess in ferritins to hedge against future scarcity [1, 2]; and when iron is limited, they prioritize its use by shutting down the synthesis of iron-requiring enzymes that are abundant but not essential [23].

Enteric bacteria also compensate for iron deficiency by importing manganese to be used in its place. Iron enzymes fall into several classes: those that use redox-active heme, iron-sulfur clusters, and mono- or di-nuclear iron centers to catalyze electron-transfer reactions, and those that employ iron-sulfur and mononuclear iron centers as surface catalysts that activate substrates for non-redox reactions. In the non-redox mononuclear enzymes the ferrous iron atom typically binds substrate and facilitates

catalysis by electrostatically stabilizing an oxyanionic intermediate. Divalent manganese can also play this role, and because it shares the coordination preferences of iron, it can substitute directly into what is normally an iron-binding protein and confer activity that approaches that of the iron-loaded enzyme. It is presumably for this reason that the dedicated manganese importers of *Escherichia coli* (MntH) and *Salmonella typhimurium* (MntH and SitABC) are repressed by iron-loaded Fur protein during iron-replete conditions but are induced when Fur is demetallated during iron limitation [13, 31]. Interestingly, under the latter circumstances the iron-dependent enzymes superoxide dismutase (FeSOD) and ribonucleotide reductase (NrdAB) are replaced by manganese-dependent isozymes (MnSOD and NrdEF) [22, 30] . Manganese cannot effectively substitute directly into the original iron enzymes because they fail to poise manganese at the reduction potential needed for catalysis [4, 6, 22, 43].

The MntH importer is also induced > 20-fold by the transcriptional activator OxyR in response to hydrogen peroxide stress, causing a large (*ca*. 20-fold) rise in intracellular manganese [4, 19]. Hydrogen peroxide readily oxidizes the exposed ferrous cofactors of non-redox mononuclear iron enzymes such as peptide deformylase, threonine dehydrogenase, and ribulose-5-phosphate epimerase, leading to dissociation of ferric iron and inactivation of the enzyme [3, 15, 16, 32, 38] . Replacement of the iron with a manganese cation, which H_2O_2 does not oxidize, apparently restores activity and maintains the function of the pathways to which these enzymes belong [3, 15, 16, 32, 38]. These observations suggest that *E. coli* relies upon manganese only when iron is scarce or H_2O_2 is present, and thus far growth defects have been documented for *mntH* null mutants only under those conditions [4].

The similarities between iron and manganese may also create problems, however. Investigators have long recognized that high levels of extracellular manganese can inhibit bacterial growth. In principle, this effect might result if manganese outcompetes iron for the metal-binding sites of proteins that cannot function with manganese, such as the NrdAB ribonucleotide reductase. Other plausible targets would be the metal binding sites of ferrochelatase, which subsequently inserts ferrous iron into porphyrins in the final step of heme synthesis, and that of the Isc iron-sulfur-cluster assembly machinery.

Examination of the regulation of MntH synthesis has turned up evidence of multiple controls that limit manganese content. MntR is a transcriptional factor that, when bound by Mn^{2+}, represses *mntH* transcription [18, 33]. Further, excess manganese can be redirected out of the cytoplasm by the MntR:Mn-directed induction of manganese efflux pumps. The identification of these systems in *E. coli* (MntP), *Streptococcus pneumoniae* (MntE), and *Neisseria spp.* (MntX) suggest that bacteria strive to remove excess manganese before levels become toxic [34, 40, 42]. Manganese overloading might occur when MntH-containing cells enter manganese-rich habitats or if manganese enters the cell through less-specific divalent cation importers.

Recent evidence has predicted that a third player, termed MntS, is also involved in manganese homeostasis [42]. The *mntS* gene is expressed as an RNA that is predicted to have complex secondary structure; this RNA is termed RybA. Within the RNA lies a short open reading frame that encodes a very small protein of 42 amino acids, known as MntS [42]. This protein is expressed. The *mntS* transcript is repressed by MntR:Mn, suggesting that it plays a role only when manganese is scarce [42]. Mutants that lack MntS are defective at MntR-mediated repression of *mntH* transcription, as if MntR fails

to acquire manganese [42]. Strains that overexpress MntS are hypersensitive to exogenous manganese [42]. These data suggest that MntS may help make manganese available to potential manganese-binding proteins. One possibility is that the MntS protein, which seems too small to be an enzyme, might be a manganese chaperone.

In this study, we explored the physiological role of MntS. We confirmed that MntS enables manganese binding to authentic client proteins but that it also exacerbates the ability of excess manganese to poison iron-specific cellular functions, such as heme synthesis. The *mntS* phenotype is epistatic with *mntP*, and we suspect that MntS is an inhibitor of that export system.

3.2 MATERIALS AND METHODS

3.2.1 Reagents

All antibiotics, β-mercaptoethanol, β-NADH, bovine xanthine oxidase, casein acid hydrolysate, cytochrome *C* from equine heart, deamino-NADH, desferoxamine mesylate (DFO), diethylenetriamine pentaacetic acid (DTPA), 2,2'-dipyridyl (DIP), ethyl acetate, ferric chloride, ferrous ammonium sulfate, 30% hydrogen peroxide, 8-hydroxyquinoline-5-sulphonic acid, *E. coli* manganese-containing superoxide dismutase, manganese (II) chloride tetrahydrate, 2-[*N*-morpholino]ethanesulfonic acid (MES), *o*-dianisidine dihydrochloride, *o*-nitrophenyl-β-D-galactopyranoside (ONPG), potassium ferricyanide, potassium cyanide, tricine, and xanthine were purchased from Sigma. Ethylenediamine tetraacetic acid (EDTA), guanidine hydrochloride, hydrochloric acid, and 3-(*N*-morpholino) propane-sulfonic acid (MOPS) were purchased from Fisher

Scientific; Coomassie protein assay reagent and albumin standard, from Thermo Scientific; sodium dithionite, from Fluka; and glacial acetic acid, from J.T.Baker.

3.2.2 Bacterial strain and plasmid construction

All strains and plasmids used in this study are listed in Table 3.1. Chromosomal null deletions were generated using the λ Red recombination method [11]. All oxygen-sensitive strains were constructed under anaerobic conditions to ensure that suppressor mutations were not selected during outgrowth. Mutations were introduced into new strains by P1-transduction [26]. All mutations were confirmed by PCR analysis or blue/white selection with Xgal. When necessary, the antibiotic cassette was removed by FLP-mediated excision [11]. Note that the *mntS*-null deletion removes the MntS open reading frame.

For single-copy *lacZ* transcriptional fusions, the promoter region of given genes were amplified by PCR using primers designed with restriction sites. The product was digested and inserted into pSJ501, a plasmid derivative of pAH125 modified to express the chloramphenicol acetyl transferase gene (*cat*) flanked by FLP sites for selection under anaerobic conditions. The resulting plasmid constructs were confirmed by restriction analysis and sequencing. Plasmids were then integrated into the λ attachment site, while the wild-type genes remained at their native positions [12]. Fusions were introduced into new strains by P1-transduction, and the chloramphenicol-resistance cassette was removed by FLP-mediated excision [11].

The plasmid pMntS2 (pLW131) was generated by amplifying the 150 nt upstream of the *mntS* transcriptional start site, followed by 205 nt of the RNA sequence (including

the complete MntS open reading frame) by PCR. The product was digested with SalI and XbaI and ligated into similarly digested pACYC184 (a low copy number plasmid that is maintained at 15 copies/cell), which removes the tetracycline-resistance marker but retains the chloramphenicol-resistance marker for selection.

Plasmid pMntS (pLW112) was generated by amplifying the 205 nt of the RNA (encompassing only the MntS open reading frame) and the *mntS* Shine-Dalgarno sequence by PCR [42]. The product was digested with NheI and KpnI and cloned into pBAD24 (a medium copy number plasmid that is maintained at 15-20 copies/cell), in which expression is driven by *araBAD* promoter.

The plasmids pMntS-F11 (pJEM67), pMntS-F16 (pJEMS68), pMntS-E3A (pMS017), pMntS-C7A (pMS018), pMntS-C27A (pMS020), pMntS-D28A (pMS021), and pMntS-H13A (pLW125), pMntS-E3A/C7A/D28A (pLW133), pMntS-E3A/C27A/D28A (pLW134), pMntS-C7A/C27A/D28A (pLW135), and pMntS-E3A/C7A/C27A (pLW136) expressing mutant *mntS* alleles were created by site-directed mutagenesis on the template pLW112 using Pfu Turbo polymerase from Stratagene. Briefly, 60-mer primers were designed with the mutation of interest located in the center of the sequence (Table 3.2) . Both forward and reverse complements were ordered. Mutagenesis was performed in a mixture (50 µl) containing 50 ng template DNA, 400 nM each primer complement, 200 µM dNTPs, and 2.5 units Pfu Turbo polymerase. Typical cycling conditions were as follows: 95°C/3 min; 18 cycles of 95°C/30 s, 55°C/1 min, 68°C/2.5 min/kb. The resulting mixture was digested with DpnI at 37°C for more than 1 hr to remove original plasmid DNA template, then transformed into TOP10

electrocompetent *E. coli* cells followed by selection on ampicillin plates. All resulting plasmids constructs were confirmed by sequencing.

3.2.3 Growth conditions

Luria broth (LB) and base M9 minimal salts were of standard composition [26]. Base MOPS minimal salts were prepared without $FeSO_4$ and micronutrients [28]. M9 and MOPS medium were supplemented with 0.2% glucose, 0.2% casamino acids, 0.5 mM tryptophan (lacking in casamino acids). Media were supplemented with 100 μg/ml ampicillin, 20 μg/ml chloramphenicol, 30 μg/ml kanamycin sulfate, or 12.5 μg/ml tetracycline HCl when antibiotic selection was needed. Anaerobic cultures were grown in an anaerobic chamber (Coy Laboratory Products Inc.) under an atmosphere of 85% N_2/10% H_2/5% CO_2. Aerobic cultures were grown under room air with vigorous shaking.

To ensure that cells were growing exponentially, overnight cultures were diluted to OD_{600} 0.005 and grown at 37°C to an approximate OD_{600} of 0.12. Cells were then subcultured again into fresh aerobic medium to OD_{600} 0.0025 and grown at 37°C to an approximate OD_{600} of 0.25 prior to analysis. Strains harboring pMntS or Δ*mntP* began exhibiting slower growth approximately 2 hr after the addition of manganese. Thus, enzyme activities were typically measured 2.5 hr after treatment with manganese.

Strains carrying pBAD24-derived plasmids were grown with ampicillin overnight and then diluted into fresh medium to OD_{600} 0.005. After approximately four doublings, 50 mM L(+)arabinose was added to induce MntS expression. Cultures were grown for an

additional 30 to 45 minutes, subcultured again into fresh aerobic medium with ampicillin and 50 mM L(+)arabinose to OD_{600} 0.0025, and grown at 37°C.

Strains lacking *hemA* were grown in anaerobic LB overnight and then diluted into fresh anaerobic medium to OD_{600} 0.005. After approximately three generations of growth, 0.25 mM 5-ALA was added to the medium. Cultures were grown for two additional generations, subcultured again into fresh aerobic medium with 1 mM 5-ALA to OD_{600} 0.005, and grown aerobically at 37°C.

3.2.4 Cell viability

Anaerobic overnight cultures were diluted to OD_{600} 0.005 and grown anaerobically at 37°C to an OD_{600} of approximately 0.1. Cells were then subcultured again into fresh aerobic medium to OD_{600} 0.0025 and grown at 37°C with vigorous shaking. At intervals, aliquots of cells were removed and serially diluted into aerobic medium. The diluted samples were mixed with anaerobic top agar and poured onto anaerobic medium agar plates. Colonies were counted after 24 (LB medium) or 48 hours (defined medium) of anaerobic incubation at 37°C.

3.2.5 Enzyme assays

All enzyme assays were performed at room temperature. Protein concentrations were determined by the Bradford assay using bovine serum albumin as the standard.

β-galactosidase activity

To prepare extracts, cells were centrifuged, washed twice, resuspended in 1/30 the original culture volume with ice-cold 50 mM Tris-HCl buffer (pH 8), and lysed by French press. Cell debris was removed by centrifugation, and β-galactosidase activity in cell extracts was determined by ONPG hydrolysis using standard procedures [26].

Superoxide dismutase activity

Extracts were prepared same as above for β-galactosidase activity but resuspended in 1/100 the original culture volume. SOD activity was measured in cell extracts using the xanthine oxidase/cytochrome *C* method [25]. A *sodB* (encoding FeSOD) mutant was used to track MnSOD activity. The fraction of MnSOD that was active in the cell extracts was determined after extracts were subjected to partial denaturation and renaturation in the presence of manganese to ensure full activation of MnSOD protein [20, 22]. Briefly, MnSOD was denatured at pH 3.8 in the presence of 5 mM Tris-HCl,/2.5 M guanidinium chloride/20 mM 8-hydroxyquinoline-5-sulphonic acid/0.1 mM EDTA for approximately 12 hr in the dark and then renatured at pH 7.8 in the presence of 5 mM HEPES/0.1 mM $MnCl_2$ for 2 periods of approximately 12 hr each. Excess metal was removed by dialysis at pH 7.8 in 5 mM Tris-HCl/0.1 mM EDTA for 2 periods of 4 hr each. The entire reconstitution process was performed at 4°C. Since measurements were determined from the fraction of protein that survived the procedure, I occasionally observed greater than 100% active MnSOD. Purchased *E. coli* manganese-containing SOD was used as a control for the reconstitution procedure.

Hydroperoxidase I (HPI) activity

To prepare extracts, cells were washed twice with ice-cold 50 mM potassium phosphate buffer (pH 7.8), then resuspended in 1/30 the original culture volume and lysed by French press in ice-cold 10 mM potassium phosphate buffer (pH 6.4). Cell debris was removed by centrifugation, and HPI, the KatG catalase, was specifically assayed through its ability to act as a peroxidase. Extracts were added to 300 μM *o*-dianisidine, 900 μM H_2O_2, and 10 mM KPi (pH 6.4), and the oxidation of *o*-dianisidine was monitored at A_{460}.

NADH dehydrogenase I (Ndh1) activity

Cells were centrifuged and washed twice with ice-cold 50 mM MES buffer (pH 6.0). Final resuspension was in 1/60 the original culture volume. Cells were lysed by French press, and cell debris was removed by centrifugation. Inverted membrane vesicles were isolated from the supernatant by ultra-centrifugation at 100,000 x *g* for 2 hours, 4°C. Inverted vesicles were resuspended in ice-cold 50 mM MES buffer (pH 6.0) at 1/120 the original culture volume. Vesicles were assayed immediately for NADH dehydrogenase activity at A_{340} with either 120 μM NADH or 60 μM deamino-NADH as the substrate. Ndh2 can only use NADH as a substrate, while Ndh1 can use both deamino-NADH and NADH with equal efficiency [8, 24].

NADH dehydrogenase II (Ndh2) activity

Inverted membrane vesicles were isolated as described above. Resuspended inverted vesicles were diluted 5-fold into 50 mM KPi (pH 7.8) and held at 0°C overnight to eliminate NdhI activity, which is unstable at this pH. The inverted vesicles were incubated with 3 mM KCN to block respiration by inhibiting cytochrome oxidase function, then assayed for Ndh-2 activity by monitoring NADH oxidation at A_{340} in the presence of 200 μM $K_3Fe(CN)_6$, which acts as an oxidant to remove electrons from Ndh2. This enables the enzyme to continue to turn over in the absence of cytochrome oxidase function.

3.2.6 Electron paramagnetic resonance (EPR) measurements of unincorporated intracellular iron

The pool of intracellular chelatable iron was quantified by standard procedures [44] from one-liter cultures that were grown aerobically at 37°C in LB for 2.5 hr with or without 500 μM $MnCl_2$. Briefly, cells were centrifuged and resuspended in 37°C LB at 1/100 the original culture volume containing 10 mM DTPC (pH 7.0) to block further iron import and 20 mM DFO (pH 8.0) to facilitate oxidation of intracellular unincorporated ferrous iron to EPR-detectable ferric iron. The cell mixture was incubated aerobically with vigorous shaking at 37°C for 15 min and then centrifuged. Cell pellets were washed twice with ice-cold 20 mM Tris-HCl/10% glycerol (pH 7.4), and finally resuspended in 150 μl of the same buffer. The cell density was recorded and samples were loaded into a quartz EPR tube. Samples were frozen on dry ice and stored at -80°C for no longer than one week. EPR standards consisted of $FeCl_3$ dissolved in 20 mM Tris-HCl/10%

glycerol/1 mM DFO (pH 7.4); the iron concentration in the standard was determined using ε_{mM} at 420 nM of 2.865 cm^{-1}. EPR spectra were acquired on a Varion Century E-112 X-band spectrophotometer at 15 K using a Varian TE102 cavity using 10 mW power, 12.5 G modulation amplitude, 4000 gain, 32 ms time constant, and 100 kHz modulation frequency. EPR spectra for samples were normalized to cell density and converted to intracellular iron concentrations using the following conversion: 1 ml of bacteria culture at 1 OD_{600} equals 0.52 µl of intracellular volume [14].

3.2.7 Detection of manganese by EPR

Reduced manganese (Mn^{2+}) spectra were detected from one-liter cultures that were grown aerobically at 37°C in LB for 2.5 hr with or without 500 µM $MnCl_2$. Briefly, cells were washed twice and resuspended in 1/2000 the original culture volume with ice-cold 100 mM Tris-HCl/150 mM NaCl/5% glycerol (pH 7.6). Samples were normalized to similar densities, approximately 75 OD_{600}, and loaded into a quartz EPR tube. Samples were frozen on dry ice and stored at -80°C for no longer than one week. EPR spectra were acquired at 110 K using 2 mW power, 5 G modulation amplitude, 20000 gain, 32 ms time constant, and 100 kHz modulation frequency. Same parameters were used at 30 K, except that 2500 gain was used.

3.2.8 Inductively coupled plasma-mass spectrometry (ICP-MS) of intracellular iron and manganese

The pool of intracellular iron and manganese was quantified from one-liter cultures that were grown aerobically at 37°C in LB for 2.5 hr with or without 500 µM

$MnCl_2$. Cells were centrifuged, washed twice with ice-cold 20 mM Tris-HCl/1 mM EDTA (pH 7.4), then once with ice-cold 20 mM Tris-HCl (pH 7.4). Cells were resuspended in ice cold 20 mM Tris-HCl (pH 7.4) to 1/500 the original culture volume and lysed by French press. Cell debris was removed by centrifugation. The metal content was determined at the University of Georgia Center for Applied Isotope Studies and normalized to total protein in the lysates.

3.2.9 Porphyrin quantification

Porphyrins were extracted from 100 ml cultures that were grown aerobically at 37°C in LB for 2.5 hr with or without 500 μM $MnCl_2$ using a modified procedure [27]. Cells were centrifuged, washed twice with ice-cold 50 mM Tris-HCl (pH 8.0), then resuspended in room temperature ethyl acetate/glacial acetic acid (3:1, v/v) to 1/100 the original culture volume and lysed by sonication on ice. Cell debris was removed by centrifugation at room temperature and the non-aqueous (top-layer) phase was washed twice with 1 ml ddH_2O to remove residual water soluble contaminants, taking care not to disturb the intermediate phase. Porphyrins were then extracted from the solution by the addition of 0.5 ml 3M HCl and the absorbance of the aqueous (bottom-layer) phase was assessed at 408 nm. Porphyrin levels were normalized to optical cell density (OD_{600}).

3.3 RESULTS

3.3.1 MntS facilitates manganese delivery to manganese-dependent enzymes when manganese is scarce

The fact that MntS is expressed only when manganese levels are low suggested that it might help activate metalloenzymes under those conditions. Manganese confers activity to non-redox mononuclear enzymes during H_2O_2 stress, and it is an essential cofactor for the manganese-dependent NrdEF ribonucleotide reductase and MnSOD superoxide dismutase[6, 10, 22]. The role of MntS in these processes was therefore examined.

E. coli Hpx^- mutants (*katG katE ahpCF*) cannot degrade H_2O_2 [35, 36], and their growth in the presence of H_2O_2 requires the import of manganese [4]. Under this condition manganese import ensues when the OxyR regulator senses H_2O_2 and induces MntH [18, 19, 25]. In our standard defined medium, the *mntS* mutants exhibited a protracted lag when moderate (15 μM) amounts of H_2O_2 were supplied (Fig. 3.1). The lag was suppressed when high levels of manganese were included in the medium. The phenotype was complemented by a plasmid expressing *mntS* under its native promoter (Fig. 3.2). This result suggests that MntS helped deliver manganese to mononuclear metalloenzymes during the period before the MntH transporter had imported manganese to high levels.

Using these conditions of oxidative stress, we were able to test whether MntS acts exclusively as an ancillary protein to either the MntR transcription factor or the MntH importer. MntS has been shown to help activate MntR [42], but Figure 3.3 demonstrates

that MntS helps outgrowth even in an *mntR*-null background. Figure 3.4 shows that both MntH (panel A) and MntS (panel B) each confer benefits in the absence of the other.

We suspect that MntS promoted manganese insertion into non-redox mononuclear enzymes, but we were unable to directly test this idea because manganese dissociates from them during extract preparation. Instead, we examined the metallation status of MnSOD under unstressed growth conditions. This enzyme closes around the bound manganese atom and does not allow it to dissociate *in vitro* [43]. In previous studies we demonstrated that this enzyme is only partially populated with manganese in our standard minimal medium, because the cell makes little effort to import the metal [4]. Cell extracts were prepared, the MnSOD activity was assayed, and then the activity was assayed a second time after reversible denaturation and reconstitution in the presence of manganese. The latter procedure fully activates the enzyme, and comparison of the pre- and post-reconstitution activities allows us to appraise what fraction of the enzyme was initially active. In wild-type cells only about 30% of the enzymes were active prior to reconstitution (Fig. 3.5). The value was 15% in *mntS* mutants. Conversely, overexpression of the MntS protein from a plasmid using its native promoter caused full MnSOD activation (Fig. 3.5). These data confirmed that MntS helps provide manganese to enzymes.

Notably, Hpx$^-$ *mntS* mutants exhibited full MnSOD activation (Fig. 3.5). We suspected that this reflected the fact that H_2O_2-stressed cells contain high levels of manganese due to their robust MntH induction. To see whether MntS is needed for MnSOD activation only at low intracellular levels of manganese, we examined its effect in *mntH* mutants that were supplemented with varying amounts of manganese. When

MntH is absent, manganese can enter the cell less efficiently through other, non-specific divalent metal import systems. We found that whereas supplementation with 0.4 μM manganese enabled full MnSOD activation in MntS-proficient strains, about 10-fold more manganese was needed in *mntS* mutants (Fig. 3.6). These data affirm that MntS assists in metallation when intracellular manganese levels are low but is dispensable when levels are high.

Finally, we examined the function of NrdEF, the manganese-dependent ribonucleotide reductase. NrdEF activity can be monitored when *nrdAB* null mutants are shifted from anoxic medium to aerated medium. In this circumstance the oxygen-sensitive NrdDG ribonucleotide reductase stops working, and the absence of NrdAB leaves NrdEF as the only reductase that can function. NrdEF is induced and activated only in iron-deficient cells, and so these studies were performed in strains lacking the Feo, ZupT, and siderophore-dependent iron-import systems (Δ*tonB* Δ*feoABC* Δ*zupT*) [25]. As reported previously, in this circumstance cells exhibit a protracted lag, during which iron is progressively depleted and MntH and NrdEF are induced, prior to outgrowth that requires the manganese-activated NrdEF [25]. Invariably this lag was slightly longer for *mntS*-deficient cells (Fig. 3.7A). More strikingly, the lag was greatly reduced when MntS was overproduced from its native promoter on a plasmid and manganese was supplemented (Fig. 3.7B). Gene-fusion data showed that *mntS* had no effect on the transcription or translation of the *nrdHIEF* operon (data not shown). We infer that during this transition period MntS somehow assisted with the activation of NrdEF. In total, our data indicate that MntS facilitates manganese binding to a variety of enzymes, under conditions where manganese influx is limited.

3.3.2 In manganese-rich medium overproduced MntS disrupts metal pools

Waters *et al.* showed that wild type *E. coli* cells overexpressing MntS were sensitive to manganese on zone-of-inhibition plates [25]. We confirmed that the phenotype also occurs in aerobic liquid medium (Fig. 3.8). Growth characteristically failed after several generations.

Wild-type cells grown in LB medium typically contained about 5 μM total manganese (Fig. 3.9A). SOD activity measurements allow us to conclude that the majority of this manganese was incorporated into SodA (data not shown). The manganese level rose to about 15 μM when MntS was overproduced (Fig. 3.9A). If manganese was supplemented in the medium (0.5 mM), manganese levels rose to approximately 35 μM in the wild-type strain and approximately 140 μM upon MntS overproduction (Fig. 3.9A). The increase in intracellular manganese was also observed by EPR using intact whole-cells; the manganese spectrum that was observed did not match that of MnSOD, indicating that the manganese had exceeded its carrying capacity.

In contrast, ICP-MS data showed that manganese-supplemented cells exhibited a 5-fold reduction in total intracellular iron when MntS was overproduced (Fig. 3.10). Most of this iron is incorporated into proteins, and so whole-cell EPR analysis was performed to measure the pool of loosely bound intracellular iron. Manganese treatment lowered the pool of loose iron in wild-type cells from approximately 100 to approximately 40 μM. However, the effect was much more severe when MntS was overproduced, as the pool fell from approximately 90 to approximately 2 μM (Fig. 3.9B).

We sought the reason for this collapse of the iron pool. Iron acquisition by *E. coli* is regulated by the Fur transcription factor; in its iron-metallated form, Fur inhibits

synthesis of iron-import systems. Transcriptional fusions demonstrated that the combination of MntS overproduction and manganese supplementation essentially eliminated the expression of *iucC* and *fhuA* (Fig. 3.11). Elimination of Fur restored full expression, eradicating the effects of both manganese and MntS. The *fur* mutation also restored the intracellular iron pools (Fig. 3.9B) and obviated the growth defect (Fig. 3.8). This phenotypic suppression resulted from iron import rather than *ryhB* expression, since Δ*ryhB* had no affect on the growth of MntS overproducing cells grown with manganese (Fig. 3.12).

Fe^{2+}-bound Fur could not be mediating the super-repressive action of Fur in manganese-supplemented MntS overproducers, since iron was vanishingly scarce. Instead, it is likely that in these Mn-rich cells Fur acted with Mn^{2+} as a cofactor. Manganese can substitute for iron in this protein in vitro and in vivo, and the Mn-bound form of the protein is a capable repressor [13, 18]

3.3.3 Metal imbalance blocks growth by inhibiting the synthesis of heme

Iron serves as a cofactor for the activation of mono- and di-nuclear iron enzymes, iron-sulfur proteins, and heme proteins. The combination of manganese overload and iron deficiency is unlikely to disrupt the pathways of the first group of enzymes: the two redox-active iron enzymes, SOD and ribonucleotide reductase, can be replaced by manganese-using isozymes. Similarly, non-redox mononuclear iron enzymes can be activated by manganese. However, manganese cannot assemble in iron-sulfur or heme cofactors, and we wondered whether excess manganese coupled with iron deficiency would compromise one or the other.

Iron-sulfur clusters are assembled upon the IscU scaffold protein and then transferred to client enzymes, including some that are essential for growth. It is not yet clear how the assembly system initially binds cytoplasmic iron atoms, but it seemed possible that manganese might competitively inhibit this process or might simply block it through iron deficiency. We assayed the activity of NADH dehydrogenase I, a respiratory enzyme that requires nine iron-sulfur clusters for function. This enzyme activity is sharply diminished in cells that have even partial defects in iron-sulfur assembly. However, it remained at normal levels during manganese intoxication (Fig. 3.13). Further, there was no increase in the transcription of the *iscR* and *sufA* genes (Fig. 3.14). These genes are strongly induced when iron-sulfur synthesis is hindered, due to conversion of the IscR[2Fe-2S] transcription factor to its apoprotein form [29]. Collectively, these data indicate that excess manganese did not disrupt iron-sulfur assembly, and so the growth defect did not result from the loss of an iron-sulfur enzyme.

Heme is a cofactor for relatively few enzymes in *E. coli*: catalases G and E, cytochrome o and bd oxidases, succinate dehydrogenase, and the nitrite and sulfite reductases. Mutant studies show that only the cytochrome oxidases are important for growth in LB medium. We found that catalase G activity was 3.5-fold lower in manganese-supplemented cells overexpressing MntS compared to those carrying the empty vector (Fig. 3.15A). The low activity did not result from decreased transcription of *katG*, since the *katG* transcription rate was essentially unchanged (Fig. 3.16).

We then tested cytochrome oxidase activity by measuring the NADH oxidase activity of inverted cell membrane vesicles. Membranes prepped from cells overproducing MntS in the presence of high manganese showed 3-fold lower NADH

oxidation compared to cells expressing empty vector (Fig. 3.15B). This activity depends upon the upstream enzymes, NADH dehydrogenase I or NADH dehydrogenase II, but these were not diminished (Fig. 3.13). These data suggested that MntS interfered with heme biosynthesis. Cytochrome oxidase activity is only essential under aerobic conditions, since during anoxia its role is compensated for by the induction of fermentative enzymes. In fact, MntS did not interfere with the growth of cells under anoxic conditions, supporting the idea that it specifically toxifies cells by diminishing cytochrome oxidase activity.

The heme biosynthetic pathway (Fig. 3.17A) is controlled by HemA in ways that involve its transcription, protein stability, and allosteric control. To test whether manganese affected this step, we created a *hemA*-null deletion. These mutants required 5-aminolevulinate to grow in aerated medium (Fig. 3.17B) but were proficient in anoxic medium, when respiration is dispensable. Notably, 5-aminolevulinate did not suppress the manganese sensitivity of *hemA* cells overexpressing MntS (Fig. 3.17B); thus, the manganese-induced block was apparently downstream of HemL. A likely target was HemH, the ferrochelatase that inserts iron into protoporphyrin IX to produce protoheme. When this activity is inhibited by treatment of cells with dipyridyl, metal-free porphyrins accumulate. We found that cells overproducing MntS accumulated 10-fold more porphyrins when treated with manganese compared to cells expressing empty vector (Fig. 3.18). We infer that HemH likely fails to function properly when the iron/manganese balance is perturbed.

Growth inhibition occurs gradually rather than immediately (Fig. 3.8), no matter what dose of manganese is added. This observation fits the idea that manganese prevents

the activation of new cytochrome oxidase: once heme synthesis is blocked, several generations are required for titers of extant active enzyme to decline enough, through dilution, that growth fails.

3.3.4 MntS protein exerts manganese toxicity

The *mntS* ORF lies within the *rybA* message. RybA was first identified by microarray as a small RNA[41]. Northern blots showed seven mRNA constructs all containing the same 5'end, but different 3'ends, with the shortest construct corresponding to the 205 nucleotide MntS transcript [42]. It was not clear whether the *mntS* gene affected manganese poisoning by acting as a sRNA, by encoding a protein, or both. Analysis of the *mntS* ORF indicates conservation of the ORF among related species, as silent substitutions greatly predominated over non-silent ones. Only two of fifteen single-base changes resulted in codon switches. Further, the ORF length was unchanged, indicating selection against stop mutations, and a Shine-Dalgarno sequence was maintained in the appropriate position.

To test this idea experimentally, we constructed two separate frame-shift mutants of *mntS*, at Phe11 and Phe16. Cells expressing pMntS-F11 and pMntS-F16 alleles were no longer sensitive to manganese (Fig. 3.19A). The Fur-regulon was also de-repressed (Fig. 3.19C), and catalase G activity was restored (Fig. 3.19D). These data suggested that *mntS* was functioning as a protein and not a small RNA. Further, while small RNAs typically require the RNA chaperone, *hfq*, to function, deletion of *hfq* had no affect on manganese sensitivity, since Δ*hfq* mutants grew just as poorly as wild type cells when overexpressing MntS in manganese-rich conditions (Fig. 3.19B). Taken together, these

data indicate that *mntS* is most likely exerting Mn toxicity through its action as a small protein.

3.3.5 MntS overproduction mimics the effect of eliminating the MntP manganese exporter

In principle MntS could elevate the level of intracellular manganese by increasing the rate of influx, by delivering manganese to proteins that bind it, or by inhibiting export. The first possibility is unlikely, because MntS imposes its effect even in the absence of the primary manganese importer, MntH (Fig. 3.4B). The second possibility, which MntS might act as a manganese chaperone within the cell, was examined in several ways. We tested whether purified MntS would facilitate the metallation of SodA apoprotein in vitro, but saw no effect (data not shown). Isothermal calometry titration studies did not indicate any binding. Finally, we tested the role of the plausible metal-binding residues. Mutation of the conserved Glu, Cys, Asp, and His residues—individually or as in combinations—did not eliminate its ability to confer manganese toxicity (Fig. 3.20). Since these constitute the only residues known to bind manganese in biology, we conclude that MntS is not a manganese-binding protein.

The *mntP* gene is, alongside *mntH* and *mntS*, the third member of the MntR regulon. Manganese-loaded MntR induces *mntP* when manganese levels rise [42]. MntP is a manganese-efflux pump, and *mntP* mutants were sensitive to manganese on solid media [42], a phenotype similar to that of MntS overexpression. This phenotype recurred in liquid medium, and it was relieved by deletion of *fur* (Fig. 3.21A). To evaluate the hypothesis that MntS overproduction might act through the inhibition of MntP, we

examined the other phenotypes. The *mntP* mutants contained elevated levels of manganese and very low levels of iron (Figs. 3.22A and 3.21B). The *iucC* and *fhuA* genes were repressed by Fur (Fig. 3.21C). Catalase G activity was reduced 5-fold, and porphyrins accumulated to levels similar to those of cells overproducing MntS (Fig. 3.21D). All of these observations supported the notion that MntS might confer manganese sensitivity by inhibiting MntP function.

We then overexpressed *mntS* in Δ*mntP* mutants, to examine whether MntS had any further affect on the manganese metabolism. We observed no change in the concentration of intracellular manganese and iron in Δ*mntP* mutants overexpressing MntS compared to those expressing empty vector (Fig. 3.22B). Furthermore, overproduction of MntS in Δ*mntP* mutants did not increase manganese sensitivity (Fig. 3.23A), even when cells were grown with lower manganese concentrations (Fig. 3.24). Likewise, Δ*mntP* mutants portray similar manganese sensitivity to Δ*mntP* Δ*mntS* mutants, which suggests that *mntS* has no further affect when MntP is not functioning (Fig. 3.23B). Taken together, these data indicate that the *mntP*-null deletion is epistatic to overexpression of MntS with respect to manganese toxicity. Thus, MntS most likely elevates intracellular manganese levels by inhibiting manganese export through MntP. When the environmental level of manganese is low, this has the effect of modestly increasing the intracellular manganese and of thereby enhancing manganese entry into proteins. When external manganese is high, MntP failure forces the accumulation of abundant manganese, which toxifies the cell by blocking iron import and preventing heme synthesis.

3.4 DISCUSSION

E. coli is an iron-dependent organism. Its biology and metabolism are configured around the catalytic capabilities of iron. When *E. coli* is starved for iron or stressed by hydrogen peroxide, it uses manganese in place of iron. Although the two metals are quite similar, *E. coli* prefers not to use manganese during routine iron-rich growth because the kinetics of manganese are not as well suited for enzymes as is iron. Their similarities also make it difficult for the cell to distinguish between the two metals. To lessen these problems, *E. coli* strives to maintain low intracellular manganese levels – So low, in fact, that the manganese-dependent redox enzymes, SodA and NrdEF, are bound to the wrong metal or have no cofactor and fail to function during iron-replete growth. Only during iron-limitation or hydrogen peroxide stress does the cell import enough manganese that these enzymes are more stoichiometrically bound by their cognate metal, manganese.

In this work, I showed that the small protein MntS facilitates manganese delivery to both SodA and NrdEF during normal aerobic growth when manganese is low. MntS also helps cells tolerate hydrogen peroxide, probably by making manganese more available to mononuclear enzymes that normally would function with iron as a metal cofactor. Furthermore, *mntS* seems to be dispensable during manganese-replete conditions. Taken together, *mntS* is most likely useful during periods of transition when iron is unavailable and manganese is needed.

The mechanism by which MntS makes manganese more available to these enzymes is still unclear. I initially perceived MntS as a possible manganese-chaperone due to its small size and the presence of several potential metal-binding residues. Studies show that metalloproteins fail to function when an essential metal-binding residue is

mutated. Our data show that the predicted metal-binding residues are not essential for MntS function, since MntS remained active when the residues were mutated to alanine. Furthermore, purified MntS protein is unable to activate apo-SodA protein in cell extracts when manganese is provided (data not shown). Based on these data, it is unlikely that MntS functions as a manganese-chaperone that directly binds manganese and delivers it to proteins. Ongoing studies in our lab show that the mechanism by which MntS functions to make manganese more available to proteins when manganese is limited is much more complex than originally perceived.

3.4.1 Manganese poisoning of iron-dependent processes by overexpression of MntS or deletion of *mntP*

It appears as though *E. coli* has evolved to keep intracellular manganese concentrations low relative to iron levels. This makes sense when manganese rises to toxic levels, it outcompetes iron for sites in iron-containing proteins. Iron depletion and hydrogen peroxide stress exacerbate the competition even further. Likewise, I observed that overexpression of MntS in manganese-replete conditions causes cellular processes to fail by disrupting the intracellular manganese/iron metal balance; i.e., MntS-overproducing cells contain excessively high intracellular manganese concentrations and are iron-deficient. Our *in vivo* data strongly suggest that when manganese is plentiful and iron is scarce, Fur binds manganese and actively represses iron-acquisition genes, thereby suppressing iron entry. Heme-containing enzymes like catalase and the respiratory oxidases fail, not only because iron is low, but because heme biosynthesis (HemH, the ferrochelatase) is poisoned by the abundance of intracellular manganese.

Manganese poisoning does not just result from blocking iron import, because cells lacking iron uptake genes grow well in our media. Their fitness is enhanced by induction of *ryhB*, which promotes iron-sparing through the elimination of abundant but dispensable iron-containing proteins. Furthermore, iron also has the capacity to sneak through other non-specific divalent metal transporters just as manganese does, which permits cell growth for iron-deficient cells. During manganese toxicity, *ryhB* transcription is turned off (data not shown), which forces cells to rely on low-affinity iron transporters for iron uptake. Extracellular manganese may competively inhibit these transporters.

Excess intracellular manganese might also inhibit other metal transporters, such as the ferrous iron uptake system Feo. This membrane spanning system translocates ferrous iron from the environment into the cytosol. It is possible that manganese could mimic the iron product released and clog Feo intracellularly, i.e. mimic product inhibition.

It is true that manganese cannot bind in place of iron in iron-sulfur clusters, but it seemed possible that manganese could interfere with the Fe-S cluster assembly process. However, our data show that it does not seem to affect the assembly process at all, since the iron-sulfur cluster-containing proteins, Ndh-1 and IscR, remain active during manganese toxicity. How cells specify iron for this process when manganese is replete remains a mystery.

Ligand affinity and metal geometry play a role in the process of excluding one metal over another, since both attributes influence metal binding. In addition, I imagine that the intracellular ratio of manganese to iron plays a critical role in helping cells to

discriminate between the two metals. This would be truly beneficial, since manganese and iron share similar ligand affinities and can inappropriately bind and affect the function of regulators, transporters, and enzymes *in vitro*. The data represented in this work indicate that the transcriptional repressor, Fur, can bind manganese in addition to iron *in vivo*. MntR may also bind iron *in vivo* [13, 18], since manganese titration only minimally reduces *mntH* transcription in a *fur*-null mutant (data not shown). The reduction is MntR dependent, since the decrease was not observed *mntR*-null mutants

Why do cells choose to use the mononuclear protein Fur, which inaccurately senses the available intracellular free iron pool, over the iron-sulfur cluster containing protein, which is more effective at reporting on iron due to its inherent specificity? Other organisms, such as *Bradyrhyzobium*, use heme as an indicator for iron availability [17]. Similar to *E. coli*, manganese metabolism is interconnected with that of iron. However, *Bradyrhyzobium* uses manganese to directly influence iron import by diminishing the binding affinity of heme to the iron transport regulator, Irr [17]. This implies that when manganese concentrations rise, so does iron.

3.4.2 Regulating intracellular manganese concentrations

During iron is abundant, manganese is almost entirely excluded from the cell due to repression of *mntH* by Fur:Fe plus MntR:Mn. All other manganese is redirected out of the cytoplasm through MntP. When iron levels diminish, derepression of *mntH* by Fur promotes manganese entry into the cell via MntH. Since the cell is in need of more manganese, MntR is deactivated. This causes further induction of *mntH*. MntS is also induced by deactivation of MntR to make manganese more available by possibly

inhibiting already synthesized MntP protein. Once the desired manganese level is reached or iron returns, MntR:Mn^{2+} will repress *mntS* and induce *mntP* to rid the cell of excess manganese. *mntH* will also return to normal levels. If MntR fails to repress *mntS* or induce *mntP* when iron becomes available, then manganese concentrations will rise to toxic levels and outcompete iron for binding-sites in enzymes.

Thus, it appears that both MntP and MntS are expressed only intermittently when *E. coli* cells are transitioning from iron-deplete to iron-replete growth. For other organisms residing in manganese-rich environments, MntP might be expressed at a steady state to prevent manganese poisoning of iron-dependent cellular processes.

3.4.3 Do MntS and RybA act within the same physiological pathway to increase manganese availability?

The *mntS* open reading frame resides within the *rybA* gene, which transcribes a small RNA of unknown function. A handful of other small RNAs encoding protein products, known as dual-functioning regulatory small RNAs, have been identified in several bacteria. The most extensively studied dual-functioning sRNA in *E. coli* is SgrS, which encodes a 43 amino acid protein called SgrT. Both SgrS and SgrT act independently within the same physiological pathway to promote recovery from glucose-phosphate stress [5, 7]. It would be interesting to know whether MntS and RybA act in conjunction with each other to increase manganese availability during iron-limitation.

3.5 TABLES

Table 3.1. Bacterial strains and plasmids used in this study.

Strains	Genotype	Reference
MG1655	F⁻ wild type	*E. coli* CGSC
LC106	Δ*ahpF::kan* Δ(*katG::*Tn*10*)1 Δ(*katE12::*Tn*10*)	[37]
BW25113	*lacI rrnB* Δ*lacZ hsdK* Δ*araBAD* Δ*rhaBAD*	[11]
LSW120	As MG1655 Δ*mntS::cat*	This study
MS025	As MG1655 Δ*mntP::cat*	This study
MS023	As MG1655 Δ(*mntS-mntR*)1*::cat*	This study
CAG18493	λ⁻ *rph-1 zbh-29::*Tn*10*	*E. coli* GSC
AA30	As LC106 Δ*mntH2::cat*	[4]
AA99	As MG1655 Δ*mntH2::cat*	[4]
JEM84	As MG1655 Δ(*nrdA-nrdB*)*1::cat*	[22]
JEM609	As MG1655 Δ*lacZ*1 Δ*tonB1* Δ*feoABC* Δ*zupT::cat*	[22]
JEM1136	As MG1655 Δ*lacZ*1 Δ*tonB1* Δ*feoABC* Δ*zupT* Δ(*nrdA-nrdB*)*1*	This study
JEM1253	As JEM1136 with pACYC184	This study
JEM722	As MG1655 Δ*lacZ*1 Δ*tonB1* Δ*feoABC* Δ*zupT* Δ(*nrdH-nrdF*)1 Δ(*nrdA-nrdB*)*1::cat~zbf::*Tn*10*	[22]
JEM1254	As JEM1136 with pLW131	This study
JEM1171	As MG1655 Δ*mntS::kan~zbh-29::*Tn*10*	This study
JEM1177	As LC106 Δ*mntS::kan~zbh-29::*Tn*10*	P1(JEM1171) X LC106
JEM1255	As JEM1177 with pACYC184	This study
JEM1256	As JEM1177 with pLW131	This study
JEM1181	As JEM609 Δ*mntS::kan~zbh-29::*Tn*10*	P1(JEM1171) X JEM609
JEM1202	As BW25113 Δ*sodB1::cat*	This study
JEM1208	As LC106 Δ*sodB1::cat*	P1(JEM1202) X LC106
JEM1212	As LC106 Δ*mntS::kan~zjf-29::*Tn*10* Δ*sodB1::cat*	P1(JEM1202) X JEM1177
JEM1222	As LC106 with pLW131	This study
JEM1214	As MG1655 Δ(*mntS-mntR*)1*::kan~zbh-29::*Tn*10*	P1(CAG18493) X MS023
JEM1216	As LC106 Δ(*mntS-mntR*)1*::kan~zbh-29::*Tn*10*	P1(JEM1214) X LC106
JEM1223	As JEM1216 with pACYC184	This study
JEM1224	As JEM1216 with pLW131	This study
JEM1227	As LC106 Δ(*mntS-mntR*)1*::kan~zbh-29::*Tn*10 ΔmntH2::cat*	P1(AA99) X JEM1216
JEM1233	As MG1655 Δ*sodB1*	P1(JEM1202) X MG1655
JEM1234	As MG1655 Δ*sodB1* Δ*mntS*	This study
JEM1311	As JEM1234 with pLW131	This study
JEM1244	As MG1655 with pDT1-16	This study
JEM271	As MG1655 Δ*lacZ1* pColV	This study

Table 3.1. (continued)

JEM1369	As JEM271 with pBAD24	This study
JEM1370	As JEM271 with pLW112	This study
GS45	As MG1655 Δ*lacZ1 attλ*::[pSJ501::f*huA'-lacZ*+]~*cat*	Lab stock
JEM1395	As GS45 with pBAD24	This study
JEM1396	As GS45 with pLW112	This study
OD502	As MG1655 Δ*(sufABCDSE)19::kan*	Lab stock
JEM1397	As OD502 with pBAD24	This study
JEM1398	As OD502 with pLW112	This study
AL441	As Δ*lacZ1 attλ*::[pSJ501::*katG'*-lacZ+]~*cat*	Lab stock
JEM1405	As AL441 with pBAD24	This study
JEM1406	As AL441 with pLW112	This study
JEM659	As BW25113 Δ*hfq1::cat*	This study
JEM1408	As MG1655 Δ*hfq1::cat*	P1(JEM659) X JEM1407
JEM1409	As JEM1408 with pBAD24	This study
JEM1410	As JEM1408 with pLW112	This study
JW1316-1	Δ(*araD-araB*)*567* Δ*lacZ4787*(::*rrnB-3*) λ⁻ Δ*tyrR760::kan rph-1* Δ(*rhaD-rhaB*)*568 hsdR514*	*E. coli* CGSC
JEM1413	MG1655 Δ*sodB1* Δ*tyrR760::kan*	P1(JW1316-1) X JEM1233
JEM1506	MG1655 Δ*sodB1* Δ*mntS ΔtyrR760::kan*	P1(JW1316-1) X JEM1234
JEM913	MG1655 Δ*lacZ1* Δ*fur-731*	This study
JEM1417	JEM913 with pBAD24	This study
JEM1421	JEM913 with pLW112	This study
JEM1425	JEM913 *attλ*::[pSJ501::*katG'-lacZ*+]~*cat*	P1(AL441) X JEM913
JEM1427	JEM1425 with pBAD24	This study
JEM1428	JEM1425 with pLW112	This study
JEM1431	JEM913 attλ::[pSJ501::katG'-lacZ+] Δ*ryhB1::cat*	This study
JEM1447	JEM1431 with pBAD24	This study
JEM1448	JEM1431 with pLW112	This study
JEM1453	MG1655 ΔP_{katG}::*tetRA*-23 with pBAD24	This study
JEM1454	MG1655 ΔP_{katG}::*tetRA*-23 with pLW112	This study
JEM1455	JEM913 attλ::[pSJ501::katG'-lacZ+] Δ*mntH2::cat*	This study
JEM1457	MG1655 ΔP_{katG}::*tetRA*-23 Δ*fur-731::kan*	This study
JEM1459	JEM913 attλ::[pSJ501::katG'-lacZ+] Δ*iscR::cat*	This study
JEM981	MG1655 Δ*lacZ1* Δ*fur-731::kan* with pColV	This study
JEM1463	JEM981 with pBAD24	This study
JEM1464	JEM981 with pLW112	This study
JEM1465	MG1655 Δ*lacZ1 attλ*::[pSJ501::f*huA'-lacZ*+]~*cat* Δ*fur-731::kan* with pBAD24	This study
JEM1466	MG1655 Δ*lacZ1 attλ*::[pSJ501::f*huA'-lacZ*+]~*cat* Δ*fur-731::kan* with pLW112	This study
SJ169	MG1655 Δ*lacZ1 attλ*::[pSJ501::*iscR'-lacZ*+]~*cat*	Lab stock
JEM1474	SJ169 with pBAD24	This study
JEM1475	SJ169 with pLW112	This study

Table 3.1. (continued)

SJ253	MG1655 Δ*lacZ1 attλ*::[pSJ501::*sufA'-lacZ*+]~*cat*	Lab stock
JEM1476	SJ253 with pBD24	This study
JEM1477	SJ253 with pLW112	This study
JS248	MG1655 Δ*aroB1::cat*	Lab stock
JEM1494	JEM1234 Δ*aroB1::cat*	P1(JS248) X JEM1234
JEM1522	JEM1233 Δ*mntP::kan*	P1(MS025) X JEM1233
JEM1524	JEM1234 Δ*mntP::kan*	P1(MS025) X JEM1234
JEM1538	MG1655 Δ*lacZ1* Δ*fur-731* Δ*ryhB::cat* with pBAD24	This study
JEM1540	MG1655 Δ*lacZ1* Δ*fur-731* Δ*ryhB::cat* with pLW112	This study
SMA1091	MG1655 Δ*lacZ1* Δ*hemA::kan attλ*::[pSJ501::*hemA'-lacZ*+]	Lab stock
JEM1579	SMA1091 with pBAD24	This study
JEM1580	SMA1091 with pLW112	This study
AA171	MG1655 Δ*lacZ1 attλ*::[pSJ501::*mntH'-lacZ*+]~*cat*	[4]
JEM1609	JEM913 *attλ*::[pSJ501::*mntH'-lacZ*+]~*cat*	P1(AA171) X JEM913
JEM1647	JEM913 *attλ*::[pSJ501::*mntH'-lacZ*+]	This study
JEM1651	JEM1647 Δ*mntH2::cat*	P1(AA99) X JEM1647
AA46	MG1655 Δ*mntR1::cat*	Lab stock
JEM1667	JEM1647 Δ*mntR1::cat*	P1(AA46) X JEM1647
JEM1611	JEM913 Δ*mntS attλ*::[pSJ501::*mntH'-lacZ*+]~*cat*	This study
JEM1649	JEM913 Δ*mntS attλ*::[pSJ501::*mntH'-lacZ*+]	This study
JEM1653	JEM1649 Δ*mntH2::cat*	P1(AA99) X JEM1649
JEM1663	BW25113 Δ*mntP2::cat*	This study
JEM1682	SMA1091 Δ*mntP2::cat*	P1(JEM1663) X SMA1091
JEM1683	JEM1682 with pBAD24	This study
JEM1684	JEM1682 with pLW112	This study
JEM1715	MG1655 Δ*mntS* Δ*mntP::kan*	This study
JEM1719	JEM271 Δ*mntP::kan*	P1(MS025) X JEM71
JEM1713	MG1655 Δ*lacZ1 attλ*::[pSJ501::f*huA'-lacZ*+]	This study
JEM1720	JEM1713 Δ*mntP::kan*	P1(MS025) X JEM1713
JEM1714	MG1655 Δ*lacZ1 attλ*::[pSJ501::f*huA'-lacZ*+] Δ*fur-731*	This study
JEM1722	JEM1714 Δ*mntP::kan*	P1(MS025) X JEM1714
JEM1718	MG1655 Δ*lacZ1* Δ*fur-731* with pColV	This study
JEM1724	JEM1718 Δ*mntP::kan*	P1(MS025) X JEM1718
MG1655/pBAD24	MG1655 with pBAD24	This study
MG1655/pLW112	MG1655 with pLW112	This study

Table 3.1. (continued)

JEM1726	MS025 with pBAD24	This study
JEM1727	MS025 with pLW112	This study
JEM1571	MG1655 with pJEM67	This study
JEM1575	MG1655 with pJEM68	This study
JEM1603	JEM271 with pJEM67	This study
JEM1604	JEM271 with pJEM68	This study
JEM1290	MG1655 with pMS17	This study
JEM1291	MG1655 with pMS18	This study
JEM1293	MG1655 with pMS20	This study
JEM1294	MG1655 with pMS21	This study
JEM1295	MG1655 with pLW125	This study
JEM1335	MG1655 with pLW133	This study
JEM1336	MG1655 with pLW134	This study
JEM1337	MG1655 with pLW135	This study
JEM1338	MG1655 with pLW136	This study

Plasmid	**Relevant characteristics**	**Reference**
pBAD24	Amp^R ColE1	Lab stock
pLW112	pBAD24 containing *mntS* ORF and its own Shine-Dalgarno	[42]
pJEM67	pBAD24 containing *mntS*-(Phe11 +1 frameshift)	This study
pJEM68	pBAD24 containing *mntS*-(Phe16 +1 frameshift)	This study
pMS17	pBAD24 containing *mntS*-(E3A)	This study
pMS18	pBAD24 containing *mntS*-(C7A)	This study
pMS20	pBAD24 containing *mntS*-(C27A)	This study
pMS21	pBAD24 containing *mntS*-(D28A)	This study
pLW125	pBAD24 containing *mntS*-(H13A)	This study
pLW133	pBAD24 containing *mntS*-(E3A/C7A/D28A)	This study
pLW134	pBAD24 containing *mntS*-(E3A/C27A/D28A)	This study
pLW135	pBAD24 containing *mntS*-(C7A/C27A/D28A)	This study
pLW136	pBAD24 containing *mntS*-(E3A/C7A/C27A)	This study
pACYC184	Tet^R Cam^R	[21]
pLW131	pACYC184 containing *rybA* (includes *mntS* ORF)	This study
pKD3	*bla* FRT *cat* FRT PS1 PS2 oriR6K	[11]
pKD46	*bla* P_{BAD} *gam bet exo* pSC101 oriTS	[11]
pCP20	*bla cat cI857* λP_R *flp* pSC101 oriTS	[9]
pSJ501	pAH125 derivative with *cat* flanked by *flp* sites	Lab stock
pDT1-16	pBR322 containing *sodA* under *tac* promoter, Amp^R	Lab stock

Table 3.2. Primers used for site directed mutagenesis in this study.

Primer	Sequence
MntS-Phe11 +1frameshift	5′-TGAATGAGTTCAAGAGGTGTATGCGCGTGTaTTAGTCATTCTC CCTTTAAAGTACGGTTA-3′
MntS-Phe16 +1frameshift	5′-AGGTGTATGCGCGTGTTTAGTCATTCTCCCTaTTAAAGTACGGTT AATGCTGCTCTCTAT-3′
MntS-Glu3Ala	5′-AGGAGGTCTTATGAATGcGTTCAAGAGGTGTATGCGCGTGTTTA GTCATTCTCCCTTTAA-3′
MntS-Cys7Ala	5′-AGGAGGTCTTATGAATGAGTTCAAGAGGgcTATGCGCGTGTTTA GTCATTCTCCCTTTAA-3′
MntS-Cys27Ala	5′-AAGTACGGTTAATGCTGCTCTCTATGTTGgcCGATATGGTCAACA ACAAACCGCAGCAAG-3′
MntS-Asp28Ala	5′-GTACGGTTAATGCTGCTCTCTATGTTGTGCGcTATGGTCAACA ACAAACCGCAGCAAGAT-3′
MntS-His13Ala	5′-GTTCAAGAGGTGTATGCGCGTGTTTAGTgcTTCTCCCTTTAAAGT ACGGTTAATGCTG-3′
MntS-E3A/C7A/D28A	5′-AGGAGGTCTTATGAATGcGTTCAAGAGGgcTATGCGCGTGTTT AGTCATTCTCCCTTTAA-3′
MntS-E3A/C27A/D28A	5′-AAGTACGGTAATGCTGCTCTCTATGTTGgcCGCTATGGTCAACA ACAAACCGCAGCAAG-3′
MntS-C7A/C27A/D28A	5′-AAGTACGGTTAATGCTGCTCTCTATGTTGgcCGcTATGGTCAACA ACAAACCGCAGCAAG-3′
MntS-E3A/C7A/C27A	5′-AGGAGGTCTTATGAATGcGTTCAAGAGGgcTATGCGCGTGTTTA GTCATTCTCCCTTTAA-3′

3.6 FIGURES

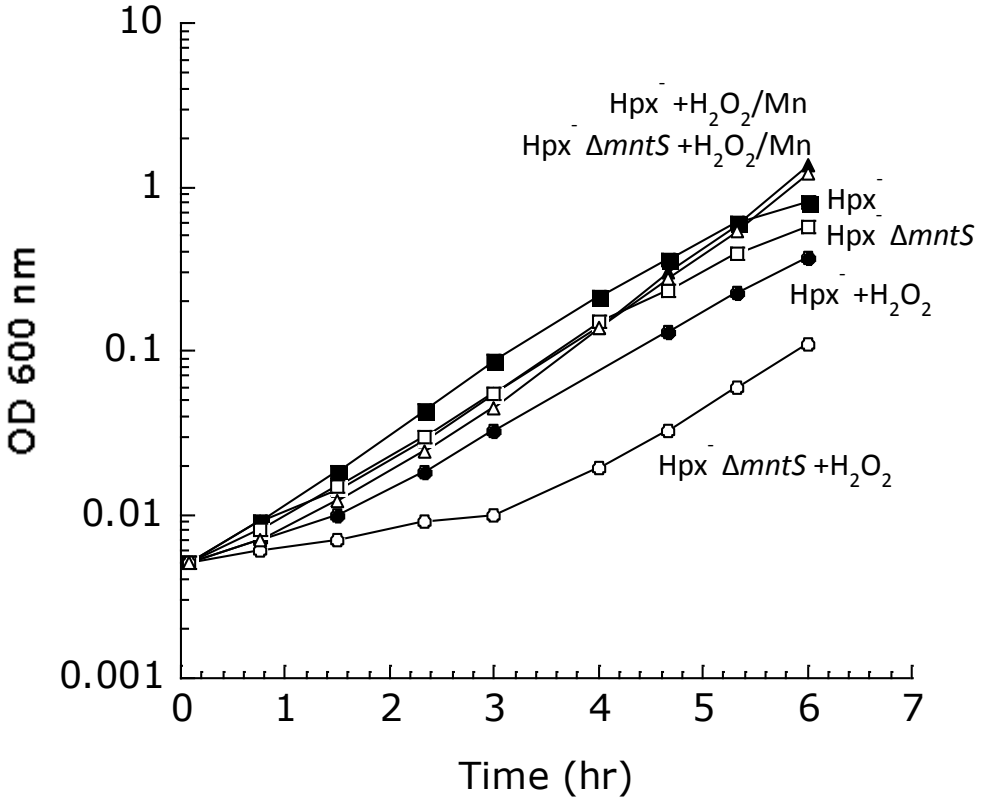

Figure 3.1. *mntS* helps cells cope with H_2O_2 stress. Cells were pre-cultured in anaerobic M9 glucose/casamino acids medium and then diluted at time zero into the same aerobic medium containing 0, 15 μM H_2O_2, or 15 μM H_2O_2/5 μM $MnCl_2$. Strains were LC106 (Hpx^-) and JEM1177 (Hpx^- Δ*mntS*).

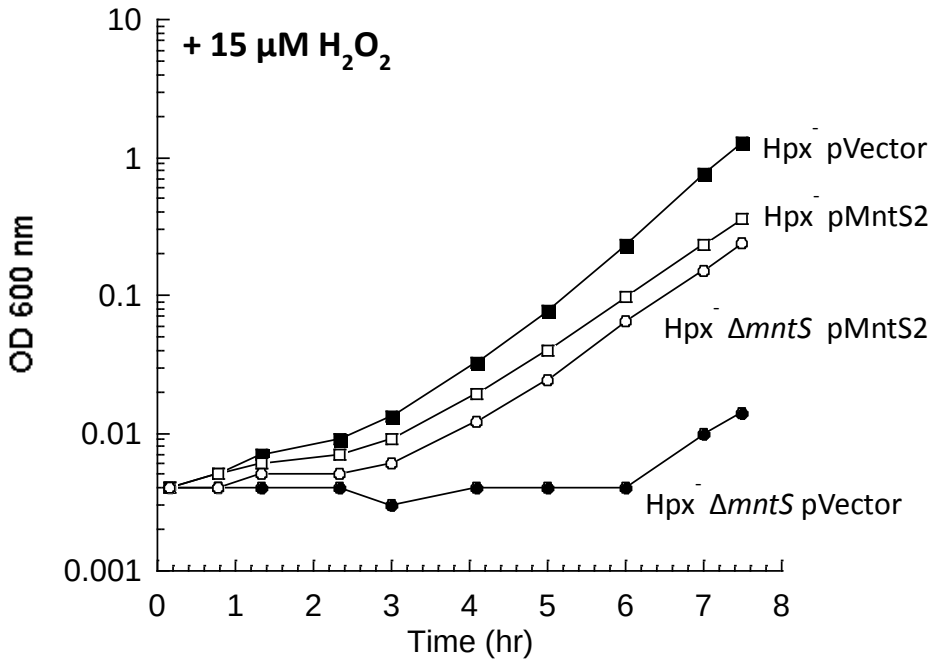

Figure 3.2. Growth defect observed is specific to Δ*mntS*, since growth is restored by complementation with pMntS. Cells were pre-cultured in anaerobic M9 glucose/casamino acids medium and then diluted at time zero into the same aerobic medium containing 15 µM H_2O_2. Strains used were LC106 (Hpx⁻) and JEM1177 (Hpx⁻ Δ*mntS*) expressing pMntS2 (pLW131, *mntS* under its native promoter).

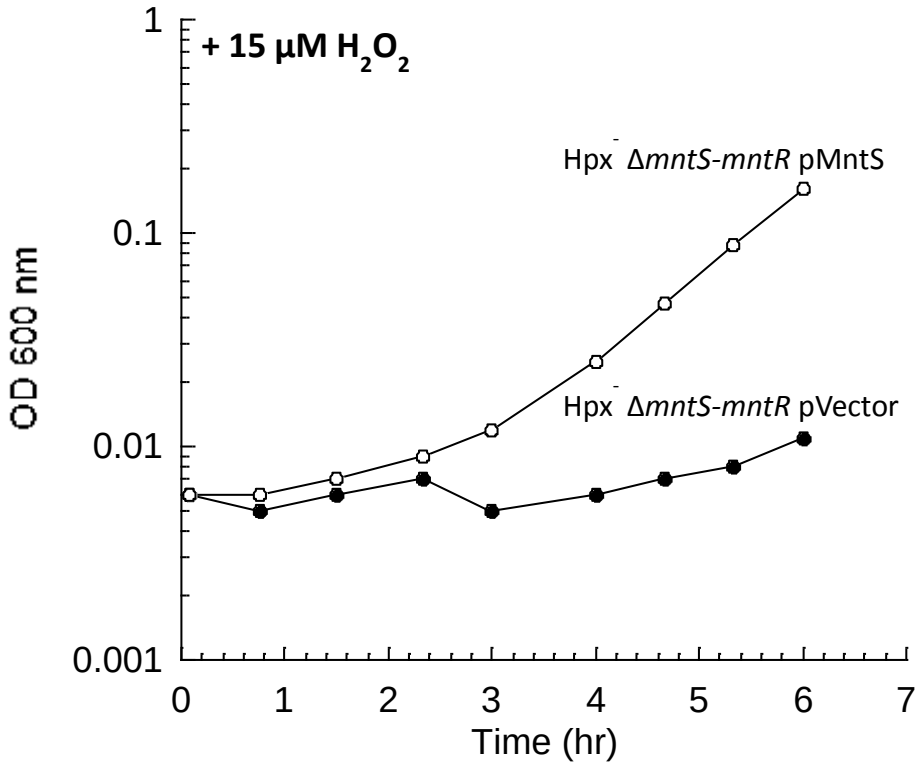

Figure 3.3. *mntS*-null mutants are not poisoned by manganese via failure of MntR. Cells were pre-cultured in anaerobic M9 glucose/casamino acids medium and then diluted at time zero into the same aerobic medium containing 15 µM H_2O_2. Strains used were JEM1216 (Hpx$^-$ Δ(*mntS-mntR*)) expressing empty vector (pACYC184) or pMntS2 (pLW131, *mntS* under its native promoter).

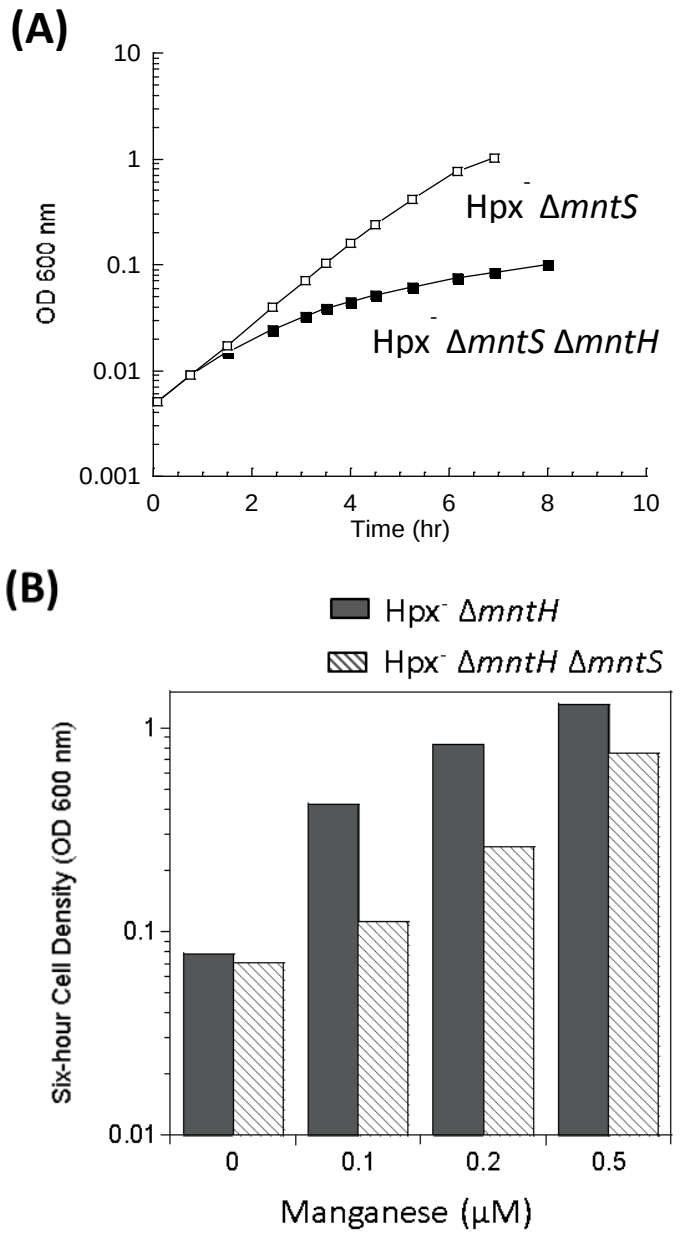

Figure 3.4. MntH and MntS function independent of each other. Cells were pre-cultured in anaerobic M9 glucose/casamino acids medium and then diluted at time zero into the same aerobic medium.

A. MntH functions in the absence of *mntS.* Strains were JEM1177 (Hpx⁻ Δ*mntS*) and JEM1227 (Hpx⁻ Δ*mntS* Δ*mntH*).

B. MntS functions in the absence of *mntH*. OD_{600} of strains AA30 (Hpx⁻ Δ*mntH*) and JEM1227 (Hpx⁻ Δ*mntH* Δ*mntS*) grown in the presence of increasing concentrations of $MnCl_2$ for 6 hr.

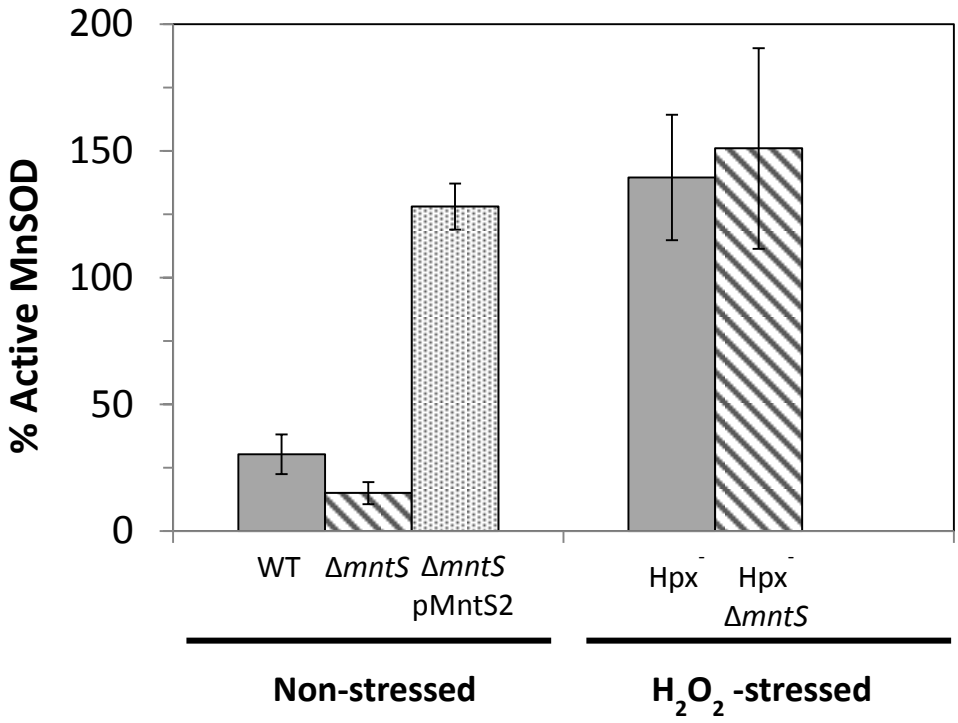

Figure 3.5. MntS ensures manganese is inserted into MnSOD in non-stressed/manganese-poor cells. The fraction of active MnSOD was measured in cell extracts prepared from cultures grown aerobically to 0.25 OD_{600} in M9 glucose/casamino acids medium. Data represent the mean of three independent cultures. All strains contain the *sodB*-null allele. Strains were JEM1233 (WT), JEM1234 (Δ*mntS*), JEM1311 (Δ*mntS* with pMntS2, *mntS* under the control of its native promoter), JEM1208 (Hpx^-), and JEM1212 (Hpx^- Δ*mntS*).

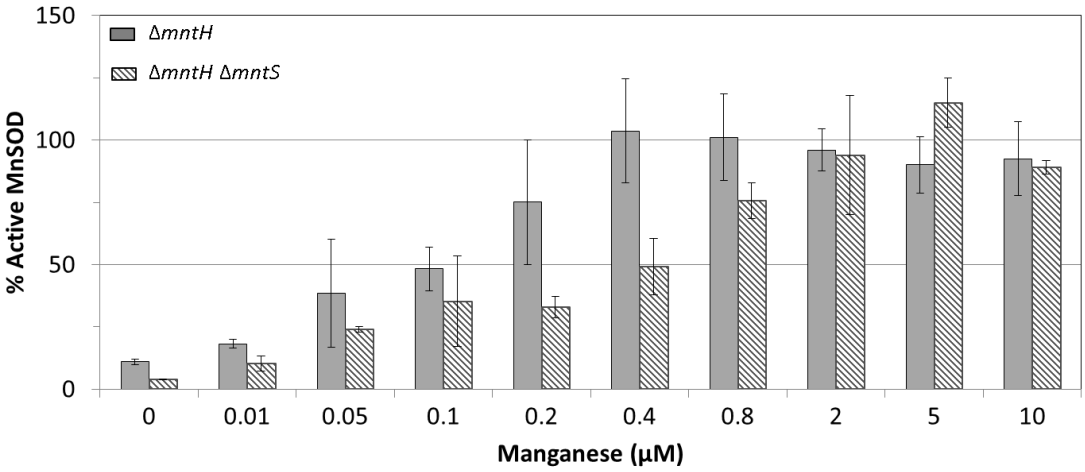

Figure 3.6. MntS helps activate MnSOD when manganese concentrations are low. The fraction of active MnSOD was measured in cell extracts prepared from cultures grown aerobically to 0.25 OD_{600} in M9 glucose/casamino acids medium supplemented with increasing concentrations of $MnCl_2$. Data represent the mean of three independent cultures. All strains contain the *sodB*-null allele. Strains were JEM1235 (Δ*mntH*) and JEM1237 (Δ*mntH* Δ*mntS*).

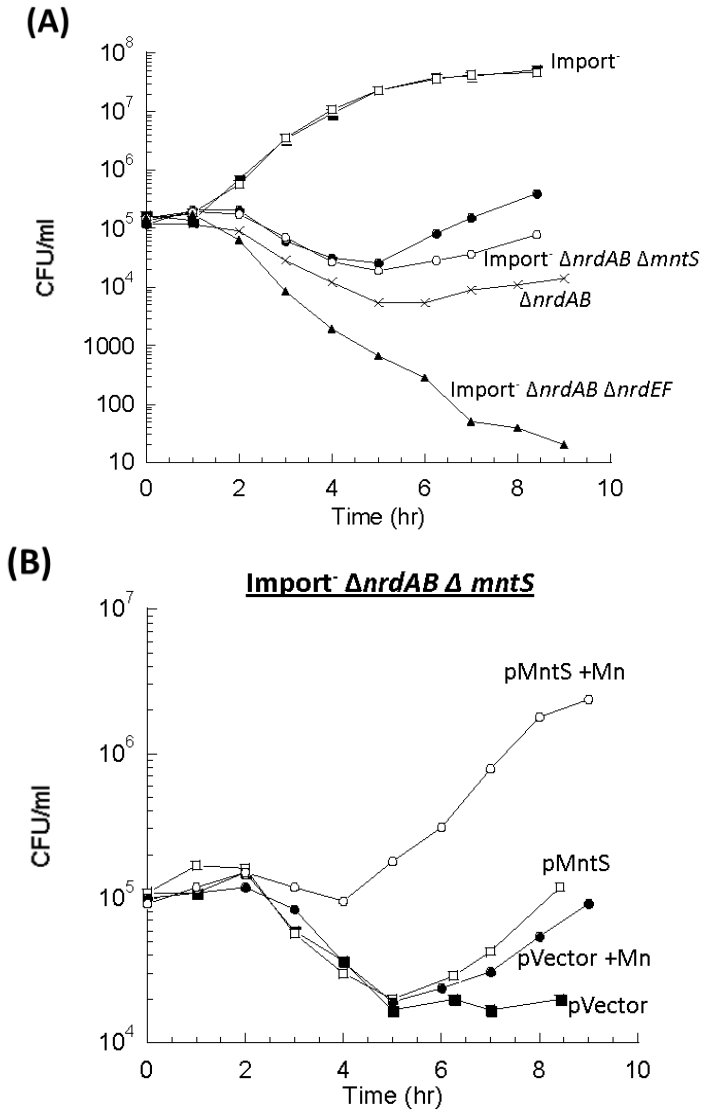

Figure 3.7. MntS helps activate the manganese-dependent RNR, NrdEF. Cells pre-cultured in anaerobic MOPS glucose/casamino acids medium were diluted into aerobic medium at time zero and viability was monitored by anaerobic plating. "Import-minus" strains contain Δ*tonB* Δ*feoABC* Δ*zupT* null alleles and therefore have reduced iron import.

A. Strains were JEM609 (Import$^-$), JEM1181 (Import$^-$ Δ*mntS*), JEM1136 (Import$^-$ Δ*nrdAB*), JEM1836 (Import$^-$ Δ*nrdAB* Δ*mntS*), JEM722 (Import$^-$ Δ*nrdAB* Δ*nrdHIEF*), and JEM84 (Δ*nrdAB*).

B. Viability of Import$^-$ Δ*nrdAB* Δ*mntS* (JEM1183) harboring empty vector (pACYC184) or pMntS2 (pLW131, *mntS* under the control of its native promoter) grown in MOPS glucose/casamino acids medium with or without 50 μM $MnCl_2$.

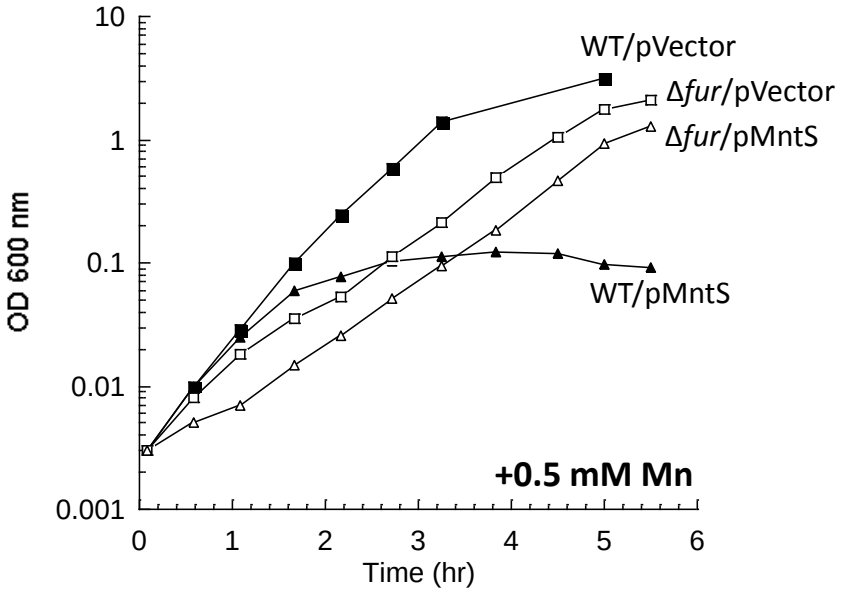

Figure 3.8. MntS overproducing cells are manganese sensitive. Cells were pre-cultured in aerobic LB medium and then diluted at time zero into fresh LB/arabinose medium with or without 0.5 mM $MnCl_2$. Strains were MG1655 (WT) and JEM913 (Δ*fur*) harboring empty vector (pBAD24) or pMntS (pLW112, *mntS* expression driven by the *araBAD* promoter). Data represent the mean of three independent cultures.

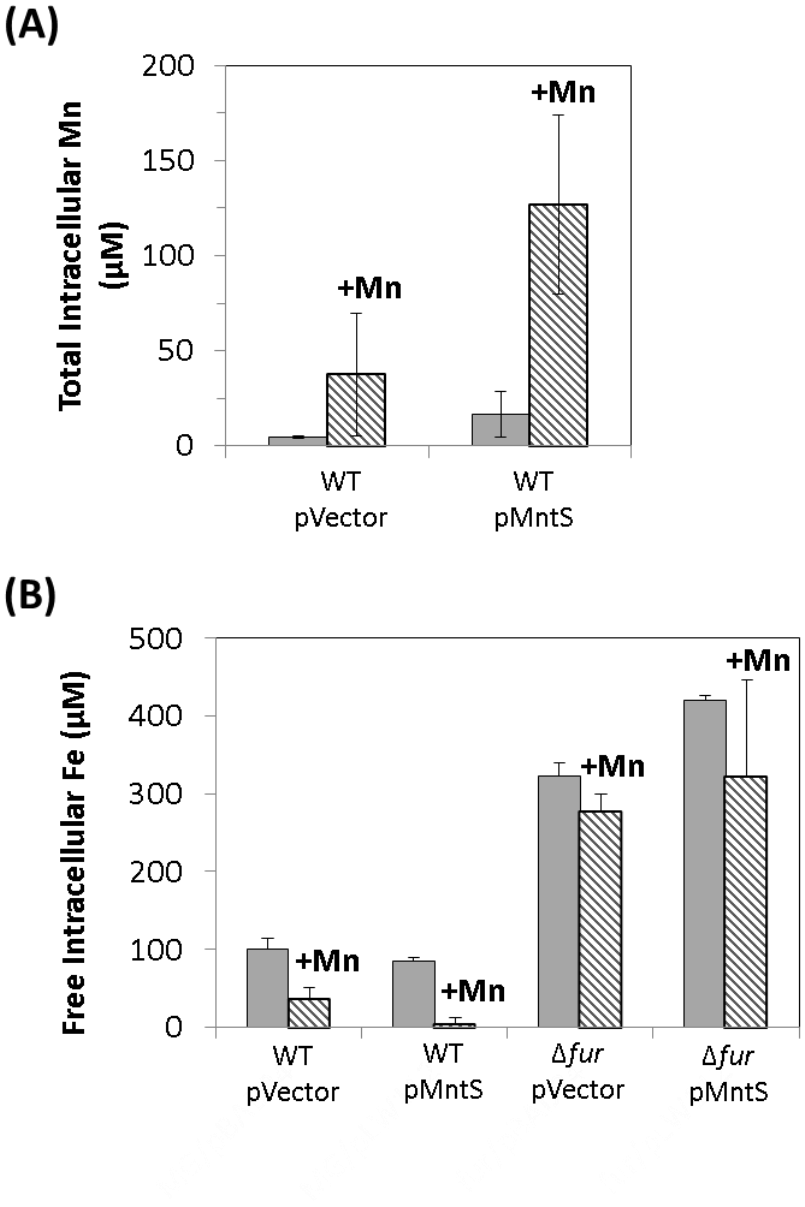

Figure 3.9. MntS overproducing cells are loaded with manganese and contain very low amounts of available free iron. Cells pre-cultured in aerobic LB medium were diluted into fresh LB/arabinose medium with or without 0.5 mM $MnCl_2$ and harvested after 2.5 hr of aerobic growth. Data represent the mean of three independent cultures. Strains were MG1655 (WT) and JEM913 (Δ*fur*) harboring empty vector (pBAD24) or pMntS (pLW112, *mntS* expression driven by the *araBAD* promoter).

A. Total intracellular manganese measured by ICP-MS.

B. The concentration of available intracellular iron measured by EPR.

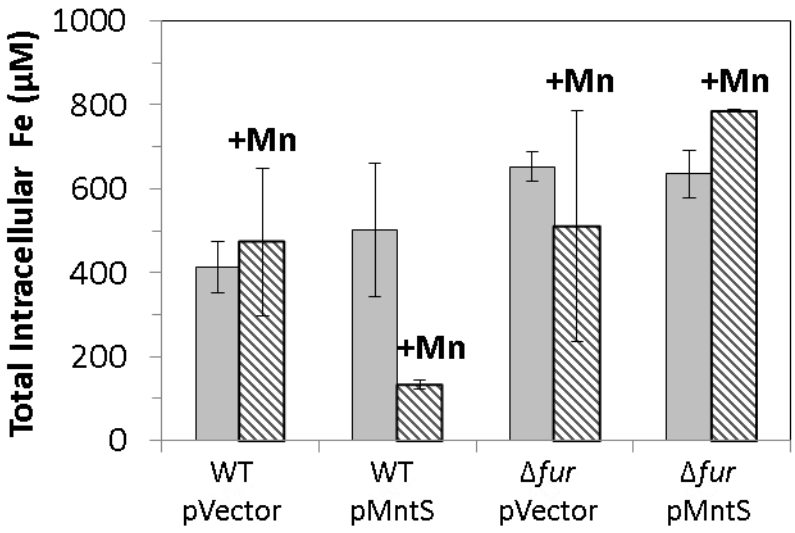

Figure 3.10. Intracellular iron concentrations are low in MntS overexpressing cells grown in Mn-replete conditions. Cells pre-cultured in aerobic LB medium were diluted into fresh LB/arabinose medium with or without 0.5 mM $MnCl_2$ and harvested after 2.5 hr of aerobic growth, followed by ICP-MS analysis. Data represent the mean of three independent cultures. Strains were MG1655 (WT) and JEM913 (Δ*fur*) harboring empty vector (pBAD24) or pMntS (pLW112, *mntS* expression driven by the *araBAD* promoter).

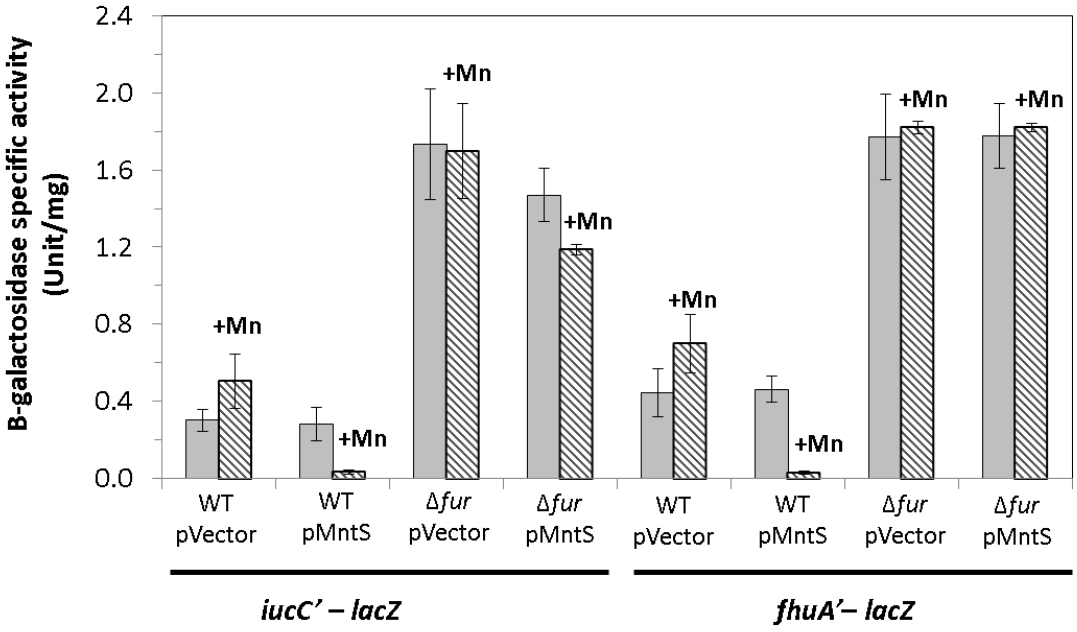

Figure 3.11. The Fur regulon is profoundly repressed via Fur during manganese toxicity. Cells were grown in aerobic LB/arabinose medium with or without 0.5 mM $MnCl_2$ and aerated for 2.5 hr before harvesting. Data represent the mean of three independent cultures. Strains bearing *iucC'-lacZ* were JEM1369 (WT/pBAD24), JEM1370 (WT/pLW112), JEM1463 (Δ*fur* /pBAD24), and JEM1464 (Δ*fur*/pLW112). Strains bearing *fhuA'-lacZ* were JEM1395 (WT/pBAD24), JEM1396 (WT/pLW112), JEM1465 (Δ*fur* /pBAD24), and JEM1466 (Δ*fur*/pLW112). Note that pMntS (pLW112) contains *mntS* expression driven by the *araBAD* promoter.

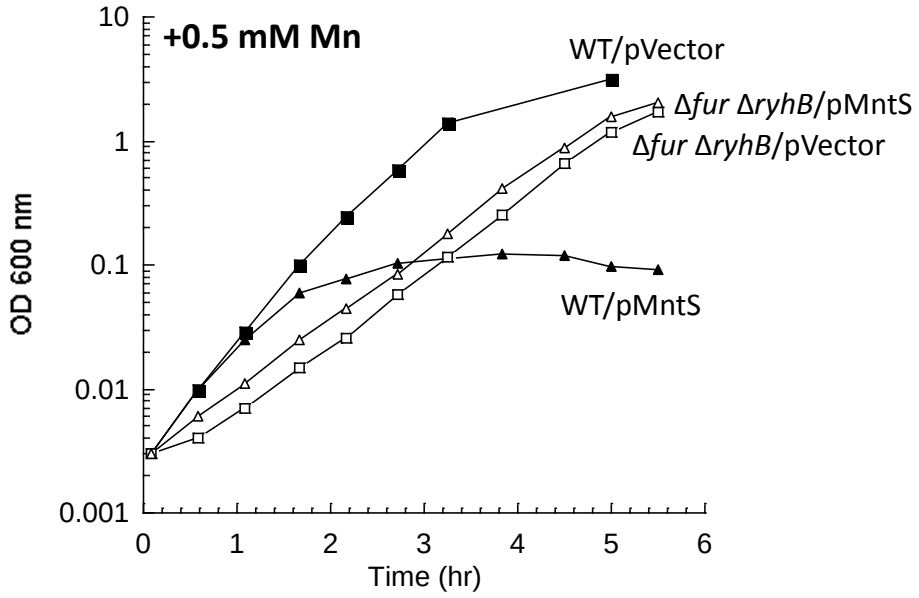

Figure 3.12. Restored growth in Δ*fur*/pMntS mutants is due to iron import and not an increase in RyhB synthesis. Cells were pre-cultured in aerobic LB medium and then diluted at time zero into fresh LB/arabinose medium with 0.5 mM $MnCl_2$. Strains were MG1655 (WT) and JEM1538/JEM1540 (Δ*fur* Δ*ryhB*) harboring empty vector (pBAD24) or pMntS (pLW112, *mntS* expression driven by the *araBAD* promoter).

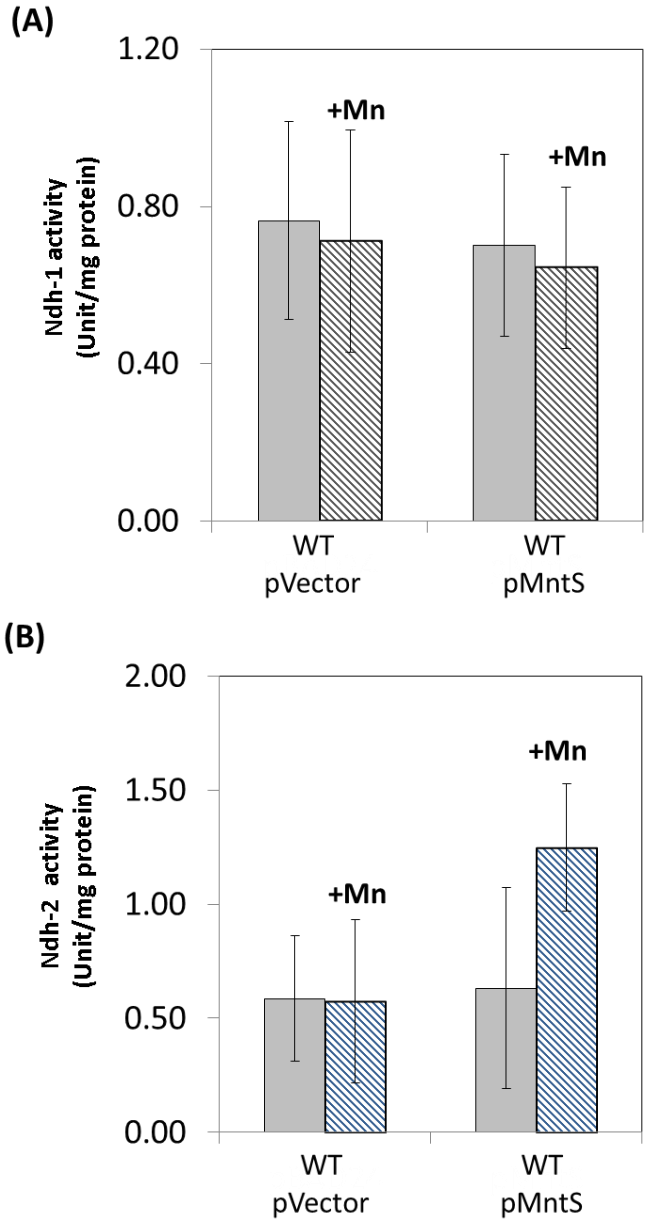

Figure 3.13. NADH dehydrogenase levels remain normal during manganese intoxication. Cells lacking the *suf* operon were pre-cultured in aerobic LB medium, and then diluted into fresh LB/arabinose medium with or without 0.5 mM $MnCl_2$. Measurements of **(A)** Ndh-1and **(B)** Ndh-2 activity were determined after 2.5 hr of manganese treatment. Data represent the mean of three independent cultures. Strains were OD502 (Δ*suf*) harboring empty vector (pBAD24) or pMntS (pLW112, *mntS* expression driven by the *araBAD* promoter).

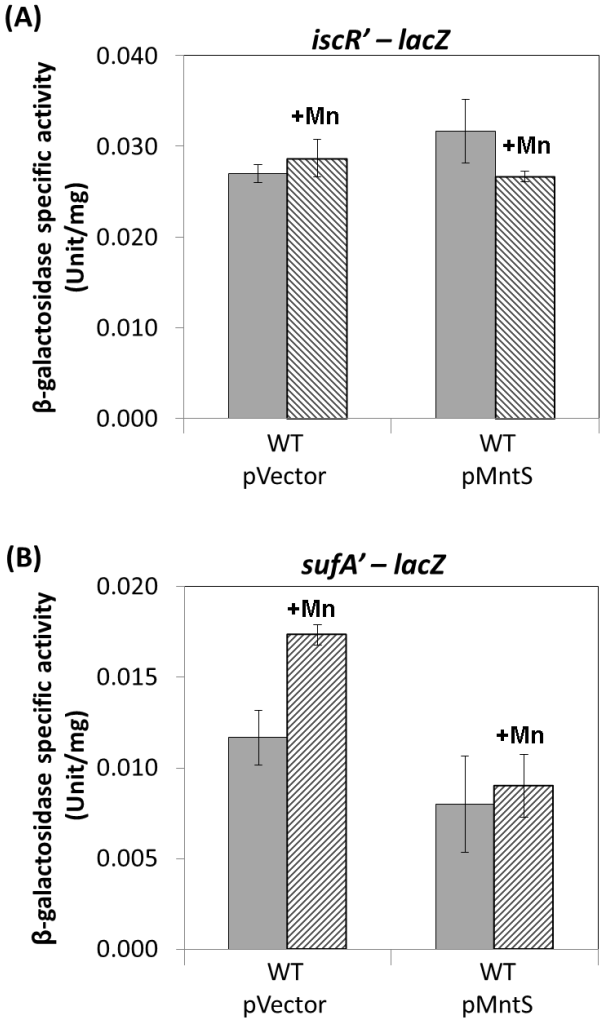

Figure 3.14. Transcription of the *iscR* and *sufA* genes were not induced during manganese intoxication. Cells were grown in anaerobic LB/arabinose medium with or without 0.5 mM $MnCl_2$ and aerated for 2.5 hr before harvesting. Data represent the mean of three independent cultures.

A. Expression of *iscR* measured from JEM1474 (WT/pBAD24) and JEM1475 (WT/pLW112).

B. Expression of *sufA* measured from JEM1476 (WT/pBAD24) and JEM1477 (WT/pLW112).

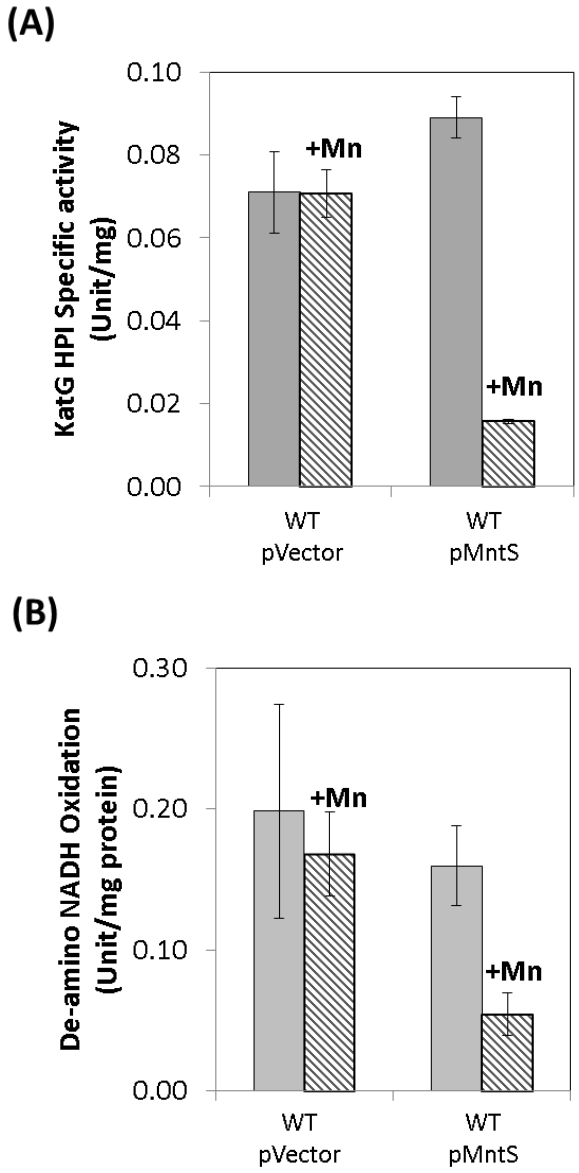

Figure 3.15. Heme-containing enzymes, catalase and cytochrome oxidase, fail to function properly during manganese toxicity. Cells were grown in anaerobic LB/arabinose medium with or without 0.5 mM $MnCl_2$ and aerated for 2.5 hr before harvesting. Data represent the mean of three independent cultures.

A. HPI activity was determined from strains JEM1405 (WT/pBAD24) and JEM1406 (WT/pLW112).

B. Deamino-NADH oxidation was determined from strains lacking the *suf* operon, JEM1397 (WT/pBAD24) and JEM1398 (WT/pLW112). Note that the *suf* operon was deleted to prevent the cell from turning it on in the event that the main iron-sulfur cluster assembly system (*isc*) was failing.

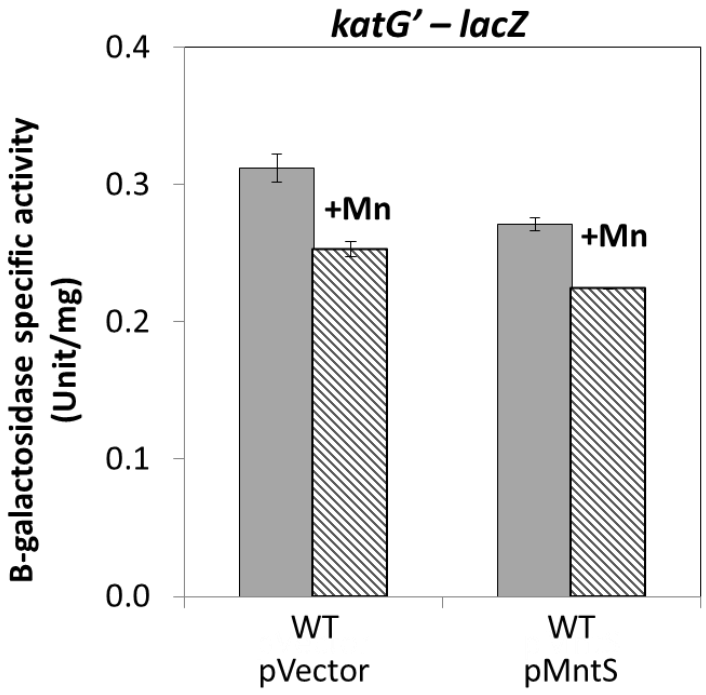

Figure 3.16. Low HPI activity does not result from decreased transcription of *katG*. Cells bearing the *katG'-lacZ* transcriptional fusion were pre-cultured in aerobic LB, and then diluted into LB/arabinose medium with or without 0.5 mM $MnCl_2$. Cells were harvested after 2.5 hr treatment. Strains were AL441 harboring empty vector (pBAD24) or pMntS (pLW112).

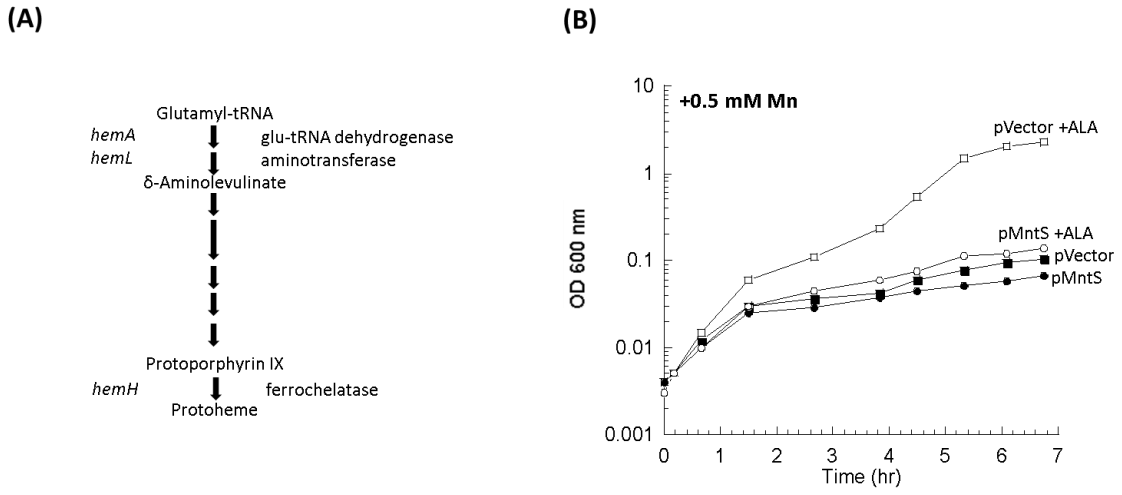

Figure 3.17. Supplementation with 5-ALA does not suppress manganese sensitivity in Δ*hemA* mutants overexpressing MntS.

A. Heme biosynthetic pathway displayed with genes on the left and corresponding protein products on the right.

B. Cells lacking *hemA* were pre-cultured in anaerobic LB medium, and then diluted at time zero into fresh aerobic LB/arabinose medium with or without 5-ALA. Strains were SMA1091 (Δ*hemA*) harboring empty vector (pBAD24) or pMntS (pLW112, *mntS* expression driven by the *araBAD* promoter).

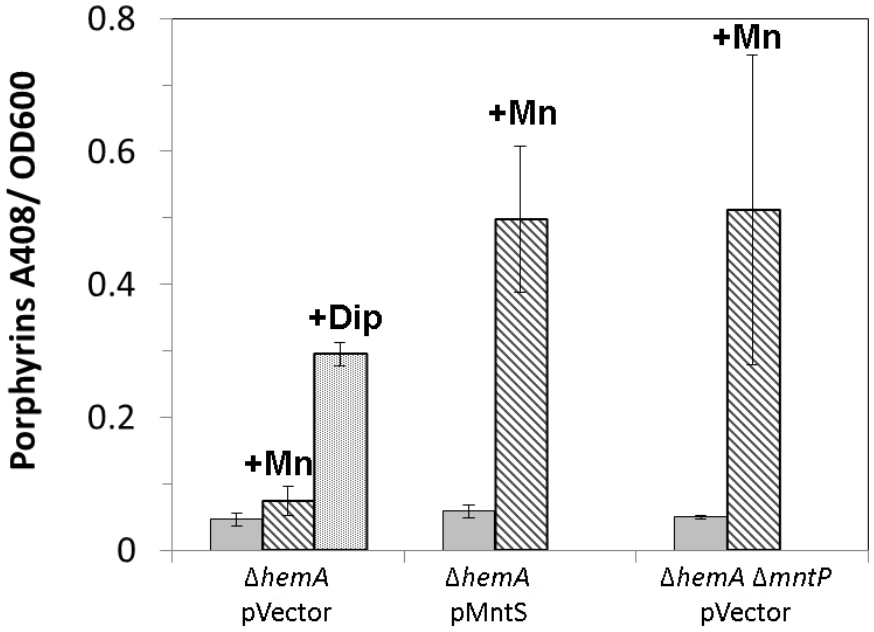

Figure 3.18. Manganese sensitive cells accumulate porphyrins. *hemA*-null mutants were grown in aerobic LB/arabinose medium supplemented with 1 mM 5-ALA. Cells were harvested 2.5 hr after treatment with or without 0.5 mM $MnCl_2$ or 100 μM DIP. Data represent the mean of three independent cultures. Strains were JEM1579 (Δ*hemA*/pBAD24), JEM1580 (Δ*hemA*/pLW112), JEM1683 (Δ*mntP*/pBAD24).

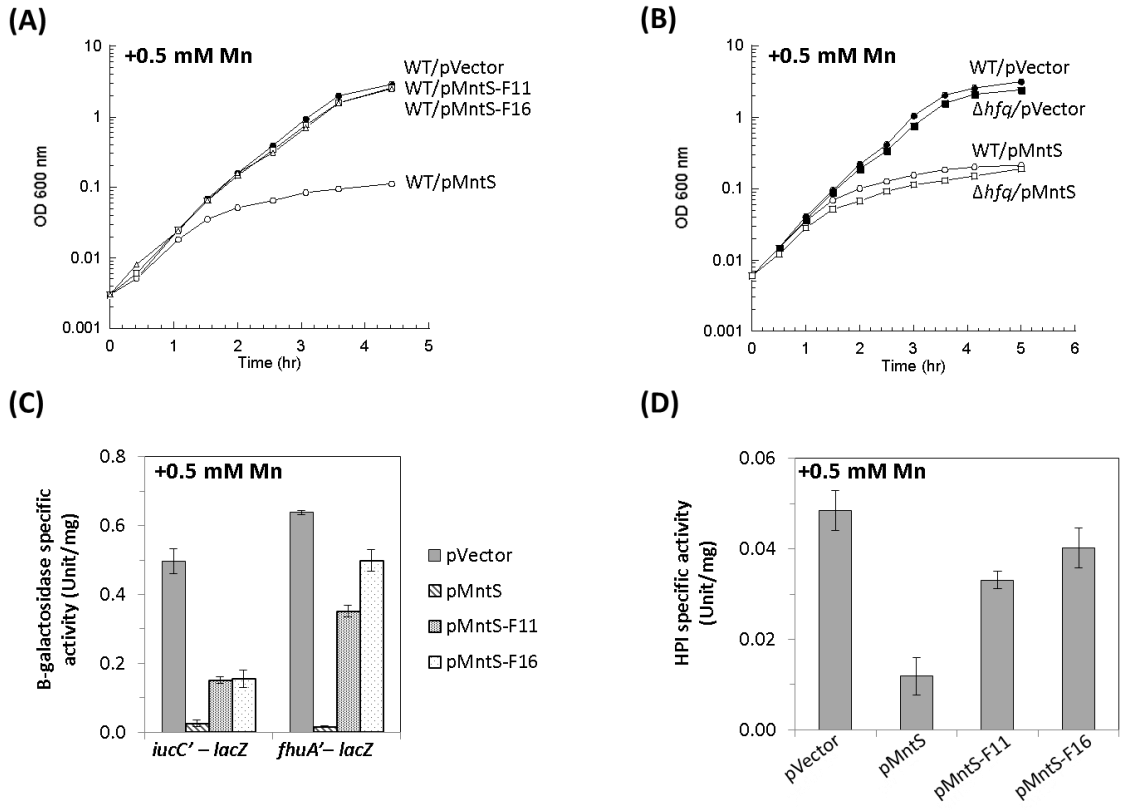

Figure 3.19. MntS functions as a protein to confer manganese sensitivity. Cells were cultured in aerobic LB/arabinose supplemented with 0.5 mM $MnCl_2$ 2.5 hr before harvesting. Data represent the mean of three independent cultures. Plasmids used were empty vector (pBAD24), pMntS (pLW112, *mntS* driven by the *araBAD* promoter), pMntS-F11 (pJEM67, *mntS* containing a frameshift at F11), or pMntS-F16 (pJEM68, *mntS* containing a frameshift at F16).

A. Cell growth over time of WT (MG1655) cells.

B. Cell growth over time of WT (MG1655) and Δ*hfq* (JEM1407) mutants.

C. Transcription levels of the Fur regulated genes *iucC'-lacZ* and *fhuA'-lacZ* in WT strains (JEM271 and GS45, respectively) harboring indicated plasmids.

D. HPI activity determined from WT (GS45) strains harboring indicated plasmids.

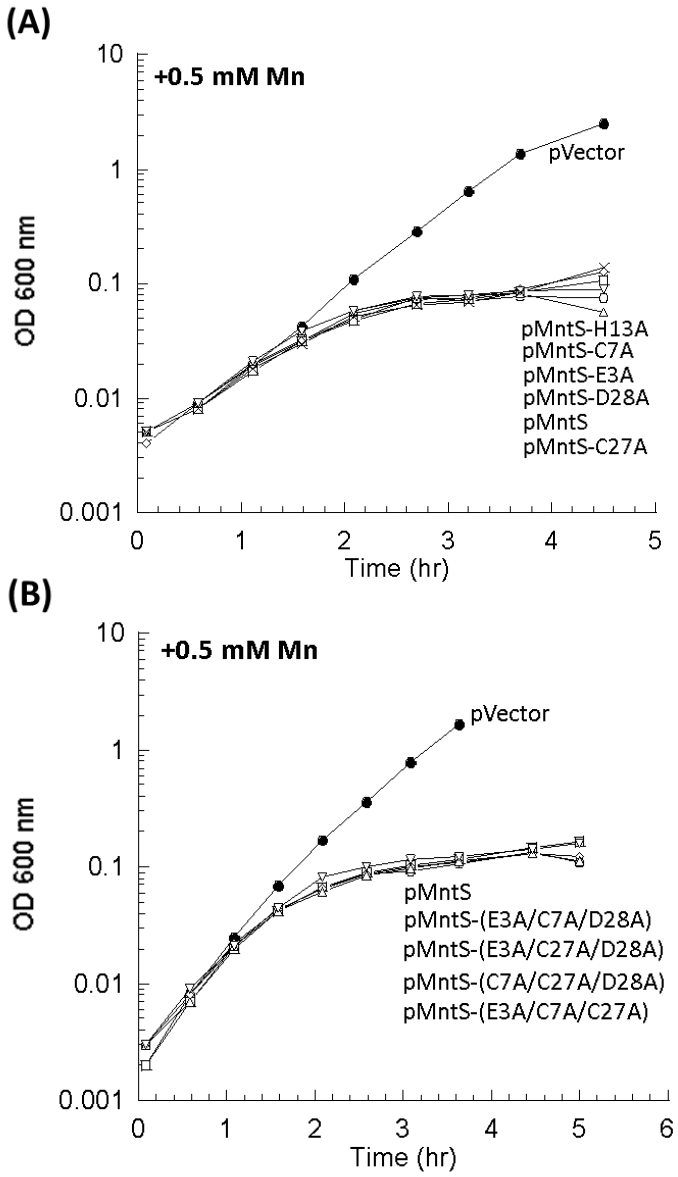

Figure 3.20. MntS mutant alleles still show manganese sensitivity. WT (MG1655) cells harboring mutant pMntS derivatives were pre-cultured in aerobic LB medium and then diluted at time zero into fresh LB/arabinose medium with or without 0.5 mM $MnCl_2$. MntS protein expression is induced by arabinose.

A. Plasmids were pMntS-E3A (pMS017), pMntS-C7A (pMS018), pMntS-C27A (pMS020), pMntS-D28A (pMS021), and pMntS-H13A (pLW125).

B. Plasmids were pMntS-(E3A/C7A/D28A) (pLW133), pMntS-(E3A/C27A/D28A) (pLW134), pMntS-(C7A/C27A/D28A) (pLW135), and pMntS-(E3A/C7A/C27A) (pLW136).

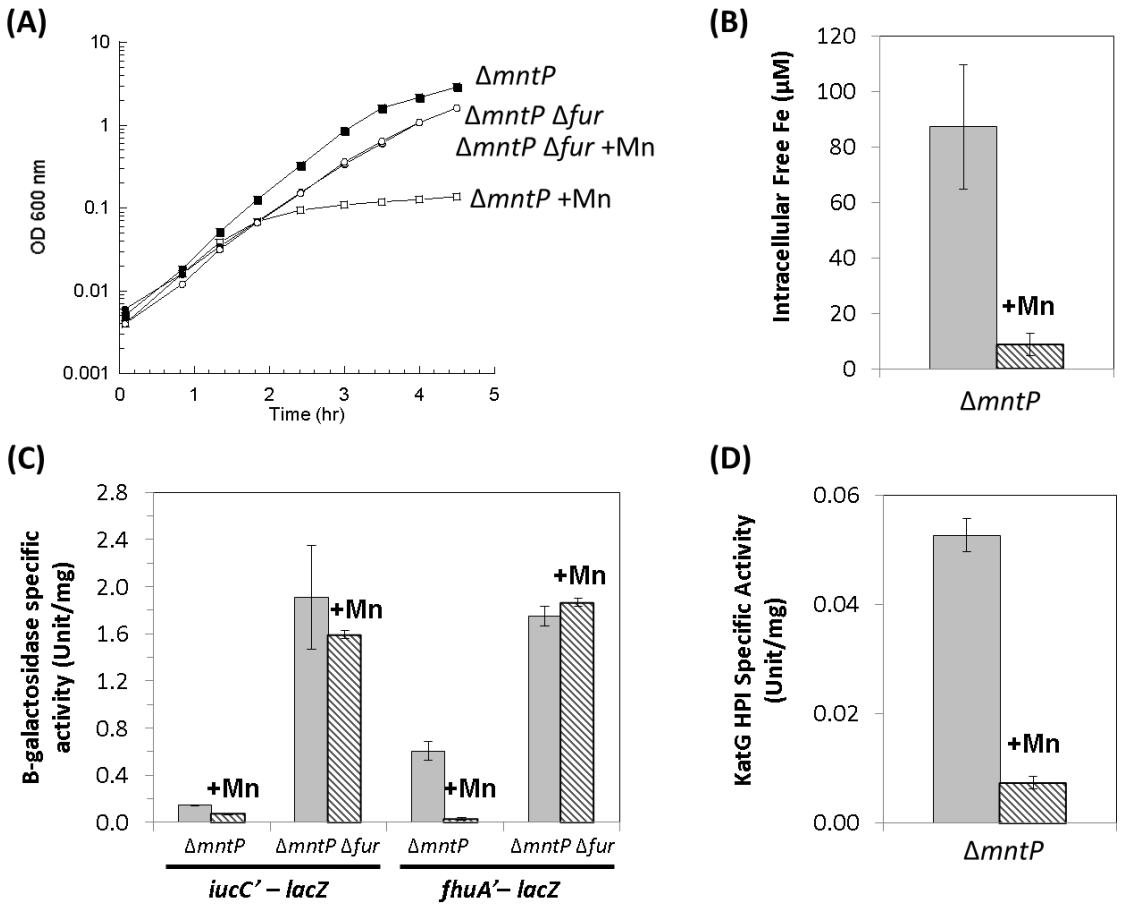

Figure 3.21. Manganese sensitivity in Δ*mntP* mutants is due to repression of the Fur regulon, which suppresses iron entry. Cells were grown for 2.5 hr in aerobic LB medium with or without 0.5 mM $MnCl_2$. Data represents the mean of three independent cultures.

A. Cell growth over time of JEM1720 (Δ*mntP*) and JEM1722 (Δ*mntP* Δ*fur*).

B. Intracellular free iron was determined from JEM1726 (Δ*mntP*).

C. Transcription levels of the Fur regulated genes *iucC'-lacZ* or *fhuA'-lacZ* from strains JEM1719 (Δ*mntP*) and JEM1724 (Δ*mntP* Δ*fur*) or JEM1720 (Δ*mntP*) and JEM1722 (Δ*mntP* Δ*fur*), respectively.

D. Catalase G activity from MS025 (Δ*mntP*).

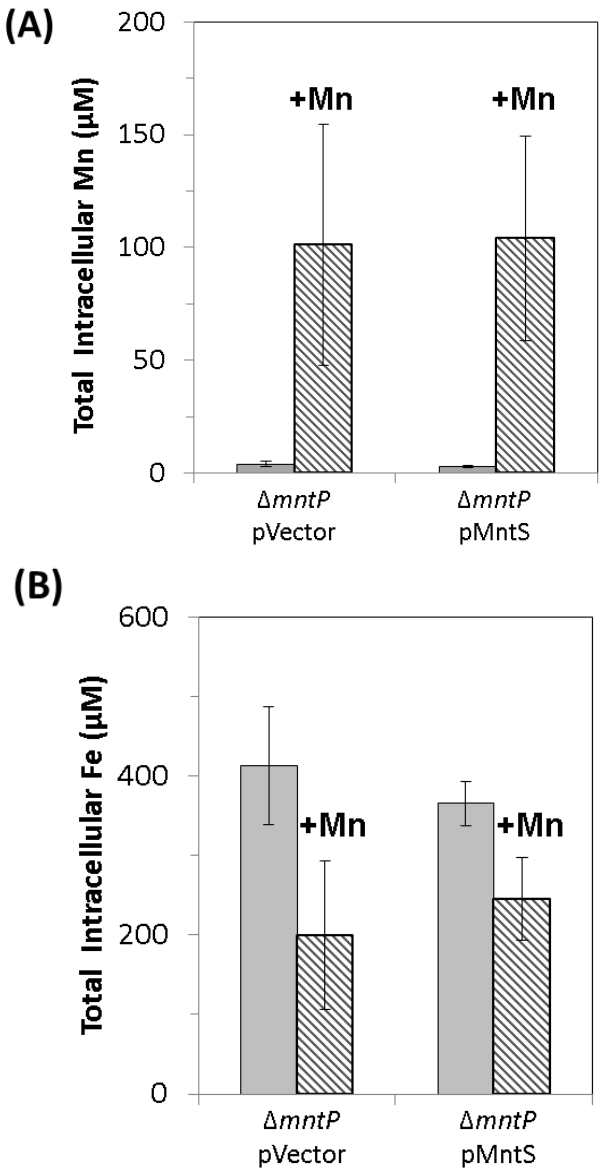

Figure 3.22. *mntP*-null mutants are loaded with manganese and contain very little intracellular iron. Cells pre-cultured in aerobic LB medium were diluted into fresh LB/arabinose medium with or without 0.5 mM $MnCl_2$ and harvested after 2.5 hr of aerobic growth, followed by ICP-MS analysis. Data represent the mean of three independent cultures. Strains were MS025 (Δ*mntP*) harboring empty vector (pBAD24) or pMntS (pLW112, *mntS* driven by the *araBAD* promoter).

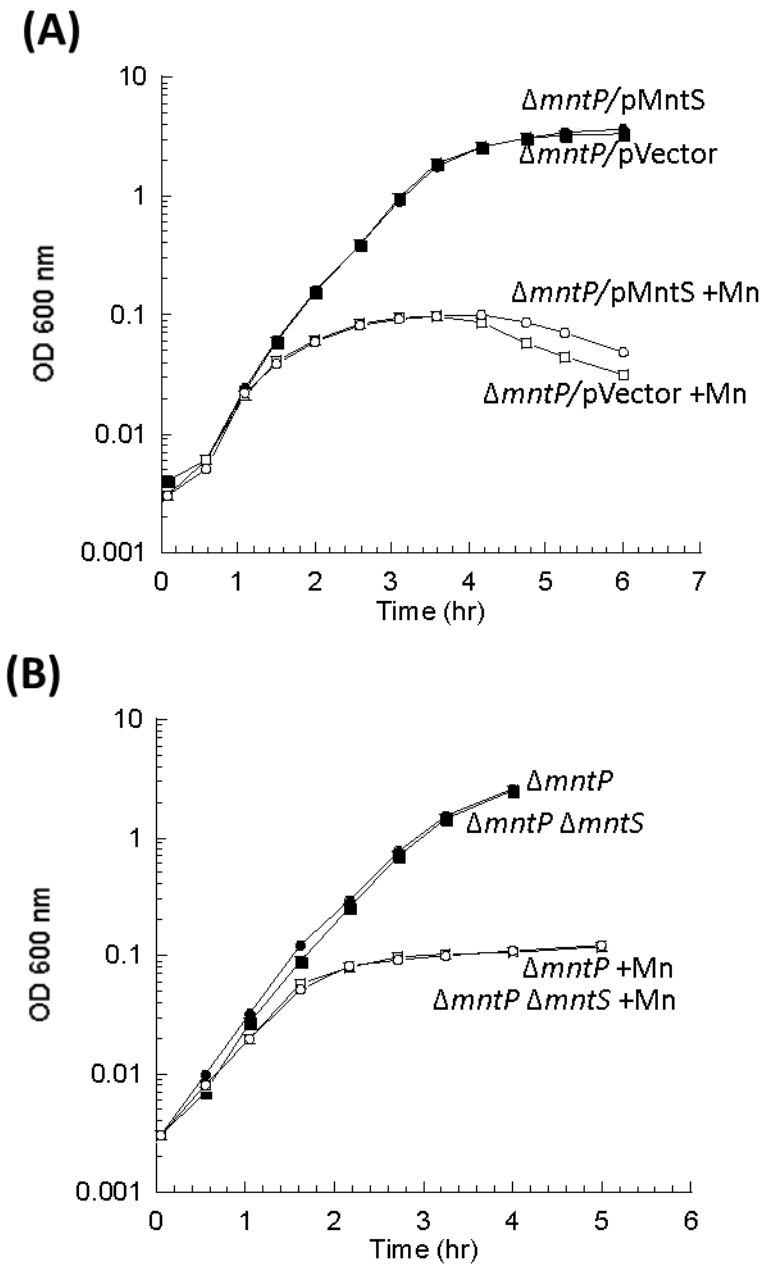

Figure 3.23. The *mntP*-null mutation is epistatic to overproduction of MntS with respect to manganese sensitivity. Cells were pre-cultured in aerobic LB medium and then diluted at time zero into fresh LB/arabinose medium with or without 0.5 mM $MnCl_2$.
A. Strains were JEM1726 (Δ*mntP*/pBAD24) and JEM1727 (Δ*mntP*/pLW112, *mntS* driven by *araBAD* promoter).
B. Strains were MS025 (Δ*mntP*) and JEM1715 (Δ*mntP* Δ*mntS*).

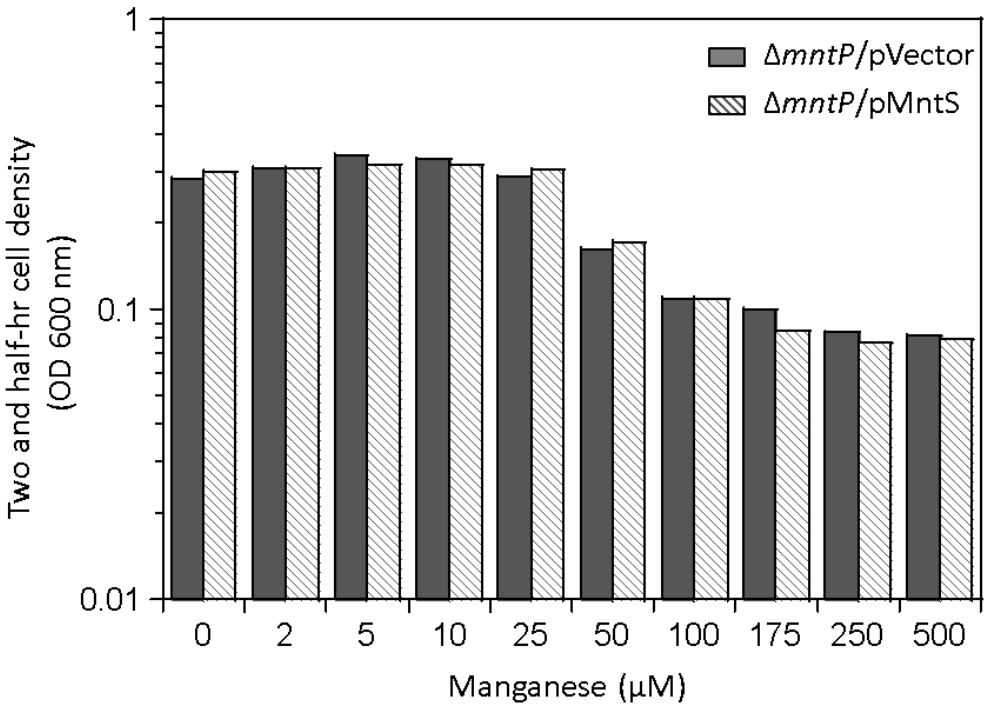

Figure 3.24. Overproduction of MntS does not make Δ*mntP* mutants more sensitive to manganese. Cells pre-cultured in aerobic LB medium were diluted at time zero into fresh LB/arabinose medium with increasing concentrations of $MnCl_2$. Strains were MS025 (Δ*mntP*) harboring empty vector (pBAD24) or pMntS (pLW112, *mntS* driven by the *araBAD* promoter).

3.7 REFERENCES

1. **Andrews, S. C.** 1998. Iron storage in bacteria. Adv. Microb. Physiol. **40:**281-351.

2. **Andrews, S. C., A. K. Robinson, and F. Rodriguez-Quinones.** 2003. Bacterial iron homeostasis. FEMS Microbiol. Rev. **27:**215-237.

3. **Anjem, A., and J. A. Imlay.** 2012. Mononuclear iron enzymes are primary targets of hydrogen peroxide stress. J. Biol. Chem. **287:**15544-15556.

4. **Anjem, A., S. Varghese, and J. A. Imlay.** 2009. Manganese import is a key element of the OxyR response to hydrogen peroxide in *Escherichia coli*. Mol. Microbiol. **72:**844-858.

5. **Balasubramanian, D., and C. K. Vanderpool.** 2013. Deciphering the interplay between two independent functions of the small RNA regulator SgrS in *Salmonella*. J. Bacteriol. **195:**4620-4630.

6. **Beyer, W. F.,Jr, and I. Fridovich.** 1991. In vivo competition between iron and manganese for occupancy of the active site region of the manganese-superoxide dismutase of *Escherichia coli*. J. Biol. Chem. **266:**303-308.

7. **Bobrovskyy, M., and C. K. Vanderpool.** 2013. Regulation of bacterial metabolism by small RNAs using diverse mechanisms. Annu. Rev. Genet.

8. **Calhoun, M. W., and R. B. Gennis.** 1993. Demonstration of separate genetic loci encoding distinct membrane-bound respiratory NADH dehydrogenases in *Escherichia coli*. J. Bacteriol. **175:**3013-3019.

9. **Cherepanov, P. P., and W. Wackernagel.** 1995. Gene disruption in *Escherichia coli*: TcR and KmR cassettes with the option of Flp-catalyzed excision of the antibiotic-resistance determinant. Gene. **158:**9-14.

10. **Cotruvo, J. A.,Jr, and J. Stubbe.** 2010. An active dimanganese(III)-tyrosyl radical cofactor in *Escherichia coli* class Ib ribonucleotide reductase. Biochemistry. **49:**1297-1309.

11. **Datsenko, K. A., and B. L. Wanner.** 2000. One-step inactivation of chromosomal genes in *Escherichia coli* K-12 using PCR products. Proc Natl. Acad. Sci. U. S. A. **97:**6640-6645.

12. **Haldimann, A., and B. L. Wanner.** 2001. Conditional-replication, integration, excision, and retrieval plasmid-host systems for gene structure-function studies of bacteria. J. Bacteriol. **183:**6384-6393.

13. **Ikeda, J. S., A. Janakiraman, D. G. Kehres, M. E. Maguire, and J. M. Slauch.** 2005. Transcriptional regulation of *sitABCD* of *Salmonella enterica* serovar Typhimurium by MntR and Fur. J. Bacteriol. **187:**912-922.

14. **Imlay, J. A., and I. Fridovich.** 1991. Assay of metabolic superoxide production in *Escherichia coli*. J. Biol. Chem. **266:**6957-6965.

15. **Jang, S., and J. A. Imlay.** 2010. Hydrogen peroxide inactivates the *Escherichia coli* Isc iron-sulphur assembly system, and OxyR induces the Suf system to compensate. Mol. Microbiol. **78:**1448-1467.

16. **Jang, S., and J. A. Imlay.** 2007. Micromolar intracellular hydrogen peroxide disrupts metabolism by damaging iron-sulfur enzymes. J. Biol. Chem. **282:**929-937.

17. **Johnston, A. W., J. D. Todd, A. R. Curson, S. Lei, N. Nikolaidou-Katsaridou, M. S. Gelfand, and D. A. Rodionov.** 2007. Living without Fur: the subtlety and complexity of iron-responsive gene regulation in the symbiotic bacterium *Rhizobium* and other alpha-proteobacteria. Biometals. **20:**501-511.

18. **Kehres, D. G., A. Janakiraman, J. M. Slauch, and M. E. Maguire.** 2002. Regulation of *Salmonella enterica* serovar Typhimurium *mntH* transcription by H_2O_2, Fe(2+), and Mn(2+). J. Bacteriol. **184:**3151-3158.

19. **Kehres, D. G., M. L. Zaharik, B. B. Finlay, and M. E. Maguire.** 2000. The NRAMP proteins of *Salmonella typhimurium* and *Escherichia coli* are selective manganese transporters involved in the response to reactive oxygen. Mol. Microbiol. **36:**1085-1100.

20. **Kirby, T., J. Blum, I. Kahane, and I. Fridovich.** 1980. Distinguishing between Mn-containing and Fe-containing superoxide dismutases in crude extracts of cells. Arch. Biochem. Biophys. **201:**551-555.

21. **Kullik, I., M. B. Toledano, L. A. Tartaglia, and G. Storz.** 1995. Mutational analysis of the redox-sensitive transcriptional regulator OxyR: regions important for oxidation and transcriptional activation. J. Bacteriol. **177:**1275-1284.

22. **Martin, J. E., and J. A. Imlay.** 2011. The alternative aerobic ribonucleotide reductase of *Escherichia coli*, NrdEF, is a manganese-dependent enzyme that enables cell replication during periods of iron starvation. Mol. Microbiol. **80:**319-334.

23. **Masse, E., and S. Gottesman.** 2002. A small RNA regulates the expression of genes involved in iron metabolism in *Escherichia coli*. Proc. Natl. Acad. Sci. U. S. A. **99:**4620-4625.

24. **Matsushita, K., T. Ohnishi, and H. R. Kaback.** 1987. NADH-ubiquinone oxidoreductases of the *Escherichia coli* aerobic respiratory chain. Biochemistry. **26:**7732-7737.

25. **McCord, J. M., and I. Fridovich.** 1969. Superoxide dismutase. An enzymic function for erythrocuprein (hemocuprein). J. Biol. Chem. **244:**6049-6055.

26. **Miller, J. H. (ed.),** 1972. Experiments in Molecular Genetics. Cold Springs Harbor Laboratory, Cold Springs Harbor, NY.

27. **Nakayashiki, T., and H. Inokuchi.** 1997. Effects of starvation for heme on the synthesis of porphyrins in *Escherichia coli.* Mol. Gen. Genet. **255:**376-381.

28. **Neidhardt, F. C., P. L. Bloch, and D. F. Smith.** 1974. Culture medium for enterobacteria. J. Bacteriol. **119:**736-747.

29. **Nesbit, A. D., J. L. Giel, J. C. Rose, and P. J. Kiley.** 2009. Sequence-specific binding to a subset of IscR-regulated promoters does not require IscR Fe-S cluster ligation. J. Mol. Biol. **387:**28-41.

30. **Niederhoffer, E. C., C. M. Naranjo, K. L. Bradley, and J. A. Fee.** 1990. Control of *Escherichia coli* superoxide dismutase (*sodA* and *sodB*) genes by the ferric uptake regulation (*fur*) locus. J. Bacteriol. **172:**1930-1938.

31. **Osman, D., and J. S. Cavet.** 2011. Metal sensing in *Salmonella*: implications for pathogenesis. Adv. Microb. Physiol. **58:**175-232.

32. **Park, S., X. You, and J. A. Imlay.** 2005. Substantial DNA damage from submicromolar intracellular hydrogen peroxide detected in Hpx$^-$ mutants of *Escherichia col*i. Proc. Natl. Acad. Sci. U. S. A. **102:**9317-9322.

33. **Patzer, S. I., and K. Hantke.** 2001. Dual repression by Fe(2+)-Fur and Mn(2+)-MntR of the *mntH* gene, encoding an NRAMP-like Mn(2+) transporter in *Escherichia coli*. J. Bacteriol. **183:**4806-4813.

34. **Rosch, J. W., G. Gao, G. Ridout, Y. D. Wang, and E. I. Tuomanen.** 2009. Role of the manganese efflux system *mntE* for signalling and pathogenesis in *Streptococcus pneumoniae*. Mol. Microbiol. **72:**12-25.

35. **Seaver, L. C., and J. A. Imlay.** 2001. Alkyl hydroperoxide reductase is the primary scavenger of endogenous hydrogen peroxide in *Escherichia coli*. J. Bacteriol. **183:**7173-7181.

36. **Seaver, L. C., and J. A. Imlay.** 2001. Hydrogen peroxide fluxes and compartmentalization inside growing *Escherichia coli*. J. Bacteriol. **183:**7182-7189.

37. **Seaver, L. C., and J. A. Imlay.** 2004. Are respiratory enzymes the primary sources of intracellular hydrogen peroxide? J. Biol. Chem. **279:**48742-48750.

38. **Sobota, J. M., and J. A. Imlay.** 2011. Iron enzyme ribulose-5-phosphate 3-epimerase in *Escherichia coli* is rapidly damaged by hydrogen peroxide but can be protected by manganese. Proc. Natl. Acad. Sci. U. S. A. **108:**5402-5407.

39. **Stintzi, A., C. Barnes, J. Xu, and K. N. Raymond.** 2000. Microbial iron transport via a siderophore shuttle: a membrane ion transport paradigm. Proc. Natl. Acad. Sci. U. S. A. **97:**10691-10696.

40. **Veyrier, F. J., I. G. Boneca, M. F. Cellier, and M. K. Taha.** 2011. A novel metal transporter mediating manganese export (MntX) regulates the Mn to Fe intracellular ratio and *Neisseria meningitidis* virulence. PLoS Pathog. **7:**e1002261.

41. **Wassarman, K. M., F. Repoila, C. Rosenow, G. Storz, and S. Gottesman.** 2001. Identification of novel small RNAs using comparative genomics and microarrays. Genes Dev. **15:**1637-1651.

42. **Waters, L. S., M. Sandoval, and G. Storz.** 2011. The *Escherichia coli* MntR miniregulon includes genes encoding a small protein and an efflux pump required for manganese homeostasis. J. Bacteriol. **193:**5887-5897.

43. **Whittaker, M. M., and J. W. Whittaker.** 1997. Mutagenesis of a proton linkage pathway in *Escherichia coli* manganese superoxide dismutase. Biochemistry. **36:**8923-8931.

44. **Woodmansee, A. N., and J. A. Imlay.** 2002. Quantitation of intracellular free iron by electron paramagnetic resonance spectroscopy. Methods Enzymol. **349:**3-9.

CHAPTER 4: CONCLUSIONS

4.1 SUMMARY OF CURRENT WORK

4.1.1 NrdEF is a manganese-dependent ribonucleotide reductase that enables cell replication during periods of iron-starvation

DNA synthesis in *E. coli* has long been known to rely upon NrdD, an oxygen-sensitive ribonucleotide reductase, in anaerobic habitats, and NrdAB, an oxygen-dependent isozyme, in aerobic habitats. The goal of this work was to assess the physiological role of the NrdAB homologue, NrdEF. Its function was not apparent, as it is not active under standard laboratory growth conditions. Prior work had hinted that NrdAB might be vulnerable to oxidative stress and that NrdEF might be induced to compensate, but I found that this was not so. Instead, NrdEF is a manganese-dependent enzyme that becomes functional only when iron is scarce; by doing so, it allows DNA synthesis to proceed when NrdAB, an iron-dependent enzyme, cannot be activated.

4.1.2 MntS and MntP make manganese more available to enzymes

Iron is involved in many cellular processes and is essential for almost all organisms. However, it is sometimes scarce in the contemporary aerobic world due to oxidation. When *Escherichia coli* is deficient in iron or stressed by hydrogen peroxide, it apparently uses manganese rather than iron to populate enzymes. When iron becomes available, excess manganese is exported out of the cell through the efflux pump, MntP. High levels of intracellular manganese are deleterious to bacteria. The goal of this work was to assess which cellular processes fail during manganese toxicity and to identify the physiological role of the small protein, MntS. Prior work had demonstrated that MntS

overexpression or deletion of *mntP* made cells more vulnerable to high concentrations of manganese. In this work, I showed that these cells were loaded with manganese and contained low levels of iron, due to repression of Fur-regulated iron-uptake genes. This metal imbalance ultimately resulted in the cell's inability to synthesize heme. I also found that the *mntP* deletion was epistatic to overproduction of MntS. Thus, MntS likely makes manganese more available to proteins by inhibiting MntP. This attribute is most likely beneficial during periods of transition from iron-replete to iron-deplete conditions.

4.2 FUTURE DIRECTIONS

4.2.1 What is the physiological relevance for the regulation of *nrdHIEF* by apo-IscR?

In this work, I showed that Fur represses *nrdHIEF* transcription in iron-replete conditions, while apo-IscR activates transcription. Since iron-loaded NrdEF is poorly active, the repression of *nrdHIEF* by Fur:Fe makes sense. However, the physiological logic for the *nrdHIEF* induction by apo-IscR is puzzling. It plausibly stems from the role of YfaE, a [2Fe-2S] enzyme, in activating NrdAB. When iron-sulfur synthesis is impeded—the situation that is sensed by IscR—YfaE may become unavailable to activate NrdAB, and so a shift to NrdEF could be salutary. Alternatively, apo-IscR may serve as an adjunct indicator of iron deficiency [7]. To test this hypothesis, one could grow cells in manganese-replete conditions so that the Fur protein is actively repressing *nrdHIEF*, and then measure whether or not apo-IscR can activate transcription. If *nrdHIEF* transcription increased, then it would suggest that apo-IscR serves to assist the cell in

measuring iron deficiency specifically. This would be useful in manganese-rich conditions, since abundant manganese can restore the repressor activity of Fur protein.

It would also be nice to determine if apo-IscR directly binds to the promoter of *nrdHIEF* and activates transcription or acts through an auxiliary protein. *In vitro* transcription could be used to determine the effect of IscR protein on the promoter region of *nrdHIEF*. No change in *in vitro* transcript levels would imply that the regulation by IscR is indirect or that an additional *nrdHIEF* transcription factor is needed.

4.2.2 What parameters determine metal specificity of NrdB and NrdF *in vivo*?

The physical features that determine the metal specificities of NrdB and NrdF are unclear; data from other workers established that each of these enzymes can bind either iron or manganese *in vitro* [2, 4]. Binding constants have not been determined, but the results of this investigation indicate that they can be metallated with either metal *in vivo*, too. Although the NrdF tyrosyl radical is generated in iron-loaded cells, the enzyme activity is evidently insufficient to drive replication. One possibility is that the electronic effect of the metal upon the radical—which is evidenced by the metal-dependency of the radical EPR spectrum—might control its reduction potential and thereby influence how adept the radical is at abstracting and then returning the cysteinyl electron during the course of the catalytic cycle. In addition, crystal structures of NrdF indicate that despite their similarities, the ligand sphere around iron does not exactly match that around manganese, a structural difference that might similarly degrade electron conduction [3]. Both physiological and structural parameters seem to determine which metals load and activate these redox metalloenzymes *in vivo*.

In contrast to NrdF, the wild-type NrdB activation process appears to effectively exclude its non-cognate metal, manganese. The process of loading iron into NrdB is catalyzed by YfaE [5]. YfaE has been proposed to bind a [2Fe-2S] cluster that potentially delivers iron to NrdB, thereby excluding the interference of other metals or oxidants in the iron-loading process. My data show that the combination of H_2O_2 and manganese imposes an absolute requirement for YfaE to catalyze NrdB activation. Thus, it would be interesting to determine how YfaE helps accomplish NrdB activation *in vivo*.

4.2.3 Does NrdEF help pathogens tolerate the iron restriction that is imposed by the host?

Iron sequestration is a key host strategy used by mammals to suppress invasion by bacteria, and so would-be pathogens rely upon iron-acquisition and -sparing strategies. NrdEF is found in many of them. An initial interpretation was that its role might be in tolerating the oxidative stress that is created by macrophages; however, the results of the current study suggest that it may help pathogens to tolerate the iron restriction that is imposed by the host.

Panosa, *et al.* (2010) demonstrated that NrdEF was not essential, but advantageous, for the growth of *Salmonella* Typhimurium inside macrophages and epithelial cell lines during early infection as *nrdEF* mutants exhibited slightly diminished virulence compared to wild type cells [8]. One could further test whether reactive oxygen species or iron-limitation is the key stress in which NrdEF is required for pathogenicity by using Phox (-/-) knockout mice. These transgenic mice are incapable of

generating reactive oxygen species, but still chelate metals away from invading microbes during infection.

4.2.4 Can enteric bacteria persist in the absence of iron?

It was previously believed that that ribonucleotide reductase imposed an absolute requirement for iron upon bacteria, until researchers began to identify and characterize iron-independent homologues that use manganese. One wonders, now, whether enteric bacteria might adapt to dwindling iron levels so efficiently that growth could be established without it. To date *Borrelia burgdorferi* is the sole organism known to grow under rigorously iron-deplete conditions; although it harvests its deoxynucleosides from its host [9], related *Borrelia* species employ a ribonucleotide reductase that is a homologue of the *E. coli* NrdEF enzyme. Lactic acid bacteria, which also eschew major iron-dependent pathways, including the TCA cycle and respiratory chains, also rely on NrdEF homologues [1].

The dependency for iron in modern bacteria, such as *E. coli*, is most likely inherited from ancestral microbes that first evolved in an anaerobic world where iron was readily available. In many contemporary habitats, iron is periodically unavailable. Perhaps lactic acid bacteria and *Borrelia* species are examples of life evolving new strategies that help cells cope with iron scarcity. The use of NrdEF by *E. coli* may lessen the need for iron during aerobiosis, but iron is still required for other aspects of growth, such as for heme and isoprenoid synthesis. Some organisms use an alternate method to synthesize isoprenoids via the mevalonate pathway. These genes could be expressed in *E. coli* to possibly enable anaerobic growth with out iron. However, iron is still required

during anoxic growth for activation of the anaerobic ribonucleotide reductase, NrdDG. To my knowledge, *E. coli* has not established a way around these pathways. Perhaps future organisms will be able to persist in the absence of iron.

4.2.5 How is manganese imported in *mntH* mutants?

During the course of this work, several pieces of data indicated that manganese is continually imported in the absence of *mntH*: (i) a small percentage of the manganese-dependent superoxide dismutase is still active in *mntH* mutants and (ii) the deletion of *mntH* does not completely rescue cells overproducing MntS during manganese toxicity. Genome scanning suggests that *E. coli* does not contain any other dedicated manganese transporter. It is possible that manganese could enter through non-specific divalent metal transporters, such as Feo and ZupT. However, the manganese-dependent ribonucleotide reductase, NrdEF, displays some residual activity and permits minimal growth in *nrdAB mntH* compared to *nrdAB nrdEF* mutants, even in the absence of *tonB*, *feo*, and *zupT*.

Several other transporters have been shown to import other divalent metals, such as magnesium, zinc, nickel, cobalt, and calcium. These transporters include the inner membrane magnesium transporter CorA, the P-type ATPase transporter MgtA, and the proton symporter PitA that imports inorganic phospates [10-12]. Each of these transporters could be examined in turn by measuring the metallation status of MnSOD in an *mntH*-null mutant background supplementation with manganese. Low MnSOD activity would suggest that that specific transporter was the culprit for continual manganese import in *mntH* mutants.

4.2.6 Is HemH poisoned by manganese?

HemH, ferrochelatase, is the terminal enzyme in the heme biosynthetic pathway that catalyzes the insertion of ferrous iron into protoporphyrin IX to make protoheme. Reports show that ferrochelatase can catalyze the insertion of a variety of divalent metals, including iron, nickel, zinc, cobalt, and copper, while manganese inhibits [6]. Accumulation of porphyrins during manganese toxicity suggested to me that HemH might be inhibited by manganese. HPLC-MS could be used to identify which porphyrin analog is accumulating. If the major product obtained was protoporphyrin IX, then one might predict that manganese was directly interfering with iron loading into the substrate. Results show that manganese inhibits the eukaryotic ferrochelatase by preventing product release after manganese is inserted into the porphyrin ring [6]. *In vitro* measurements of HemH activity would be used to confirm that the manganese-containing heme is not released from HemH and that the low activity observed for heme-containing enzymes during manganese toxicity results from the lack of heme cofactor.

4.2.7 Does MntS inhibit MntP function?

In this work I eluded to the idea that MntS makes manganese more available by inhibiting MntP (Chapter 3). It makes sense when *E. coli* cells need to respond quickly to sporadic periods of iron-depletion. The ideal method to this hypothesis, would be to make lipid membranes containing MntP and test whether the addition of purified MntS would directly prevent manganese import. Manganese uptake could also be measured in log-phase cultures spiked with radiolabeled manganese. To monitor efflux, cells can be collected after time has elapsed and resuspended in media lacking the isotope. Mutant

mntS alleles could be used to further identify essential residues for recognition of MntP and vice versa.

The *mntS* gene also transcribes a small RNA, termed RybA. It is possible that RybA could inhibit translation of MntP by promoting degradation of the transcript. Western-blots could be used to identify the stability of MntP with respect to RybA. If the life time of the MntP transcript is shortened in the presence of RybA, then one might imagine that when iron becomes scarce, RybA is induced to prevent the synthesis of MntP protein, while MntS is induced to inhibit already existing MntP protein. Collectively, MntS and RybA would function to increase manganese availability.

4.2.8 Do metal chaperones exist that help allocate iron and manganese to proteins?

Metal chaperones have been a long standing hypothesis for how bacteria might distinguish and distribute metals with in the cytosol. To date, no such chaperones have been identified that carry iron or manganese. If such a protein existed, it would need to have a K_D for the metal low enough to allow it to retain the metal during transport, yet high enough to be able to release the metal to the target protein. It would also need to be recognized by several proteins, which seems implausible as there are an enormous amount of iron-dependent proteins.

Alternatively, the word chaperone could be loosely defined as a small molecule that solubilizes metals and prevents metals from binding low affinity sites on proteins. Histidine, cysteine, and inorganic phosphates can all bind divalent metals and mobilize them inside cells. These metabolites are much more abundant and thus it might be more feasible for the cell to use them.

4.3 REFERENCES

1. **Archibald, F.** 1983. *Lactobacillus plantarum*, an organism not requiring iron. FEMS Microbiology Letters. **19:**29-32.

2. **Atta, M., P. Nordlund, A. Aberg, H. Eklund, and M. Fontecave.** 1992. Substitution of manganese for iron in ribonucleotide reductase from *Escherichia coli.* Spectroscopic and crystallographic characterization. J. Biol. Chem. **267:**20682-20688.

3. **Boal, A. K., J. A. Cotruvo Jr., J. Stubbe, and A. C. Rosenzweig.** 2010. Structural basis for activation of class Ib ribonucleotide reductase. Science. **329:**1526-1530.

4. **Cotruvo, J. A., Jr., and J. Stubbe.** 2010. An active dimanganese(III)-tyrosyl radical cofactor in *Escherichia coli* class Ib ribonucleotide reductase. Biochemistry. **49:**1297-1309.

5. **Hristova, D., C. H. Wu, W. Jiang, C. Krebs, and J. Stubbe.** 2008. Importance of the maintenance pathway in the regulation of the activity of *Escherichia coli* ribonucleotide reductase. Biochemistry. **47:**3989-3999.

6. **Medlock, A. E., M. Carter, T. A. Dailey, H. A. Dailey, and W. N. Lanzilotta.** 2009. Product release rather than chelation determines metal specificity for ferrochelatase. J. Mol. Biol. **393:**308-319.

7. **Outten, F. W., O. Djaman, and G. Storz.** 2004. A *suf* operon requirement for Fe-S cluster assembly during iron starvation in *Escherichia coli*. Mol. Microbiol. **52:**861-872.

8. **Panosa, A., I. Roca, and I. Gibert.** 2010. Ribonucleotide reductases of *Salmonella typhimurium*: transcriptional regulation and differential role in pathogenesis. PLoS One. **5:**e11328.

9. **Posey, J. E., and F. C. Gherardini.** 2000. Lack of a role for iron in the Lyme disease pathogen. Science. **288:**1651-1653.

10. **Smith, R. L., and M. E. Maguire.** 1998. Microbial magnesium transport: unusual transporters searching for identity. Mol. Microbiol. **28:**217-226.

11. **Snavely, M. D., J. B. Florer, C. G. Miller, and M. E. Maguire.** 1989. Magnesium transport in *Salmonella typhimurium*: 28Mg2+ transport by the CorA, MgtA, and MgtB systems. J. Bacteriol. **171:**4761-4766.

12. **Wang, S. Z., Y. Chen, Z. H. Sun, Q. Zhou, and S. F. Sui.** 2006. *Escherichia coli* CorA periplasmic domain functions as a homotetramer to bind substrate. J. Biol. Chem. **281:**26813-26820.

APPENDIX A: EXPRESSION OF THE *E. COLI* TRX2 AND GRX1 ARE NOT INDUCED DURING HYDROGEN PEROXIDE STRESS TO COMPENSATE FOR INACTIVATION OF THE PRIMARY THIOREDOXIN, TRX1, SINCE IT REMAINS ACTIVE

Organisms inadvertently generate endogenous H_2O_2 as part of aerobic metabolism [18]. The amount of endogenous H_2O_2 produced is dependent upon the nature of the organism and its environmental surroundings. *E. coli* cells are exposed to H_2O_2 stress when other microorganisms and plants secrete redox-cycling drugs into the environment [12]. These drugs are produced to poison competing microbes and plants. Animals and humans also combat invading microbes in a similar way by bombarding infected areas with superoxide and H_2O_2 [8].

Because of the ubiquity of H_2O_2, *E. coli* has developed defense mechanisms against its toxic effects. Many of the proteins involved in protection against H_2O_2 stress are regulated by the OxyR transcription factor. OxyR has evolved cysteine residues that directly sense H_2O_2 [1, 9]. The oxidation of OxyR results in a conformation change and the formation of an intramolecular disulfide bond. Oxidized OxyR induces genes involved in the scavenging of H_2O_2 (*katG* and *ahpCF*), the regulation of free iron (*dps* and *fur*), the reduction of disulfide bonds (*trxC*, *grxA*, and *gor*), the uptake of manganese (*mntH*), and the biosynthesis of Fe-S clusters (*sufABCDSE*) [24]. OxyR is important and at least some of the genes regulated by OxyR are required for protection against H_2O_2 stress. Alkyl hydroperoxide reductase (encoded by *ahpC*) uses reactive sulfhydryls to scavenge low levels of H_2O_2. Hydroperoxidase I and II (encoded by *katG* and *katE*, respectively) also scavenge H_2O_2. Together, these defenses help wild type *E. coli* cells to sustain a steady-state level of H_2O_2 below 20 nM [21].

In order to study the toxic effects of H_2O_2 stress at physiological levels, Hpx^- mutants were made, which lack the H_2O_2 scavenging enzymes (*katE katG ahp*) [18, 19]. During growth experiments, ~1 micromolar H_2O_2 accumulates inside these cells [18, 19]. Continuous H_2O_2 stress can damage biomolecules via the Fenton reaction, in which ferrous iron reacts with H_2O_2 to produce ferric iron and a hydroxyl radical. The hydroxyl radical produced is highly reactive and will oxidize most anything near by. [7, 15].

Finally, researchers have repeatedly investigated the hypothesis that H_2O_2 causes disulfide stress by oxidation of cysteine residues of cytosolic proteins. Two groups have showed that there was little change in the protein disulfide content of the cytosol when yeast cells and *Bacillus subtilis* were treated with 1 mM H_2O_2 [5, 10]. Furthermore, free cysteine reacts with H_2O_2 at a rate of only 2-21 $M^{-1}s^{-1}$ [22]. At this rate the half-time for the oxidation of cysteine residues on a typical protein would take about 20 hours with 1 µM H_2O_2. Only two known proteins, AhpC and OxyR, have evolved activated cysteine residues that specifically interact with micromolar levels of H_2O_2 at physiological rates of ~10^7 $M^{-1}s^{-1}$ [3, 6, 14, 23]. The question still remains, is it possible that H_2O_2 oxidizes other protein thiols in the cytosol? Trx2 (encoded by *trxC*) and Grx1 (encoded by *grxA*) function as part of the disulfide reduction systems in *E. coli*, which keep the cytosol reduced [14, 16]. Since OxyR induces the transcription of *trxC* and *grxA*, I wondered whether continuous H_2O_2 stress could lead to the oxidation of certain protein thiols, such as Trx1 (encoded by *trxA*).

To assess whether or not *trxC* and/or *grxA* were necessary for growth during H_2O_2 stress, mutants were made in Hpx^- and wild type (MG1655) backgrounds [2]. The *trxC grxA* double mutant must rely on Trx1 as a reductant for 3'-phosphoadenylylsulfate

(PAPS) reductase, which is part of sulfate assimilation [11, 16, 17]. These mutants may also require Trx1 for ribonucleotide reductase NrdAB function, in the event that the alternate aerobic ribonucleotide reductase NrdEF or its electron donor partner protein NrdH fails to be expressed.

No growth defect was observed in the single and the double mutants lacking *trxC* and *grxA* in either wild type or Hpx$^-$ backgrounds (Fig. A.1). Hpx$^-$ *trxC grxA trxA* cells grow poorly without a reduced sulfur source compared to Hpx$^-$ *trxC grxA* (Fig. A.2). The ability of Hpx$^-$ *trxC grxA* to assimilate sulfate and replicate its DNA, indicates that H_2O_2 stress does not completely oxidize Trx1. Thus, Trx1 retains enough activity to allow cells to survive during protracted H_2O_2 stress. These observations also suggest that H_2O_2 either has no effect on sulfhydryls present in the cytoplasm, or, under our conditions, any proteins that are damaged by H_2O_2 may not be necessary for growth. Despite my effort, I do not yet know why *trxC* and *grxA* are induced during H_2O_2 stress.

A.1 MATERIALS AND METHODS

A.1.1 Bacterial strain construction

The bacterial strains used in this study are described in Table A.1. All oxygen-sensitive strains were constructed under anaerobic conditions to ensure that suppressor mutations were not selected during outgrowth. The λ Red recombinase method was used to create null mutations [2]. Mutations were introduced into new strains by P1-transduction [13]. The resulting mutations were confirmed by PCR analysis. When necessary, the antibiotic cassette was removed by FLP-mediated excision [2].

A.1.2 Growth conditions

Cells were grown in medium that contained minimal A salts [13], 1 mM $MgSO_4$, 5 mg/liter thiamine, 0.2 % glucose, 0.5 mM aromatic amino acids, 0.5 mM histidine, and 0.5 mM tryptophan. Anaerobic cultures were grown in an anaerobic chamber (Coy Laboratory Products Inc.) under an atmosphere of 85% nitrogen, 10% hydrogen, and 5% carbon dioxide. Aerobic cultures were grown under room air with vigorous shaking. All cultures were grown at 37°C unless specified elsewhere.

To ensure that cells were growing exponentially before they were exposed to oxygen, anaerobic overnight cultures were diluted to OD_{600} 0.005 into fresh anaerobic medium and grown to an approximate OD_{600} of 0.12. Cells were then subcultured again into fresh aerobic medium to OD_{600} 0.005 and aerobic growth was followed over time.

A.2 TABLES

Table A.1. Bacterial strains used in this study.

Strain	Genotype	Reference
BW25113	*lacI rrnB* Δ*lacZ hsdK* Δ*araBAD* Δ*rhaBAD*	[2]
MG1655	F^- wild type	*E. coli* CGSC
LC106	Δ*ahpF::kan* Δ(*katG::*Tn*10*)1 Δ(*katE12::*Tn*10*)	[20]
JEM59	As BW25113 Δ*trxC1::cat*	This study
JEM61	As MG1655 Δ*trxC1::cat*	This study
JEM62	As LC106 Δ*trxC1::cat*	Lab strain
JEM68	As BW25113 Δ*grxA1::cat*	This study
JEM74	As MG1655 Δ*grxA1::cat*	This study
JEM70	As LC106 Δ*grxA1::cat*	Lab strain
JEM76	As MG1655 Δ*trxC1* Δ*grxA1::cat*	This study
JEM72	As LC106 Δ*trxC1* Δ*grxA1::cat*	This study
JEM100	As BW25113 Δ*trxA1::cat*	This study
JEM136	As MG1655 Δ*trxC1* Δ*grxA1* Δ*trxA1::cat*	This study
JEM130	As LC106 Δ*trxC1* Δ*grxA1* Δ*trxA1::cat*	This study

A.3 FIGURES

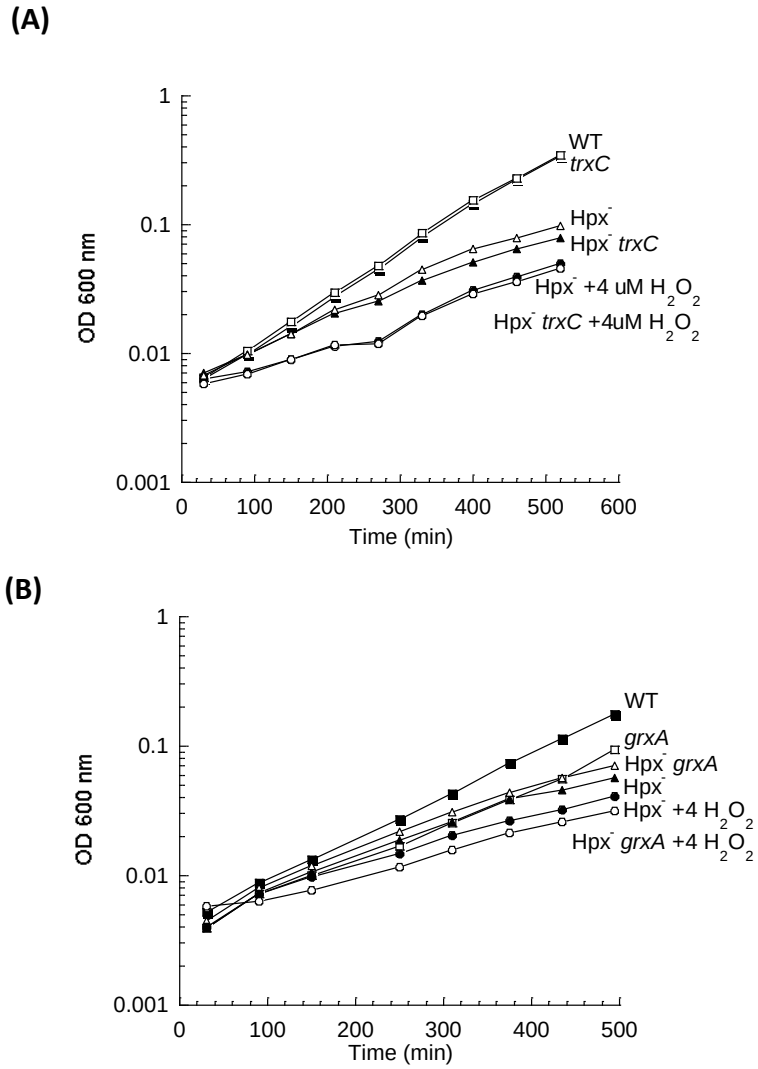

Figure A.1. Cell lacking *trxC* or *grxA* show no growth defect. Anaerobic overnight cultures were diluted to 0.005 OD_{600} in anaerobic defined medium. After five generations of anaerobic growth (~0.1 OD_{600}), cells were diluted into aerobic medium with 0 or 4 μM H_2O_2 and growth was monitored.

A. Strains were WT (MG1655), Δ*trxC* (JEM61), Hpx$^-$ (LC106), and Hpx$^-$ Δ*trxC* (JEM62).

B. Strains were WT (MG1655), Δ*grxA* (JEM74), Hpx$^-$ (LC106), and Hpx$^-$ Δ*grxA* (JEM70).

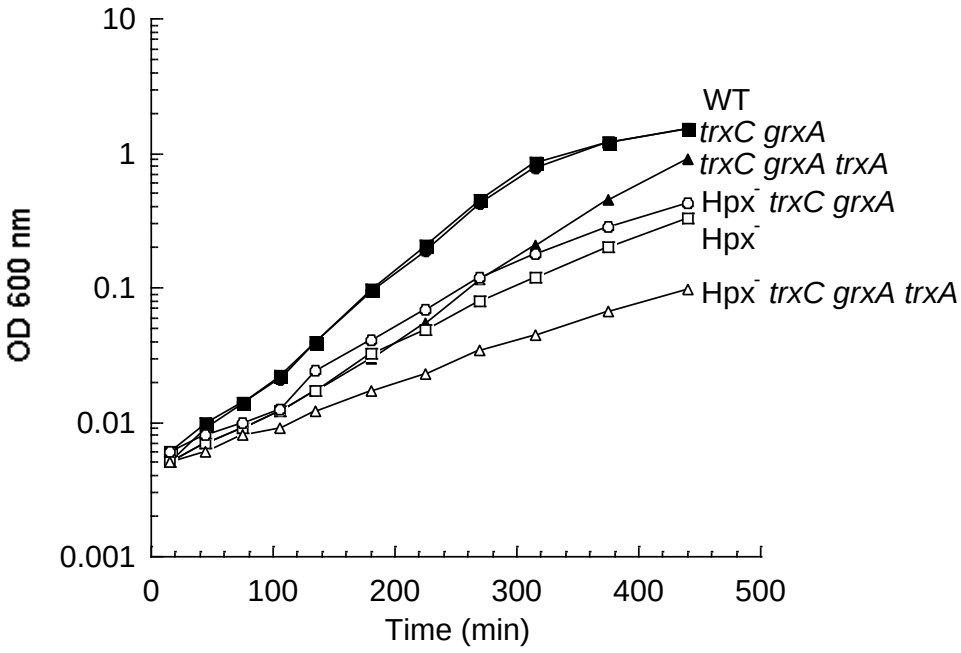

Figure A.2. Trx1 is still functional during H_2O_2 stress. Anaerobic overnight cultures were diluted to 0.005 OD_{600} in anaerobic defined medium. After five generations of anaerobic growth (~0.1 OD_{600}), cells were diluted into aerobic medium growth was monitored. Strains were WT (MG1655), Δ*trxC* Δ*grxA* (JEM76), Δ*trxC* Δ*grxA* Δ*trxA* (JEM136), Hpx$^-$ (LC106), Hpx$^-$ Δ*trxC* Δ*grxA* (JEM72), and Hpx$^-$ Δ*trxC* Δ*grxA* Δ*trxA* (JEM130).

A.4 REFERENCES

1. **Aslund, F., M. Zheng, J. Beckwith, and G. Storz.** 1999. Regulation of the OxyR transcription factor by hydrogen peroxide and the cellular thiol---disulfide status. Proc. Natl. Acad. Sci. U. S. A. **96:**6161-6165.

2. **Datsenko, K. A., and B. L. Wanner.** 2000. One-step inactivation of chromosomal genes in *Escherichia coli* K-12 using PCR products. Proc. Natl. Acad. Sci. U. S. A. **97:**6640-6645.

3. **Ellis, H. R., and L. B. Poole.** 1997. Roles for the two cysteine residues of AhpC in catalysis of peroxide reduction by alkyl hydroperoxide reductase from *Salmonella typhimurium*. Biochemistry. **36:**13349-13356.

4. **Hochgrafe, F., J. Mostertz, D. Albrecht, and M. Hecker.** 2005. Fluorescence thiol modification assay: oxidatively modified proteins in *Bacillus subtilis*. Mol. Microbiol. **58:**409-425.

5. **Imlay, J. A.** 2003. Pathways of oxidative damage. Annu. Rev. Microbiol. **57:**395-418.

6. **Jang, S., and J. A. Imlay.** 2007. Micromolar intracellular hydrogen peroxide disrupts metabolism by damaging iron-sulfur enzymes. J. Biol. Chem. **282:**929-937.

7. **Klebanoff, S. J.** 1975. Antimicrobial mechanisms in neutrophilic polymorphonuclear leukocytes. Semin. Hematol. **12:**117-142.

8. **Kona, J., and T. Brinck.** 2006. A combined molecular dynamics simulation and quantum chemical study on the mechanism for activation of the OxyR transcription factor by hydrogen peroxide. Org. Biomol. Chem. **4:**3468-3478.

9. **Le Moan, N., G. Clement, S. Le Maout, F. Tacnet, and M. B. Toledano.** 2006. The *Saccharomyces cerevisiae* proteome of oxidized protein thiols: contrasted functions for the thioredoxin and glutathione pathways. J. Biol. Chem. **281:**10420-10430.

10. **Lillig, C. H., A. Potamitou, J. Schwenn, A. Vlamis-Gardikas, and A. Holmgren.** 2003. Redox regulation of 3'-phosphoadenylylsulfate reductase from *Escherichia coli* by glutathione and glutaredoxins. J. Biol. Chem. **278:**22325-22330.

11. **Mehdy, M. C.** 1994. Active oxygen species in plant defense against pathogens. Plant Physiol. **105:**467-472.

12. **Miller, J. H. (ed.),** 1972. Experiments in molecular genetics. Cold Springs Harbor Laboratory, Cold Springs Harbor, NY.

13. **Paget, M. S., and M. J. Buttner.** 2003. Thiol-based regulatory switches. Annu. Rev. Genet. **37:**91-121.

14. **Park, S., X. You, and J. A. Imlay.** 2005. Substantial DNA damage from submicromolar intracellular hydrogen peroxide detected in Hpx^- mutants of *Escherichia coli*. Proc. Natl. Acad. Sci. U. S. A. **102:**9317-9322.

15. **Ritz, D., and J. Beckwith.** 2001. Roles of thiol-redox pathways in bacteria. Annu. Rev. Microbiol. **55:**21-48.

16. **Russel, M., P. Model, and A. Holmgren.** 1990. Thioredoxin or glutaredoxin in *Escherichia coli* is essential for sulfate reduction but not for deoxyribonucleotide synthesis. J. Bacteriol. **172:**1923-1929.

17. **Seaver, L. C., and J. A. Imlay.** 2001. Alkyl hydroperoxide reductase is the primary scavenger of endogenous hydrogen peroxide in *Escherichia coli*. J. Bacteriol. **183:**7173-7181.

18. **Seaver, L. C., and J. A. Imlay.** 2001. Hydrogen peroxide fluxes and compartmentalization inside growing *Escherichia coli*. J. Bacteriol. **183:**7182-7189.

19. **Seaver, L. C., and J. A. Imlay.** 2004. Are respiratory enzymes the primary sources of intracellular hydrogen peroxide? J. Biol. Chem. **279:**48742-48750.

20. **Storz, G., and J. A. Imlay.** 1999. Oxidative stress. Curr. Opin. Microbiol. **2:**188-194.

21. **Winterbourn, C. C., and D. Metodiewa.** 1999/8. Reactivity of biologically important thiol compounds with superoxide and hydrogen peroxide. Free Radical Biology and Medicine. **27:**322-328.

22. **Zheng, M., F. Aslund, and G. Storz.** 1998. Activation of the OxyR transcription factor by reversible disulfide bond formation. Science. **279:**1718-1721.

23. **Zheng, M., X. Wang, B. Doan, K. A. Lewis, T. D. Schneider, and G. Storz.** 2001. Computation-directed identification of OxyR DNA binding sites in *Escherichia coli*. J. Bacteriol. **183:**4571-4579.

APPENDIX B: *KATG* TRANSCRIPTION IS HIGHLY REPRESSED IN *Δ FUR* MUTANTS

Hydroperoxidase I (HPI, encoded by *katG*) is a heme-containing enzyme that catalyzes the dismutation of H_2O_2 to water and oxygen. Its transcription is induced in response to low concentrations of H_2O_2 by the positive activator OxyR [11].

During the course of investigating the physiological role of *mntS*, I observed a significant (approximately 4-fold) reduction of HPI activity in *E. coli fur* mutants. This decrease roughly correlated with an approximately 2-fold decrease in *katG* transcription, as measured using a P_{katG}'-*lacZ* transcriptional fusion. Similar observations for both HPI activity and *katG* transcription were previously reported by Heorter *et al*. (2005). In this study, I investigated why *katG* transcription was down-regulated when *fur* was deleted.

In *E. coli*, Fur protein bound to iron binds to the promoters of most iron-acquisition genes and represses transcription. Metallated Fur also represses the transcription of *ryhB*, a small regulatory RNA that when expressed promotes degradation of mRNA encoding iron-containing proteins that are abundant, but not essential. Genes that are targeted for degradation by RyhB appear to be down-regulated in the absence of Fur protein. In such cases, Fur appears to function as a positive regulator. I examined whether induction of *ryhB* in *fur* mutants affected *katG* transcription. No change in either *katG* transcription or HPI activity was observed when *ryhB* was deleted in *fur* mutants (Fig. B.1). These data imply that the reduction in *katG* transcription was not due to degradation of *katG* mRNA.

Metallated Fur also represses the transcription of *mntH*, a manganese importer [6, 10]. Since manganese can potentially inhibit heme biosynthesis and HPI activity requires

heme, I next examined whether manganese import inhibited *katG* transcription. Neither *katG* transcription nor HPI activity were affected when *mntH* was deleted in *fur* mutants or when LB medium was supplemented with manganese (Fig. B.2). These data indicated that manganese was also not involved in the regulation or activity of *katG*.

IscR is another global transcriptional regulator that responds to intracellular iron concentrations. Its transcription is regulated indirectly by Fur through RyhB [3]. Deletion of *iscR* in combination with the *fur*-null allele showed a slight increase in both *katG* transcription (to 80% of wild type cells) and HPI activity (to 40% of wild type cells) compared to *fur* mutants alone (Fig. B.2.). The increase was not significant enough to conclude that IscR played a role in regulating *katG*. I also did not test whether deletion of *fur* influenced *katG* transcription in the *iscR*-null mutant background.

Taken together, the above data suggest that Fur protein possibly occludes a repressor from binding to the promoter region of *katG*. For example, Fur is capable of blocking H-NS, a histone-like nucleoid structuring protein, from repressing the transcription of *ftnA*, which encodes ferritin [9]. Since H-NS is essential for growth, I instead replaced the promoter region of *katG* with the *tetRA* expression system instead. This system allows *katG* to be induced when tetracycline is present in the medium. Using this system, I found that HPI activity still remained low in *fur* mutants (Fig. B.3). These data suggest that H-NS is not involved in down-regulating *katG* and that such regulation observed is indicative of a small RNA. RyhB can be excluded from the possible lists as its deletion does not affect *katG* transcription in the *fur* mutant containing P_{tet}-*katG* (Fig. B.3). Thus, Fur modulates expression of *katG* possibly through another

small RNA. The next step would be to measure *katG* transcription levels in an *hfq*-null mutant and to make a translational fusion to *katG.*

B.1 MATERIALS AND METHODS

B.1.1 Bacterial strain construction

The bacterial strains used in this study are described in Table B.1. The λ red recombinase method was used to create null mutations [2]. Mutations were introduced into new strains by P1-transduction [8]. The resulting mutations were confirmed by PCR analysis. When necessary, the antibiotic cassette was removed by FLP-mediated excision [2].

For construction of single-copy transcriptional *lacZ* fusion to *katG,* the promoter region of *katG* was amplified by PCR using primers designed with restriction sites. The product was digested and inserted into pSJ501, a plasmid derivative of pAH125 modified to express the chloramphenicol acetyl transferase gene (cat) flanked by FLP sites for selection. The resulting plasmid constructs were confirmed by sequencing. Plasmids were then integrated into the λ attachment site, while the wild-type *katG* gene remained at its native position. Fusions were introduced into new strains by P1-transduction and the chloramphenicol-resistance cassette was removed by FLP-mediated excision.

For the construction of tetracycline inducible *katG* gene, I used the λ red recombinase method to replace the *katG* promoter region with *tetRA* [7]. The coding sequence of *tetRA* (shown in bold type) was amplified from JRE520 genomic DNA with the following primers 5′-ATTACTTGAAGGATATGAAGCTAAAACTAGGTGGGTA CGTTG**TAGGTGGGTACGTTG**-3′ and 5′-TGCTCATCAATGTGCTCCCCTCTAC

AGTGTTTGGTGACGAAATAA**TTGGTGACGAAATAA**-3′ which are flanked by sequences from the *katG* promoter region. Products were electrophoresed on a 1% agarose gel. Resulting band was excised, purified, and transformed into BW25113 harboring the temperature-sensitive plasmid pKD46. Transformants were selected on LB containing tetracycline, the resulting mutation was confirmed by PCR analysis, and P1 transduction was used to move P_{tet}-*katG* fusion into recipient strains. The *tetRA* expression system lays 23 bp upstream of the *katG* translational start site and directly buds up against the *katG* transcriptional start. Approximately 166 bp upstream of the *katG* transcription start site was removed and replaced by the Tet promoter.

The plasmid pMntS (pLW112) was generated by amplifying the 205 nt of the RNA (encompassing the MntS open reading frame only) and its own Shine-Dalgarno sequence by PCR [12]. The product was digested with NheI and KpnI and cloned into pBAD24 (a medium copy number plasmid that is maintained at 15-20 copies/cell), which is driven by *araBAD* promoter.

B.1.2 Growth conditions

Cells were grown in standard LB medium at 37°C. Overnight cultures were diluted to OD_{600} 0.005 into fresh medium and grown to an approximate OD_{600} of 0.12. Cells were then subcultured again into fresh aerobic medium to OD_{600} 0.005 with or with out 0.5 mM $MnCl_2$. Cells harboring P_{tet}-*katG* were cultured in medium containing 50 ng/ml tetracycline HCl. Cells were harvested after approximately 2.5 hr of growth and enzyme activities were measured.

Strains carrying pBAD24-derived plasmids were grown with ampicillin overnight, then diluted into fresh medium to OD_{600} 0.005. After approximately four doublings, 50 mM L(+)arabinose was added to induce MntS expression. Cultures were grown for an additional 30 to 45 minutes, then subcultured again into fresh aerobic medium with ampicillin and 50 mM L(+)arabinose to OD_{600} 0.0025 and grown at 37°C.

B.1.3 Enzyme assays

All enzyme assays were performed at room temperature and protein concentrations were determined by the Bradford assay using bovine serum albumin as the standard.

β-galactosidase activity

To prepare extracts, cells were centrifuged, washed twice, resuspended in 1/30 the original culture volume with ice-cold 50 mM Tris-HCl buffer (pH 8), and lysed by French press. Cell debris was removed by centrifugation, and β-galactosidase activity in cell extracts was determined by ONPG hydrolysis using standard procedures [8].

Hydroperoxidase I (HPI) activity

To prepare extracts, cells were washed twice with ice-cold 50 mM potassium phosphate buffer (pH 7.8), then resuspended in 1/30 the original culture volume and lysed by French press in ice-cold 10 mM potassium phosphate buffer (pH 6.4). Cell debris was removed by centrifugation and HPI, the KatG catalase, was specifically assayed through its ability to act as a peroxidase. Extracts were added to 300 μM *o*-

dianisidine, 900 μM H_2O_2, and 10 mM KPi (pH 6.4), and the oxidation of *o*-dianisidine was monitored at A_{460}.

B.2 TABLES

Table B.1. Bacterial strains and plasmids used in this study.

Strain	Genotype	Reference
BW25113	*lacI rrnB* Δ*lacZ hsdK* Δ*araBAD* Δ*rhaBAD*	[2]
JRE520	*ompR1009*::Tn*10*d Tet^R	J.M. Slauch
MG1655	F^- wild type	*E. coli* CGSC
AL441	As MG1655 Δ*lacZ1 att*λ*.*::[pSJ501::*katG´-lacZ*$^+$]~*cat*	Lab strain
JEM1405	As AL441 with pBAD24	This study
JEM1406	As AL441 with pLW112	This study
JEM1425	As AL441 Δ*fur-731*	This study
JEM1427	As JEM1425 with pBAD24	This study
JEM1428	As JEM1425 with pLW112	This study
JEM1431	As JEM1425 Δ*ryhB::cat*	This study
JEM1447	As JEM1447 with pBAD24	This study
JEM1448	As JEM1448 with pLW112	This study
JEM1455	As JEM1425 Δ*mntH2::cat*	This study
JEM1459	As JEM1425 Δ*iscR::cat*	This study
JEM1449	As BW25113 ΔP_{katG}*::tetRA*-23	This study
JEM1451	As MG1655 ΔP_{katG}*::tetRA*-23	This study
JEM1457	As MG1655 ΔP_{katG}*::tetRA*-23 Δ*fur-731::kan*	This study
JEM1478	As MG1655 ΔP_{katG}*::tetRA*-23 Δ*fur-731::kan* Δ*ryhB::cat*	This study

Plasmids	Relevant characteristics	Reference
pSJ501	pAH125 derivative with *cat* flanked by *flp* sites	[5]
pKD3	*bla* FRT *cat* FRT PS1 PS2 oriR6K	[2]
pKD46	*bla* P_{BAD} *gam bet exo* pSC101 oriTS	[2]
pCP20	*bla cat cI857* λP_R *flp* pSC101 oriTS	[1]
pBAD24	Amp^R, ColE1	[4]
pLW112	pBAD24 containing *mntS* ORF and its own Shine-Dalgarno	[12]

B.3 FIGURES

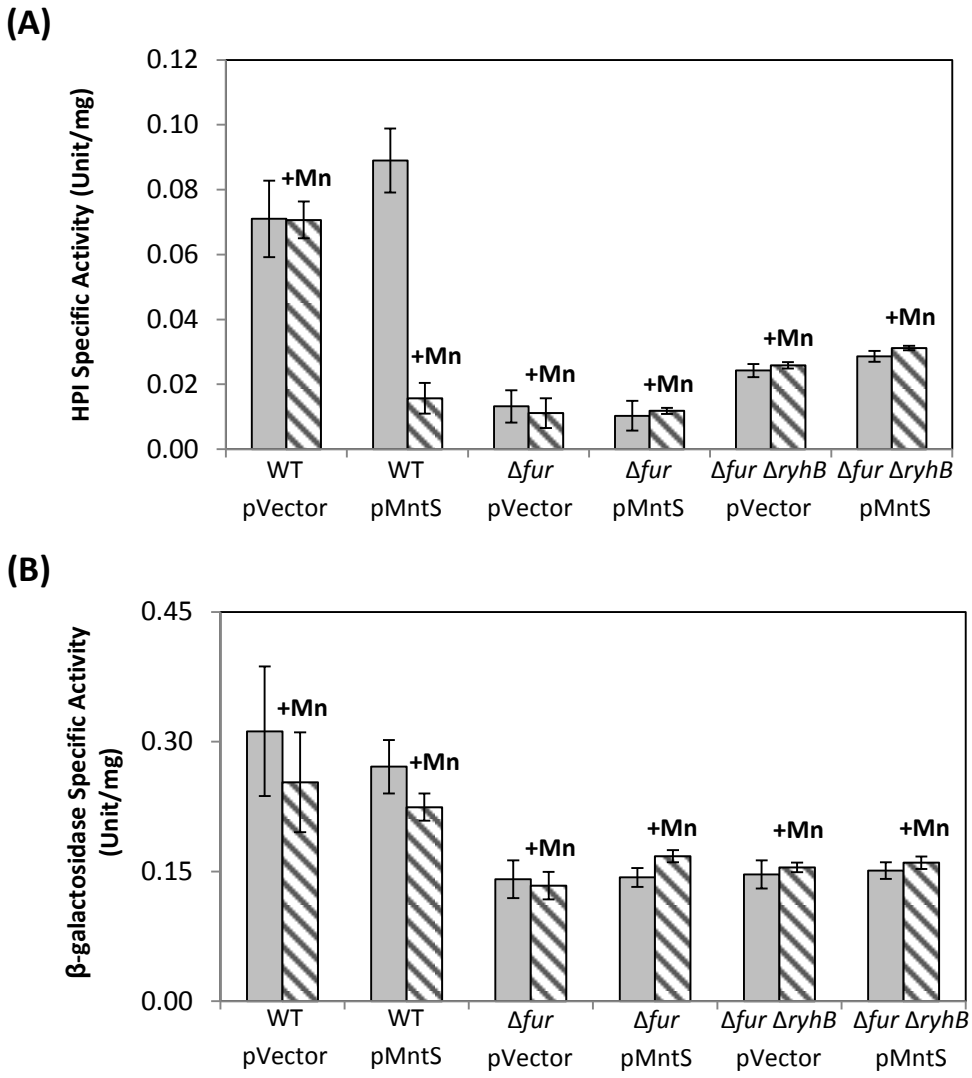

Figure B.1. (A) Low HPI activity and (B) *katG* transcription in Δ*fur* mutants is not due to increased RyhB synthesis. Cells pre-cultured in LB medium were diluted into fresh LB/arabinose medium with or without 0.5 mM $MnCl_2$. Cells were harvested after 2.5 hr of growth and enzyme activity was analyzed. The data shown are the mean of three independent experiments. All strains contain both the *lacZ*-null and P_{katG}-*lacZ* alleles. Strains were WT (AL441), Δ*fur* (JEM1425), and Δ*fur* Δ*ryhB* (JEM1431) harboring empty pVector (pBAD24) or pMntS (pLW112, *mntS* driven by *araBAD* promoter).

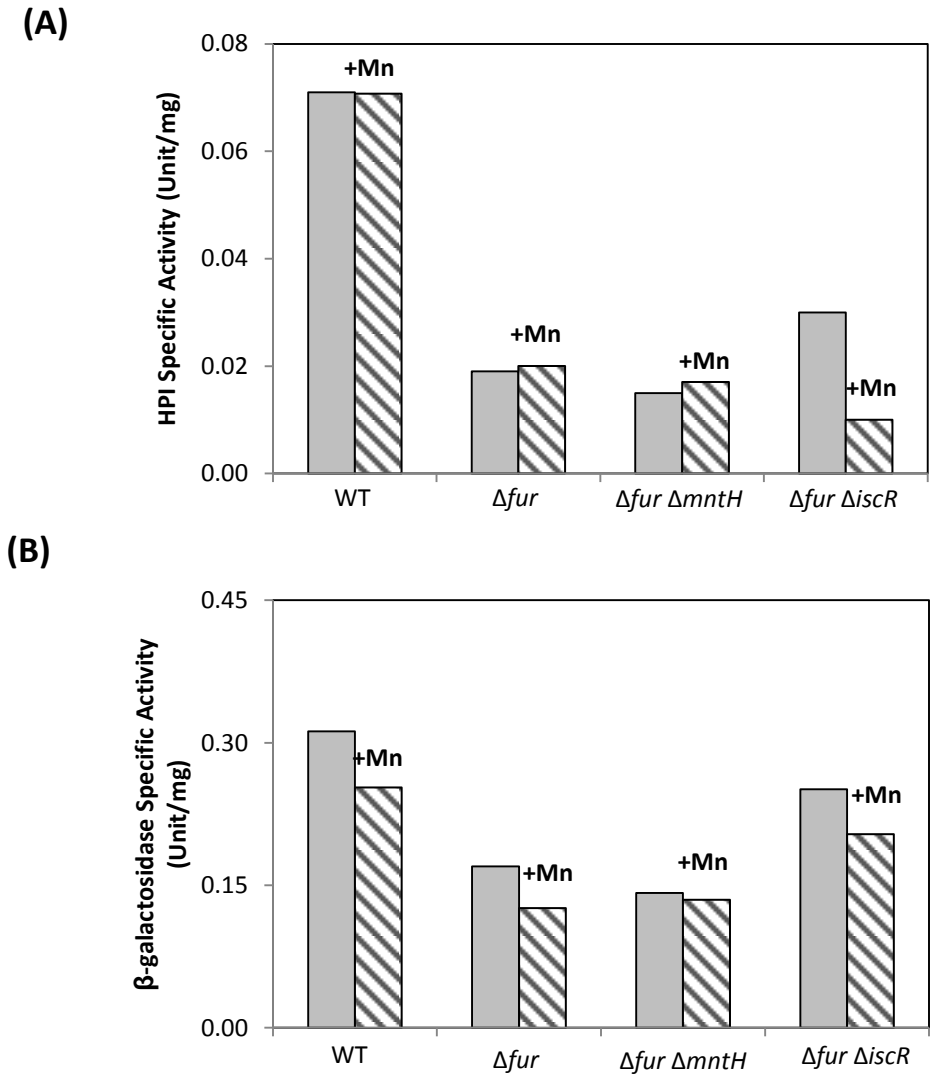

Figure B.2. (A) Low HPI activity and (B) *katG* transcription in Δ*fur* mutants is not due to manganese import or induction of *iscR*. Cells pre-cultured in LB medium were diluted into fresh LB/arabinose medium with or without 0.5 mM $MnCl_2$. Cells were harvested after 2.5 hr of growth and enzyme activity was analyzed. All strains contain both the *lacZ*-null and P_{katG}-*lacZ* alleles. Strains were WT (AL441), Δ*fur* (JEM1425), Δ*fur* Δ*mntH* (JEM1455), and Δ*fur* Δ*iscR* (JEM1459).

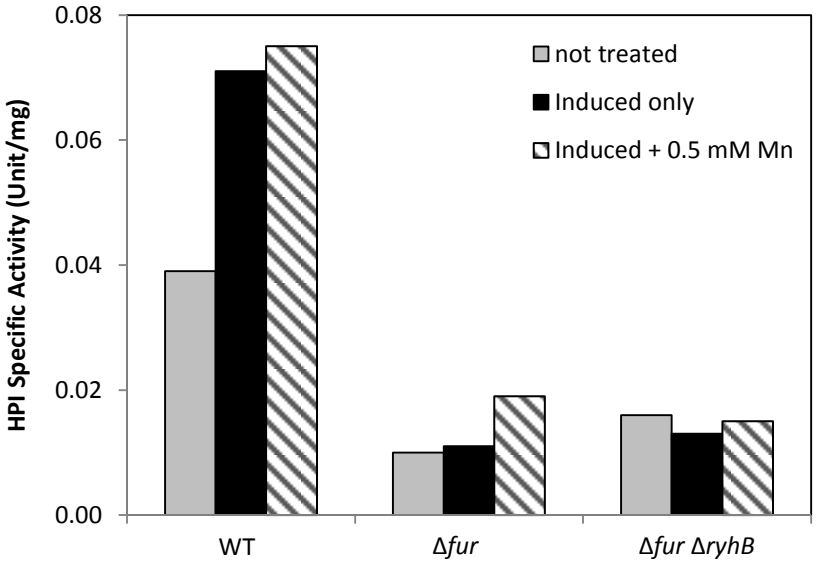

Figure B.3. Fur regulates *katG* expression downstream of transcription. Cells pre-cultured in LB medium were diluted into fresh LB/arabinose medium with or without 0.5 mM $MnCl_2$. Cells were harvested after 2.5 hr of growth and enzyme activity was assessed. All strains contain both the *lacZ*-null and P_{tet}-*katG* alleles. Transcription of *katG* was not induced for samples labeled as not treated. Strains were WT (JEM1451), Δ*fur* (JEM1457), and Δ*fur ΔryhB* (JEM1478).

B.4 REFERENCES

1. **Cherepanov, P. P., and W. Wackernagel.** 1995. Gene disruption in E*scherichia coli*: Tc^R and Km^R cassettes with the option of Flp-catalyzed excision of the antibiotic-resistance determinant. Gene. **158:**9-14.

2. **Datsenko, K. A., and B. L. Wanner.** 2000. One-step inactivation of chromosomal genes in *Escherichia coli* K-12 using PCR products. Proc. Natl. Acad. Sci. U. S. A **97:**6640-6645.

3. **Desnoyers, G., A. Morissette, K. Prevost, and E. Masse.** 2009. Small RNA-induced differential degradation of the polycistronic mRNA i*scRSUA*. EMBO J. **28:**1551-1561.

4. **Guzman, L. M., D. Belin, M. J. Carson, and J. Beckwith.** 1995. Tight regulation, modulation, and high-level expression by vectors containing the arabinose P_{BAD} promoter. J. Bacteriol. **177:**4121-4130.

5. **Jang, S., and J. A. Imlay.** 2010. Hydrogen peroxide inactivates the *Escherichia coli* Isc iron-sulphur assembly system, and OxyR induces the Suf system to compensate. Mol. Microbiol. **78:**1448-1467.

6. **Kehres, D. G., A. Janakiraman, J. M. Slauch, and M. E. Maguire.** 2002. Regulation of *Salmonella enterica* serovar Typhimurium *mntH* transcription by H_2O_2, Fe^{2+}, and Mn^{2+}. J. Bacteriol. **184:**3151-3158.

7. **Merighi, M., C. D. Ellermeier, J. M. Slauch, and J. S. Gunn.** 2005. Resolvase-in vivo expression technology analysis of the *Salmonella enterica* serovar Typhimurium PhoP and PmrA regulons in BALB/c mice. J. Bacteriol. **187:**7407-7416.

8. **Miller, J. H. (ed.),** 1972. Experiments in molecular genetics. Cold Springs Harbor Laboratory, Cold Springs Harbor, NY.

9. **Nandal, A., C. C. Huggins, M. R. Woodhall, J. McHugh, F. Rodriguez-Quinones, M. A. Quail, J. R. Guest, and S. C. Andrews.** 2010. Induction of the ferritin gene (*ftnA*) of *Escherichia coli* by Fe^{2+}-Fur is mediated by reversal of H-NS silencing and is RyhB independent. Mol. Microbiol. **75:**637-657.

10. **Patzer, S. I., and K. Hantke.** 2001. Dual repression by Fe^{2+}-Fur and Mn^{2+}-MntR of the mntH gene, encoding an NRAMP-like Mn^{2+} transporter in *Escherichia coli.* J. Bacteriol. **183:**4806-4813.

11. **Tartaglia, L. A., G. Storz, and B. N. Ames.** 1989. Identification and molecular analysis of OxyR-regulated promoters important for the bacterial adaptation to oxidative stress. J. Mol. Biol. **210:**709-719.

12. **Waters, L. S., M. Sandoval, and G. Storz.** 2011. The *Escherichia coli* MntR miniregulon includes genes encoding a small protein and an efflux pump required for manganese homeostasis. J. Bacteriol. **193:**5887-5897.

APPENDIX C: *HEMA* TRANSCRIPTION IS DOWN-REGULATED DURING MANGANESE TOXICITY

HemA (glu-tRNA dehydrogenase, encoded by *hemA*) catalyzes the first step in the heme biosynthetic pathway [11, 12]. The regulation of *hemA* is not well understood. During the course of investigating the physiological role of *mntS*, I observed a 3-fold decrease in *hemA* transcription for cells overexpressing MntS in manganese-rich conditions compared to cells harboring empty vector (Fig. C.1). There are only two known transcriptional regulators that induce *hemA* transcription: ArcA and Fnr [2]. I found that neither ArcA nor Fnr seem to be responsible for decreased *hemA* transcription in cells overexpressing MntS during manganese-replete conditions, since the phenotype still occurred in the absence of *arcA* or *fnr* (Fig. C.2).

MntS overexpressing cells are sensitive to manganese and contain low amounts of available iron, which results from repression of the Fur regulon (discussed in chapter 3). Deletion of *fur* in these cells restored intracellular iron levels beyond wild type cells and relieved manganese sensitivity. Deletion of *fur* in cells overexpressing MntS also restored *hemA* transcription to wild type levels but did not further increase *hemA* transcription in wild type cells (Fig. C.1), which indicated that Fur does not directly induce *hemA* transcription.

IscR, in addition to Fur, is another global regulator that senses intracellular iron. IscR is a dual transcriptional regulator that exists in two forms: holo (bound to an iron-sulfur cluster) and apo (containing no iron-sulfur cluster) [4, 7] . Holo-IscR tends to repress transcription of genes, while apo-IscR activates transcription, but was also shown to repress *hyaA* [10]. *iscR*-null mutants showed a 2-fold increase in *hemA* transcription

levels compared to wild type cells (Fig. C.3), which suggested that IscR represses *hemA* transcription. Overexpression of MntS in Δ*iscR* mutants does not affect *hemA* transcript levels, unless manganese is present (Fig. C.3). Only then, do you see a 2-fold decrease in *hemA* transcription. Note that the *hemA* transcript levels never fall below wild type levels when *iscR* is deleted (Fig. C.3). Thus, *hemA* is still affected by manganese toxicity, but Δ*iscR* lessens the effect.

I next examined which form of IscR was responsible for repression of *hemA*, by complementing the *iscR*-null allele with plasmids expressing IscR or Apo-IscR. To my surprise, I found that both forms of IscR repressed *hemA* transcription. Since IscR may exist inside the cell as both forms, I can only conclude that Apo-IscR represses transcription of *hemA*. A typical type 2 IscR-binding motif (AxxxCCxxAxxxXxxxTAxGGxxxT) [10] is visible within the promoter region of *hemA* (Fig. C.4). However, the predicted motif is unusual in that it falls upstream of the -35 element and does not overlap it at all. Typical repressors bind near the -10 or -35 elements and block polymerase from binding.

In conclusion, Apo-IscR is a likely candidate for repression of *hemA* transcription. When iron is limited, Apo-IscR shuts down heme biosynthesis.

C.1 MATERIALS AND METHODS

C.1.1 Bacterial strain construction

The bacterial strains used in this study are described in Table C.1. The λ red recombinase method was used to create null mutations [3]. Mutations were introduced into new strains by P1-transduction [9]. The resulting mutations were confirmed by PCR

analysis. When necessary, the antibiotic cassette was removed by FLP-mediated excision [3].

For construction of single-copy transcriptional *lacZ* fusion to *hemA,* the promoter region of *hemA* was amplified by PCR using primers designed with restriction sites. The product was digested and inserted into pSJ501, a plasmid derivative of pAH125 modified to express the chloramphenicol acetyl transferase gene (cat) flanked by FLP sites for selection. The resulting plasmid constructs were confirmed by sequencing. Plasmids were then integrated into the λ attachment site, while the wild-type *hemA* gene remained at its native position. Fusions were introduced into new strains by P1-transduction and the chloramphenicol-resistance cassette was removed by FLP-mediated excision.

The plasmid pMntS (pLW112) was generated by amplifying the 205 nt of the RNA (encompassing the MntS open reading frame) and its own Shine-Dalgarno sequence by PCR [13]. The product was digested with NheI and KpnI and cloned into pBAD24 (medium copy number plasmid that is maintained at 15-20 copies/cell), which is driven by *araBAD* promoter.

C.1.2 Growth conditions

Cells were grown in standard LB medium at 37°C. Overnight cultures were diluted to OD_{600} 0.005 into fresh medium and grown to an approximate OD_{600} of 0.12. Cells were then subcultured again into fresh aerobic medium to OD_{600} 0.005 with or with out 0.5 mM $MnCl_2$. Cells were harvested after approximately 2.5 hr of growth and enzyme activity was measured.

Strains carrying pBAD24 derived plasmids were grown with ampicillin overnight, then diluted into fresh medium to OD_{600} 0.005. After approximately four doublings, 50 mM L(+)arabinose was added to induce MntS expression. Cultures were grown for an additional 30 to 45 minutes, then subcultured again into fresh aerobic medium with ampicillin and 50 mM L(+)arabinose to OD_{600} 0.0025 and grown at 37°C.

C.1.3 β-galactosidase activity

To prepare extracts, cells were centrifuged, washed twice, resuspended in ice-cold 50 mM Tris-HCl buffer (pH 8), and lysed by French press. Cell debris was removed by centrifugation, and β-galactosidase activity in cell extracts was determined by ONPG hydrolysis using standard procedures [9]. Protein concentrations were determined by the Bradford assay using bovine serum albumin as the standard.

C.2 TABLES

Table C.1. Bacterial strains and plasmids used in this study.

Strain	Genotype	Reference
BW25113	*lacI rrnB* Δ*lacZ hsdK* Δ*araBAD* Δ*rhaBAD*	[3]
MG1655	F^- wild type	*E. coli* CGSC
SMA1023	As MG1655 Δ*lacZ1 attλ::*[pSJ501::*hemA´-lacZ*$^+$]	Lab strain
JEM1468	As SMA1023 with pBAD24[5]	This study
JEM1469	As SMA1023 with pLW112	This study
SMA1073	As MG1655 Δ*lacZ1* Δ*fur-731::kan attλ::*[pSJ501::*hemA´-lacZ*$^+$]	Lab strain
JEM1482	As SMA1073 with pBAD24	This study
JEM1483	As SMA1073 with pLW112	This study
SMA1101	As MG1655 Δ*lacZ1* Δ*iscR::cat attλ::*[pSJ501::*hemA´-lacZ*$^+$]	Lab strain
JEM1555	As SMA1101 with pBAD24	This study
JEM1556	As SMA1101 with pLW112	This study
JEM1557	As JEM1468 Δ*fnr*(Bsm-Mlu)::Ω($Spec^R$)~*zcj::*Tn*10*	This study
JEM1559	As JEM1468 Δ*fnr*(Bsm-Mlu)::Ω($Spec^R$)~*zcj::*Tn*10*	This study
JEM1543	As JEM1468 Δ*arcA44::kan*	This study
JEM1545	As JEM1469 Δ*arcA44::kan*	This study
JEM1561	As MG1655 Δ*lacZ1* Δ*iscR attλ::*[pSJ501::*hemA´-lacZ*$^+$]	This study
JEM1565	As JEM1561 with pACYC184	This study
JEM1566	As JEM1561 with pPK7312	This study
JEM1567	As JEM1561 with pPK7867	This study

Plasmids	Relevant characteristics	Reference
pSJ501	pAH125 derivative with *cat* flanked by *flp* sites	[6]
pKD3	*bla* FRT *cat* FRT PS1 PS2 oriR6K	[3]
pKD46	*bla* P_{BAD} *gam bet exo* pSC101 oriTS	[3]
pCP20	*bla cat cI857* λP_R *flp* pSC101 oriTS	[1]
pBAD24	Amp^R, ColE1	Lab stock
pLW112	pBAD24 containing *mntS* ORF and its own Shine-Dalgarno	[13]
pACYC184	Tet^R Cam^R	[8]
pPK7312	pACYC184 containing EcoRI 1303-bp *FRT-kan-FRT* StuI-EcoRV 985-bp *iscR*	[10]
pPK7867	pACYC184 containing EcoRI 1303-bp *FRT-kan-FRT* StuI-EcoRV 985-bp *iscR*-C92A/C98A/C104A	[10]

C.3 FIGURES

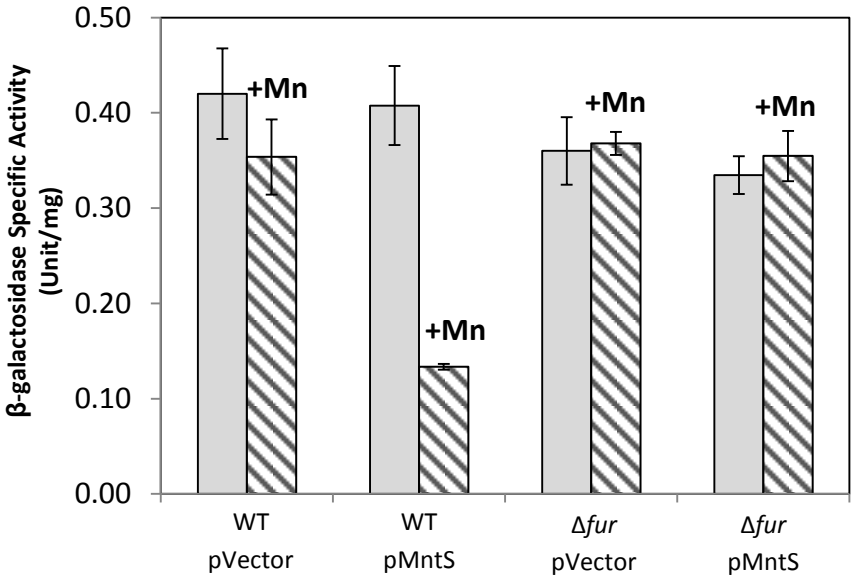

Figure C.1. *hemA* transcription is down-regulated during manganese toxicity. Cells pre-cultured in LB medium were diluted into fresh LB/arabinose medium with or without 0.5 mM $MnCl_2$. Cells were harvested after 2.5 hr of growth and enzyme activity was analyzed. The data shown are the mean of three independent experiments. All strains contain both the *lacZ*-null and P_{hemA}-*lacZ* alleles. Strains were WT (SMA1023) and Δ*fur* (SMA1073) harboring empty pVector (pBAD24) or pMntS (pLW112, *mntS* driven by *araBAD* promoter).

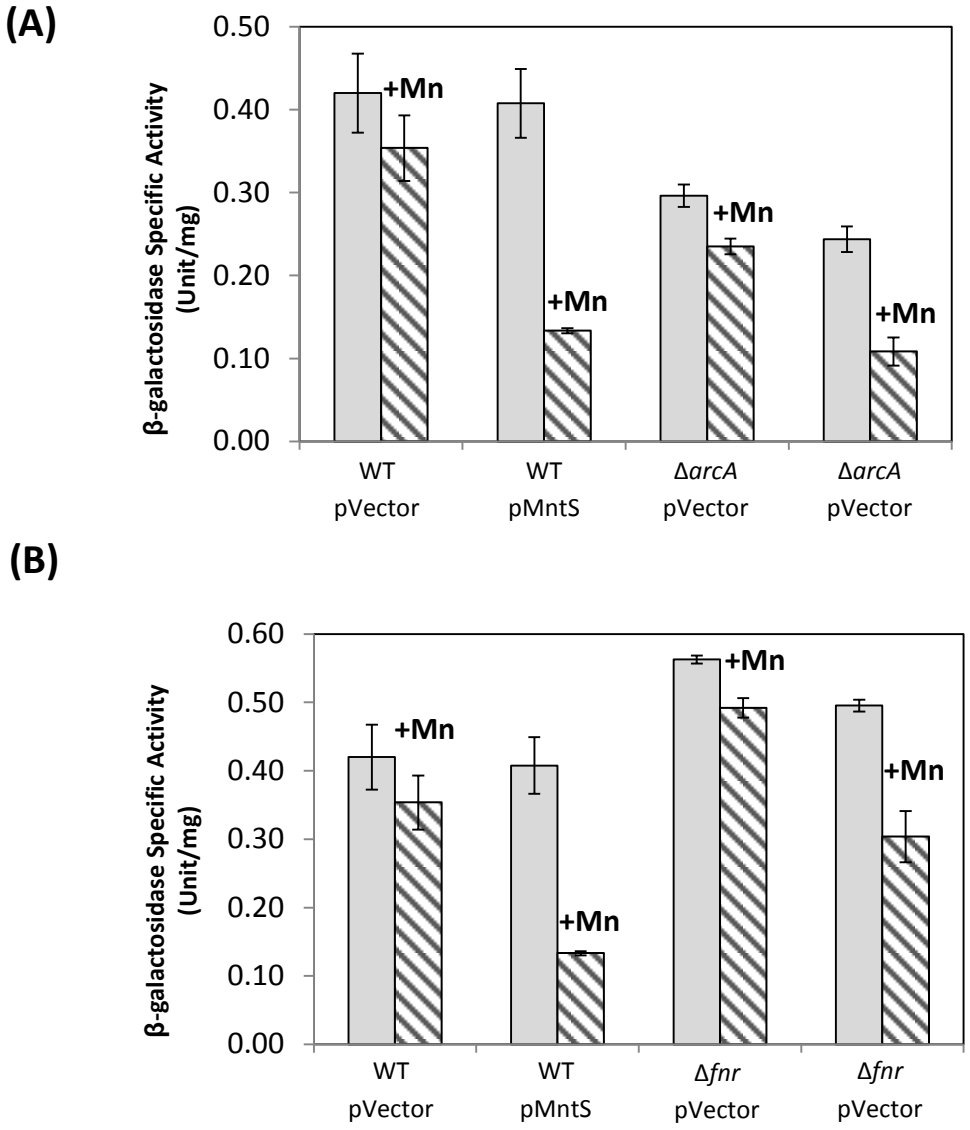

Figure C.2. ArcA and FNR are not responsible for decreased *hemA* transcription during manganese toxicity. Cells pre-cultured in LB medium were diluted into fresh LB/arabinose medium with or without 0.5 mM $MnCl_2$. Cells were harvested after 2.5 hr of growth and enzyme activity was analyzed. The data shown are the mean of three independent experiments. All strains contain both the *lacZ*-null and P_{hemA}-*lacZ* alleles.
A. Strains were WT (SMA1023) and Δ*arcA* (JEM1543) harboring empty pVector (pBAD24) or pMntS (pLW112, *mntS* driven by *araBAD* promoter).
B. Strains were WT (SMA1023) and Δ*fnr* (JEM1557) harboring empty pVector (pBAD24) or pMntS (pLW112, *mntS* driven by *araBAD* promoter).

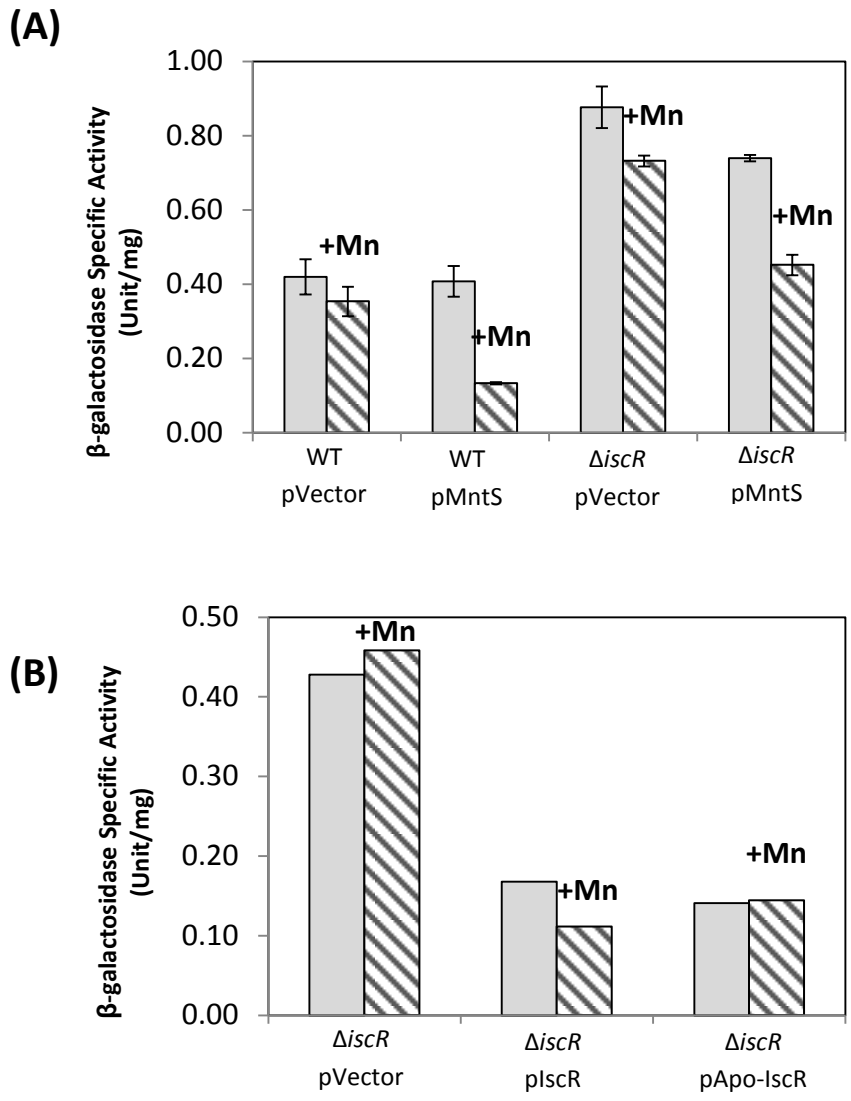

Figure C.3. IscR regulates *hemA*. Cells pre-cultured in LB medium were diluted into fresh LB/arabinose medium with or without 0.5 mM $MnCl_2$. Cells were harvested after 2.5 hr of growth and enzyme activity was analyzed. All strains contain both the *lacZ*-null and P_{hemA}-*lacZ* alleles.

A. The data shown are the mean of three independent experiments. Strains were WT (SMA1023) and Δ*iscR* (SMA1101) harboring empty pVector (pBAD24) or pMntS (pLW112, *mntS* driven by *araBAD* promoter).

B. Strains were Δ*iscR* (JEM1561) harboring empty pVector (pACYC184), pIscR (pPK7312), or pApo-IscR (pPK7867, *iscR*-C92A/C98A/C104A).

5’-GTTGTCTTA*ATTG**CC*AG*AA*TCTAACGGCT*T*TC*GG*CAA*T*TACTCCAAAAGG

GGGCGCTCTCTTTTATTGATCTTACGCATCCTGTATGATGCAAGCAGACT

AACCCTATCAACGTTGGTATTATTTCCCGCAGACATGACCCTTTTA-‘3

+1

***hemA* ORF**

Figure C.4. Alignment of the *hemA* genomic locus. Sequence showing the -10 and -35 regions (double underlined), the predicted type 2 IscR-binding motif (single underline, with critical bases italicized), transcriptional start site (+1), and the *hemA* open reading frame (gray).

C.4 REFERENCES

1. **Cherepanov, P. P., and W. Wackernagel.** 1995. Gene disruption in *Escherichia coli*: Tc^R and Km^R cassettes with the option of Flp-catalyzed excision of the antibiotic-resistance determinant. Gene. **158:**9-14.

2. **Darie, S., and R. P. Gunsalus.** 1994. Effect of heme and oxygen availability on *hemA* gene expression in *Escherichia coli*: role of the *fnr*, *arcA*, and *himA* gene products. J. Bacteriol. **176:**5270-5276.

3. **Datsenko, K. A., and B. L. Wanner.** 2000. One-step inactivation of chromosomal genes in *Escherichia coli* K-12 using PCR products. Proc. Natl. Acad. Sci. U. S. A. **97:**6640-6645.

4. **Fontecave, M., and S. Ollagnier-de-Choudens.** 2008. Iron-sulfur cluster biosynthesis in bacteria: Mechanisms of cluster assembly and transfer. Arch. Biochem. Biophys. **474:**226-237.

5. **Guzman, L. M., D. Belin, M. J. Carson, and J. Beckwith.** 1995. Tight regulation, modulation, and high-level expression by vectors containing the arabinose P_{BAD} promoter. J. Bacteriol. **177:**4121-4130.

6. **Jang, S., and J. A. Imlay.** 2010. Hydrogen peroxide inactivates the *Escherichia coli* Isc iron-sulphur assembly system, and OxyR induces the Suf system to compensate. Mol. Microbiol. **78:**1448-1467.

7. **Johnson, D. C., D. R. Dean, A. D. Smith, and M. K. Johnson.** 2005. Structure, function, and formation of biological iron-sulfur clusters. Annu. Rev. Biochem. **74:**247-281.

8. **Kullik, I., M. B. Toledano, L. A. Tartaglia, and G. Storz.** 1995. Mutational analysis of the redox-sensitive transcriptional regulator OxyR: regions important for oxidation and transcriptional activation. J. Bacteriol. **177:**1275-1284.

9. **Miller, J. H. (ed.),** 1972. Experiments in Molecular Genetics. Cold Springs Harbor Laboratory, Cold Springs Harbor, NY.

10. **Nesbit, A. D., J. L. Giel, J. C. Rose, and P. J. Kiley.** 2009. Sequence-specific binding to a subset of IscR-regulated promoters does not require IscR Fe-S cluster ligation. J. Mol. Biol. **387:**28-41.

11. **Randau, L., S. Schauer, A. Ambrogelly, J. C. Salazar, J. Moser, S. Sekine, S. Yokoyama, D. Soll, and D. Jahn.** 2004. tRNA recognition by glutamyl-tRNA reductase. J. Biol. Chem. **279:**34931-34937.

12. **Schauer, S., S. Chaturvedi, L. Randau, J. Moser, M. Kitabatake, S. Lorenz, E. Verkamp, W. D. Schubert, T. Nakayashiki, M. Murai, K. Wall, H. U. Thomann, D. W. Heinz, H. Inokuchi, D. Soll, and D. Jahn.** 2002. *Escherichia coli* glutamyl-tRNA reductase. Trapping the thioester intermediate. J. Biol. Chem. **277:**48657-48663.

13. **Waters, L. S., M. Sandoval, and G. Storz.** 2011. The *Escherichia coli* MntR miniregulon includes genes encoding a small protein and an efflux pump required for manganese homeostasis. J. Bacteriol. **193:**5887-5897.

APPENDIX D: DOES MNTS WORK AS A SMALL RNA IN ADDITION TO ITS FUNCTION AS A PROTEIN?

D.1 INTRODUCTION

The *mntS* gene was first identified using comparative genomics and microarrays [11]. It is expressed as a small RNA that is predicted to have complex secondary structure; this small RNA is termed RybA. Within the RNA lies a short open reading frame that encodes a novel small protein of 42 amino acids, known as MntS [12]. MntS facilitates manganese delivery to enzymes, such as MnSOD and NrdEF (discussed in Chapter 3). It also helps *E. coli* cells cope with hydrogen peroxide stress, possibly by allocating manganese to non-redox mononuclear enzymes (discussed in Chapter3). The mechanism by which MntS functions to make manganese available to these enzymes is not clear. Based on the genetic characterization of *mntS*, it is plausible that MntS could function as both a protein and a small RNA. Here, I examined how *mntS* functions to activate MnSOD and NrdEF and helps cells cope with hydrogen peroxide stress.

D.2 RESULTS

D.2.1 A small RNA helps activate MnSOD

MntS was first hypothesized to be a metal chaperone, since it is too small to possess enzymatic activity and its coding sequence contains several potential metal binding residues (Glu, Cys, Asp, His) that are conserved. Strains overexpressing mutant *mntS* alleles, in which these metal binding residues were exchanged with the non-metal binding amino acid alanine, were still able to activate MnSOD to similar levels as the native *mntS* gene (Fig. D.2). Combining the mutations did not diminish this function of

MntS (Fig. D.3). Furthermore, purified MntS protein was incapable of influencing the metallation of apo-MnSOD in cell extracts (Fig. D.4). These data argue against the idea that MntS functions as a metal chaperone that binds manganese, but they do not eliminate the idea that MntS functions as a protein and possibly a small RNA.

To decipher the mechanistic capability of MntS, I constructed several plasmids expressing mutant *mntS* alleles that were incapable of expressing the MntS protein. Only the MntS open reading frame plus its Shine-Dalgarno were cloned into the plasmids. These mutations included an amber stop codon inserted at Met1 and Met8 and three independent frame-shift mutations at Phe4, Phe11, and Phe16. MnSOD activation was observed for all mutations (Fig. D.5), despite no MntS protein being made. Arabinose induction was also necessary to see the increase in MnSOD activation (Fig. D.6). Deletion of the entire chromosomal *mntS* gene (including RybA) did not affect the function of MntS when expressed from the plasmid (Fig. D.7). These data suggested that the *mntS* alleles expressed from the plasmid might possess small RNA activity that functions independent of the *mntS* chromosomal gene.

Many small RNAs require the Hfq chaperone to function. An *hfq*-null mutation showed decreased MnSOD activation compared to wild type cells (Fig. D.8B). MntS expressed from a plasmid was also incapable of activating MnSOD in the absence of *hfq* (Fig. D.8A). This data further suggested that a small RNA was involved in the activation of MnSOD and might possibly be transcribed from the MntS plasmid. It is not RyhB, since deletion of *ryhB* had no affect on the metallation status of MnSOD (Fig. D.9).

D.2.2 Val10 residue is important for MntS/RybA function

The fact that *mntS*-Met1stop showed full activation of MnSOD suggested that *mntS* translation might initiate elsewhere. Examination of the MntS coding region revealed two alternative translational start sites: Met8 and Val10 (Fig. D.10). Met8 is not as well conserved (sometimes Ile (ATA) or Leu (CTG)) and does not have a strong Shine-Dalgarno site upstream of it, while Val10 is conserved and is always encoded by the GTG codon, rather than GTC, GTA, or GTT. GTG is a rare codon that occurs about 14% of the time and can code for Met at the start of a protein translational sequence. Val10 also has a decent Shine-Dalgarno site that encompasses the Arg6 codon, which is strictly conserved as AGG when it could be five other codons (AGA or CGN). Moreover, Val10 is important for MnSOD activation by MntS, whereas Met1 and Met8 are not (Fig. D.11). MntS remained active when Val10 was mutated to another start codon (ATG) or amino acid codon (GTT or GTC) (Fig. D.11), indicating that Val10 might be an alternate start site or contain a region that is critical for RNA base-pairing. To our surprise, mutation of the possible Shine-Dalgarno sequence to a weaker (Arg6Ile) or stronger (Lys5Arg) sequence did not significantly affect MnSOD activation by MntS (Fig. 11). Mutation of the downstream residue, Phe11 (TTT), to the stop codon (TAG) also inactivated MntS, while mutation of the upstream residue, Arg9 (AGG), had no effect (Fig. D.12). Taken together, these data give rise to a possible consensus sequence of RTgtTK (target site TRyrRA), in which the second and fifth nucleotides are critical for small RNA base-pairing. Note that these results are only suggestive, since a small amount of residual protein being produced could be sufficient to affect the results that I observed. Replacement of the native *mntS* with several of the mutant alleles on the

chromosome revealed to me that overproduction may affect the outcome of MnSOD activation (Fig. D.13), making the results even more complicated to interpret.

D.2.3 MntS possibly functions as a small RNA to help activate NrdEF

MntS helped NrdEF function (discussed in Chapter 3). Iron limited mutants harboring the *mntS* chromosomal alleles, *mntS*-F16 or *mntS*-M1M8stop, grew better than Δ*mntS* mutants, but not as well as *mntS*$^{+}$ mutants (Fig. D.14). This data suggests a small RNA function. Strains expressing *mntS*-F11stop allele grew similarly to Δ*mntS* (Fig. D.14), which suggested that this region is necessary for the small RNA function.

D.2.4 MntS confers both protein and small RNA function during hydrogen peroxide stress

A transient lag is observed for Hpx^{-} Δ*mntS* mutants during aerobic growth, which suggests that *mntS* is needed during initial aeration when manganese concentrations are low. This growth defect was not observed for Hpx^{-} *mntS*-M1M8stop mutants (Fig. D.15C), suggesting that *mntS* may function as a small RNA. Hpx^{-} strains encoding *mntS*-F11stop and *mntS*-F16 frameshift alleles display an intermediate growth defect (Fig. D.15A, B).

D.3 CONCLUSION

It appears that the *mntS* gene may function as a small RNA, in addition to a protein, to assist activation of multiple enzymes. This is not unheard of, as there are several examples that have been identified among bacteria. The most well studied dual

functioning small RNA/protein combo is SgrS and SgrT of *E. coli*. The two function collectively to eliminate glucose-phosphate stress [1, 2]. For *mntS*, one might imagine that when iron is scarce, the MntS protein is induced possibly to inhibit the already synthesized MntP protein thereby preventing manganese export, while the small RNA, RybA, or a portion there of might associate with MntS is induced possibly to prevent translation of the MntP transcript. Responding together would permit the accumulation of manganese and ensure a rapid response to iron scarcity.

D.4 MATERIALS AND METHODS

D.4.1 Strain and plasmid constructions

All strains and plasmids used in this study are listed in Table D.1. Chromosomal null deletions were generated using the λ Red recombination method [4]. All oxygen-sensitive strains were constructed under anaerobic conditions to ensure that suppressor mutations were not selected during outgrowth. Mutations were introduced into new strains by P1-transduction [8]. All mutations were confirmed by PCR analysis or blue/white selection with Xgal. When necessary, the antibiotic cassette was removed by FLP-mediated excision [4]. Note that the *mntS*-null deletion removes the entire MntS open reading frame from the translational start ATG to +129 bp, *mntS2* (*mntS*-RNA) removes sequence from the translational start ATG to +278 bp, and the *mntS3* (*mntS*-promoter) removes sequence from the +1 transcriptional start site to +278 bp (Fig. D.1).

The plasmid pMntS (pLW112) was generated by amplifying the 205 nt of the RNA (encompassing only the MntS open reading frame) and its own Shine-Dalgarno sequence by PCR (Fig. D.1) [12]. The product was digested with NheI and KpnI and

cloned into pBAD24 (a medium copy number plasmid that is maintained at 15-20 copies/cell), in which expression is driven by *araBAD* promoter.

The plasmids expressing mutant *mntS* alleles (Table D.1) were created by site-directed mutagenesis on the template pLW112 using Pfu Turbo polymerase from Stratagene. Briefly, 60-mer primers were designed with the mutation of interest located in the center of the sequence (Table D.2). Both forward and reverse complements were ordered. Mutagenesis was performed in a mixture (50 µl) containing 50 ng template DNA, 400 nM each primer complement, 200 µM dNTPs, and 2.5 units Pfu Turbo polymerase. Typical cycling conditions were as follows: 95°C/3 min; 18 cycles of 95°C/30 s, 55°C/1 min, 68°C/2.5 min/kb. The resulting mixture was digested with DpnI at 37°C for more than 1 hr to remove original plasmid DNA template, then transformed into TOP10 electrocompetent *E. coli* cells followed by selection on ampicillin plates. Note that all resulting plasmids constructs were confirmed by sequencing.

Validated plasmids containing *mntS* mutant alleles were transferred to the *E. coli* chromosome as follows. The *mntS* region was amplified using 60-mer primers that contained homology to the beginning and end of the *mntS* open reading frame on the plasmid (20 bp) and additional homology to the flanking sequences upstream and downstream of *mntS* (40 bp). The PCR product was digested with DpnI to degrade parental plasmid, ethanol precipitated to remove salts and to concentrate, and then electroporated into the *mntS::cat-sacB* mutant (LSW245) that also contained a mini-lambda cassette with the lambda-red recombineering genes. Prior to electroporation, LSW245 was grown at 30 °C to 0.4 OD_{600}, heat-shocked for 15 min at 42°C, and washed in sterile cold 10% glycerol. Cultures were recovered after 3 hr at 30 °C in SOC medium

and plated on minimal M63-5% sucrose plates for 3 days. Single colonies were struck out on LB at 37°C and candidates were patched onto LB, LB plus chloramphenicol, and LB plus tetracycline to confirm gene replacement. Candidates showing growth only on LB were tested for the presence of the *mntS* allele by PCR and gel electrophoresis and then subsequently verified by sequence analysis. The chloramphenicol-resistance gene *cat*) was inserted 6 bp after *rybA* on the chromosome using the λ Red recombination method [4] and forward primer 5'-CAGTAGTTGACCTGAACGGCGGCTCGCTCTAT CTTCTGTAGGCTGGAGCTGCTTCG-3' and reverse primer 5'-AAGAGTGGAAAGG GGTCCGCATCCGCGAGCCGCAATATCATATGAATATCCTCCTTAG-3'. The resulting constructs thus inked the chromosomal *mntS* mutant alleles to *cat*, which allowed mutations to be introduced into new strains by P1-transduction [8]. All mutations were confirmed by sequence analysis.

D.4.2 Growth conditions

Luria broth (LB) and base M9 minimal salts were of standard composition [8]. Base MOPS minimal salts were prepared without $FeSO_4$ and micronutrients [9]. M9 and MOPS medium were supplemented with 0.2% glucose, 0.2% casamino acids, 0.5 mM tryptophan (lacking in casamino acids). Media were supplemented with 100 μg/ml ampicillin, 20 μg/ml chloramphenicol, 30 μg/ml kanamycin sulfate, or 12.5 μg/ml tetracycline HCl when antibiotic selection was needed. Anaerobic cultures were grown in an anaerobic chamber (Coy Laboratory Products Inc.) under an atmosphere of 85% N_2/10% H_2/5% CO_2. Aerobic cultures were grown under room air with vigorous shaking.

To ensure that cells were growing exponentially, overnight cultures were diluted to OD_{600} 0.005 and grown at 37°C to an approximate OD_{600} of 0.12. Cells were then subcultured again into fresh aerobic medium to OD_{600} 0.0025 and grown at 37°C to an approximate OD_{600} of 0.25 prior to analysis. Strains harboring pMntS exhibited slower growth, approximately 2 hr after incubation with manganese. Thus, enzyme activities were typically measured 2.5 hr after treatment with manganese.

Strains carrying pBAD24-derived plasmids were grown with ampicillin overnight and then diluted into fresh medium to OD_{600} 0.005. After approximately four doublings, 50 mM L(+)arabinose was added to induce MntS expression. Cultures were grown for an additional 30 to 45 minutes, subcultured again into fresh aerobic medium with ampicillin and 50 mM L(+)arabinose to OD_{600} 0.0025, and grown at 37°C.

D.4.3 Cell viability

Anaerobic overnight cultures were diluted to OD_{600} 0.005 and grown anaerobically at 37°C to an OD_{600} of approximately 0.1. Cells were then subcultured again into fresh aerobic medium to OD_{600} 0.0025 and grown at 37°C with vigorous shaking. At intervals, aliquots of cells were removed and serially diluted into aerobic medium. The diluted samples were mixed with anaerobic top agar and poured onto anaerobic medium agar plates. Colonies were counted after 24 (LB medium) or 48 hours (defined medium) of anaerobic incubation at 37°C.

D.4.4 Superoxide dismutase activity

To prepare extracts, cells were centrifuged, washed twice, resuspended to 1/100 the original culture volume in ice-cold 50 mM Tris-HCl buffer (pH 8), and lysed by French press. Cell debris was removed by centrifugation, and SOD activity was measured in cell extracts using the xanthine oxidase/cytochrome *c* method [7]. A *sodB* (encoding FeSOD) mutant was used to track MnSOD activity. The fraction of MnSOD that was active in the cell extracts was determined after extracts were subjected to partial denaturation and renaturation in the presence of manganese to ensure full activation of MnSOD protein [5, 6]. Briefly, MnSOD was denatured at pH 3.8 in the presence of 5 mM Tris-HCl/2.5 M guanidinium chloride/20 mM 8-hydroxyquinoline-5-sulphonic acid/0.1 mM EDTA for approximately 12 hr in the dark and then renatured at pH 7.8 in the presence of 5 mM HEPES/0.1 mM $MnCl_2$ for 2 periods of approximately 12 hr each. Excess metal was removed by dialysis at pH 7.8 in 5 mM Tris-HCl/0.1 mM EDTA for 2 periods of 4 hr each. The entire reconstitution process was performed at 4°C. Since measurements were determined from the fraction of protein that survived the procedure, we occasionally observed greater than 100% active MnSOD. Purchased *E. coli* manganese-containing SOD was used as a control for the reconstitution procedure (approximately 90-110 % reactivation was observed).Protein concentrations were determined by the Bradford assay using bovine serum albumin as the standard.

D.4.5 Purification of MntS protein

Purification of MntS protein was performed by Laurie S. Waters. A GST-MntS fusion protein was overproduced in BL21 (DE3), purified on glutathione sepharose,

eluted with PreScission protease, purified on a size exclusion column, and dialyzed against 50 mM Tris-HCl/ 150 mM NaCl/ 0.1% dodecyl β-D-maltoside, pH 8.0. The concentration of the final protein was estimated at 9 μM (or 50 μg/ml), based on the Bradford assay, and the purity was estimated to be at least 50% (possibly >85%) by Coomassie-stained gel. Note that both of these numbers are only estimates and probably under-represent the true amount of purified protein, since MntS does not bind the Coomassie dye well.

D.4.6 *In vitro* manganese uptake by apo-MnSOD in cell extracts

Apo-MnSOD was prepared from a Δ*sodB* Δ*mntS* mutant overexpressing MnSOD (pDT1-16). Briefly, overnight cells were diluted into fresh LB plus ampicillin to 0.01 OD_{600} and grown at 37°C. MnSOD expression was induced by the addition 400 μM IPTG at 0.15 OD_{600}. Cells were harvested after incubation at 15°C for 24 hr, centrifuged, washed twice, resuspended in ice-cold 50 mM Tris-HCl buffer (pH 8.0), and lysed by French press. Cell debris was removed by centrifugation, extracts were subjected to partial denaturation, and SOD activity was measured as described above.

Ice-cold 200 μM $MnCl_2$ and 20 μl of purified MntS protein (stock concentration 9 μM) was added to the prepared cell extracts containing Apo-MnSOD protein in 50 mM KP_i/ 0.1 mM EDTA buffer (pH 7.8) on ice. After removing a zero time reference sample, the mixture was transferred to a preheated tube at 37°C. Aliquot samples were removed and transferred to ice-cold tubes to stop the reaction at the specified times. Samples were stored on ice for no longer than 30 min before SOD activity was measured using the xanthine oxidase/cytochrome *c* method [7].

D.5 TABLES

Table D.1. Bacterial strains and plasmids used in this study.

Strains	Genotype	Reference
MG1655	F^- wild type	*E. coli* CGSC
LC106	Δ*ahpF::kan* Δ(*katG::*Tn*10*)1 Δ(*katE12::*Tn*10*)	[10]
BW25113	*lacI rrnB* Δ*lacZ hsdK* Δ*araBAD* Δ*rhaBAD*	[4]
LSW120	As MG1655 Δ*mntS::cat*	This study
CAG18493	λ^- *rph-1 zbh-29::*Tn*10*	*E. coli* CGSC
JEM1136	As MG1655 Δ*lacZ*1 Δ*tonB1* Δ*feoABC* Δ*zupT* Δ(*nrdA-nrdB*)*1*	This study
JEM1171	As MG1655 Δ*mntS::kan~zbh-29::*Tn*10*	This study
JEM1177	As LC106 Δ*mntS::kan~zbh-29::*Tn*10*	P1(JEM1171) X LC106
JEM1183	As JEM1136 Δ*mntS::kan~zbh-29::*Tn*10*	P1(JEM1171) X JEM1136
JEM1202	As BW25113 Δ*sodB1::cat*	This study
JEM1233	As MG1655 Δ*sodB1*	P1(JEM1202) X MG1655
JEM1234	As MG1655 Δ*sodB1* Δ*mntS*	This study
LSW245	Δ*mntS::cat-sacB* mini-λ::Tet^R	L.S. Waters
LSW261A	*mntS*-WT	This study
LSW262A	*mntS*-(M1stop)	This study
LSW263A	*mntS*-(V10stop)	This study
KRG003	*mntS*-(Phe16 +1 frameshift)	This study
KRG001D	*mntS*-(F11stop)	This study
KRG002B	*mntS*-(M1stopM8stop)	This study
JEM1507	Δ*sodB1::cat mntS*-(WT)	P1(JEM1202) X LSW261A
JEM1509	Δ*sodB1::cat mntS*-(M1stop)	P1(JEM1202) X LSW262A
JEM1511	Δ*sodB1::cat mntS*-(V10stop)	P1(JEM1202) X LSW263A
JEM1641	Δ*sodB1::cat mntS*-(F11stop)	P1(JEM1202) X KRG001D
JEM1643	Δ*sodB1::cat mntS*-(M1stopM8stop)	P1(JEM1202) X KRG002B
JEM1679	Δ*sodB1::cat mntS*-(Phe16 +1 frameshift)	P1(JEM1202) X KRG003
JEM1678	*mntS*-(Phe16 +1 frameshift) with pKD46	This study
JEM1685	*mntS*-(F11stop) with pKD46	This study
JEM1686	*mntS*-(M1stopM8stop) with pKD46	This study
JEM1689	*mntS*-(Phe16 +1 frameshift)~*zji-297::cat*	This study
JEM1691	*mntS*-(F11stop)~*zji-297::cat*	This study
JEM1693	*mntS*-(M1stopM8stop)~*zji-297::cat*	This study
JEM1702	As LC106 *mntS*-(Phe16 +1 frameshift)~*zji-297::cat*	P1(JEM1689) X LC106
JEM1705	As LC106 *mntS*-(F11stop)~*zji-297::cat*	P1(JEM1691) X LC106

Table D.1. (continued)

JEM1706	As LC106 *mntS*-(M1stopM8stop)~*zji-297::cat*	P1(JEM1693) X LC106
JEM1708	As JEM1136 *mntS*-(Phe16 +1 frameshift)~*zji-297::cat*	P1(JEM1689) X JEM1136
JEM1710	As JEM1136 *mntS*-(M1stopM8stop)~*zji-297::cat*	P1(JEM1691) X JEM1136
JEM1712	As JEM1136 *mntS*-(F11stop)~*zji-297::cat*	P1(JEM1693) X JEM1136
LSW191	As MG1655 Δ*mntS2*	This study
JEM1375	As LSW191 Δ*sodB1::cat*	P1(JEM1202) X LSW191
LSW193	As MG1655 Δ*mntS3*	This study
JEM1377	As LSW193 Δ*sodB1::cat*	P1(JEM1202) X LSW191
JEM659	As BW25113 Δ*hfq1::cat*	This study
JEM1345	Δ*sodB1* Δ*hfq1*	This study
JEM1346	Δ*sodB1* Δ*mntS* Δ*hfq1*	This study
JEM1365	Δ*sodB1* Δ*ryhB::cat*	This study
JEM1367	Δ*sodB1* Δ*mntS* Δ*ryhB::cat*	This study
JEM1361	Δ*sodB1* Δ*hfq1* Δ*ryhB::cat*	This study
JEM1363	Δ*sodB1* Δ*mntS* Δ*hfq1* Δ*ryhB::cat*	This study

Plasmid	**Relevant characteristics**	**Reference**
pBAD24	Amp^R ColE1	Lab stock
pLW112	pBAD24 containing *mntS* ORF and its own Shine-Dalgarno	[12]
pJEM67	pBAD24 containing *mntS*-(Phe11 +1 frameshift)	This study
pJEM68	pBAD24 containing *mntS*-(Phe16 +1 frameshift)	This study
pJEM69	pBAD24 containing *mntS*-(V10M)	This study
pJEM70	pBAD24 containing *mntS*-(K5R)	This study
pJEM71	pBAD24 containing *mntS*-(V10, gtg →gtt)	This study
pJEM72	pBAD24 containing *mntS*-(V10A)	This study
pJEM74	pBAD24 containing *mntS*-(R6I)	This study
pMS17	pBAD24 containing *mntS*-(E3A)	This study
pMS18	pBAD24 containing *mntS*-(C7A)	This study
pMS19	pBAD24 containing *mntS*-(S14A)	This study
pMS20	pBAD24 containing *mntS*-(C27A)	This study
pMS21	pBAD24 containing *mntS*-(D28A)	This study
pLW125	pBAD24 containing *mntS*-(H13A)	This study
pLW129	pBAD24 containing *mntS*-(M1stop)	This study
pLW133	pBAD24 containing *mntS*-(E3A/C7A/D28A)	This study
pLW134	pBAD24 containing *mntS*-(E3A/C27A/D28A)	This study
pLW135	pBAD24 containing *mntS*-(C7A/C27A/D28A)	This study
pLW136	pBAD24 containing *mntS*-(E3A/C7A/C27A)	This study
pLW138	pBAD24 containing *mntS*-(M1stopM8stopV10stop)	This study
pLW139	pBAD24 containing *mntS*-(Phe4 +2 frameshift)	This study

Table D.1. (continued)

pLW141	pBAD24 containing *mntS*-(M8stop)	This study
pLW142	pBAD24 containing *mntS*-(M1stopE3stop)	This study
pLW143	pBAD24 containing *mntS*-(M1stopC7stop)	This study
pLW144	pBAD24 containing *mntS*-(M1stopM8stop)	This study
pLW145	pBAD24 containing *mntS*-(R9stop)	This study
pLW146	pBAD24 containing *mntS*-(M1stopR9stop)	This study
pLW147	pBAD24 containing *mntS*-(V10stop)	This study
pLW148	pBAD24 containing *mntS*-(M1stopV10stop)	This study
pLW149	pBAD24 containing *mntS*-(F11stop)	This study
pLW150	pBAD24 containing *mntS*-(M1stopF11stop)	This study
pKD3	*bla* FRT *cat* FRT PS1 PS2 oriR6K	[4]
pKD46	*bla* P_{BAD} *gam bet exo* pSC101 oriTS	[4]
pCP20	*bla cat cI857* λP_R *flp* pSC101 oriTS	[3]
pDT1-16	pBR322 containing *sodA* under *tac* promoter, Amp^R	Lab stock

Table D.2. Primer sequences used for construction of *mntS* alleles by site directed mutagenesis.

Primer	Sequence
MntS-Phe4 +2 frameshift	5′-aggaggtcttATGAATGAGTggTCAAGAGGTGTATGCGCGTGTTTAGTCATTCTCCCTTT-3′
MntS-Phe11 +1frameshift	5′-TGAATGAGTTCAAGAGGTGTATGCGCGTGTaTTAGTCATTCTCCCTTTAAAGTACGGTTA-3′
MntS-Phe16 +1frameshift	5′-AGGTGTATGCGCGTGTTTAGTCATTCTCCCTaTTAAAGTACGGTTAATGCTGCTCTCTAT-3′
MntS-Glu3Ala	5′-AGGAGGTCTTATGAATGcGTTCAAGAGGTGTATGCGCGTGTTTAGTCATTCTCCCTTTAA-3′
MntS-Cys7Ala	5′-AGGAGGTCTTATGAATGAGTTCAAGAGGgcTATGCGCGTGTTTAGTCATTCTCCCTTTAA-3′
MntS-Cys27Ala	5′-AAGTACGGTTAATGCTGCTCTCTATGTTGgcCGATATGGTCAACAACAAACCGCAGCAAG-3′
MntS-Asp28Ala	5′-GTACGGTTAATGCTGCTCTCTATGTTGTGCGcTATGGTCAACAACAAACCGCAGCAAGAT-3′
MntS-His13Ala	5′-GTTCAAGAGGTGTATGCGCGTGTTTAGTgcTTCTCCCTTTAAAGTACGGTTAATGCTG-3′
Mnts-Ser14Ala	5′-TTCAAGAGGTGTATGCGCGTGTTTAGTCATgCTCCCTTTAAAGTACGGTTAATGCTGCTC-3′
MntS-E3A/C7A/D28A	5′-AGGAGGTCTTATGAATGcGTTCAAGAGGgcTATGCGCGTGTTTAGTCATTCTCCCTTTAA-3′
MntS-E3A/C27A/D28A	5′-AAGTACGGTAATGCTGCTCTCTATGTTGgcCGCTATGGTCAACAACAAACCGCAGCAAG-3′
MntS-C7A/C27A/D28A	5′-AAGTACGGTTAATGCTGCTCTCTATGTTGgcCGcTATGGTCAACAACAAACCGCAGCAAG-3′
MntS-E3A/C7A/C27A	5′-AGGAGGTCTTATGAATGcGTTCAAGAGGgcTATGCGCGTGTTTAGTCATTCTCCCTTTAA-3′
MntS-M1stop	5′-cgacgggattagcaagtcaggaggtcttTAGAATGAGTTCAAGAGGTGTATGCGCGTG-3′
MntS-M1stopE3stop	5′-gttttttgggctagcAGGAGGTCTTtagAATtAGTTCAAGAGGTGTATGCGCGTGTTTA-3′
MntS-M1stopC7stop	5′-AATGAGTTCAAGAGGTGaATGCGCGTGTTTAGTCATTCTCCCTTTAAAGTACGGTTAATG-3′
MntS-M8stop	5′-AATGAGTTCAAGAGGTGTtaGCGCtaGTTTAGTCATTCTCCCTTTAAAGTACGGTTAATG-3′
MntS-M1stopM8stopV10stop	5′-AATGAGTTCAAGAGGTGTtaGCGCtaGTTTAGTCATTCTCCCTTTAAAGTACGGTTAATG-3′
MntS-R9stop	5′-AATGAGTTCAAGAGGTGTATGtGaGTGTTTAGTCATTCTCCCTTTAAAGTACGGTTAATG-3′
MntS-M1stopR9stop	5′-AATGAGTTCAAGAGGTGTATGtGaGTGTTTAGTCATTCTCCCTTTAAAGTACGGTTAATG-3′
MntS-F11stop	5′-AATGAGTTCAAGAGGTGTATGCGCGTGTAGAGTCATTCTCCCTTTAAAGTACGGTTAATG-3′
MntS-M1stopF11stop	5′-AATGAGTTCAAGAGGTGTATGCGCGTGTAGAGTCATTCTCCCTTTAAAGTACGGTTAATG-3′

Table D.2. (continued)

MntS-Val10stop	5′-AATGAGTTCAAGAGGTGTATGCGCtaGTTTAGTCATTCTCCCTTTAAAGTACGGTTAATG-3′
MntS-M1stopV10stop	5′-AATGAGTTCAAGAGGTGTATGCGCtaGTTTAGTCATTCTCCCTTTAAAGTACGGTTAATG-3′
MntS-Val10Met	5′-TTATGAATGAGTTCAAGAGGTGTATGCGCaTGTTTAGTCATTCTCCCTTTAAAGTACGGT-3′
MntS-Val10Ala	5′-AGGTCTTATGAATGAGTTCAAGAGGTGTATGCGCGcGTTTAGTCATTCTCCCTTT-3′
MntS-V10 (gtg→gtt)	5′-TTATGAATGAGTTCAAGAGGTGTATGCGCGTtTTTAGTCATTCTCCCTTTAAGTACGGT-3′
MntS-K5R	5′-AGCAGGAGGTCTTATGAATGAGTTCAgGAGGTGTATGCGCGTGTTTAGTCATTCTCCCTT-3′
MntS-R6I	5′-AGCAGGAGGTCTTATGAATGAGTTCAAGAtaTGTATGCGCGTGTTTAGTCATTCTCCCTT-3′

D.6 FIGURES

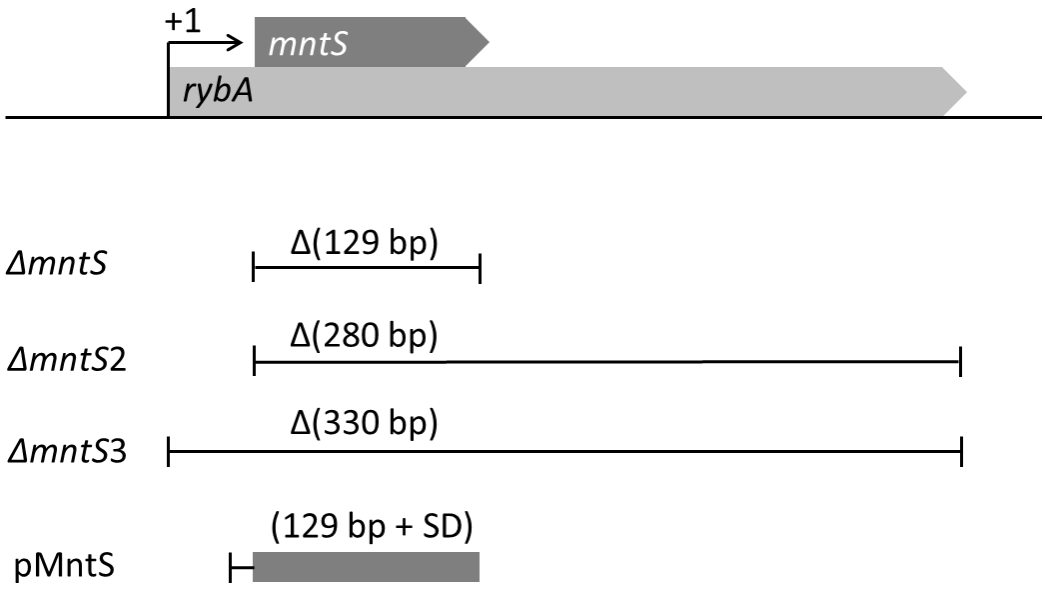

Figure D.1. Diagram of *mntS* constructs. Both *rybA* and *mntS* are transcribed from the same transcriptional start site (+1). Within the RybA sRNA transcript lays a short open reading frame that encodes the small protein MntS. Several chromosomal deletions were made: *ΔmntS*, which removes the entire MntS open reading frame (129 bp) starting from the translational start site (ATG); *mntS*2, which removes the entire MntS open reading frame (129 bp) plus the downstream untranslated region (151 bp); and *mntS*3, which removes the entire RybA transcript (330 bp) that encompasses the MntS open reading frame. The MntS open reading frame including its own Shine-Dalgarno sequence was cloned into pBAD24, resulting in the plasmid construct pMntS. This plasmid was used as a DNA template for site-directed mutagenesis of the *mntS* gene.

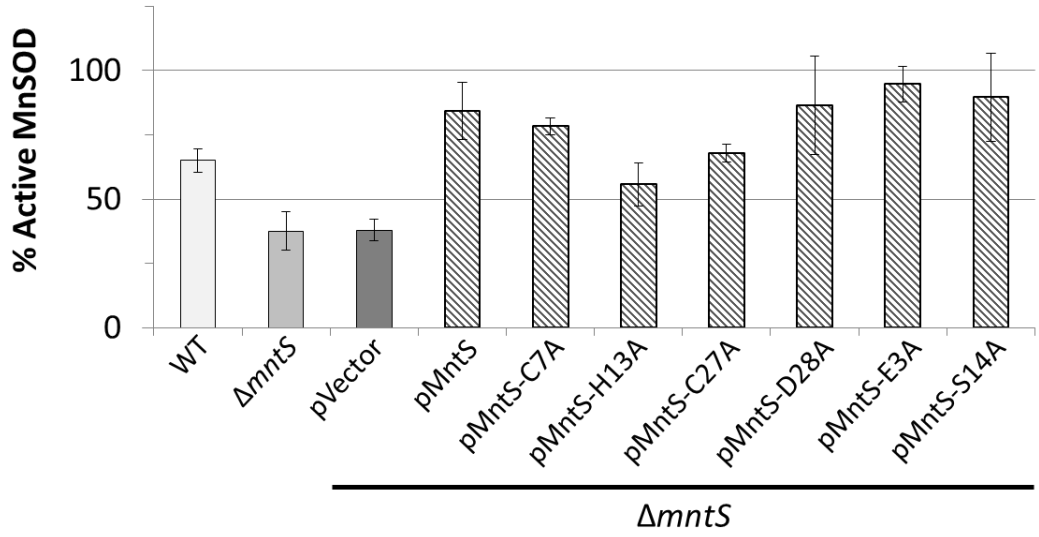

Figure D.2. Mutation of possible metal-binding residues does not inactivate MntS function. The fraction of active MnSOD was measured in cell extracts prepared from cultures grown aerobically to 0.25 OD_{600} in LB/arabinose medium. Data represent the mean of three independent cultures. All strains contain the *sodB*-null allele. Strains were JEM1233 (WT) and JEM1234 (Δ*mntS*) harboring empty vector (pBAD24), pMntS (pLW112, *mntS* driven by the *araBAD* promoter), pMntS-C7A (pMS18), pMntS-H13A (pLW125), pMntS-C27A (pMS20), pMntS-D28A (pMS21), pMntS-E3A (pMS17) or pMntS-S14A (pMS19).

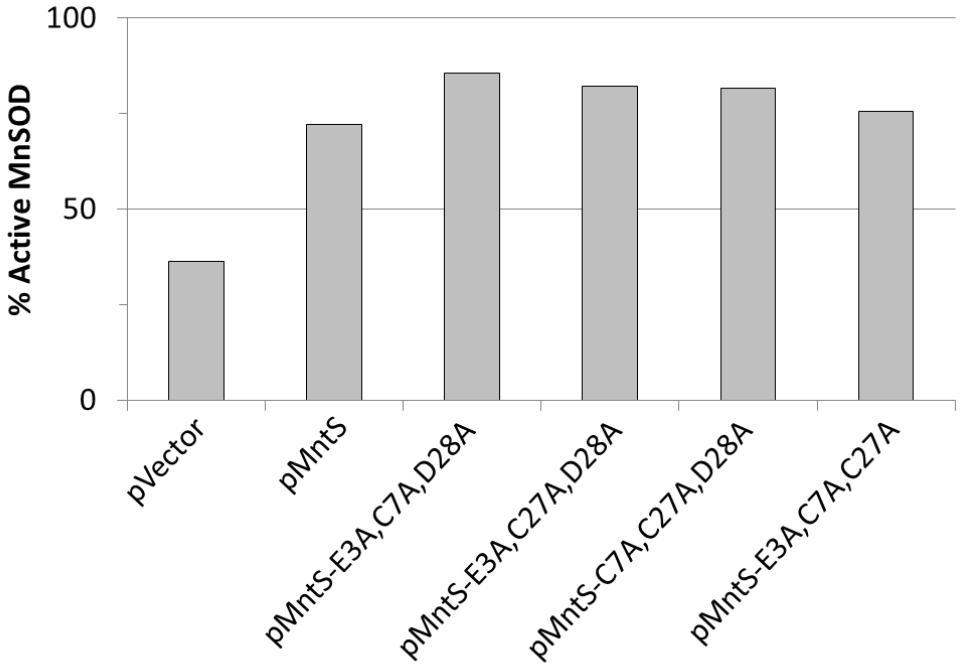

Figure D.3. Mutation of possible metal-binding residues in triplet does not inactivate MntS function. The fraction of active MnSOD was measured in cell extracts prepared from cultures grown aerobically to 0.25 OD_{600} in LB/arabinose medium. All strains contain the *sodB*-null allele. Strains were JEM1234 (Δ*mntS*) harboring empty vector (pBAD24), pMntS (pLW112, *mntS* driven by the *araBAD* promoter), pMntS-(E3A/C7A/ D28A) (pLW133), pMntS-(E3A/C27A/D28A) (pLW134), pMntS-(C7A/C27A/D28A) (pLW135) or pMntS-(E3A/C7A/C27A) (pLW136).

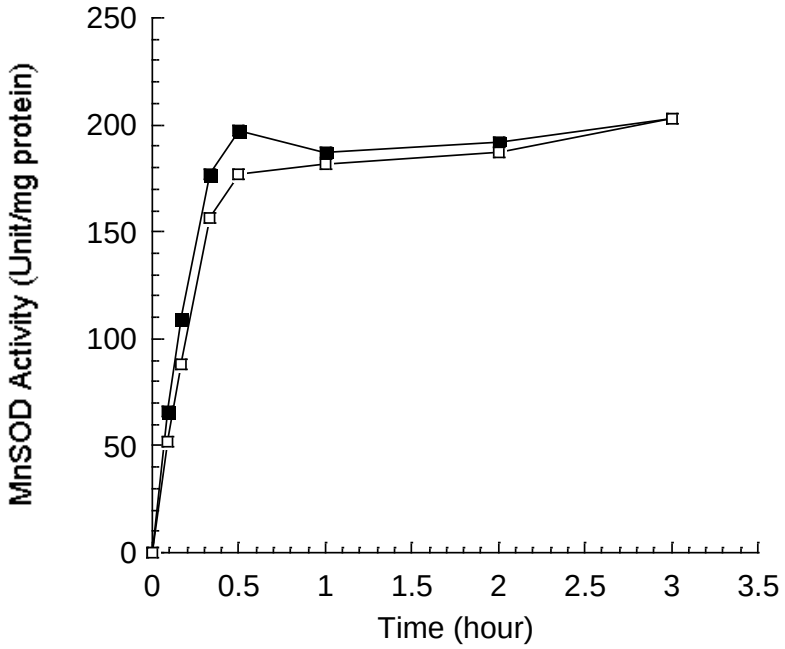

Figure D.4. Purified MntS protein does not help activate MnSOD in cell extracts. Cell extracts were prepared from Δ*sodB* Δ*mntS* mutants overexpressing MnSOD (pDT-16). Apo-MnSOD was prepared by denaturing proteins in cell extracts. Buffer (filled symbols) or purified MntS (360 nM) protein (empty symbols) was added at time zero to denatured cell extracts in the presence of 200 μM $MnCl_2$, aliquots were removed at times indicated, and SOD activity was measured.

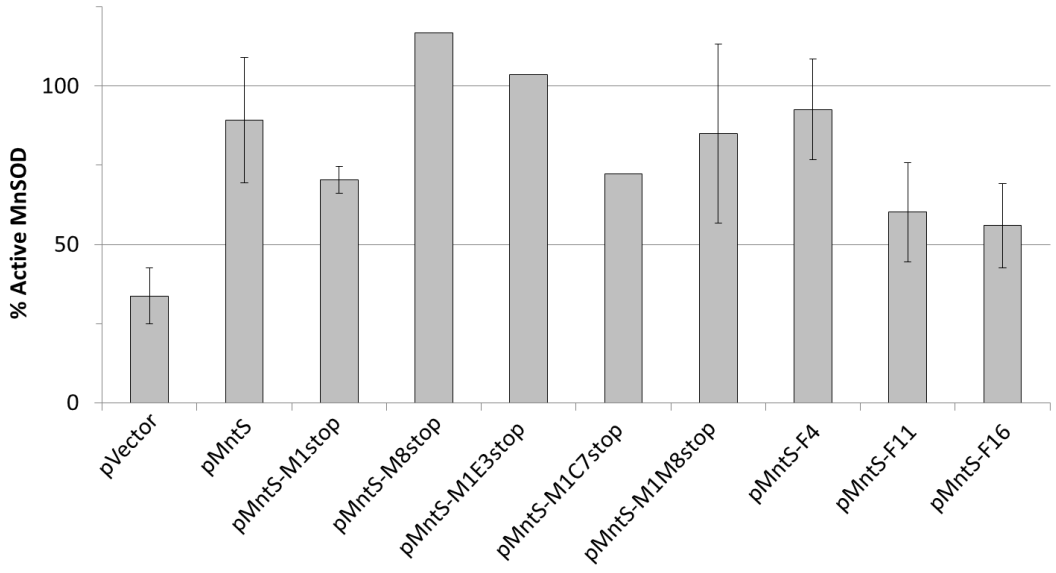

Figure D.5. MntS still functions to activate MnSOD when MntS protein is not made. The fraction of active MnSOD was measured in cell extracts prepared from cultures grown aerobically to 0.25 OD_{600} in LB/arabinose medium. Data represent the mean of three independent cultures. All strains contain Δ*sodB* and Δ*mntS*-null mutations. Plasmids were empty vector (pBAD24), pMntS (pLW112, *mntS* driven by the *araBAD* promoter), pMntS-M1stop (pLW129), pMntS-M8stop (pLW141), pMntS-M1E3stop (pLW142), pMntS-M1C7stop (pLW143), pMntS-M1M8stop (pLW144), pMntS-F4 (pLW139), pMntS-F11 (pJEM67) or pMntS-F16 (pJEM68).

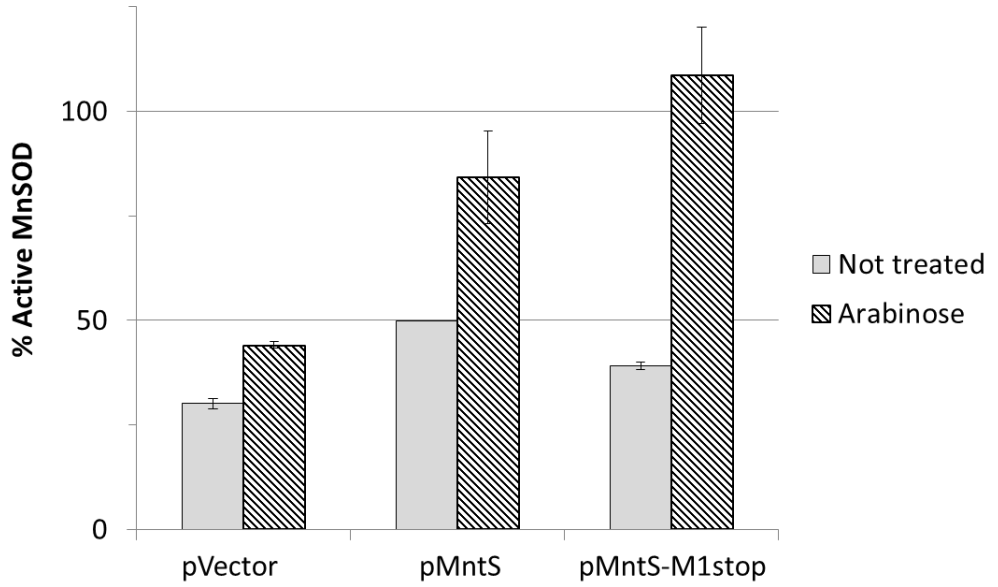

Figure D.6. MnSOD activation observed by overexpression of MntS requires induction with arabinose. The fraction of active MnSOD was measured in cell extracts prepared from cultures grown aerobically to 0.25 OD_{600} in LB medium with or without arabinose. Data represent the mean of three independent cultures measured from JEM1234 (Δ*sodB* Δ*mntS*) harboring empty vector (pBAD24), pMntS (pLW112, *mntS* driven by the *araBAD* promoter) or pMntS-M1stop (pLW129).

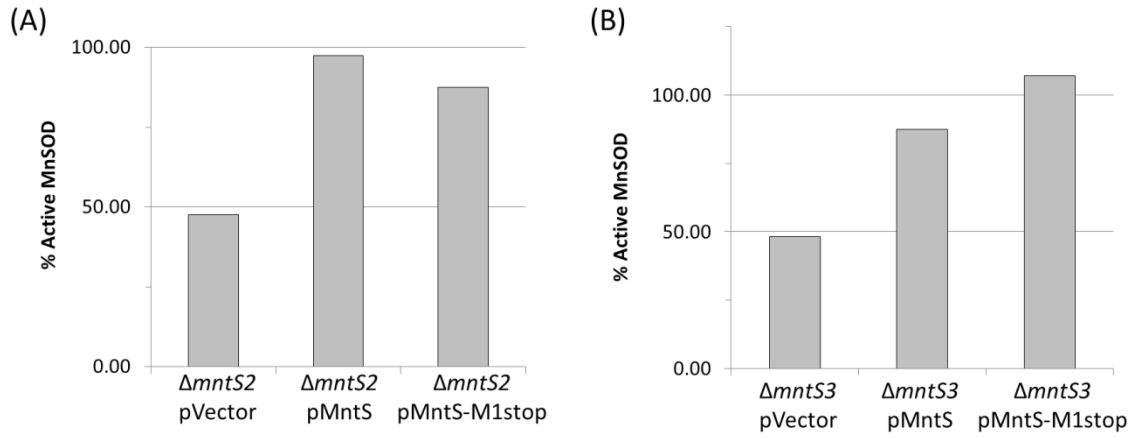

Figure D.7. MntS expressed from a plasmid functions independently of the *mntS* and RybA allele on the chromosome. The fraction of active MnSOD was measured in cell extracts prepared from cultures grown aerobically to 0.25 OD_{600} in LB/arabinose medium. Plasmids were empty vector (pBAD24), pMntS (pLW112, *mntS* driven by the *araBAD* promoter) or pMntS-M1stop (pLW129).

A. Strain was JEM1375 (Δ*sodB* Δ*mntS*2, which lacks small RNA RybA)

B. Strain was JEM1377 (Δ*sodB* Δ*mntS*3, which lacks entire *mntS/rybA* transcript and promoter region).

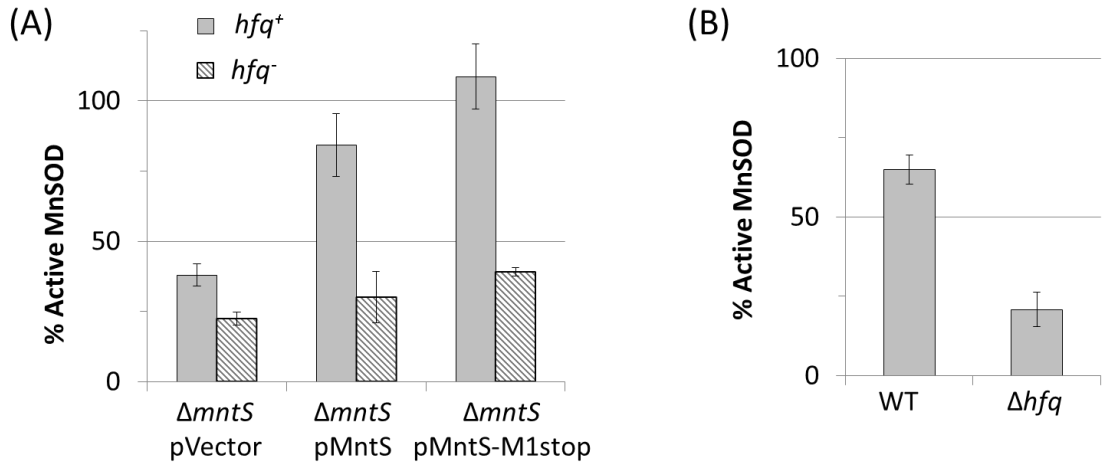

Figure D.8. The function of MntS is Hfq dependent for the activation of MnSOD. The fraction of active MnSOD was measured in cell extracts prepared from cultures grown aerobically to 0.25 OD_{600} in LB/arabinose medium. Data represent the mean of three independent cultures.

A. Strains were JEM1234 (Δ*sodB* Δ*mntS*) and JEM1346 (Δ*sodB* Δ*mntS* Δ*hfq*) expressing empty vector (pBAD24), pMntS (pLW112, *mntS* driven by the *araBAD* promoter) or pMntS-M1stop (pLW129).

B. Strains were JEM1233 (Δ*sodB*) and JEM1345 (Δ*sodB* Δ*hfq*).

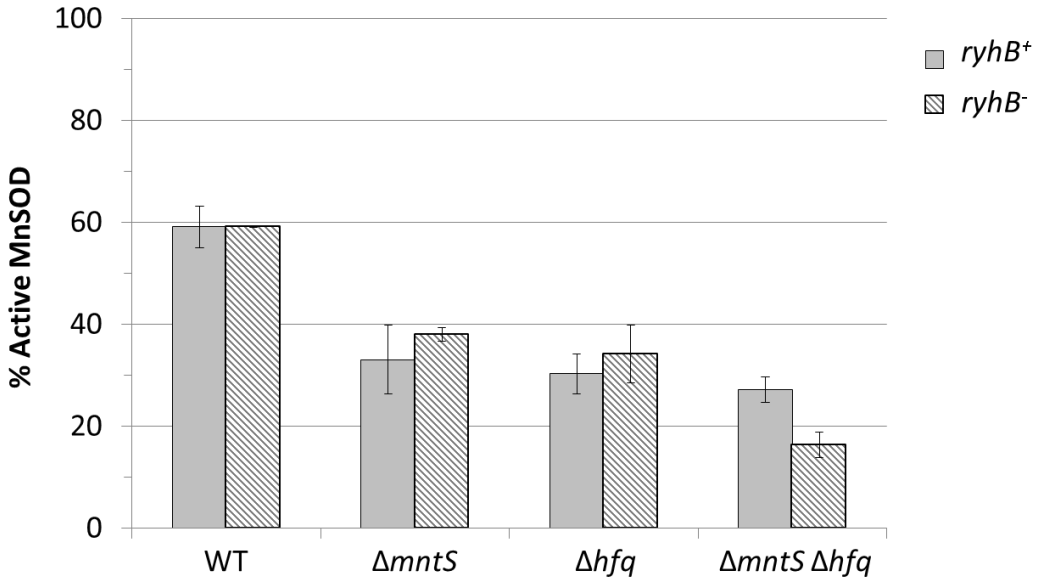

Figure D.9. RyhB does not affect activation of MnSOD. The fraction of active MnSOD was measured in cell extracts prepared from cultures grown aerobically to 0.25 OD_{600} in LB/arabinose medium. Data represent the mean of three independent cultures. All strains contain the *sodB*-null allele. Strains were JEM1233 (WT), JEM1234 (Δ*mntS*), JEM1345 (Δ*hfq*), JEM1346 (Δ*mntS* Δ*hfq*), JEM1365 (Δ*ryhB*), JEM1367 (Δ*mntS* Δ*ryhB*), JEM1361 (Δ*hfq* Δ*ryhB*), and JEM1363 (Δ*mntS* Δ*hfq* Δ*ryhB*).

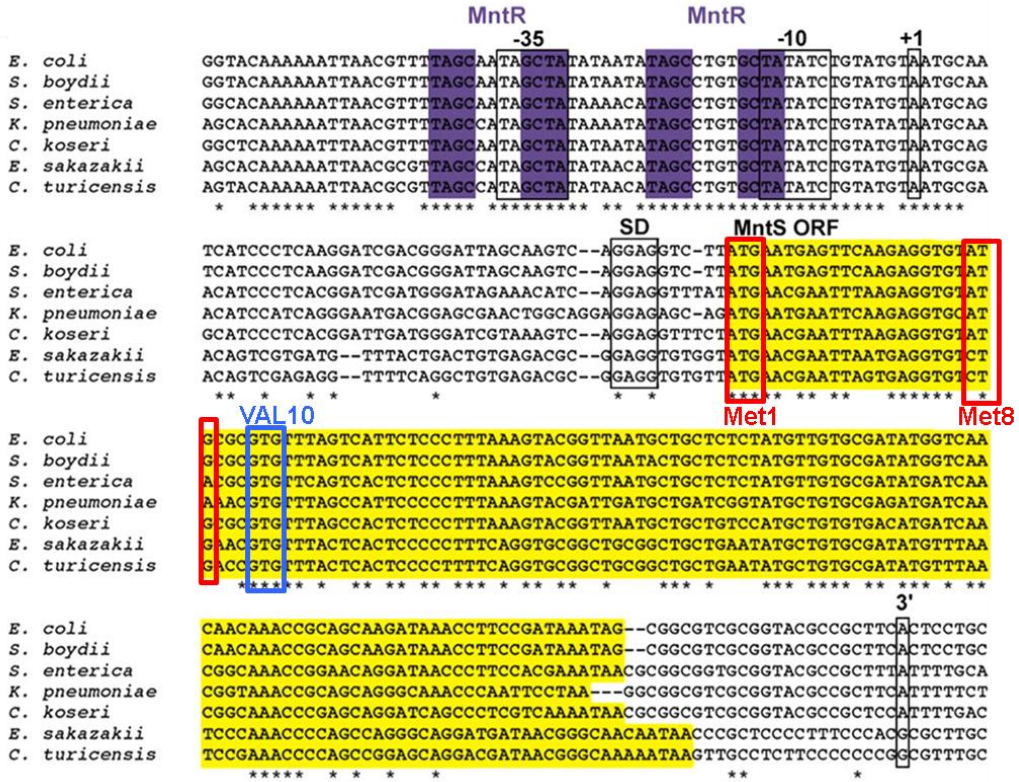

Figure D.10. Sequence alignment of *mntS* locus. Species abbreviations are: *Escherichia coli*, *Shigella boydii*, *Salmonella enterica*, *Citrobacter koseri*, *Klebsiella pneumoniae*, *Enterobacter sakazakii*, and *Cronobacter turicensis* [12].

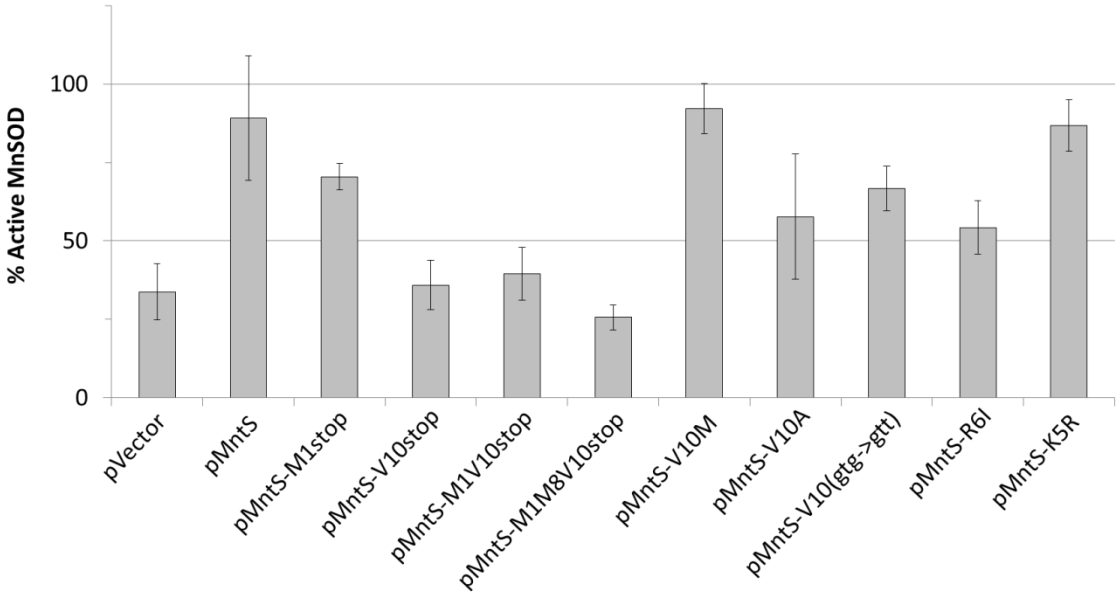

Figure D.11. The V10 residue is important for MntS function and may encode an alternate translational start site. The fraction of active MnSOD was measured in cell extracts prepared from cultures grown aerobically to 0.25 OD_{600} in LB/arabinose medium. Data represent the mean of three independent cultures. All strains contain the *sodB* and *mntS*-null alleles. Plasmids were empty vector (pBAD24), pMntS (pLW112, *mntS* driven by the *araBAD* promoter), pMntS-M1stop (pLW129), pMntS-V10stop (pLW147), pMntS-M1V10stop (pLW148), pMntS-M1M8V10stop (pLW138), pMntS-V10M (pJEM69), pMntS-V10A (pJEM72), pMntS-V10 (gtg to gtt) (pJEM71), pMntS-R6I (pJEM74) or pMntS-K6R (pJEM70).

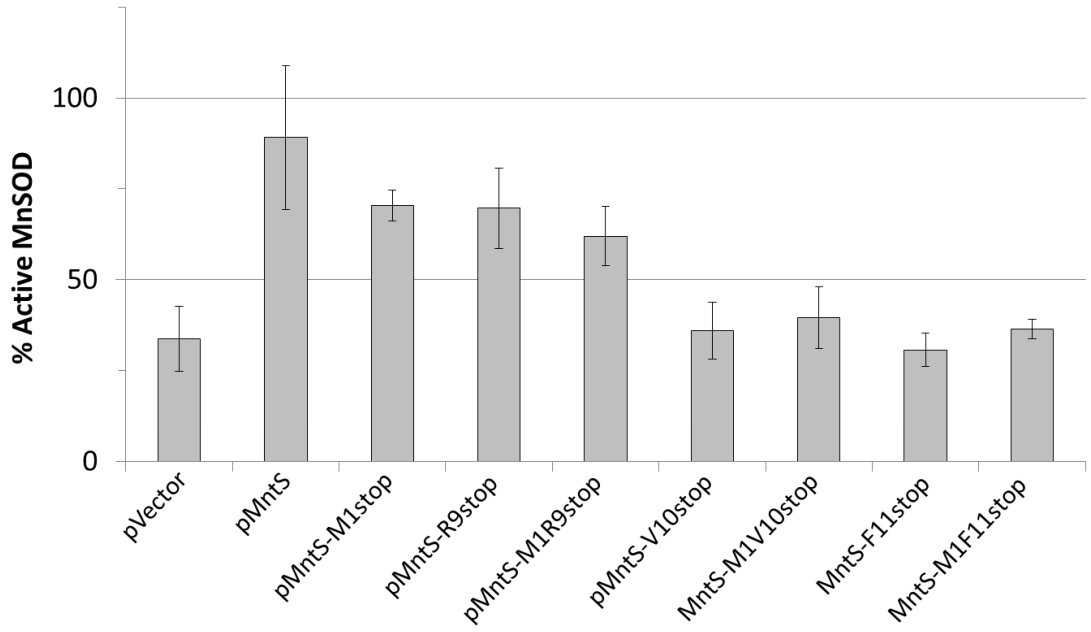

Figure D.12. Residues V10 and F11 are important for MntS function, while R9 is not. The fraction of active MnSOD was measured in cell extracts prepared from cultures grown aerobically to 0.25 OD_{600} in LB/arabinose medium. Data represent the mean of three independent cultures. All strains contain the *sodB* and *mntS*-null alleles. Plasmids were empty vector (pBAD24), pMntS (pLW112, *mntS* driven by the *araBAD* promoter), pMntS-M1stop (pLW129), pMntS-R9stop (pLW145), pMntS-M1R9stop (pLW146), pMntS-V10stop (pLW147), pMntS-M1V10stop (pLW148), pMntS-F11stop (pLW149) or pMntS-M1F11stop (pLW150).

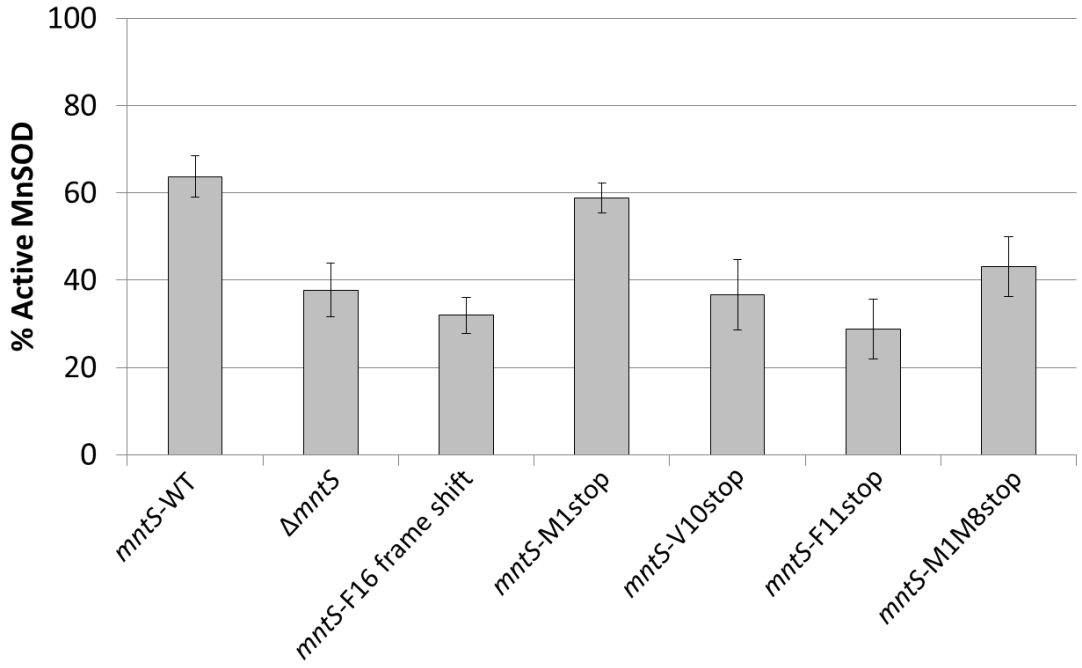

Figure D.13. The *mntS* chromosomal mutations show low activation of MnSOD. The fraction of active MnSOD was measured in cell extracts prepared from cultures grown aerobically to 0.25 OD_{600} in LB/arabinose medium. Data represent the mean of three independent cultures. All strains contain the *sodB*-null allele. Strains were JEM1507 (*mntS*-WT), JEM1234 (Δ*mntS*), JEM1679 (*mntS*-F16 frameshift), JEM1509 (*mntS*-M1stop), JEM1511 (*mntS*-V10stop), JEM1641 (*mntS*-F11stop), and JEM1643 (*mntS*-M1M8stop).

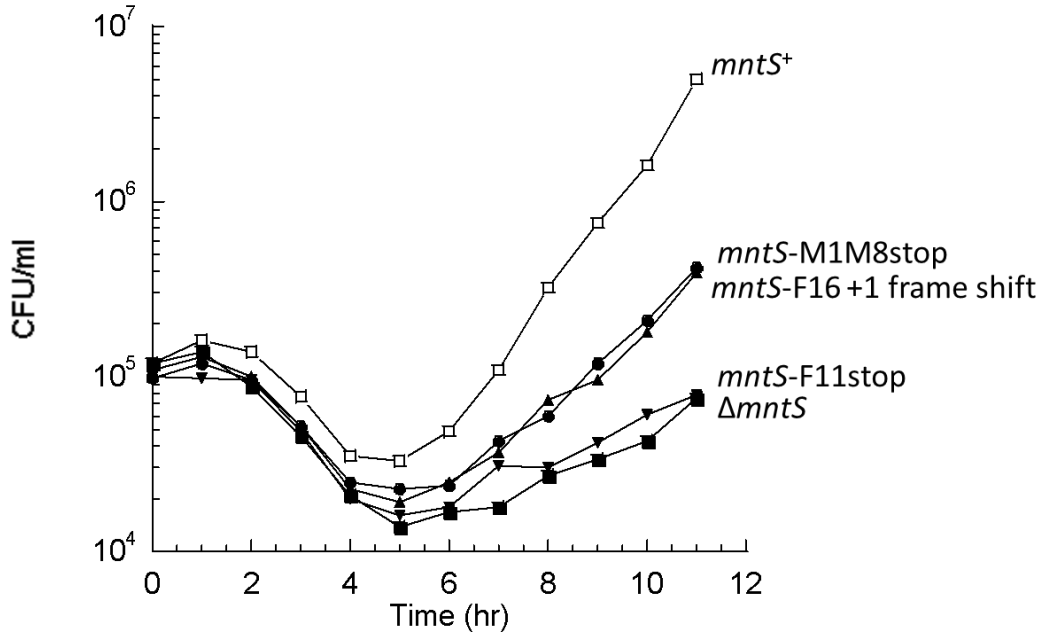

Figure D.14. MntS functions as both a protein and small RNA to activate NrdEF. Cells pre-cultures in anaerobic MOPS glucose/casamino acids medium were diluted into aerobic medium at time zero and viability was monitored by anaerobic plating. All strains contain Δ*tonB* Δ*feoABC* Δ*zupT* Δ*nrdAB* null alleles and therefore have reduced iron import. Strains were JEM1136 (*mntS*$^+$), JEM1183 (Δ*mntS*), JEM1708 (*mntS*-F16 frameshift), JEM1710 (*mntS*-M1M8stop), and JEM1712 (*mntS*-F11stop).

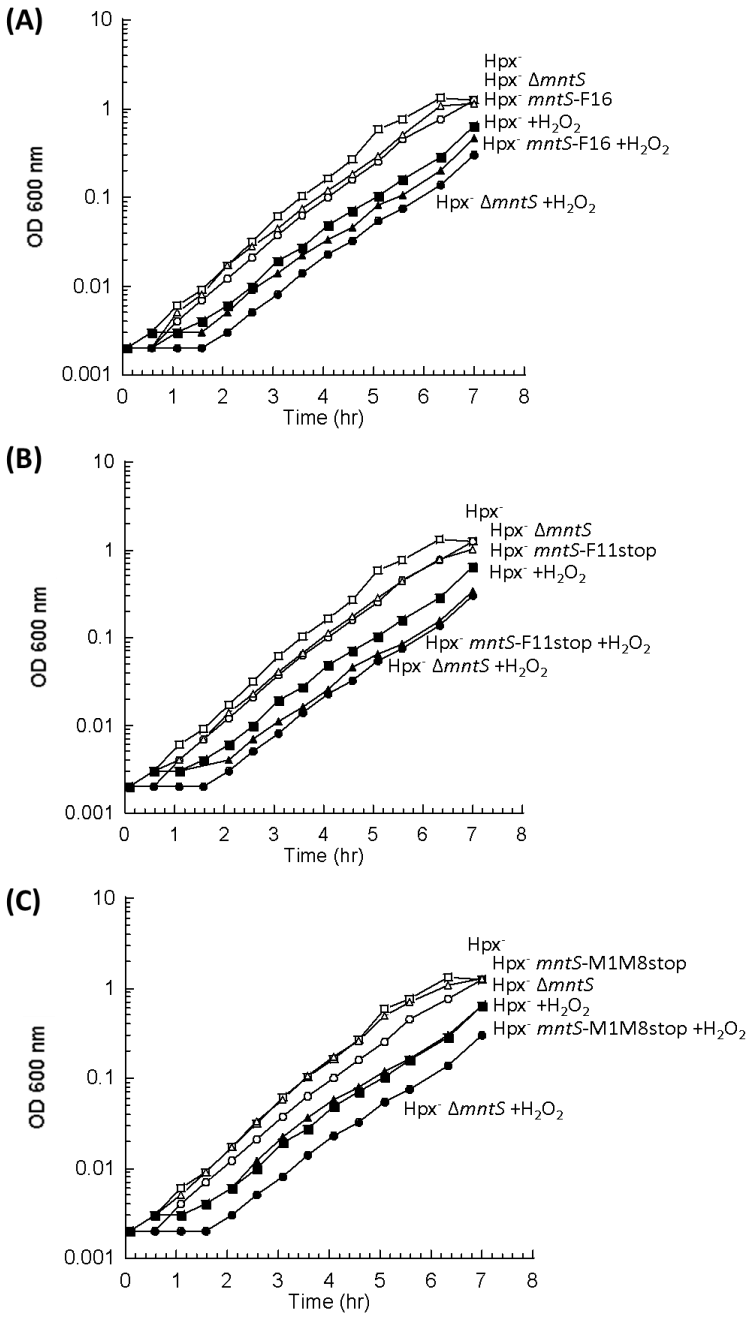

Figure D.15. MntS functions as both a protein and small RNA to help cells cope with hydrogen peroxide stress. Cells were pre-cultured in anaerobic M9 glucose/casamino acids medium and then diluted at time zero into the same aerobic medium containing 0 or 15 μM H_2O_2. Strains were LC106 (Hpx^-), JEM1177 (Hpx^- Δ*mntS*), JEM1702 (Hpx^- *mntS*-F16 frameshift), JEM1705 (Hpx^- *mntS*-F11stop), and JEM1706 (Hpx^- *mntS*-M1M8stop).

D.7 REFERENCES

1. **Balasubramanian, D., and C. K. Vanderpool.** 2013. Deciphering the interplay between two independent functions of the small RNA regulator SgrS in *Salmonella*. J. Bacteriol. **195:**4620-4630.

2. **Bobrovskyy, M., and C. K. Vanderpool.** 2013. Regulation of bacterial metabolism by small RNAs using diverse mechanisms. Annu. Rev. Genet.

3. **Cherepanov, P. P., and W. Wackernagel.** 1995. Gene disruption in *Escherichia coli:* Tc^R and Km^R cassettes with the option of Flp-catalyzed excision of the antibiotic-resistance determinant. Gene. **158:**9-14.

4. **Datsenko, K. A., and B. L. Wanner.** 2000. One-step inactivation of chromosomal genes in *Escherichia coli* K-12 using PCR products. Proc. Natl. Acad. Sci. U. S. A. **97:**6640-6645.

5. **Kirby, T., J. Blum, I. Kahane, and I. Fridovich.** 1980. Distinguishing between Mn-containing and Fe-containing superoxide dismutases in crude extracts of cells. Arch. Biochem. Biophys. **201:**551-555.

6. **Martin, J. E., and J. A. Imlay.** 2011. The alternative aerobic ribonucleotide reductase of *Escherichia coli*, NrdEF, is a manganese-dependent enzyme that enables cell replication during periods of iron starvation. Mol. Microbiol. **80:**319-334.

7. **McCord, J. M., and I. Fridovich.** 1969. Superoxide dismutase. An enzymic function for erythrocuprein (hemocuprein). J. Biol. Chem. **244:**6049-6055.

8. **Miller, J. H. (ed.),** 1972. Experiments in molecular genetics. Cold Springs Harbor Laboratory, Cold Springs Harbor, NY.

9. **Neidhardt, F. C., P. L. Bloch, and D. F. Smith.** 1974. Culture medium for enterobacteria. J. Bacteriol. **119:**736-747.

10. **Seaver, L. C., and J. A. Imlay.** 2004. Are respiratory enzymes the primary sources of intracellular hydrogen peroxide? J. Biol. Chem. **279:**48742-48750.

11. **Wassarman, K. M., F. Repoila, C. Rosenow, G. Storz, and S. Gottesman.** 2001. Identification of novel small RNAs using comparative genomics and microarrays. Genes Dev. **15:**1637-1651.

12. **Waters, L. S., M. Sandoval, and G. Storz.** 2011. The *Escherichia coli* MntR miniregulon includes genes encoding a small protein and an efflux pump required for manganese homeostasis. J. Bacteriol. **193:**5887-5897.